

# Identification and characterisation of vacuolar proton-pumping pyrophosphatase genes in bread wheat

Daniel Jamie Menadue

B. Sc. (Hons)

A thesis submitted for the degree of  
Doctor of Philosophy

Faculty of Sciences  
School of Agriculture, Food & Wine  
The University of Adelaide



THE UNIVERSITY  
*of* ADELAIDE

June 2018



# Table of Contents

List of Figures.....	iv
List of Tables.....	viii
List of Abbreviations .....	ix
Abstract .....	xiii
Declaration .....	xiv
List of Publications.....	xv
List of Conference Presentations .....	xv
List of Awards .....	xv
Acknowledgments .....	xvi
<b>Chapter 1 - Literature review and research aims .....</b>	<b>1</b>
Current constraints to Australian wheat production .....	2
Vacuolar proton-pumping pyrophosphatases.....	3
Proposed mechanisms regarding the role of type I H <sup>+</sup> -PPases .....	4
Phenotypes of transgenic plants constitutively expressing H <sup>+</sup> -PPase genes .....	16
H <sup>+</sup> -PPase genes and bread wheat .....	30
Research aims.....	34
References .....	35
<b>Chapter 2 - Metabolite profiling of <i>AVP1</i> over-expressing and loss-of-function Arabidopsis.....</b>	<b>41</b>
Key message .....	45
Abstract.....	45
Introduction.....	46
Materials and Methods.....	50
Results.....	54
Discussion .....	60
Conclusions.....	66
Acknowledgements.....	67
References .....	68
Tables.....	72
Figures.....	78
Additional Data.....	84
<b>Chapter 3 - Assessing the salt tolerance of <i>AVP1</i> expressing transgenic wheat.....</b>	<b>91</b>
Abstract.....	95
Introduction.....	96

Experimental Methods .....	100
Results .....	105
Discussion.....	108
Conclusions .....	114
Acknowledgements .....	115
References.....	116
Figures .....	123
Supplementary Tables .....	128
Supplementary Figures.....	129
<b>Chapter 4 - <i>TaVP</i> homeolog expression profiling in bread wheat.....</b>	<b>133</b>
Summary .....	137
Introduction .....	138
Results .....	140
Discussion.....	146
Experimental Procedures .....	150
Acknowledgements .....	155
References.....	155
Tables .....	162
Figures .....	166
Supplementary Tables .....	173
Supplementary Figures.....	175
Additional Information .....	185
<b>Chapter 5 - Phenotypic characterisation of <i>TaVP</i> over-expressing bread wheat .....</b>	<b>193</b>
Highlight .....	197
Abstract .....	197
Introduction .....	198
Materials and methods .....	201
Results .....	208
Discussion.....	213
Conclusions .....	218
Acknowledgements .....	219
References.....	220
Tables .....	223
Figures .....	228
Supplementary Figures.....	234

Additional Information.....	238
<b>Chapter 6 - General discussion .....</b>	<b>253</b>
Review of research aims .....	254
Summary of research findings.....	255
Implications for future research.....	257
Other relevant areas for future research .....	263
Concluding remarks .....	268
References .....	270

# List of Figures

<b>Chapter 1 - Literature review and research aims.....</b>	<b>1</b>
Figure 1: Proposed role of AVP1 in promoting auxin transport.....	8
Figure 2: Proposed role of AVP1 in regulating cytosolic PP <sub>i</sub> levels.....	10
Figure 3: Proposed role of AVP1 in sucrose phloem loading. ....	13
Figure 4: Phenotypes of transgenic plants constitutively expressing <i>AVP1</i> under stressed and non-stressed conditions.....	24
<b>Chapter 2 - Metabolite profiling of <i>AVP1</i> over-expressing and loss-of-function Arabidopsis.....</b>	<b>41</b>
Fig. 1 Molecular characterisation of <i>AVP1</i> over-expressing and <i>fugu5</i> mutant Arabidopsis lines .....	78
Fig. 2 Growth phenotypes of Arabidopsis seedlings on basal MS media and MS + 2 % sucrose .....	79
Fig. 3 Growth parameters of wild-type (WT), <i>AVP1</i> mutant ( <i>fugu5-1</i> , <i>fugu5-2</i> , <i>fugu5-3</i> ) and <i>35S:AVP1</i> over-expressing seedlings on basal MS media with and without 2 % sucrose (Suc) for 8 d. ....	80
Fig. 4 Percent (%) change in metabolite concentrations relative to wild-type in 8 d-old <i>AVP1</i> mutant ( <i>fugu5-1</i> , <i>fugu5-2</i> , and <i>fugu5-3</i> ) and <i>35S:AVP1</i> over-expressing Arabidopsis seedlings on basal MS media without nutrients or sugars. ....	81
Fig. 5 Metabolite changes in 8 d-old <i>fugu5</i> mutant Arabidopsis seedlings relative to wild-type.....	82
Fig. 6 Metabolite changes in 8 d-old <i>35S:AVP1</i> transgenic Arabidopsis seedlings relative to wild-type. ....	83
Fig. A1 Gene expression analysis of <i>35S:AVP1</i> over-expressing Arabidopsis. ....	86
Fig. A2 Transgene expression and growth phenotypes of <i>AVP1-1</i> , <i>AVP1-2</i> and <i>35S:AVP1</i> transgenic Arabidopsis seedlings.....	87
Fig. A3 Growth parameters of 8 d-old <i>AVP1-1</i> , <i>AVP1-2</i> and <i>35S:AVP1</i> transgenic Arabidopsis on basal MS media with and MS media with 2 % sucrose (Suc).....	88
Fig. A4 Preliminary phenotypic analysis of wild-type and <i>fugu5</i> Arabidopsis mutants.	89
<b>Chapter 3 - Assessing the salt tolerance of <i>AVP1</i> expressing transgenic wheat .....</b>	<b>91</b>

Figure 1: Transgene presence and expression analysis of <i>ubi:AVP1</i> transgenic and null segregant (nulls) wheat lines.....	123
Figure 2: Sequence analysis of the <i>AVP1</i> transgene in <i>ubi:AVP1</i> transgenic wheat lines. ....	124
Figure 3: Phenotypic characteristics of 6 d-old <i>ubi:AVP1</i> and null segregant (nulls) wheat seedlings .....	125
Figure 4: Growth characteristics of <i>ubi:AVP1</i> transgenic and null segregant (nulls) wheat lines following 3 weeks in hydroponic conditions under 0 mM NaCl and 150 mM NaCl. ....	126
Figure 5: Leaf and root Na <sup>+</sup> , Cl <sup>-</sup> and K <sup>+</sup> concentrations in <i>ubi:AVP1</i> transgenic and null segregant (nulls) wheat lines in hydroponics under 0 mM NaCl and 150 mM NaCl...	127
Supplementary Figure 1: Transgene presence and expression analysis of <i>rab17:AVP1</i> transgenic and null segregant (nulls) wheat lines. ....	129
Supplementary Figure 2: Phenotypic characteristics of 6 d-old <i>rab17:AVP1</i> and null segregant (nulls) wheat seedlings. ....	130
Supplementary Figure 3: Growth characteristics of <i>rab17:AVP1</i> transgenic and null segregant (nulls) wheat lines following 3 weeks in hydroponics under 0 mM NaCl and 150 mM NaCl.....	131
Supplementary Figure 4: Leaf and root ion concentrations in <i>rab17:AVP1</i> transgenic and null segregant (nulls) wheat lines in hydroponics under 0 mM NaCl and 150 mM NaCl .....	132
<b>Chapter 4 - <i>TaVP</i> homeolog expression profiling in bread wheat.....</b>	<b>133</b>
Figure 1: Intron-exon analysis and amino acid alignment of <i>TaVP</i> homeologs.....	166
Figure 2: Phylogenetic analysis of type I H <sup>+</sup> -PPases. ....	167
Figure 3: <i>TaVP</i> expression profile at seedling stage.....	168
Figure 4: <i>TaVP</i> expression profile at third leaf stage. ....	169
Figure 5: <i>TaVP</i> expression profile at second tiller stage. ....	170
Figure 6: <i>TaVP</i> expression profile at grain development stage. ....	171
Figure 7: Heat map of <i>TaVP</i> gene expression through time.....	172
Supplementary Figure 1: Complete type I and II H <sup>+</sup> -PPase amino acid alignment.....	176
Supplementary Figure 2: Alignment of 15 identified <i>TaVP</i> homeologs with <i>Vigna radiata</i> H <sup>+</sup> -PPase (VrVP1) protein sequence.....	178

Supplementary Figure 3: Phylogenetic analysis of type I and type II H <sup>+</sup> -PPases.....	179
Supplementary Figure 4: RNAseq expression data of IWGSCv2 scaffolds.....	180
Supplementary Figure 5: Expression of <i>TaVP3-A</i> in Vigour18 cDNA samples.....	181
Supplementary Figure 6: Melt curve analysis of <i>TaVP</i> homeolog specific primers ....	182
Supplementary Figure 7: Sequencing of <i>TaVP4-D</i> PCR product amplified from <i>Gladius</i> genomic DNA (gDNA) and pooled cDNA. ....	184
Figure A1: Growth phenotypes of B31 yeast strains after 2 d growth with 0 mM, 50 mM and 100 mM NaCl. ....	186
Figure A2: Growth phenotypes of B31 yeast strains after 3 d growth with 0 mM, 50 mM and 100 mM NaCl. ....	187
Figure A3: Growth phenotypes of B31 yeast strains after 4 d growth with 0 mM, 50 mM and 100 mM NaCl. ....	188
<b>Chapter 5 - Phenotypic characterisation of <i>TaVP</i> over-expressing bread wheat .....</b>	<b>193</b>
Fig. 1: Molecular characterisation of wild-type, <i>TaVP</i> transgenic and null segregant wheat lines. ....	228
Fig. 2: Days to flowering and visual phenotype of wild-type, <i>TaVP</i> transgenic and null segregant wheat lines.....	229
Fig 3: Smoothed projected shoot area of wild-type, <i>TaVP</i> transgenic and null segregant wheat lines 13, 19 and 38 DAP. ....	230
Fig. 4: Relative growth rates of wild-type, <i>TaVP</i> transgenic and null segregant wheat lines 13-17, 19-25 and 32-38 DAP. ....	231
Fig. 5: Cumulative water use of wild-type, <i>TaVP</i> transgenic and null segregant wheat lines 17, 25 and 38 DAP.....	232
Fig. 6: Na <sup>+</sup> , Cl <sup>-</sup> and K <sup>+</sup> concentrations of wild-type, <i>TaVP</i> transgenic and null segregant wheat lines in 4 <sup>th</sup> leaf samples collected at 38 DAP. ....	233
Fig. S1: Transformation vectors used to generate transgenic bread wheat (cv. Fielder) constitutively over-expressing the <i>TaVP1-B</i> and <i>TaVP2-B</i> genes.....	234
Fig. S2: Greenhouse layout of wild-type, <i>TaVP</i> transgenic and null segregant wheat lines. ....	235
Fig. S3: Cumulative water use of wild-type, <i>TaVP</i> transgenic and null segregant wheat lines under control (0 mM NaCl) and saline (150 mM NaCl) conditions from 13-116 DAP. ....	236



Fig. S4: Osmotic stress tolerance (OST) of wild-type, <i>TaVP</i> transgenic and null segregant wheat lines in the first 5 d following salt treatment. ....	237
Fig. A1: Cumulative water use of wild-type Fielder plants under various salt treatment levels in two methodologies. ....	240
Fig. A2: Biomass measurements of wild-type Fielder plants after 30 d and 38 d growth in two salt treatment methodologies. ....	241
Fig. A3: 4 <sup>th</sup> leaf Na <sup>+</sup> , Cl <sup>-</sup> and K <sup>+</sup> concentration of wild-type Fielder plants under various NaCl conditions. ....	242
Fig. A4: Root Na <sup>+</sup> , Cl <sup>-</sup> and K <sup>+</sup> concentration of wild-type Fielder plants under various NaCl conditions ....	243
Fig. A5: Analysis of soil in treatment Method 1.....	244
Fig. A6: Analysis of soil in treatment Method 2.....	245
Fig. A7: Overview of the hydroponics system used to assess seedling vigour of T <sub>1</sub> <i>TaVP</i> over-expressing wheat lines. ....	251

# List of Tables

<b>Chapter 1 - Literature review and research aims.....</b>	<b>1</b>
Table 1: Summary of phenotypic characteristics of transgenic plants constitutively expressing H <sup>+</sup> -PPase genes.....	25
<b>Chapter 2 - Metabolite profiling of <i>AVP1</i> over-expressing and loss-of-function Arabidopsis.....</b>	<b>41</b>
Table 1 Details of PCR primers and related thermocycling settings used for gene presence and expression analysis of all Arabidopsis lines.....	72
Table 2 Metabolite concentrations (picomole mg <sup>-1</sup> dry weight ± standard error of the mean) in 8 d-old pooled seedlings of wild-type (WT), <i>AVP1</i> mutant ( <i>fugu5-1</i> , <i>fugu5-2</i> and <i>fugu5-3</i> ) and <i>35S:AVP1</i> over-expressing Arabidopsis lines on basal MS media. ...	73
Table A1 Metabolite concentrations (picomole mg <sup>-1</sup> dry weight ± standard error of the mean) in 8 d-old pooled seedlings of wild-type (WT), and <i>AVP1-1</i> and <i>AVP1-2</i> transgenic Arabidopsis lines on basal MS media.....	84
<b>Chapter 3 - Assessing the salt tolerance of <i>AVP1</i> expressing transgenic wheat .....</b>	<b>91</b>
Supplementary Table 1: Details of primers used to amplify and sequence the <i>AVP1</i> transgene in gDNA samples of the <i>ubi:AVP1-1</i> , <i>ubi:AVP1-2</i> and <i>ubi:AVP1-3</i> transgenic wheat lines. ....	128
<b>Chapter 4 - <i>TaVP</i> homeolog expression profiling in bread wheat.....</b>	<b>133</b>
Table 1: Details of the 15 <i>TaVP</i> homeologs identified in the bread wheat genome. .	162
Supplementary Table 1: qRT-PCR primer details. ....	173
Supplementary Table 2: Details of H <sup>+</sup> -PPase sequences used in phylogenetic analysis. ....	174
<b>Chapter 5 - Phenotypic characterisation of <i>TaVP</i> over-expressing bread wheat .....</b>	<b>193</b>
Table 1: Phenotypic characteristics of wild-type, <i>TaVP</i> over-expressing and null segregant wheat lines at maturity. ....	223
Table A1: Initial seed weight and daily total biomass measurements (mg FW ± SEM) of wild-type, T <sub>1</sub> <i>TaVP</i> transgenic and null segregant wheat seedlings.....	248
Table A2: Daily total root length measurements (cm ± SEM) of wild-type, T <sub>1</sub> <i>TaVP</i> transgenic and null segregant wheat seedlings. ....	249
Table A3: Daily shoot biomass measurements (cm ± SEM) of wild-type, T <sub>1</sub> <i>TaVP</i> transgenic and null segregant wheat seedlings. ....	250

## List of Abbreviations

3'	three prime of nucleic acid sequence
5'	five prime of nucleic acid sequence
~	approximately
°C	degrees Celsius
(-)	negative control (water)
ACPFG	Australian Centre for Plant Functional Genomics
ANOVA	analysis of variance
ATP	adenosine triphosphate
AVP1	type I <i>Arabidopsis thaliana</i> vacuolar proton-pumping pyrophosphatase
AVP2	type II <i>Arabidopsis thaliana</i> vacuolar proton-pumping pyrophosphatase
B	billion
bp	(nucleic acid) base pairs
Ca <sup>2+</sup>	calcium ion
CaCl <sub>2</sub>	calcium chloride
Ca(NO <sub>3</sub> ) <sub>2</sub>	calcium nitrate
Cd	cadmium
cDNA	complementary deoxyribonucleic acid
CDS	coding deoxyribonucleic acid sequence
Cl <sup>-</sup>	chloride ion
cm	centimetre
cM	centimorgan
CuSO <sub>4</sub>	copper sulfate
cv.	cultivar
d	day(s)
DAP	days after planting
dNTP	deoxynucleotide triphosphate
dS/m	deciSiemens per metre
E221D	amino acid substitution in AVP1 which increases functional activity
EC <sub>1:5</sub>	Electrical conductivity of 1:5 (soil:water) extract

EC <sub>e</sub>	Electrical conductivity of a saturated soil extract
EDTA	Ethylenediaminetetraacetic acid
EST	expressed sequence tag
g	gram(s)
gDNA	genomic deoxyribonucleic acid
GL mix	Goldilocks soil mix
GM	genetically modified
GSDS2.0	Gene Structure Display Server version 2.0
h	hour(s)
H <sup>+</sup>	hydrogen cation (proton)
H <sup>+</sup> -ATPase	proton-pumping adenosine triphosphatase
H <sup>+</sup> -PPase	vacuolar proton-pumping pyrophosphatase
H <sub>2</sub> O	water
ha	hectare(s)
HCl	hydrochloric acid
HVP	type I <i>Hordeum vulgare</i> vacuolar proton-pumping pyrophosphatase
IWGSC	International Wheat Genome Sequencing Consortium
K <sup>+</sup>	potassium ion
Kg	kilogram(s)
KNO <sub>3</sub>	potassium nitrate
KH <sub>2</sub> PO <sub>4</sub>	potassium phosphate
L	litre(s)
LSD	least significant difference
m	metre(s)
M	million
MgSO <sub>4</sub>	magnesium sulfate
min	minute(s)
mg	milligram(s)
Mg <sup>2+</sup>	magnesium ion
mL	millilitre(s)
mm	millimetre(s)

mM	milliMolar(s)
MnCl <sub>2</sub>	manganese chloride
Mocho	Mocho de Espiga Branca
mS	milliSiemens
MS media	Murashige and Skoog's media
MT	million tonnes
n	sample size
N	nitrogen
Na <sup>+</sup>	sodium ion
NaCl	sodium chloride
NaFe(III)	sodium iron
Na <sub>2</sub> MoO <sub>4</sub>	sodium molybdate
Na <sub>2</sub> Si <sub>3</sub> O <sub>7</sub>	sodium silicate
NCBI	National Center for Biotechnology Information
ng	nanogram(s)
NH <sub>4</sub> NO <sub>3</sub>	ammonium nitrate
NRQ	normalised relative quantity
OEX	over-expressing
OST	osmotic stress tolerance
OVP	type I <i>Oryza sativa</i> vacuolar proton-pumping pyrophosphatase
<i>P</i>	probability
P	phosphorus
PCR	polymerase chain reaction
pH	potential of hydrogen
P <sub>i</sub>	orthophosphate
PIN1	Pinformed1 (auxin efflux protein)
PP <sub>i</sub>	inorganic pyrophosphate
PSA	projected shoot area
PVC	polyvinyl chloride
qRT-PCR	quantitative real-time polymerase chain reaction
QTL	quantitative trait loci

RGR	relative growth rate
RNA	ribonucleic acid
RO	reverse osmosis
s	second(s)
SEM	standard error of the mean
sPSA	smoothed projected shoot area
sRGR	smoothed relative growth rate
Suc	sucrose
t/ha	tonnes per hectare
T <sub>1</sub>	1 <sup>st</sup> generation transgenic seed obtained from primary transformant
T <sub>2</sub>	2 <sup>nd</sup> generation transgenic seed obtained from primary transformant
TaVP	<i>Triticum aestivum</i> vacuolar proton-pumping pyrophosphatase
U	unit(s)
μl	microliter(s)
μM	micromolar
μmol	micromole(s)
μS	microSiemens
UC mix	University of California soil mix (1:1 peat:sand)
UV	ultraviolet light
v/v	volume per volume
w/v	weight per volume
w/w	weight per weight
WT	wild-type
VrVP1	type I <i>Vigna radiata</i> vacuolar proton-pumping pyrophosphatase
Z10	growth stage 10 on the Zadok scale
Z13	growth stage 13 on the Zadok scale
Z22	growth stage 22 on the Zadok scale
Z75	growth stage 75 on the Zadok scale
ZmVP	type I <i>Zea mays</i> vacuolar proton-pumping pyrophosphatase
ZnSO <sub>4</sub>	zinc sulfate

# Abstract

Vacuolar proton-pumping pyrophosphatase ( $H^+$ -PPase) genes encode membrane bound proteins responsible for hydrolysing cytosolic pyrophosphate ( $PP_i$ ) and generating an electrochemical potential difference for protons ( $H^+$ ) across cellular membranes. Constitutive expression of  $H^+$ -PPase genes, in particular the *Arabidopsis thaliana* *AVP1* gene, significantly improves the growth of several plant species, under control and stress conditions. Despite considerable research, little is known about these genes in bread wheat (*Triticum aestivum*) and whether they can be utilised to improve wheat growth and/or stress tolerance.

The first focus of this research project was to further investigate the role of *AVP1* in *Arabidopsis*. Metabolomics analysis of *AVP1* mutant and *AVP1* over-expressing *Arabidopsis* lines showed the concentrations of multiple metabolites were reduced in the mutants compared to wild-type, while concentrations of many metabolites were increased in the *AVP1* over-expressing lines compared to wild-type. This analysis suggests that expression of *AVP1* could potentially influence pathways involved in the biosynthesis of ascorbic acid, tryptophan and sucrose.

The second focus of this project was to investigate the role of *AVP1* in bread wheat. To address this, transgenic wheat lines (cv. Bob White), containing constitutive (*ubi:AVP1*) and stress-inducible (*rab17:AVP1*) *AVP1* expression, were characterised under control and saline conditions. When grown in control and saline hydroponics conditions, however, no phenotypic differences were observed between the *ubi:AVP1* or *rab17:AVP1* transgenic lines and the null segregants. These findings suggest that, either *AVP1* expression does not have a beneficial impact on growth and salt tolerance in bread wheat, or that the promoters and/or experimental methodologies used to characterise these lines were not suitable.

The third focus of this project was to identify native wheat  $H^+$ -PPase (*TaVP*) genes, and to investigate the role of these genes *in vitro* and *in planta*. Using the NRGene wheat reference genome assembly, 15 *TaVP* genes were identified and were shown to vary in gene sequence and expression. Expression patterns differed greatly between genes, tissue types, developmental stages and wheat varieties, which will be useful for the development of genetic markers for breeding purposes. To characterise the role of these genes, *TaVP* homologs from the B genome were expressed in a salt-sensitive mutant yeast strain. Analysis of *TaVP* expressing yeast suggested that *TaVP2-B* and *TaVP4-B* may be more beneficial for improving salt tolerance. Transgenic wheat lines (cv. Fielder) constitutively expressing the *TaVP1-B* and *TaVP2-B* genes were generated and phenotyped in soil under control and saline conditions. The transgenic wheat lines had significantly reduced plant biomass at maturity, decreased time to flowering, and increased leaf  $Na^+$  and  $Cl^-$  accumulation. These results indicate that *TaVP1-B* and *TaVP2-B* influence ion accumulation, plant development and floral transition when constitutively expressed in bread wheat.

Overall, the findings of this research project suggest that wheat *TaVP* genes are likely to have diverse roles in regulating plant growth and salt tolerance, and variation amongst these genes could potentially be utilised to enhance the growth and stress tolerance of bread wheat through selective breeding and gene editing in the future.

## Declaration

I certify that this work contains no material which has been accepted for the award of any other degree or diploma in my name, in any university or other tertiary institution and, to the best of my knowledge and belief, contains no material previously published or written by another person, except where due reference has been made in the text. In addition, I certify that no part of this work will, in the future, be used in a submission in my name, for any other degree or diploma in any university or other tertiary institution without the prior approval of the University of Adelaide and where applicable, any partner institution responsible for the joint-award of this degree.

I acknowledge that copyright of published works contained within this thesis resides with the copyright holder(s) of those works.

I also give permission for the digital version of my thesis to be made available on the web, via the University's digital research repository, the Library Search and also through web search engines, unless permission has been granted by the University to restrict access for a period of time.

I acknowledge the support I have received for my research through the provision of an Australian Government Research Training Program Scholarship.

...

Daniel J. Menadue

8/6/2018

Date



## List of Publications

Menadue DJ, Riboni M, Baumann U, Schilling RK, Plett DC and Roy SJ. Proton-pumping pyrophosphatase ( $H^+$ -PPase) homeolog expression is a dynamic trait in bread wheat (*Triticum aestivum*). **Submitted for publication**

Menadue DJ, Riboni M, Baumann U, Schilling RK, Plett DC and Roy SJ. **2018**. "Identification and characterisation of proton-pumping pyrophosphatase genes in bread wheat (*Triticum aestivum*)" In. Grains Research Update, Strategic Steps - Enduring Profit, GRDC, Adelaide Convention Centre, pp. 137-140

## List of Conference Presentations

Menadue DJ, Riboni M, Baumann U, Schilling RK, Plett DC and Roy SJ. **20<sup>th</sup> February 2018**. "*Identification and characterisation of proton-pumping pyrophosphatase genes in bread wheat (Triticum aestivum)*" Oral presentation at the GRDC Grains Research Update, Adelaide Convention Centre, Adelaide, Australia

Menadue DJ, Riboni M, Baumann U, Schilling RK, Plett DC, Berger, B. and Roy SJ. **5<sup>th</sup> October 2017**. "*Can  $H^+$ -PPase genes improve the growth and yield of wheat (Triticum aestivum)?*" Poster presentation at Combio, Adelaide Convention Centre, Adelaide, Australia

Menadue DJ, Schilling RK, Plett DC and Roy SJ. **30<sup>th</sup> - 31<sup>st</sup> May 2016**. "*Characterising  $H^+$ -PPase genes to improve the growth and yield of wheat (Triticum aestivum)*" Poster presentation at the Gordon Research Conference on Salt and Water Stress in Plants, Les Diablerets Conference Centre, Les Diablerets, Switzerland

Menadue DJ, Schilling RK, Plett DC and Roy SJ. **29<sup>th</sup> May 2016**. "*Characterising  $H^+$ -PPase genes to improve the growth and yield of wheat (Triticum aestivum)*" Poster presentation at the Gordon Research Seminar on Salt and Water Stress in Plants, Les Diablerets Conference Centre, Les Diablerets, Switzerland

## List of Awards

**Australian Plant Phenomics Facility (APPF) - Postgraduate Internship Award, 2017**

*Awarded based on academic record, research experience and the proposed research topic, allowing the successful applicant to undertake a collaborative project with the APPF team*

**Plant Nutrition Trust - Travel Award, 2016**

*Awarded to promising students and early-career scientists working in the area of plant mineral nutrition to attend a conference or conduct a study-tour*

## Acknowledgments

Firstly, I would like to express my gratitude to my PhD supervisors, Associate Prof. Stuart Roy, Dr. Darren Plett and Dr. Rhiannon Schilling. Thank you for your continued support, encouragement, guidance and advice throughout my PhD. I have greatly enjoyed the opportunity to work with you all. Thanks also to my APPF Internship supervisor, Dr. Bettina Berger and my independent advisor Dr. Trevor Garnett, your advice and input into my research project has been greatly appreciated.

I would like to acknowledge the financial contributions made towards this project through a Grains Industry Research Scholarship from the Grains Research and Development Corporation (GRDC) and the C J Everard Scholarship from the University of Adelaide. Thank you to the Australian Plant Phenomics Facility for providing me with the opportunity to work with The Plant Accelerator team through a Postgraduate Internship Award, and to the Plant Nutrition Trust for supporting my attendance at the 2016 Gordon Research Seminar and Conference in Switzerland.

I have received endless assistance and support from countless people throughout my PhD and I would like to thank everyone in the School of Agriculture, Food and Wine that has supported me. Thank you to all past and present members of the Salt Focus Group, Ms. Melissa Pickering, Ms. Jodie Kretschmer, Dr. Matteo Riboni, Ms. Emily Thoday-Kennedy, Mr. William Heaslip, Dr. Yogendra Kalenahalli, Dr. Allison Pearson, Ms. Christine Tritterman, Ms. Laura Short, Ms. Chana Borjigin, Dr. Gordon Wellman and Dr. Ahsan Asif. Thank you for your technical advice, support and friendship.

Thanks also to the team at The Plant Accelerator, particularly Dr. Chris Brien, Dr. Nathaniel Jewell, Ms. Lidia Mischis, Ms. Nicole Bond, Ms. Fiona Groskreutz and Mr. Nicholas Sitlington Hansen for assisting me during my internship, your help was invaluable. I would also like to acknowledge Prof. Ute Roessner and Dr. Siria Natera at The University of Melbourne would carried out the metabolite extraction and analysis.

And finally, to my friends and family, thank you for all of your encouragement, support and patience, I couldn't have done it without you.

## Chapter 1 - Literature review and research aims

## Literature review

### Current constraints to Australian wheat production

In Australia, approximately 220 M ha of agricultural land is used for the production of bread wheat (*Triticum aestivum*) (ABARES, 2018). From this area of land, it is predicted that in excess of 35 M tonnes of wheat will be produced in 2018 (ABARES, 2018). Despite having high annual production compared to other countries, the average Australian wheat yield in 2017 was 2.7 t/ha, which is considerably lower than the United States of America (3.5 t/ha), the European Union (5.4 t/ha) and New Zealand (8 t/ha) (ABARES, 2017). The relatively low average yields in Australia are largely influenced by abiotic stress conditions, such low water availability, high temperatures, low nutrient availability and high soil salinity (Hochman et al., 2017). Salinity is estimated to affect 69 % of the Australian wheat belt (Rengasamy, 2006) and can reduce wheat yields by 35 % at an  $EC_e$  of 6 dS/m, and 50 % at an  $EC_e$  of 12 dS/m (El-Hendawy et al., 2017). As a result of global climate change, the prevalence of abiotic stress conditions is predicted to increase (Cubasch et al., 2001), imposing further constraints on wheat production in Australia. To prevent the substantial yield losses that occur as a result of abiotic stress conditions, and to increase average yields across Australia, high-yielding, stress tolerant bread wheat cultivars are required. The development of such cultivars can be aided through identifying genes that have a beneficial impact on the growth and yield of bread wheat under abiotic stress conditions, without imposing a yield penalty under non-stressed conditions (Gilliham et al., 2017; Roy et al., 2014). A prime candidate for such research is the vacuolar proton-pumping pyrophosphatase ( $H^+$ -PPase), which has been shown to enhance plant growth under control and various abiotic stress conditions (Gaxiola et al., 2016; Gaxiola et al., 2012; Khadilkar et al.,

2016; Schilling et al., 2017). Despite considerable research in other plant species, little is known about the potential of these genes to improve growth and stress tolerance in bread wheat.

### **Vacuolar proton-pumping pyrophosphatases**

Vacuolar proton-pumping pyrophosphatases ( $H^+$ -PPase, EC 3.6.1.1) are membrane bound proteins, which hydrolyse the phosphoanhydride bond in inorganic pyrophosphate ( $PP_i$ ), producing two orthophosphate ( $P_i$ ) ions and free energy (Baltscheffsky, 1967). The energy produced from this reaction can be utilised in a vast range of cellular processes, including generating an electrochemical potential difference for protons ( $H^+$ ) across cellular membranes (Baltscheffsky, 1967; Kim et al., 1994).  $H^+$ -PPases are single-subunit proteins with a molecular weight of approximately 80 kDa and contain 14-17 transmembrane domains (Drozdowicz and Rea, 2001). Protein crystallisation and X-ray analysis of a mung bean (*Vigna radiata*) type I  $H^+$ -PPase (VHP1), revealed six of these transmembrane domains form an inner complex, which contains one  $PP_i$  and five magnesium ( $Mg^{2+}$ ) binding sites, with the remaining transmembrane domains forming an outer wall, likely to be responsible for maintaining the structural integrity of the protein (Lin et al., 2012).

Based on enzymatic requirements,  $H^+$ -PPases can be classified into two distinct types; type I  $H^+$ -PPases, for which potassium ( $K^+$ ) and  $Mg^{2+}$  are essential cofactors, and type II enzymes, which do not require  $K^+$  but are sensitive to cytosolic calcium ( $Ca^{2+}$ ) concentrations (Leigh et al., 1992; Maeshima, 1991). Type I  $H^+$ -PPases have been shown to localise to both the tonoplast and the plasma membrane (Langhans et al., 2001; Segami et al., 2014), while type II  $H^+$ -PPases localise to the membrane of the Golgi apparatus (Mitsuda et al., 2001; Segami et al., 2010). Of these two types, it is believed that type I  $H^+$ -PPases are more common than type II  $H^+$ -PPases. In cell-

suspension cultures of *Arabidopsis* (*Arabidopsis thaliana*) seedlings, the type II H<sup>+</sup>-PPase, AVP2, has a protein abundance < 0.3 % that of the type I H<sup>+</sup>-PPase, AVP1 (Drozdowicz et al., 2000). Overall, sequence similarity among type I H<sup>+</sup>-PPases is > 85 % at the amino acid level, while similarity between type I and type II H<sup>+</sup>-PPase proteins is < 38 % (Drozdowicz et al., 2000).

Due to differences in enzyme activity, cellular localisation and protein abundance, the vast majority of research involving H<sup>+</sup>-PPases has focused on type I proteins, with the *Arabidopsis* type I H<sup>+</sup>-PPase, AVP1, being the most thoroughly characterised. As a result of extensive research, several mechanisms have been proposed regarding the function of AVP1, and it is likely that each mechanism is important at different growth stages, in certain cell-types and under different growth conditions (Schilling et al., 2017; Segami et al., 2018).

## **Proposed mechanisms regarding the role of type I H<sup>+</sup>-PPases**

### **Facilitating ion sequestration**

H<sup>+</sup>-PPase proteins have long been considered to have a significant role in vacuolar ion sequestration, due to their function in vacuole acidification (Kim et al., 1994). Ion sequestration is an important mechanism that prevents the accumulation of toxic ions, such as Na<sup>+</sup>, within the cytosol, which can inhibit cytosolic processes and thus disrupt cellular function and plant growth (Munns and Tester, 2008). This process requires ion transport proteins, such as Na<sup>+</sup>/H<sup>+</sup> transporters, the function of which are dependent on an electrochemical potential difference for H<sup>+</sup> across the tonoplast (Pope and Leigh, 1987). Therefore, H<sup>+</sup>-PPases have the ability to enhance vacuolar ion sequestration by generating a proton gradient between the vacuole and cytosol, thereby enhancing the activity of tonoplast ion transport proteins and reducing the accumulation of toxic ions within the cytosol (Nass et al., 1997).

When expressed in a highly salt sensitive mutant yeast strain (*nhx1::HIS3ena1::HIS3*), which lacks the ability to transport Na<sup>+</sup> out of the cytosol due to mutations within the Sodium Proton Antiporter 1 (NHA1) and Exclusion of Sodium via ATPase 1 (ENA1) plasma membrane Na<sup>+</sup> transporters, expression of H<sup>+</sup>-PPase genes restored growth and significantly enhanced intracellular Na<sup>+</sup> concentrations under saline conditions compared to mutants without H<sup>+</sup>-PPase expression (Brini et al., 2005; Gao et al., 2006; Gaxiola et al., 1999). In further support of this function, constitutive expression of H<sup>+</sup>-PPase genes has significantly enhanced plant growth under saline conditions compared to wild-type in a variety of plant species, including alfalfa (*Medicago sativa*) (Bao et al., 2009), Arabidopsis (Gaxiola et al., 2001; Lv et al., 2015; Wei et al., 2012), barley (*Hordeum vulgare*) (Schilling et al., 2014), cotton (*Gossypium hirsutum*) (Cheng et al., 2018; Pasapula et al., 2011; Shen et al., 2015), creeping bentgrass (*Agrostis stolonifera*) (Li et al., 2010), *Lotus corniculatus* (Bao et al., 2014), peanut (*Arachis hypogaea*) (Qin et al., 2013), poplar (*Populus trichocarpa*) (Yang et al., 2015), rice (*Oryza sativa*) (Kim et al., 2013; Zhao et al., 2006), sugar-beet (*Beta vulgaris*) (Wu et al., 2015), sugarcane (*Saccharum officinarum*) (Kumar et al., 2014), tobacco (*Nicotiana tabacum*) (Gao et al., 2006), tomato (*Lycopersicon esculentum*) (Dong et al., 2011) and wheat (Brini et al., 2007; Lv et al., 2015).

Despite enhancing growth under salt treatment, conflicting results have been reported regarding the accumulation of ions within transgenic H<sup>+</sup>-PPase expressing plants. While leaf Na<sup>+</sup> concentrations increased in salt treated transgenic alfalfa (Bao et al., 2009), Arabidopsis (Gaxiola et al., 2001; Wei et al., 2012), cotton (Cheng et al., 2018), creeping bentgrass (Li et al., 2010), *Lotus corniculatus* (Bao et al., 2014), rice (Kim et al., 2013; Zhao et al., 2006), sugar-beet (Wu et al., 2015), tobacco (Gao et al., 2006), tomato (Dong et al., 2011) and wheat (Brini et al., 2007), leaf Na<sup>+</sup> concentrations remained unaltered in salt treated transgenic Arabidopsis (Lv et al., 2015), barley (Schilling et al., 2014), wheat (Lv et al., 2015) and poplar (Yang et al., 2015)

compared to wild-type. In addition, several studies reporting improved biomass in H<sup>+</sup>-PPase expressing transgenic plants under saline conditions have not included data related to ion accumulation (Kumar et al., 2014; Pasapula et al., 2011; Qin et al., 2013; Shen et al., 2015), thus the impact of H<sup>+</sup>-PPase expression on Na<sup>+</sup> accumulation within these lines remains unknown. With the ability to maintain growth under saline conditions influenced by many factors in addition to ion sequestration, as well as conflicting evidence regarding ion accumulation in H<sup>+</sup>-PPase expressing transgenic plants, the role of H<sup>+</sup>-PPases in facilitating this process in plants remains unclear.

### **Promoting auxin transportation**

Characterisation of constitutively over-expressing *AVP1* Arabidopsis (*AVP1OX*) and *AVP1* knockout (*avp1-1*) mutants, identified a potential role of AVP1 in promoting auxin transportation (Li et al., 2005). In *AVP1OX* Arabidopsis, leaf size increased 40-60 % compared to wild-type and showed significantly enhanced root growth, while in the *avp1-1* mutants root and shoot development were severely disrupted (Li et al., 2005). Further characterisation revealed that vacuolar and cytoplasmic pH remained unaltered between *avp1-1* mutants, *AVP1OX* lines and wild-type. In addition, *avp1-1* mutants had significantly reduced plasma membrane proton-pumping adenosine triphosphatase (H<sup>+</sup>-ATPase) activity, reduced abundance of the auxin efflux protein, Pinformed 1 (PIN1), and lowered root auxin levels compared to wild-type (Li et al., 2005). Based on these results it was proposed that, in Arabidopsis, AVP1 enhances polar auxin transport through increasing abundance of the H<sup>+</sup>-ATPase and auxin efflux proteins on the plasma membrane, thus promoting auxin-dependent plant development (Li et al., 2005) (Figure 1).



This hypothesis was further investigated in the Arabidopsis *AVP1* loss-of-function mutants, *fugu5* and *vhp1-1*. Due to t-DNA insertions within the *AVP1* coding sequence, these mutants either lacked the ability, or had a reduced capacity, to hydrolyse PP<sub>i</sub> (Ferjani et al., 2011). In these lines, expression of a synthetic auxin response reporter gene (*DR5:GUS*) revealed no differences in *DR5:GUS* distribution compared to wild-type, suggesting auxin abundance was not altered in these lines (Ferjani et al., 2011). While seedling growth in the *fugu5* and *vhp1-1* mutants was reduced in a similar manner to the *avp1-1* mutants, none of the other developmental defects reported in the *avp1-1* mutants were observed in these lines. Based on these results it was concluded that the lack of heterotrophic growth (growth prior to photosynthesis) in the *fugu5* and *vhp1-1* mutants was unlikely to be the result of disrupted auxin distribution, and that the *avp1-1* phenotype was likely to be allele specific (Ferjani et al., 2011).

Further characterisation of the *avp1-1* mutants developed by Li et al., (2005) identified a second t-DNA insertion within the *GNOM* gene, which encodes a GDP/GTP exchange factor involved in polar auxin transport, and is genetically linked to the *AVP1* gene (Kriegel et al., 2015). Comparison of the *avp1* and *fugu5* mutants with *emb30-1 (gnom)*, an ethyl methanesulfonate (EMS) mutagenized line lacking GNOM function (Mayer et al., 1991), revealed free auxin levels and root auxin transport in 6 d-old *fugu5* seedlings were similar to wild-type, while in the *avp1-1* seedlings free auxin levels were higher, and root auxin transport lower, compared to wild-type (Kriegel et al., 2015). In addition, *avp1-1* seedlings also displayed a growth phenotype similar to the *gnom* mutants, while the *fugu5* seedlings did not. This study provided further evidence that the *avp1-1* phenotype was unlikely to be solely due to the lack of AVP1 function (Ferjani et al., 2011; Geldner et al., 2004; Kriegel et al., 2015). However, several studies have reported increased abundance and transport of auxin in constitutively expressing *AVP1* plants

(Gonzalez et al., 2010; Li et al., 2010; Pei et al., 2012; Yang et al., 2014), suggesting that AVP1 may still have an impact on auxin transport.

NOTE: This image has been removed according to the author's instructions.

**Figure 1: Proposed role of AVP1 in promoting auxin transport.** It has been proposed that AVP1 regulates auxin transport by mediating trafficking of the PM H<sup>+</sup>-ATPase (P-H<sup>+</sup> ATPase) and the auxin efflux protein, PIN1, to the plasma membrane. Increased abundance of H<sup>+</sup>-ATPase on the plasma membrane of *AVP1* over-expressing (*AVP1OX*) plants was proposed to alter apoplastic pH, enhancing auxin-mediated plant development as a result of increased transport of deprotonated auxin (IAA<sup>-</sup>) via PIN1. In *AVP1* knockout (*avp1-1*) plants, it was proposed that trafficking of H<sup>+</sup>-ATPase and PIN1 to the plasma membrane was reduced compared to wild-type, resulting in reduced auxin transport and, consequently, stunted growth. Further research, however, has shown a second t-DNA insertion present in these mutants is likely to be responsible for this phenotype (Kriegel et al. 2015). Figure from Li et al., 2005.

## Regulating cytosolic PP<sub>i</sub> concentrations

Another proposed role of H<sup>+</sup>-PPases is the regulation of cytosolic PP<sub>i</sub>. Analysis of *fugu5* mutant Arabidopsis seedlings, with reduced (*fugu5-1* and *fugu5-2*) or abolished (*fugu5-3*) AVP1 activity due to mutations within the *AVP1* gene, were unable to support seedling growth prior to the establishment of photosynthesis (heterotrophic growth) on Murashige and Skoog (MS) basal media (Ferjani et al., 2011). Biochemical analysis revealed 3 d-old *fugu5* seedlings contained 2.5-fold higher PP<sub>i</sub> and 50 % less sucrose than wild-type (Ferjani et al., 2011). Through the addition of sucrose to the growth media, or through expression of a soluble yeast pyrophosphatase gene with the ability to hydrolyse PP<sub>i</sub> but not translocate H<sup>+</sup>, seedling growth was restored to the *fugu5* mutants (Ferjani et al., 2011). Prior to the establishment of photosynthesis, seedlings require sucrose to support growth (Penfield et al., 2005), which is synthesised via gluconeogenesis, a cytosolic pathway that is inhibited by high concentrations of PP<sub>i</sub> (Kubota and Ashihara, 1990). Based on this knowledge, and the observed *fugu5* growth phenotypes, it was proposed that the lack of heterotrophic growth in the *fugu5* mutants was likely due to cytosolic PP<sub>i</sub> accumulation and, consequently, inhibition of the gluconeogenesis pathway (Figure 2) (Ferjani et al., 2011). It remains unclear, however, whether enhanced H<sup>+</sup>-PPase activity, and therefore increased activity of PP<sub>i</sub> dependent pathways, is responsible for the improved growth of H<sup>+</sup>-PPase over-expressing plants.

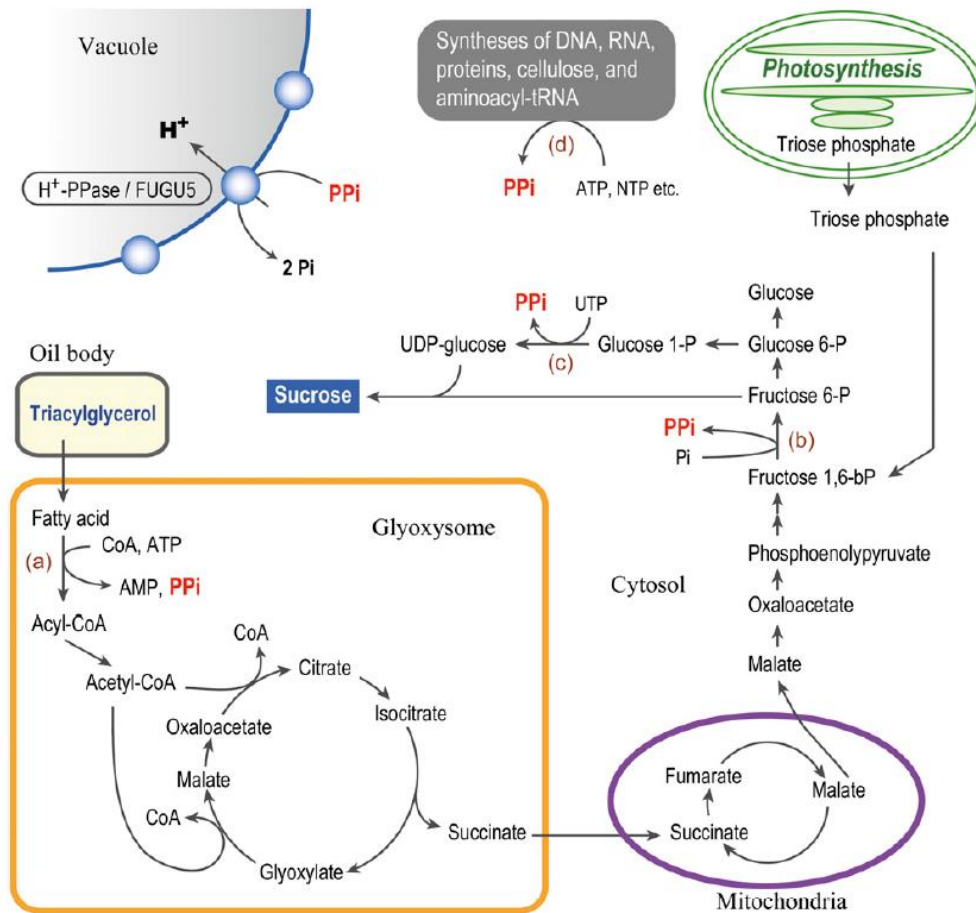


**Figure 2: Proposed role of AVP1 in regulating cytosolic PP<sub>i</sub> levels.** Pyrophosphate (PP<sub>i</sub>) is produced as a by-product of many cellular processes, such as the (d) synthesis of DNA, RNA, proteins, cellulose and aminoacyl-tRNA, as well as the (a) breakdown of triacylglycerols. During sucrose synthesis via gluconeogenesis, PP<sub>i</sub> is produced from the conversion of (b) fructose 1,6-bisphosphate → fructose 6-phosphate, and (c) glucose 1-phosphate → UDP-glucose. The PP<sub>i</sub> produced by these processes accumulates within the cytosol, high levels of which can inhibit gluconeogenesis. It is proposed that, through hydrolysing cytosolic PP<sub>i</sub>, AVP1 (H<sup>+</sup>-PPase) promotes sucrose production via gluconeogenesis and prevents cytosolic PP<sub>i</sub> accumulation. Enhanced AVP1 abundance, and therefore increased sucrose supply, is proposed to contribute to the beneficial phenotypes of AVP1 expressing transgenic plants. Figure from Ferjani et al., 2011.

## Sucrose phloem loading

AVP1 has also been proposed to function in sucrose phloem loading (Gaxiola et al., 2012). Due to phenotypic similarity of *AVP1* expressing transgenic plants to those with increased sugar supply (Hammond and White, 2011), in addition to endogenous H<sup>+</sup>-PPase proteins localising to the plasma membrane in several plant species (Langhans et al., 2001; Paez-Valencia et al., 2011; Regmi et al., 2016), it has been proposed that H<sup>+</sup>-PPases can also function in the synthesis of PP<sub>i</sub> (Gaxiola et al., 2012). This proposed mechanism suggests that, in phloem companion cells, AVP1 functions in the synthesis of PP<sub>i</sub>, thereby increasing the rate of sucrose respiration (Gaxiola et al., 2012). ATP, generated as a result of sucrose respiration, is then utilised by PM H<sup>+</sup>-ATPases to enhance the electrochemical potential difference for H<sup>+</sup> across the plasma membrane, facilitating sucrose phloem loading, and increasing source to sink transportation (Gaxiola et al., 2012) (Figure 3).

In support of this proposed mechanism, the ability of H<sup>+</sup>-PPases to function in both PP<sub>i</sub> hydrolysis and synthesis has been demonstrated in maize (*Zea mays*) (Rocha Facanha and de Meis, 1998) and the bacteria, *Rhodospirillum rubrum* (Baltscheffsky et al., 1966; Seufferheld et al., 2004). This proposed mechanism has been further investigated using autoradiography, to analyse carbon partitioning in *AVP1OX* Arabidopsis lines (Pizzio et al., 2015). When photosynthetically labelled with <sup>14</sup>CO<sub>2</sub>, accumulation of <sup>14</sup>C within *AVP1OX* leaf tissue increased 2-fold compared to wild-type, and had 40-89 % greater root H<sup>+</sup> extrusion (Pizzio et al., 2015). These results, as well as observed increases in shoot biomass, rhizosphere acidification and expression of sugar-induced ion transporters, suggested the *AVP1OX* lines had a greater ability to metabolise and transport reduced carbon compared to wild-type Arabidopsis (Pizzio et al., 2015). In support of this, genes encoding sucrose transporters have been shown to be

upregulated in the shoot and root of H<sup>+</sup>-PPase expressing transgenic Arabidopsis (Lv et al., 2015) and in sweet potato root tissue (*Ipomoea batatas*) (Fan et al., 2017). In the developing fruit of wild-type apple (*Malus domestica*), expression of the *MdVHP1* gene, encoding an apple H<sup>+</sup>-PPase, is co-ordinately upregulated with *MdSUT1*, a sucrose transporter gene (Yao et al., 2011).

When transgenic Arabidopsis with constitutive expression of *AVP1* was transformed with the *pCoYMV::RNAiAVP1* cassette, resulting in phloem-specific silencing of *AVP1*, growth was severely stunted (Pizzio et al., 2015). In comparison, only a small growth reduction was observed in Arabidopsis mutants (*avp1-2*) lacking *AVP1* at the tonoplast compared to wild-type (Pizzio et al., 2015). When *AVP1* is over-expressed specifically within phloem companion cells, transgenic Arabidopsis (*CoYMVpro:AVP1*) displayed near identical phenotypic characteristics to constitutively expressing *AVP1* Arabidopsis lines (*35S:AVP1*) (Khadilkar et al., 2016), providing further support for the importance of *AVP1* expression in phloem cells. While protein modelling has identified residues with the potential to regulate *AVP1* function, as well as the directionality of H<sup>+</sup> fluxes (Pizzio et al., 2017), the ability of plant H<sup>+</sup>-PPases to function in PP<sub>i</sub> synthesis is yet to be demonstrated *in planta*.

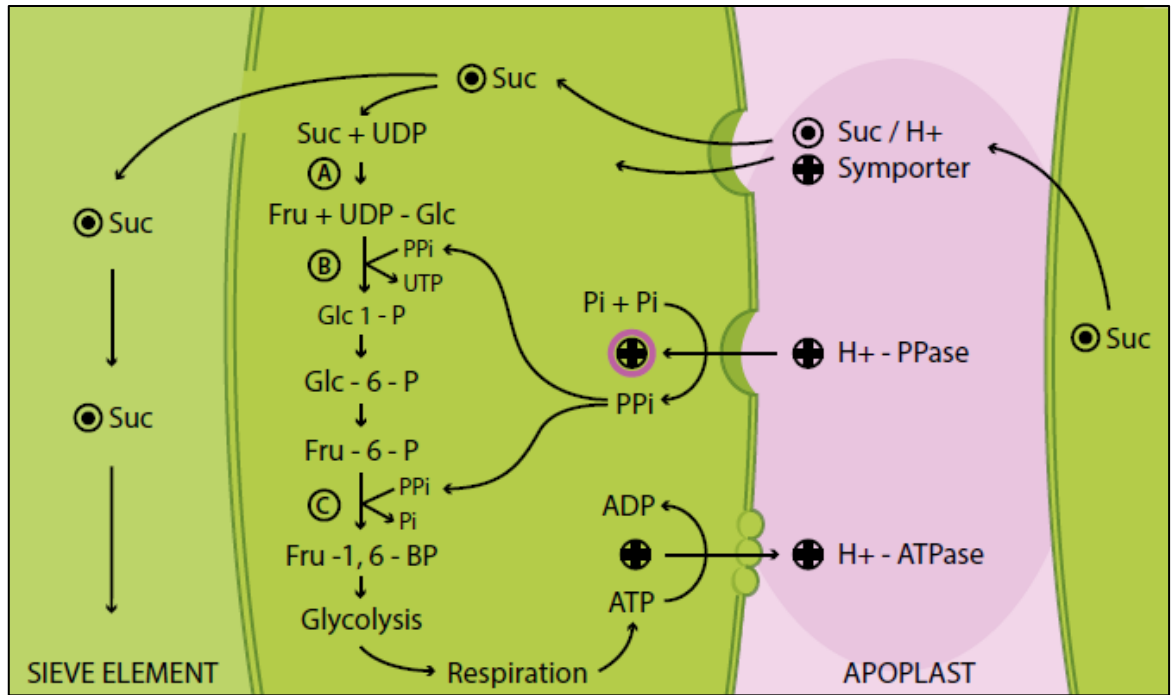


**Figure 3: Proposed role of AVP1 in sucrose phloem loading.** It has been suggested that, when localised to the plasma membrane of phloem companion cells,  $H^+$ -PPases function in  $PP_i$  synthesis, producing the  $PP_i$  required for sucrose respiration (A-C). ATP, generated as a product of this pathway, is utilised by the plasma membrane  $H^+$ -ATPase to generate an electrochemical potential difference for protons ( $\oplus$ ) across the plasma membrane, enhancing activity of sucrose-proton (Suc/ $H^+$ ) symporters ( $\odot$ ). Increased transport of sucrose, from source to sink tissues via sieve element cells, is proposed to promote growth and stress tolerance in transgenic plants over-expressing  $H^+$ -PPase genes. Figure from Gaxiola et al., 2016.

## Promoting ascorbic acid biosynthesis

Experimental evidence from transgenic barley constitutively expressing *AVP1* (*35S:AVP1*), has also implicated AVP1 in ascorbic acid synthesis via the Smirnoff-Wheeler pathway (Schilling, 2014). In plant cells, ascorbic acid (vitamin C) acts as an antioxidant, an enzyme cofactor and an electron donor (Smirnoff, 1996) and contributes to many cellular processes, including the detoxification of reactive oxygen species (Foyer et al., 1995), promotion of cell wall expansion (Horemans et al., 1994), and the regulation of cell division and expansion (Conklin, 2001). Ascorbic acid has been demonstrated to have a beneficial impact on plant development and improve tolerance to salinity (Hemavathi et al., 2010; Lisko et al., 2013), mannitol treatment (Hemavathi et al., 2010), temperature stress (Lisko et al., 2013; Stevens et al., 2008), water limitation (Eltayeb et al., 2011) and iron deficiency (Ramírez et al., 2013), conditions in which constitutive expression of H<sup>+</sup>-PPase genes have also been shown to enhance growth (Table 1). In plants, there are four known pathways by which ascorbic acid is synthesised, one of which is the Smirnoff-Wheeler pathway (Wheeler et al., 1998).

Metabolomics analysis of leaf tissue from *35S:AVP1* expressing transgenic barley, revealed a 60-80 % reduction in galactose, a key metabolite within in the Smirnoff-Wheeler pathway (Schilling, 2014). The transgenic lines also had significantly increased ascorbic acid (1.9- to 3.8-fold) and dehydroascorbic acid (13.1- to 15.0-fold) within the leaf, compared to null segregants (Schilling, 2014). Ascorbic acid synthesis via the Smirnoff-Wheeler pathway occurs predominantly within the cytosol, and produces PP<sub>i</sub> as a by-product during the conversion of mannose 1-phosphate to GDP-mannose (Smirnoff, 2000). It has been proposed that an increased rate of cytosolic PP<sub>i</sub> hydrolysis in the *35S:AVP1* transgenic barley, through the function of AVP1, enhanced ascorbic acid synthesis via the Smirnoff-Wheeler pathway,



resulting in enhanced seedling growth, larger biomass, a 10 % increase in cell number and improved stress tolerance (Schilling, 2014). Enhanced production of ascorbic acid would also provide an explanation for the increase in mesophyll cell size and number, and enhanced root and shoot development reported in *AVP1* over-expressing Arabidopsis lines (Gonzalez et al., 2010; Li et al., 2005).

In further support of this proposed function, fruit specific expression of a soluble yeast pyrophosphatase gene (*ppa*) reduced concentrations of  $PP_i$  and galactose, and increased ascorbic acid and dehydroascorbic acid content within the fruit of transgenic tomato, compared to wild-type (Osorio et al., 2013). To date, few studies have investigated metabolic changes in relation to *AVP1* expression, with only one study measuring concentrations of ascorbic acid. In the leaf of *AVP1-1* over-expressing Arabidopsis, ascorbic acid content was reported to increase by 30 % at the end of day compared to wild-type, while at midday ascorbic acid was 120 % lower than wild-type (Gonzalez et al., 2010). The only other metabolite within the Smirnoff-Wheeler pathway to be measured in this study was dehydroascorbic acid, the concentration of which remained unaltered in the *AVP1-1* seedlings compared to wild-type (Gonzalez et al., 2010). With no other metabolites within this pathway were measured and only one independent *AVP1* expressing line analysed in this study, limited conclusions can be made in regard to the role of *AVP1* expression on ascorbic acid production in the *AVP1* over-expressing lines.

To further elucidate the impact of *AVP1* expression on ascorbic acid synthesis, metabolomics analysis of both *AVP1* over-expressing and *AVP1* knockout Arabidopsis lines, such as the *fugu5* mutants, is required. Furthermore, experiments should also investigate the other proposed

roles of AVP1 by analysing alterations in the concentration of all metabolites in response to AVP1 function.

## Phenotypes of transgenic plants constitutively expressing H<sup>+</sup>-PPase genes

### Enhanced biomass and yield in non-stressed conditions

Constitutive expression of H<sup>+</sup>-PPase genes, such as the Arabidopsis *AVP1* gene, has been shown to enhance biomass, growth rate and yield both in the presence and absence of abiotic stress conditions (Table 1). Under non-stressed conditions, biomass increased up to 50 % in H<sup>+</sup>-PPase expressing transgenic Arabidopsis seedlings (Gonzalez et al., 2010; Vercruyssen et al., 2011), 33 % in mature field-grown barley (Schilling et al., 2014), 30 % in mature creeping bentgrass (Li et al., 2010), 40 % in mature lettuce (*Lactuca sativa*) (Paez-Valencia et al., 2013), 21 % in 2 week old sweet potato (Fan et al., 2017), 24 % in mature cotton (Lv et al., 2015), 35 % in 4 week old *Lotus corniculatus* (Bao et al., 2014) and 30 % in 3 week old sugar-beet (Wu et al., 2015) compared to wild-type. Growth rates under non-stressed conditions were also enhanced in transgenic Arabidopsis (Figure 4A) (Gonzalez et al., 2010), barley (Figure 4B) (Schilling, 2014), *Lotus corniculatus* (Bao et al., 2014) and potato (*Solanum tuberosum*) (Wang et al., 2014) in comparison to wild-type/null segregants. Many transgenic plants expressing H<sup>+</sup>-PPase genes have also been reported to produce significantly higher yield than wild-type plants, with increases of up to 20 % in Arabidopsis (Pizzio et al., 2015), 34 % in barley (Schilling et al., 2014), 36 % in cotton (Lv et al., 2009; Pasapula et al., 2011), and 50 % in lettuce (Paez-Valencia et al., 2013), while transgenic tomato produced a greater proportion of ripe fruit compared to wild-type (Yang et al., 2007; Yang et al., 2014).

The growth and yield improvements reported in transgenic plants expressing H<sup>+</sup>-PPases under non-stressed conditions have been attributed to many of the proposed roles of H<sup>+</sup>-PPases, and it is possible that many of these functions contribute to the beneficial phenotypes observed in these plants. In addition to improving growth under non-stressed conditions, constitutive expression of H<sup>+</sup>-PPase genes also enhances growth under various abiotic stress conditions, including high salinity, low water availability and low nutrient availability.

### **Improved growth and yield in saline conditions**

Initially, H<sup>+</sup>-PPases were considered to function solely in the acidification of the vacuole (Kim et al., 1994) and as such, considerable research has focused on utilising H<sup>+</sup>-PPase genes to enhance the salinity tolerance of plants. The first study to demonstrate the ability of constitutive *AVP1* expression to improve salt tolerance was in transgenic *Arabidopsis*, in which the transgenic plants were able to maintain growth under 200 mM NaCl treatment, while the wild-type plants were not (Figure 4C) (Gaxiola et al., 2001). In soil containing 100 mM NaCl, leaf Na<sup>+</sup> was 20-40 % higher in *AVP1* transgenic *Arabidopsis* than wild-type, while the leaf K<sup>+</sup> concentration was 26-39 % greater than wild-type (Gaxiola et al., 2001). Since this initial study, constitutive expression of various H<sup>+</sup>-PPase genes has been shown to enhance plant growth, ion accumulation and yield under saline conditions in many transgenic plants (Table 1). Examples include *AVP1* expressing alfalfa (Bao et al., 2009), bentgrass (Li et al., 2010) and rice (Kim et al., 2013; Zhao et al., 2006); transgenic tomato constitutively expressing the apple *MdVHP1* gene (Dong et al., 2011); transgenic cotton and tobacco expressing the *Thellungiella halophila* *TsVP* gene (Cheng et al., 2018; Gao et al., 2006); transgenic *Arabidopsis* expressing the bread wheat *TVP1* and *Ammopiptanthus mongolicus* *AmVP* genes (Brini et al., 2007; Wei et

al., 2012); as well as transgenic sugar-beet and *Lotus corniculatus* expressing the *Zygophyllum xanthoxylum* *ZxVP1-1* gene (Bao et al., 2014; Wu et al., 2015). In contrast to these studies, transgenic barley constitutively expressing the *Arabidopsis AVP1* (Schilling et al., 2014) and barley *HVP10* (Bovill, unpublished) genes, as well as transgenic *Arabidopsis* and bread wheat expressing the *Salicornia europaea SeVP1* and *SeVP2* genes (Lv et al., 2015), had enhanced growth under saline conditions while leaf ion concentrations remained unaltered (Figure 4D). In salt treated transgenic poplar, constitutively over-expressing the *PtVP1.1* gene, leaf  $\text{Na}^+$  decreased by 20 % under salinity treatment, compared to wild-type, while no difference in root  $\text{Na}^+$  concentrations were observed (Yang et al., 2014). Furthermore, several of the studies in which improved salt tolerance has been reported have not investigated ion accumulation within the  $\text{H}^+$ -PPase transgenic plants (Kumar et al., 2014; Pasapula et al., 2011; Qin et al., 2013; Shen et al., 2015), thus limiting the conclusions that can be made from these studies. These findings suggest that salt tolerance mechanisms vary between plant species, and that when constitutively expressed,  $\text{H}^+$ -PPases may have multiple functions in transgenic plants. While a lack of increased  $\text{Na}^+$  accumulation does not necessarily mean that vacuole sequestration is not improved, it does suggest that the improved salt tolerance of  $\text{H}^+$ -PPase expressing transgenic lines may be influenced by the involvement of  $\text{H}^+$ -PPases in other processes. To elucidate the role of  $\text{H}^+$ -PPases in vacuolar ion sequestration, ion concentrations within specific cell types of transgenic plants expressing  $\text{H}^+$ -PPase genes is required.

### **Improved growth under low water availability**

Constitutive expression of  $\text{H}^+$ -PPase genes has also been shown to enhance growth under low water availability in a variety of plant species (Table 1). After a 10 d water deficit, *AVP1* over-

expressing *Arabidopsis* plants were able to resume normal growth and advance to seed development following re-watering, while wild-type plants did not survive (Gaxiola et al., 2001). As the transgenic plants showed no alteration in stomatal conductance, this phenotype was attributed to an ability to accumulate higher levels of solutes and maintain a higher relative water content (RWC), compared to wild-type (Gaxiola et al., 2001). Similarly, pot-grown transgenic peanut constitutively expressing *AVP1*, had 22-26 % greater root and shoot biomass than wild-type when supplied with 50 % less water than control plants (Qin et al., 2013). In addition, the yield of *AVP1* transgenic peanut was 12 % higher than wild-type in a field with 50 % reduced irrigation. In contrast to *AVP1* over-expressing *Arabidopsis*, the improved drought tolerance of *AVP1* expressing peanut was attributed to enhanced stomatal conductance and increased photosynthetic capacity, enabling growth to be maintained under drought conditions (Qin et al., 2013). Improved drought tolerance has also been reported in alfalfa (Figure 4E) (Bao et al., 2009), cotton (Lv et al., 2009; Shen et al., 2015), *Lotus corniculatus* (Bao et al., 2014), maize (Li et al., 2008), sugarcane (Kumar et al., 2014) and tomato (Figure 4F) (Dong et al., 2011; Park et al., 2005) constitutively expressing  $H^+$ -PPase genes, with biomass, RWC, solute retention and photosynthetic capacity enhanced in these lines, compared to wild-type (Table 1). These plants also displayed an ability to either maintain growth during water deprivation, or to resume normal growth following rewatering (Table 1). The many phenotypes observed in  $H^+$ -PPase expressing transgenic plants in water restricted conditions, provides further evidence that  $H^+$ -PPases influence multiple processes when constitutively expressed.

## Improved growth under low nutrient availability

Another common phenotype of plants constitutively expressing H<sup>+</sup>-PPase genes is enhanced growth under low nutrient availability (Table 1). Constitutive expression of *AVP1* and *AVP1D*, a gain-of-function *AVP1* allele which has enhanced PP<sub>i</sub> hydrolysis and H<sup>+</sup> transport activity due to an amino acid substitution (E229D) (Zhen et al., 1997), significantly enhanced root and shoot biomass under low phosphorus (P) availability in *Arabidopsis*, rice and tomato (Figure 4G) (Yang et al., 2007). Despite all lines having increased biomass in low P conditions compared to sufficient P conditions, an increase in P content was detected only within the root tissue of *AVP1D* transgenic rice, and not in transgenic *Arabidopsis* or rice plants (Yang et al., 2007). Further study showed that P content in the developing fruit of *AVP1D* expressing tomato was significantly increased under low P availability, compared to wild-type (Yang et al., 2014). Immunoblot analysis also revealed increased H<sup>+</sup>-ATPase protein abundance in *AVP1* over-expressing *Arabidopsis* and *AVP1D* expressing transgenic rice (Yang et al., 2007), suggesting the lack of increased P content within the root of *AVP1D* tomato may have been the result of enhanced H<sup>+</sup>-ATPase activity and, therefore, increased transport of P from source to sink tissues (Yang et al., 2014). In a field with low available P, *AVP1D* expressing tomato produced 25 % more ripe fruit than wild-type (Figure 4H) (Yang et al., 2014). Under low P availability, transgenic barley constitutively expressing *AVP1* (Schilling, 2014) and transgenic maize constitutively expressing *TsVP* (Pei et al., 2012) showed greater shoot growth, increased root P uptake, and enhanced rhizosphere acidification compared to wild-type, with root growth also enhanced in the *TsVP* expressing maize lines. Furthermore, yield in *TsVP* expressing transgenic maize was 23-29 % greater than wild-type in soil with low available P (Pei et al., 2012). These results suggest that the enhanced growth of H<sup>+</sup>-PPase expressing transgenic plants is likely to

be the result of enhanced P uptake and transport, although the mechanism behind this remains unclear.

Transgenic plants constitutively expressing H<sup>+</sup>-PPase genes also show improved growth under low nitrogen (N) availability (Table 1). Expression of *AVP1D* in romaine lettuce (*Lactuca sativa*) significantly increased root and shoot biomass and enhanced N uptake under sufficient and low N supply, compared to wild-type (Paez-Valencia et al., 2013). In addition, ATP hydrolysis within the root of *AVP1D* transgenic lettuce was 20 % higher than wild-type, with the transgenic plants showing an increased ability to acidify the rhizosphere under both sufficient and low P supply, compared to wild-type (Paez-Valencia et al., 2013). Enhanced rhizosphere acidification has also been reported in transgenic *Arabidopsis* (Yang et al., 2007), rice (Zhao et al., 2006), tomato (Yang et al., 2014) and barley (Schilling, 2014) constitutively expressing *AVP1*, as well as *IbVP1* over-expressing sweet potato (Fan et al., 2017). Rhizosphere acidification is known to be an important mechanism contributing to nutrient uptake and is dependent on PM H<sup>+</sup>-ATPase activity (Vance et al., 2003). Therefore, upregulated H<sup>+</sup>-ATPase activity could provide an explanation for the increased growth of H<sup>+</sup>-PPase expressing plants, under both P and N limitation, however, the mechanism responsible for this remains unclear.

Growth improvements have also been reported in transgenic plants constitutively expressing H<sup>+</sup>-PPase genes under conditions of low available iron (Fe) and low available potassium (K<sup>+</sup>) (Table 1). Transgenic sweet potato constitutively over-expressing the *IbVP1* gene, displayed 40-50 % higher shoot biomass, 30-55 % increased root biomass and higher concentrations of sucrose, glucose, fructose and antioxidants under low Fe supply, compared to wild-type (Fan et al., 2017). The *IbVP1* expressing transgenic sweet potato plants also had 33-48 % greater K<sup>+</sup> uptake and an increased ability to acidify the rhizosphere compared to wild-type (Fan et al.,

2017). Under low  $K^+$  availability, transgenic bread wheat constitutively expressing the *Elymus dahuricus* *EdVP1* gene displayed a 2-fold increase in root length, root area, root volume and yield, as well as greater root  $H^+$  extrusion and increased  $K^+$  uptake, compared to wild-type (Ruan et al., 2013).

The results of these studies demonstrate that constitutive expression of  $H^+$ -PPase genes influences a wide range of cellular processes, which have the ability to enhance growth and nutrient acquisition under a wide range of conditions. However, the reasons for these phenotypes are yet to be identified. Furthermore, little research has investigated the potential of  $H^+$ -PPase genes to improve the growth and yield of bread wheat. In addition, the majority of research concerning  $H^+$ -PPase genes has focused on using constitutive expression to improve plant growth, and has not addressed the potential of these gene to improve plant growth using stress-inducible promoters, or non-genetic modification (non-GM) approaches, such as identifying beneficial  $H^+$ -PPase alleles for selective breeding or gene editing.



NOTE: This image has been removed according to the author's instructions.

**Figure 4: Phenotypes of transgenic plants constitutively expressing *AVP1* under stressed and non-stressed conditions.** Transgenic *AVP1* expressing plants have shown many beneficial phenotypes. In non-stressed conditions, (A) *AVP1* over-expressing Arabidopsis (*AVP1*) had significantly larger biomass than wild-type (Col-0) (Gonzalez et al., 2010), and (B) *AVP1* expressing transgenic barley (*35S:AVP1*) had improved heterotrophic growth compared to null segregants (nulls) (Schilling, 2014). In saline conditions, growth of (C) *AVP1* over-expressing Arabidopsis (*AVP1-1* and *AVP1-2*) was enhanced compared to wild-type (WT) (Gaxiola et al., 2001), and (D) biomass and yield of field grown *AVP1* expressing barley (*35S:AVP1*) was greatly enhanced compared to wild-type (WT) (Schilling et al., 2014). Under low water availability, growth was improved in (E) *AVP1* expressing alfalfa (L1 & L8) compared to wild-type (WT) (Bao et al., 2009) and in (F) *AVP1D* expressing tomato (*XAVP1D*) compared to vector control plants (Park et al., 2005). Under low available P, *AVP1D* expressing tomato (*AVP1D-1* and *AVP1D-2*) plants displayed significantly higher (G) biomass (Yang et al., 2007) and (H) produced a greater proportion of ripe fruit, compared to wild-type (WT) (Yang et al., 2014).

**Table 1: Summary of phenotypic characteristics of transgenic plants constitutively expressing H<sup>+</sup>-PPase genes.** H<sup>+</sup>-PPase genes from several plant species have been constitutively expressed in transgenic plants, including genes from *Arabidopsis thaliana* (*AVP1* & *AVP1D*), *Ammopiptanthus mongolicus* (*AmVP*), *Elymus dahuricus* (*EdVP1*), *Ipomoea batatas* (*IbVP1*), *Medicago truncatula* (*MtVP1*), *Oryza sativa* (*OVP1*), *Populus trichocarpa* (*PtVP1.1*), *Salicornia europaea* (*SeVP1* & *SeVP2*), *Triticum aestivum* (*TaVP1*), *Thellungiella halophila* (*TsVP*) and *Zygophyllum xanthoxylum* (*ZxVP1-1*). Studies in which these transgenic plants have been phenotyped, in both control and abiotic stress conditions (high salt (NaCl), drought, low nitrogen (N), low phosphorus (P), low iron (Fe), low potassium (K<sup>+</sup>), low temperature and high cadmium (Cd)) are listed alphabetically in order of plant species and transgene name. Following each entry are details regarding the conditions in which the transgenic plants were phenotyped, with the phenotypic information listed next to the relevant treatment. Values for phenotypic characteristics, such as shoot and root biomass (B.), root number (#), leaf and root sodium (Na<sup>+</sup>), potassium (K<sup>+</sup>), calcium (Ca<sup>2+</sup>), chloride (Cl<sup>-</sup>), sucrose (Suc), glucose (Glc), fructose (Fru) and antioxidant (AO) concentrations, photosynthetic rate (Pn), rhizosphere acidification ability (RA), and relative water content (RWC), are shown as an increase (↑) or decrease (↓) relative to wild-type (WT) or null segregant (nulls) lines (dependent on study), with (\*) indicating the H<sup>+</sup>-PPase gene in the corresponding study was co-expressed with a Na<sup>+</sup>/H<sup>+</sup> transporter (*NHX*) gene.

Plant species	Transgene	Experimental treatments	Phenotypes of H <sup>+</sup> -PPase transgenic plants (relative to WT/nulls)	Reference
<i>Alfalfa</i> ( <i>M. sativa</i> )	<b>AVP1*</b> ( <i>A. thaliana</i> )	Control Salt - 100 & 200 mM NaCl Drought - 8 d without water	No change in biomass, Pn, leaf Na <sup>+</sup> or Ca <sup>2+</sup> , 50 % ↑ in leaf K <sup>+</sup> 2.2- to 2.5-fold ↑ shoot B., 30 % ↑ Pn, ↑ Na <sup>+</sup> , ↑ K <sup>+</sup> , ↑ Ca <sup>2+</sup> (leaf & root) ↑ solute retention, ↓ water loss	(Bao et al., 2009)
<i>Arabidopsis</i> ( <i>A. thaliana</i> )	<b>AVP1</b> ( <i>A. thaliana</i> )	Control Salt - 100 mM NaCl Drought - 10 d without water	No control data presented ↑ growth, 20-40 % ↑ Na <sup>+</sup> (leaf), 26-39 % ↑ K <sup>+</sup> (leaf) ↑ growth, ↑ RWC	(Gaxiola et al., 2001)
<i>Arabidopsis</i> ( <i>A. thaliana</i> )	<b>AVP1</b> ( <i>A. thaliana</i> )	Control only	50 % ↑ leaf area & length, 25 % ↑ leaf width, ↑ cell number, ↑ growth rate, ↑ auxin	(Gonzalez et al., 2010)
<i>Arabidopsis</i> ( <i>A. thaliana</i> )	<b>AVP1</b> ( <i>A. thaliana</i> )	Control only	20 % ↑ yield, ↑ starch accumulation and remobilisation	(Pizzio et al., 2015)
<i>Arabidopsis</i> ( <i>A. thaliana</i> )	<b>AVP1</b> ( <i>A. thaliana</i> )	Control only	50 % ↑ shoot B.	(Vercruyssen et al., 2011)
<i>Arabidopsis</i> ( <i>A. thaliana</i> )	<b>AVP1</b> ( <i>A. thaliana</i> )	Control - 1 mM P <sub>i</sub> Low P - 10 μM P <sub>i</sub>	50 % ↑ yield, 62 % ↑ root B., 10 % ↑ shoot B., 22-40 % ↑ P content ↑ RA, 2.5-fold ↑ root #, 1.6-fold ↑ root B., 1.3-fold ↑ shoot B., ↑ K <sup>+</sup> (root)	(Yang et al., 2007)
<i>Arabidopsis</i> ( <i>A. thaliana</i> )	<b>AmVP</b> ( <i>A. Mongolicus</i> )	Control Salt - 200 mM NaCl Drought - 15 d without water	No difference in Na <sup>+</sup> , K <sup>+</sup> or MDA content or RWC compared to control ↑ B. (not quantified), 38-48 % ↑ Na <sup>+</sup> (leaf), no change in K <sup>+</sup> (leaf) ↑ growth maintenance (not quantified), ↑ RWC	(Wei et al., 2012)
<i>Arabidopsis</i> ( <i>A. thaliana</i> )	<b>SeVP1 &amp; SeVP2</b> ( <i>S. europaea</i> )	Control - 30 mM KNO <sub>3</sub> <sup>-</sup> Salt - 150 mM NaCl Low N - 0.1 mM KNO <sub>3</sub> <sup>-</sup> Salt + Low N - levels as above	20 % ↑ K <sup>+</sup> (leaf & root), no change in Na <sup>+</sup> (leaf & root) 20 % ↑ total B., no change in ions, 15 % ↑ N (root) 20 % ↑ total B., no change in ions, 15 % ↑ N (root), 2-fold ↑ Glc 20 % ↑ total B., no change in ions, 2-fold ↑ Glc, 2-fold ↑ Suc (root only)	(Lv et al., 2015)
<i>Arabidopsis</i> ( <i>A. thaliana</i> )	<b>TVP1</b> ( <i>T. aestivum</i> )	Control Salt - 200 mM NaCl	↓ water potential, no difference in total leaf area 20 % ↑ leaf area, 20 % ↑ RWC, 2- to 3-fold ↑ Na <sup>+</sup> (leaf), 2-fold ↑ K <sup>+</sup> (leaf)	(Brini et al., 2007)
<i>Barley</i> ( <i>H. vulgare</i> )	<b>AVP1</b> ( <i>A. thaliana</i> )	Control - 161 μS/cm (EC <sub>1.5</sub> ) Salt - 1231 μS/cm (EC <sub>1.5</sub> )	17-33 % ↑ B., 23-34 % ↑ yield, no change in Na <sup>+</sup> or K <sup>+</sup> (leaf) 30-42 % ↑ shoot B., 79-87 % ↑ yield, 29-43 % ↑ seed weight	(Schilling et al., 2014)
<i>Barley</i> ( <i>H. vulgare</i> )	<b>AVP1</b> ( <i>A. thaliana</i> )	Control	13-19 % ↑ projected root area, 21-26 % ↑ shoot B., ↑ embryo size, ↑ growth rate	(Schilling, 2014)

Plant species	Transgen	Experimental treatments	Phenotypes of H <sup>+</sup> -PPase transgenic plants (relative to WT/nulls)	Reference
<b>Bentgrass</b> ( <i>A. stolonifera</i> )	<b>AVP1</b> ( <i>A. thaliana</i> )	Control Salt - 100-300 mM NaCl	20-30 % ↑ root & shoot B., ↑ leaf Na <sup>+</sup> 20-30 % ↑ root & shoot B., ↑ leaf Na <sup>+</sup> , ↑ Na <sup>+</sup> (root), ↑ Cl <sup>-</sup> (root), ↑ chlorophyll, ↑ auxin, ↑ RWC	(Li et al., 2010)
<b>Bread wheat</b> ( <i>T. aestivum</i> )	<b>EdVP1</b> ( <i>E. dahuricus</i> )	Low K <sup>+</sup> - 0.01 mmol/L K <sup>+</sup>	2-fold ↑ root length, area & volume, ↑ # root tips, 2-fold ↑ grain yield, 33-48 % ↑ K <sup>+</sup> uptake	(Ruan et al., 2013)
<b>Bread wheat</b> ( <i>T. aestivum</i> )	<b>SeVP1 &amp; SeVP2</b> ( <i>S. europaea</i> )	Control - 30 mM KNO <sub>3</sub> <sup>-</sup> Salt - 150 mM NaCl Low N - 0.1 mM KNO <sub>3</sub> <sup>-</sup> Salt + Low N - levels as above	7-24 % ↑ shoot B., 26-111 % ↑ root B. 33-96 % ↑ shoot B., 3-fold ↑ chlorophyll content 46-115 % ↑ shoot B., 78-117 % ↑ root B., 2-fold ↑ chlorophyll content 29-74 % ↑ shoot B., 37-103 % ↑ root B., 3-fold ↑ chlorophyll content	(Lv et al., 2015)
<b>Cotton</b> ( <i>G. hirsutum</i> )	<b>AVP1</b> ( <i>A. thaliana</i> )	Control Salt - 200 mM NaCl	23-27 % ↑ yield 23-24 % ↑ shoot B., 36-41 % ↑ root B., 24-31 % ↑ yield	(Pasapula et al., 2011)
<b>Cotton</b> ( <i>G. hirsutum</i> )	<b>AVP1*</b> ( <i>A. thaliana</i> )	Control Salt - 200 mM NaCl Drought - 5 d without water	12 % ↑ yield 20 % ↑ shoot & root B., 15 % ↑ yield, 30 % ↑ Pn 15 % ↑ in root & shoot B., 20 % ↑ yield	(Shen et al., 2015)
<b>Cotton</b> ( <i>G. hirsutum</i> )	<b>TsVP</b> ( <i>T. halophila</i> )	Control Drought - 14 d without water	13 % ↑ plant height, 25-36 % ↑ yield 20 % ↑ chlorophyll, 40-50 % ↑ soluble sugars, 40-50 % ↑ RWC	(Lv et al., 2009)
<b>Cotton</b> ( <i>G. hirsutum</i> )	<b>TsVP*</b> ( <i>T. halophila</i> )	Control Salt - 250 mM NaCl Saline field - ~ 800 ppm	1.7-4.6 ↑ B. 92-118 % ↑ shoot B., 20 % ↑ Pn, 30 % ↑ Na <sup>+</sup> (leaf), 2-fold ↑ K <sup>+</sup> (leaf) 20-25 % ↑ yield, 10 % ↑ RWC, 20 % ↑ Pn, 10 % ↑ Na <sup>+</sup> (leaf), 15 % ↑ K <sup>+</sup> (leaf)	(Cheng et al., 2018)
<b>Lettuce</b> ( <i>Lacuta sativa</i> )	<b>AVPID</b> ( <i>A. thaliana</i> )	Control - 6.25 mM KNO <sub>3</sub> <sup>-</sup> Low N - 0.5 mM KNO <sub>3</sub> <sup>-</sup>	40 % ↑ shoot & 60 % ↑ root B., ↑ RA, 50 % ↑ yield 2-fold ↑ leaf area & shoot B., ↑ RA, 3-fold ↑ root B., 5-fold ↓ Glc, 2-fold ↓ Suc, 50 % ↑ root N	(Paez-Valencia et al., 2013)
<b>Lotus corniculatus</b>	<b>ZxVP1-I*</b> ( <i>Z. xanthoxylum</i> )	Control Salt - 200 mM NaCl Drought - 10 d without water	↑ growth rate, 35 % ↑ shoot B., no difference in ion content 3.3- to 3.7-fold ↑ shoot B., 50 % ↑ Na <sup>+</sup> & K <sup>+</sup> , 40 % ↑ Ca <sup>2+</sup> (leaf), 40 % ↑ Pn 16-26 % ↑ shoot B., 30 % ↑ Na <sup>+</sup> , 39 % ↑ K <sup>+</sup> , 22 % ↑ Ca <sup>2+</sup> (leaf), 39-45 % ↑ RWC, 25 % ↑ Pn	(Bao et al., 2014)

Plant species	Transgene	Experimental treatments	Phenotypes of H <sup>+</sup> -PPase transgenic plants (relative to WT/nulls)	Reference
<b>Maize</b> ( <i>Z. mays</i> )	<b>TsVP</b> ( <i>T. halophila</i> )	Control Osmotic stress - 12 % PEG600 Field - with rainout shelter	25 % ↑ soluble sugars 30-50 % ↑ proline, 30-60 % ↑ soluble sugars, 25 % ↑ total B., 20 % ↑ RWC 30 % ↑ yield	(Li et al., 2008)
<b>Maize</b> ( <i>Z. mays</i> )	<b>TsVP</b> ( <i>T. halophila</i> )	Control - 1 mM KH <sub>2</sub> PO <sub>4</sub> Low P - 5 μM KH <sub>2</sub> PO <sub>4</sub>	23 % ↑ root B., no difference in shoot B., 18-30 % ↑ P uptake 14-16 % ↑ shoot B., 37-40 % ↑ root B., ↑ RA, 42-48 % ↑ P uptake, ↑ PIN1 & AUX1 expression, 23-29 % ↑ yield, ↓ days to flowering	(Pei et al., 2012)
<b>Peanut</b> ( <i>A. hypogaea</i> )	<b>AVP1</b> ( <i>A. thaliana</i> )	Control (pot) Salt (pot) - 150 mM NaCl 50 % reduced water (pot) Low irrigation field	No control data presented 2- to 6-fold ↑ Pn, 4- to 8-fold ↑ stomatal conductance, no ion data 20 % ↑ shoot B., 3- to 5-fold ↑ Pn, 2- to 3.5-fold ↑ stomatal conductance ↑ yield (varies between 4 trials), 15 % ↑ Pn, 25 % ↑ stomatal conductance	(Qin et al., 2013)
<b>Poplar</b> ( <i>P. trichocarpa</i> )	<b>PtVP1.1</b> ( <i>P. trichocarpa</i> )	Control Salt - 150 mM NaCl	20 % ↑ K <sup>+</sup> (leaf & root), ↓ root H <sup>+</sup> flux 18-28 % ↑ shoot B., 20 % ↓ Na <sup>+</sup> (leaf), 10 % ↑ Na <sup>+</sup> (stem), 10 % ↑ K <sup>+</sup> (leaf), ↑ root H <sup>+</sup> and Na <sup>+</sup> flux	(Yang et al., 2015)
<b>Potato</b> ( <i>S. tuberosum</i> )	<b>MeVP1</b> ( <i>M. truncatula</i> )	Control only	↑ anthocyanin biosynthesis, ↑ Suc accumulation, ↑ growth rate & organ development	(Wang et al., 2014)
<b>Rice</b> ( <i>O. sativa</i> )	<b>AVP1*</b> ( <i>A. thaliana</i> )	Control Salt - 150 mM NaCl	↑ RA, few alterations in other assessed parameters 30 % ↑ root B., 10 % ↑ leaf Na <sup>+</sup> , 37-45 % ↑ Pn, 50 % ↓ H <sub>2</sub> O <sub>2</sub>	(Zhao et al., 2006)
<b>Rice</b> ( <i>O. sativa</i> )	<b>AVP1</b> ( <i>A. thaliana</i> )	Control (field) Salt - 5.8 g/L NaCl	15 % ↑ grain weight, 12 % ↑ culm weight, 10 % ↑ root B., 15 % ↑ total B. 15 % ↑ Na <sup>+</sup> (leaf & root), 40 % ↑ total B.	(Kim et al., 2013)
<b>Rice</b> ( <i>O. sativa</i> )	<b>AVP1D</b> ( <i>A. thaliana</i> )	Control - 1 mM P Low P - 10 μM P	40 % ↑ root B., 43 % ↑ P content, ↑ proportion of ripe fruit 90 % ↑ root B., 50 % ↑ shoot B., 18 % ↑ P content, ↑ K <sup>+</sup> (root)	(Yang et al., 2007)
<b>Rice</b> ( <i>O. sativa</i> )	<b>OVP1</b> ( <i>O. sativa</i> )	Control - 26°C Low temperature - 4°C Drought - 10 d without water	24 % ↑ proline (leaf) 3-fold ↑ proline (leaf), 24-35 % ↑ survival rate, ↓ electrolyte leakage 30 % ↑ RWC	(Zhang et al., 2011)

Plant species	Transgene	Experimental treatments	Phenotypes of H <sup>+</sup> -PPase transgenic plants (relative to WT/nulls)	Reference
<b>Sugar-beet</b> ( <i>B. vulgaris</i> )	<b>ZxVP1-1*</b> ( <i>Z. xanthoxylum</i> )	Control Salt - 400 mM NaCl	30 % ↑ shoot B., no difference in root or shoot ion content 19-49 % ↑ RWC, 15 % ↑ shoot B., 15-28 % ↑ Na <sup>+</sup> (leaf), 10-50 % ↓ Na <sup>+</sup> (root), no difference in K <sup>+</sup> or Ca <sup>2+</sup> (root or shoot), 40 % ↑ proline (leaf), ↑ Suc, Fru & Glu (root only)	(Wu et al., 2015)
<b>Sugarcane</b> ( <i>S. officinarum</i> )	<b>AVP1</b> ( <i>A. thaliana</i> )	Control Salt - 200 mM NaCl Drought - 14 d without water	2-fold ↑ root length & root B. Maintained normal growth, WT died (growth not quantified) Resumed normal growth after rewatering, WT died (growth not quantified)	(Kumar et al., 2014)
<b>Sweet potato</b> ( <i>I. batatas</i> )	<b>IbVP1</b> ( <i>I. batatas</i> )	Control - 100 μm Fe-EDTA Low Fe - 0 μm Fe-EDTA	10-21 % ↑ shoot B., 35-93 % ↑ root B., ↑ Suc, Glc, Fru, starch & AO 41-50 % ↑ shoot B., 30-55 % ↑ root B., ↑ Suc, Glc, Fru, starch & AO	(Fan et al., 2017)
<b>Tomato</b> ( <i>L. esculentum</i> )	<b>AVP1D</b> ( <i>A. thaliana</i> )	Control - 400 ppm P Low P - 44 ppm P	9 % ↑ root B., 12 % ↑ shoot B., 7 % ↑ fruit weight, 16 % ↑ P content 50-90 % ↑ root B., 7-68 % ↑ shoot B., 28-92 % ↑ P content, ↑ root K <sup>+</sup>	(Yang et al., 2007)
<b>Tomato</b> ( <i>L. esculentum</i> )	<b>AVP1D</b> ( <i>A. thaliana</i> )	Control - field with P fertiliser Low P - field without P	↑ RA, ↑ auxin transport, ↑ root B., 10-15 % ↑ transplant survival, ↑ P ↑ RA, ↑ auxin transport, ↑ root B., 50 % ↑ yield, 25 % ↑ ripe fruit, 2-fold ↑ fruit size	(Yang et al., 2014)
<b>Tomato</b> ( <i>L. esculentum</i> )	<b>MdVHP1</b> ( <i>Malus domestica</i> )	Control Salt - 100 mM NaCl Drought - 15 d without water	20 % ↑ leaf Na <sup>+</sup> and K <sup>+</sup> ↑ growth maintenance, 30-50 % ↑ Na <sup>+</sup> and K <sup>+</sup> (leaf) 20 % ↑ RWC, ↓ wilting, ↑ recovery after rewatering	(Dong et al., 2011)
<b>Tobacco</b> ( <i>N. tabacum</i> )	<b>TVP1</b> ( <i>T. aestivum</i> )	Control - 0 μM Cd High cadmium - 500 μM Cd	13 % ↑ chlorophyll, 83 % ↑ CAT activity, 60 % ↑ total B., 35 % ↑ germination rate, 50 % ↑ B., 5-fold ↑ chlorophyll, 15 % ↑ Cd	(Khouidi et al., 2012)
<b>Tobacco</b> ( <i>N. tabacum</i> )	<b>TsVP</b> ( <i>T. halophila</i> )	Control Salt - 200 & 300 mM NaCl	No difference in chlorophyll, Na <sup>+</sup> or MDA content, or total biomass 50 % ↑ chlorophyll, 50 % ↑ B., 20-30 % ↑ Na <sup>+</sup> (leaf), 25 % ↑ solute retention, 43-76 % ↓ MDA, 29-34 % ↓ electrolyte leakage	(Gao et al., 2006)

## H<sup>+</sup>-PPase genes and bread wheat

### Identification of wheat H<sup>+</sup>-PPases (*TaVPs*)

The first bread wheat H<sup>+</sup>-PPase gene to be identified was *TVP1*, which was amplified from a wheat root tissue cDNA library using primers specific to the 5' and 3' ends of the barley *HVP1* gene (Brini et al., 2005). Further analysis, in which the *TVP1* sequence was used to query the 158<sup>th</sup> release of the GenBank wheat expressed sequence tag (EST) database, identified 9 putative H<sup>+</sup>-PPase genes (Wang et al., 2009). Based on gene expression analysis in nulli-tetrasomic wheat (cv. Chinese Spring) lines, the 9 *TaVP* sequences were confirmed and named based on sequence similarity and chromosome location (Wang et al., 2009). The six *TaVP* sequences located on chromosome 7 were named *TaVP1-7A*, *TaVP1-7B*, *TaVP1-7D*, *TaVP2-7A*, *TaVP2-7B* and *TaVP2-7D*, while the three located on chromosome 1 were designated *TaVP3-1A*, *TaVP3-1B* and *TaVP3-1D* (Wang et al., 2009). Semi-quantitative gene expression analysis of a Chinese wheat variety (cv. Kehan 15) suggested that expression of all three *TaVP1* genes was higher in root tissue than leaf tissue, expression of the three *TaVP2* genes was higher in leaf tissue than root tissue, and expression of the three *HVP3* genes was specific to the developing seed (Wang et al., 2009). However, as these conclusions were based on the analysis of a single wheat cultivar, it remains unknown whether these expression patterns are similar among different wheat varieties. Furthermore, the conclusions of this study cannot easily be validated as, to our knowledge, the full gene sequences of the 9 identified *TaVP* homeologs remain unpublished. As such, a more comprehensive analysis using the newly available wheat genome assemblies is required to validate these 9 *TaVP* genes, and to identify additional *TaVP* genes which may not have identified through EST analysis.



## Potential role of wheat H<sup>+</sup>-PPases (TaVPs) in stress response

The potential role of the identified *TaVP* sequences in stress tolerance has been assessed through expression of the initial *TVP1* sequence in a mutant yeast (*nhx1::HIS3ena1::HIS3*) and transgenic Arabidopsis (Brini et al., 2005; Brini et al., 2007). In the salt sensitive mutant yeast strain, expression of *TVP1*, similar to expression of *AVP1* (Gaxiola et al., 1999), restored growth on saline (500 mM NaCl) media, suggesting *TVP1* may also have a beneficial role in improving plant salinity tolerance (Brini et al., 2005). In Arabidopsis constitutively expressing *TVP1*, total leaf area was 11 % and 22 % higher than wild-type when treated with 50 mM and 200 mM NaCl, respectively (Brini et al., 2007). However, as the *TVP1* sequence used for these analyses was not homeolog specific, it remains unknown whether this is a common role among all *TaVP1* homeologs (*TaVP1-7A*, *TaVP1-7B* and *TaVP1-7D*), or other *TaVP* genes (*TaVP2-7A*, *TaVP2-7B*, *TaVP2-7D*, *TaVP3-1A*, *TaVP3-1B* and *TaVP3-1D*).

In addition to characterisation in yeast and Arabidopsis, semi-quantitative gene expression analysis of the *TaVP1* and *TaVP2* genes has also been assessed in response to salinity and drought treatment (Wang et al., 2009). After 12 h exposure to 250 mM NaCl, expression of the *TaVP2* genes (*TaVP2-7A*, *TaVP2-7B* and *TaVP2-7D*) were upregulated in the root of 10 d-old seedlings (cv. Kehan 15 and FLXMM), while few changes in expression were detected in leaf tissue. Expression of the *TaVP1* genes (*TaVP1-7A*, *TaVP1-7B* and *TaVP1-7D*) remained unaltered in both leaf and root tissue under salt treatment (Wang et al., 2009). In air-dried roots of 10 d-old seedlings, used to simulate a drought stress, few changes were detected in the expression of the *TaVP1* or *TaVP2* genes up to 48 h post treatment (Wang et al., 2009). Expression of *TaVP1* genes (*TaVP1-7A*, *TaVP1-7B* and *TaVP1-7D*) also remained unaltered in the leaf tissue up to 48 h following the treatment, while expression of the *TaVP2* genes (*TaVP2-7A*, *TaVP2-7B* and

*TaVP2-7D*) decreased approximately 2.5 h after the start of the treatment (Wang et al., 2009). Analysis of tonoplast-enriched membrane vesicles, found H<sup>+</sup>-PPase protein abundance and activity to be 1.5× lower in salt treated roots compared to plants in control conditions (Wang et al., 2000). However, as this analysis was conducted prior to the identification of the wheat *TaVP* sequences, a sequence specific to the mung bean H<sup>+</sup>-PPase (*VrVP1*) was used for these measurements, which due to sequence differences, may not have provided an accurate measurement of *TaVP* abundance and activity. To further characterise the response of *TaVP* genes under abiotic stress conditions, gene expression should be analysed using quantitative real-time polymerase chain reaction (qRT-PCR) across a range of wheat varieties, throughout development. Protein abundance and activity should also be investigated once the full length gene sequences of the 9 *TaVP* homeologs have been obtained.

### **Can H<sup>+</sup>-PPase genes enhance yield and stress tolerance in bread wheat?**

Despite being used to successfully enhance the growth and stress tolerance of a wide range of plant species, including several cereal crops, the potential of H<sup>+</sup>-PPase genes to improve the growth of bread wheat remains largely unknown. To address this knowledge gap, transgenic wheat lines constitutively expressing H<sup>+</sup>-PPase genes, such as the Arabidopsis *AVP1* or wheat *TaVP* genes, would provide valuable knowledge regarding the potential application of these genes in wheat. In addition, the use of stress-inducible promoters to drive expression of H<sup>+</sup>-PPase genes has not been investigated and should be explored to determine whether beneficial phenotypes can be produced without the use of constitutive promoters.

With the current restrictions placed upon genetically modified plants within Australia (Hindmarsh and Du Plessis, 2008), in addition to H<sup>+</sup>-PPase genes having been found to underlie

quantitative trait loci (QTL) associated with salinity tolerance in barley (Shavrukov et al., 2013) and drought tolerance in maize (Wang et al., 2016), further characterisation of the native wheat *TaVP* genes could provide an alternative resource for improving the growth and stress tolerance of bread wheat. Due to limited knowledge regarding the role of *TaVP* genes, further investigation is required to identify differences in *TaVP* expression across a broad range of wheat varieties, tissue types and developmental stages, to aid in the identification of beneficial *TaVP* genes and alleles. Further investigation into the function of *TaVP* proteins, both *in vitro* and *in planta*, would provide additional information as to how these genes could be used to improve the growth and stress tolerance of bread wheat.

## Research aims

The purpose of this research project is to address the current knowledge gaps regarding the role of H<sup>+</sup>-PPases, and to investigate the potential of these genes to improve the growth and salinity tolerance of bread wheat. Specifically, this PhD research will address the following aims:

1. To investigate the role of AVP1 in plant metabolism using *Arabidopsis thaliana* as a model plant species **(Chapter 2)**
2. To evaluate the impact of constitutive and stress-inducible expression of *AVP1* on the growth and salinity tolerance of transgenic bread wheat **(Chapter 3)**
3. To utilise new genomic resources to identify and profile the expression of all bread wheat H<sup>+</sup>-PPase (*TaVP*) genes **(Chapter 4)**
4. To assess the role of wheat H<sup>+</sup>-PPases (TaVPs) through generating and phenotyping constitutively over-expressing *TaVP* wheat lines **(Chapter 5)**

## References

- ABARES** 2017. Agricultural commodity statistics 2017. Australian Bureau of Agricultural and Resource Economics and Sciences.
- ABARES** 2018. Australian crop report. Australian Bureau of Agricultural and Resource Economics and Sciences.
- Baltscheffsky H, Von Stedingk LV, Heldt HW *et al.*** 1966. Inorganic pyrophosphate: Formation in bacterial photophosphorylation. *Science* **153**, 1120-1122.
- Baltscheffsky M.** 1967. Inorganic pyrophosphate as an energy donor in photosynthetic and respiratory electron transport phosphorylation systems. *Biochemical and Biophysical Research Communications* **28**, 270-276.
- Bao AK, Wang SM, Wu GQ *et al.*** 2009. Overexpression of the *Arabidopsis* H<sup>+</sup>-PPase enhanced resistance to salt and drought stress in transgenic alfalfa (*Medicago sativa* L.). *Plant Science* **176**, 232-240.
- Bao AK, Wang YW, Xi JJ *et al.*** 2014. Co-expression of xerophyte *Zygophyllum xanthoxylum* ZxNHX and ZxVP1-1 enhances salt and drought tolerance in transgenic *Lotus corniculatus* by increasing cations accumulation. *Functional Plant Biology* **41**, 203-214.
- Brini F, Gaxiola RA, Berkowitz GA *et al.*** 2005. Cloning and characterization of a wheat vacuolar cation/proton antiporter and pyrophosphatase proton pump. *Plant Physiology and Biochemistry* **43**, 347-354.
- Brini F, Hanin M, Mezghani I *et al.*** 2007. Overexpression of wheat Na<sup>+</sup>/H<sup>+</sup> antiporter *TNHX1* and H<sup>+</sup>-pyrophosphatase *TVP1* improve salt- and drought-stress tolerance in *Arabidopsis thaliana* plants. *Journal of Experimental Botany* **58**, 301-308.
- Cheng C, Zhang Y, Chen X *et al.*** 2018. Co-expression of *AtNHX1* and *TsVP* improves the salt tolerance of transgenic cotton and increases seed cotton yield in a saline field. *Molecular Breeding* **38**, <https://doi.org/10.1007/s11032-018-0774-5>.
- Conklin PL.** 2001. Recent advances in the role and biosynthesis of ascorbic acid in plants. *Plant, Cell & Environment* **24**, 383-394.
- Cubasch U, Meehl G, Boer G *et al.*** 2001. Projections of future climate change. In *Climate Change 2001: The Scientific Basis*, 10013/epic.15750.d001 (ed. J. Houghton, Y. Ding, D. Griggs, M. Noguer, P. Van der Linden, X. Dai, K. Maskell and C. Johnson), pp. 527-582. Cambridge, UK: Cambridge University Press.
- Dong Q, Liu D, An X *et al.*** 2011. *MdVHP1* encodes an apple vacuolar H<sup>+</sup>-PPase and enhances stress tolerance in transgenic apple callus and tomato. *Journal of Plant Physiology* **168**, 2124-2133.
- Drozdowicz YM, Kissinger JC and Rea PA.** 2000. *AVP2*, a sequence-divergent, K<sup>+</sup>-insensitive H<sup>+</sup>-translocating inorganic pyrophosphatase from *Arabidopsis*. *Plant Physiology* **123**, 353-362.
- Drozdowicz YM and Rea PA.** 2001. Vacuolar H<sup>+</sup> pyrophosphatases: From the evolutionary backwaters into the mainstream. *Trends in Plant Science* **6**, 206-211.
- El-Hendawy SE, Hassan WM, Al-Suhaibani NA *et al.*** 2017. Comparative performance of multivariable agro-physiological parameters for detecting salt tolerance of wheat cultivars under simulated saline field growing conditions. *Frontiers in Plant Science* **8**, <https://doi.org/10.3389/fpls.2017.00435>.
- Eltayeb AE, Yamamoto S, Habora MEE *et al.*** 2011. Transgenic potato overexpressing *Arabidopsis* cytosolic *AtDHAR1* showed higher tolerance to herbicide, drought and salt stresses. *Breeding Science* **61**, 3-10.

- Fan W, Wang H, Wu Y *et al.* 2017. H<sup>+</sup>-pyrophosphatase *IbVP1* promotes efficient iron use in sweet potato [*Ipomoea batatas* (L.) Lam.]. *Plant Biotechnology Journal* **15**, 698-712.
- Ferjani A, Segami S, Horiguchi G *et al.* 2011. Keep an eye on PP<sub>i</sub>: The vacuolar-type H<sup>+</sup>-pyrophosphatase regulates postgerminative development in *Arabidopsis*. *Plant Cell* **23**, 2895-2908.
- Foyer CH, Souriau N, Perret S *et al.* 1995. Overexpression of glutathione reductase but not glutathione synthetase leads to increases in antioxidant capacity and resistance to photoinhibition in poplar trees. *Plant Physiology* **109**, 1047-1057.
- Gao F, Gao Q, Duan X *et al.* 2006. Cloning of an H<sup>+</sup>-PPase gene from *Thellungiella halophila* and its heterologous expression to improve tobacco salt tolerance. *Journal of Experimental Botany* **57**, 3259-3270.
- Gaxiola RA, Li J, Undurraga S *et al.* 2001. Drought- and salt-tolerant plants result from overexpression of the *AVP1* H<sup>+</sup>-pump. *Proceedings of the National Academy of Sciences* **98**, 11444-11449.
- Gaxiola RA, Rao R, Sherman A *et al.* 1999. The *Arabidopsis thaliana* proton transporters, AtNHX1 and AVP1, can function in cation detoxification in yeast. *Proceedings of the National Academy of Sciences* **96**, 1480-1485.
- Gaxiola RA, Regmi KC, Paez-Valencia J *et al.* 2016. Plant H<sup>+</sup>-PPases: Reversible enzymes with contrasting functions dependent on membrane environment. *Molecular Plant* **9**, 317-319.
- Gaxiola RA, Sanchez CA, Paez-Valencia J *et al.* 2012. Genetic manipulation of a “vacuolar” H<sup>+</sup>-PPase: From salt tolerance to yield enhancement under phosphorus-deficient soils. *Plant Physiology* **159**, 3-11.
- Geldner N, Richter S, Vieten A *et al.* 2004. Partial loss-of-function alleles reveal a role for GNOM in auxin transport-related, post-embryonic development of *Arabidopsis*. *Development* **131**, 389-400.
- Gilliham M, Able JA and Roy SJ. 2017. Translating knowledge about abiotic stress tolerance to breeding programmes. *The Plant Journal* **90**, 898-917.
- Gonzalez N, De Bodt S, Sulpice R *et al.* 2010. Increased leaf size: Different means to an end. *Plant Physiology* **153**, 1261-1279.
- Hammond JP and White PJ. 2011. Sugar signaling in root responses to low phosphorus availability. *Plant Physiology* **156**, 1033-1040.
- Hemavathi, Upadhyaya C, Akula N *et al.* 2010. Enhanced ascorbic acid accumulation in transgenic potato confers tolerance to various abiotic stresses. *Biotechnology Letters* **32**, 321-330.
- Hindmarsh R and Du Plessis R. 2008. GMO regulation and civic participation at the “edge of the world”: The case of Australia and New Zealand. *New Genetics and Society* **27**, 181-199.
- Hochman Z, Gobbett DL and Horan H. 2017. Climate trends account for stalled wheat yields in Australia since 1990. *Global Change Biology* **23**, 2071-2081.
- Horemans N, Asard H and Caubergs RJ. 1994. The role of ascorbate free radical as an electron acceptor to cytochrome b-mediated trans-plasma membrane electron transport in higher plants. *Plant Physiology* **104**, 1455-1458.
- Khadilkar AS, Yadav UP, Salazar C *et al.* 2016. Constitutive and companion cell-specific overexpression of *AVP1*, encoding a proton-pumping pyrophosphatase, enhances biomass accumulation, phloem loading, and long-distance transport. *Plant Physiology* **170**, 401-414.
- Khoudi H, Maatar Y, Gouiaa S *et al.* 2012. Transgenic tobacco plants expressing ectopically wheat H<sup>+</sup>-pyrophosphatase (H<sup>+</sup>-PPase) gene *TaVP1* show enhanced accumulation and tolerance to cadmium. *Journal of Plant Physiology* **169**, 98-103.

- Kim EJ, Zhen RG and Rea PA.** 1994. Heterologous expression of plant vacuolar pyrophosphatase in yeast demonstrates sufficiency of the substrate-binding subunit for proton transport. *Proceedings of the National Academy of Sciences* **91**, 6128-32.
- Kim YS, Kim IS, Choe YH et al.** 2013. Overexpression of the *Arabidopsis* vacuolar H<sup>+</sup>-pyrophosphatase *AVP1* gene in rice plants improves grain yield under paddy field conditions. *The Journal of Agricultural Science* **152**, 941-953.
- Kriegel A, Andrés Z, Medzihradzky A et al.** 2015. Job sharing in the endomembrane system: Vacuolar acidification requires the combined activity of V-ATPase and V-PPase. *The Plant Cell* **27**, 3383-3396.
- Kubota K and Ashihara H.** 1990. Identification of non-equilibrium glycolytic reactions in suspension-cultured plant cells. *Biochimica et Biophysica Acta (BBA) - General Subjects* **1036**, 138-142.
- Kumar T, Uzma, Khan MR et al.** 2014. Genetic improvement of sugarcane for drought and salinity stress tolerance using *Arabidopsis* vacuolar pyrophosphatase (*AVP1*) gene. *Molecular Biotechnology* **56**, 199-209.
- Langhans M, Ratajczak R, Lutzelschwab M et al.** 2001. Immunolocalization of plasma-membrane H<sup>+</sup>-ATPase and tonoplast-type pyrophosphatase in the plasma membrane of the sieve element-companion cell complex in the stem of *Ricinus communis* L. *Planta* **213**, 11-19.
- Leigh RA, Pope AJ, Jennings IR et al.** 1992. Kinetics of the vacuolar H<sup>+</sup>-pyrophosphatase: The roles of magnesium, pyrophosphate, and their complexes as substrates, activators, and inhibitors. *Plant Physiology* **100**, 1698-1705.
- Li B, Wei A, Song C et al.** 2008. Heterologous expression of the *TsVP* gene improves the drought resistance of maize. *Plant Biotechnology Journal* **6**, 146-159.
- Li J, Yang H, Ann Peer W et al.** 2005. *Arabidopsis* H<sup>+</sup>-PPase *AVP1* regulates auxin-mediated organ development. *Science* **310**, 121-125.
- Li Z, Baldwin CM, Hu Q et al.** 2010. Heterologous expression of *Arabidopsis* H<sup>+</sup>-pyrophosphatase enhances salt tolerance in transgenic creeping bentgrass (*Agrostis stolonifera* L.). *Plant, Cell & Environment* **33**, 272-289.
- Lin SM, Tsai JY, Hsiao CD et al.** 2012. Crystal structure of a membrane-embedded H<sup>+</sup>-translocating pyrophosphatase. *Nature* **484**, 399-403.
- Lisko KA, Torres R, Harris RS et al.** 2013. Elevating vitamin C content via overexpression of *myo*-inositol oxygenase and L-gulonono-1,4-lactone oxidase in *Arabidopsis* leads to enhanced biomass and tolerance to abiotic stresses. *In Vitro Cellular & Developmental Biology - Plant* **49**, 643-655.
- Lv S, Jiang P, Nie L et al.** 2015. H<sup>+</sup>-pyrophosphatase from *Salicornia europaea* confers tolerance to simultaneously occurring salt stress and nitrogen deficiency in *Arabidopsis* and wheat. *Plant, Cell & Environment* **38**, 2433-2449.
- Lv SL, Lian LJ, Tao PL et al.** 2009. Overexpression of *Thellungiella halophila* H<sup>+</sup>-PPase (*TsVP*) in cotton enhances drought stress resistance of plants. *Planta* **229**, 899-910.
- Maeshima M.** 1991. H<sup>+</sup>-translocating inorganic pyrophosphatase of plant vacuoles inhibition by Ca<sup>2+</sup>, stabilization by Mg<sup>2+</sup> and immunological comparison with other inorganic pyrophosphatases. *European Journal of Biochemistry* **196**, 11-17.
- Mayer U, Ruiz RAT, Berleth T et al.** 1991. Mutations affecting body organization in the *Arabidopsis* embryo. *Nature* **353**, 402-407.
- Mitsuda N, Enami K, Nakata M et al.** 2001. Novel type *Arabidopsis thaliana* H<sup>+</sup>-PPase is localized to the Golgi apparatus. *FEBS Letters* **488**, 29-33.
- Munns R and Tester M.** 2008. Mechanisms of salinity tolerance. *Annual Review of Plant Biology* **59**, 651-681.

- Nass R, Cunningham KW and Rao R.** 1997. Intracellular sequestration of sodium by a novel  $\text{Na}^+/\text{H}^+$  exchanger in yeast is enhanced by mutations in the plasma membrane  $\text{H}^+$ -ATPase: Insights into the mechanisms of sodium tolerance. *Journal of Biological Chemistry* **272**, 26145-26152.
- Paez-Valencia J, Patron-Soberano A, Rodriguez-Leviz A et al.** 2011. Plasma membrane localization of the type I  $\text{H}^+$ -PPase AVP1 in sieve element–companion cell complexes from *Arabidopsis thaliana*. *Plant Science* **181**, 23-30.
- Paez-Valencia J, Sanchez-Lares J, Marsh E et al.** 2013. Enhanced proton translocating pyrophosphatase activity improves nitrogen use efficiency in romaine lettuce. *Plant Physiology* **161**, 1557-1569.
- Park S, Li J, Pittman JK et al.** 2005. Up-regulation of a  $\text{H}^+$ -pyrophosphatase ( $\text{H}^+$ -PPase) as a strategy to engineer drought-resistant crop plants. *Proceedings of the National Academy of Sciences* **102**, 18830-18835.
- Pasapula V, Shen G, Kuppu S et al.** 2011. Expression of an *Arabidopsis* vacuolar  $\text{H}^+$ -pyrophosphatase gene (*AVP1*) in cotton improves drought- and salt tolerance and increases fibre yield in the field conditions. *Plant Biotechnology Journal* **9**, 88-99.
- Pei L, Wang J, Li K et al.** 2012. Overexpression of *Thellungiella halophila*  $\text{H}^+$ -pyrophosphatase gene improves low phosphate tolerance in maize. *PLoS ONE* **7**, <https://doi.org/10.1371/journal.pone.0043501>.
- Penfield S, Graham S and Graham IA.** 2005. Storage reserve mobilization in germinating oilseeds: *Arabidopsis* as a model system. *Biochemical Society Transactions* **33**, 380-383.
- Pizzio GA, Hirschi KD and Gaxiola RA.** 2017. Conjecture regarding posttranslational modifications to the arabidopsis type I proton-pumping pyrophosphatase (*AVP1*). *Frontiers in Plant Science* **8**, <https://doi.org/10.3389/fpls.2017.01572>.
- Pizzio GA, Paez-Valencia J, Khadilkar AS et al.** 2015. *Arabidopsis* type I proton-pumping pyrophosphatase expresses strongly in phloem, where it is required for pyrophosphate metabolism and photosynthate partitioning. *Plant Physiology* **167**, 1541-1553.
- Pope A and Leigh R.** 1987. Some characteristics of anion transport at the tonoplast of oat roots, determined from the effects of anions on pyrophosphate dependent proton transport. *Planta* **172**, 91-100.
- Qin H, Gu Q, Kuppu S et al.** 2013. Expression of the *Arabidopsis* vacuolar  $\text{H}^+$ -pyrophosphatase gene *AVP1* in peanut to improve drought and salt tolerance. *Plant Biotechnology Reports* **7**, 345-355.
- Ramírez L, Bartoli CG and Lamattina L.** 2013. Glutathione and ascorbic acid protect *Arabidopsis* plants against detrimental effects of iron deficiency. *Journal of Experimental Botany* **64**, 3169-3178.
- Regmi KC, Zhang S and Gaxiola RA.** 2016. Apoplasmic loading in the rice phloem supported by the presence of sucrose synthase and plasma membrane-localized proton pyrophosphatase. *Annals of Botany* **117**, 257-68.
- Rengasamy P.** 2006. World salinization with emphasis on Australia. *Journal of Experimental Botany* **57**, 1017-1023.
- Rocha Facanha A and de Meis L.** 1998. Reversibility of  $\text{H}^+$ -ATPase and  $\text{H}^+$ -pyrophosphatase in tonoplast vesicles from maize coleoptiles and seeds. *Plant Physiology* **116**, 1487-95.
- Roy SJ, Negrão S and Tester M.** 2014. Salt resistant crop plants. *Current Opinion in Biotechnology* **26**, 115-124.



- Ruan L, Zhang J, Xin X *et al.* 2013. *Elymus dahuricus* H<sup>+</sup>-PPase *EdVP1* enhances potassium uptake and utilization of wheat through the development of root system. *Journal of soil science and plant nutrition* **13**, 716-729.
- Schilling RK. 2014. "Evaluating the abiotic stress tolerance of transgenic barley expressing an *Arabidopsis* vacuolar H<sup>+</sup>-pyrophosphatase gene (*AVP1*)". PhD thesis. Adelaide, Australia. The University of Adelaide.
- Schilling RK, Marschner P, Shavrukov Y *et al.* 2014. Expression of the *Arabidopsis* vacuolar H<sup>+</sup>-pyrophosphatase gene (*AVP1*) improves the shoot biomass of transgenic barley and increases grain yield in a saline field. *Plant Biotechnology Journal* **12**, 378-386.
- Schilling RK, Tester M, Marschner P *et al.* 2017. *AVP1*: One protein, many roles. *Trends in Plant Science* **22**, 154-162.
- Segami S, Asaoka M, Kinoshita S *et al.* 2018. Biochemical, structural, and physiological characteristics of vacuolar H<sup>+</sup>-pyrophosphatase. *Plant & Cell Physiology* <https://doi.org/10.1093/pcp/pcy054>.
- Segami S, Makino S, Miyake A *et al.* 2014. Dynamics of vacuoles and H<sup>+</sup>-pyrophosphatase visualized by monomeric green fluorescent protein in *Arabidopsis*: Artifactual bulbs and native intravacuolar spherical structures. *The Plant Cell* **26**, 3416-3434.
- Segami S, Nakanishi Y, Sato MH *et al.* 2010. Quantification, organ-specific accumulation and intracellular localization of type II H<sup>+</sup>-pyrophosphatase in *Arabidopsis thaliana*. *Plant & Cell Physiology* **51**, 1350-1360.
- Seufferheld M, Lea CR, Vieira M *et al.* 2004. The H<sup>+</sup>-pyrophosphatase of *Rhodospirillum rubrum* is predominantly located in polyphosphate-rich acidocalcisomes. *Journal of Biological Chemistry* **279**, 51193-51202.
- Shavrukov Y, Bovill J, Afzal I *et al.* 2013. *HVP10* encoding V-PPase is a prime candidate for the barley *HvNax3* sodium exclusion gene: evidence from fine mapping and expression analysis. *Planta* **237**, 1111-1122.
- Shen G, Wei J, Qiu X *et al.* 2015. Co-overexpression of *AVP1* and *AtNHX1* in cotton further improves drought and salt tolerance in transgenic cotton plants. *Plant Molecular Biology Reporter* **33**, 167-177.
- Smirnoff N. 1996. Botanical briefing: The function and metabolism of ascorbic acid in plants. *Annals of Botany* **78**, 661-669.
- Smirnoff N. 2000. Ascorbic acid: Metabolism and functions of a multi-faceted molecule. *Current Opinion in Plant Biology* **3**, 229-235.
- Stevens R, Page D, Gouble B *et al.* 2008. Tomato fruit ascorbic acid content is linked with monodehydroascorbate reductase activity and tolerance to chilling stress. *Plant, Cell & Environment* **31**, 1086-1096.
- Vance CP, Uhde-Stone C and Allan DL. 2003. Phosphorus acquisition and use: Critical adaptations by plants for securing a nonrenewable resource. *New Phytologist* **157**, 423-447.
- Vercruyssen L, Gonzalez N, Werner T *et al.* 2011. Combining enhanced root and shoot growth reveals cross talk between pathways that control plant organ size in *Arabidopsis*. *Plant Physiology* **155**, 1339-1352.
- Wang BS, Ratajczak R and Zhang JH. 2000. Activity, amount and subunit composition of vacuolar-type H<sup>+</sup>-ATPase and H<sup>+</sup>-PPase in wheat roots under severe NaCl stress. *Journal of Plant Physiology* **157**, 109-116.
- Wang JW, Wang HQ, Xiang WW *et al.* 2014. A *Medicago truncatula* H<sup>+</sup>-pyrophosphatase gene, *MtVP1*, improves sucrose accumulation and anthocyanin biosynthesis in potato (*Solanum tuberosum* L.). *Genetics and Molecular Research* **13**, 3615-26.

- Wang X, Wang H, Liu S et al.** 2016. Genetic variation in *ZmVPP1* contributes to drought tolerance in maize seedlings. *Nature Genetics* **48**, 1233-41.
- Wang Y, Xu H, Zhang G et al.** 2009. Expression and responses to dehydration and salinity stresses of V-PPase gene members in wheat. *Journal of Genetics and Genomics* **36**, 711-720.
- Wei Q, Hu P and Kuai BK.** 2012. Ectopic expression of an *Ammopiptanthus mongolicus* H<sup>+</sup>-pyrophosphatase gene enhances drought and salt tolerance in *Arabidopsis*. *Plant Cell, Tissue and Organ Culture* **110**, 359-369.
- Wheeler GL, Jones MA and Smirnoff N.** 1998. The biosynthetic pathway of vitamin C in higher plants. *Nature* **393**, 365-369.
- Wu GQ, Feng RJ, Wang SM et al.** 2015. Co-expression of xerophyte *Zygophyllum xanthoxylum* *ZxNHX* and *ZxVP1-1* confers enhanced salinity tolerance in chimeric sugar beet (*Beta vulgaris* L.). *Frontiers in Plant Science* **6**, <https://doi.org/10.3389/fpls.2015.00581>.
- Yang H, Knapp J, Koirala P et al.** 2007. Enhanced phosphorus nutrition in monocots and dicots over-expressing a phosphorus-responsive type I H<sup>+</sup>-pyrophosphatase. *Plant Biotechnology Journal* **5**, 735-745.
- Yang H, Zhang X, Gaxiola RA et al.** 2014. Over-expression of the *Arabidopsis* proton-pyrophosphatase *AVP1* enhances transplant survival, root mass, and fruit development under limiting phosphorus conditions. *Journal of Experimental Botany* **65**, 3045-3053.
- Yang Y, Tang RJ, Li B et al.** 2015. Overexpression of a *Populus trichocarpa* H<sup>+</sup>-pyrophosphatase gene *PtVP1.1* confers salt tolerance on transgenic poplar. *Tree Physiology* **35**, 663-77.
- Yao YX, Dong QL, You CX et al.** 2011. Expression analysis and functional characterization of apple *MdVHP1* gene reveals its involvement in Na<sup>+</sup>, malate and soluble sugar accumulation. *Plant Physiology and Biochemistry* **49**, 1201-1208.
- Zhang J, Li J, Wang X et al.** 2011. *OVP1*, a vacuolar H<sup>+</sup>-translocating inorganic pyrophosphatase (V-PPase), overexpression improved rice cold tolerance. *Plant Physiology and Biochemistry* **49**, 33-38.
- Zhao FY, Zhang XJ, Li PH et al.** 2006. Co-expression of the *Suaeda salsa* *SsNHX1* and *Arabidopsis* *AVP1* confer greater salt tolerance to transgenic rice than the single *SsNHX1*. *Molecular Breeding* **17**, 341-353.
- Zhen R, Kim E and Rea P.** 1997. The molecular and biochemical basis of pyrophosphate-energized proton translocation at the vacuolar membrane. *Advances in Botanical Research* **25**, 297-337.

**Chapter 2 - Metabolite profiling of *AVP1* over-expressing and  
loss-of-function Arabidopsis**

## Statement of Authorship

Title of Paper	Expression of the proton-pumping pyrophosphatase gene, <i>AVP1</i> , regulates metabolism in <i>Arabidopsis thaliana</i> seedlings
Publication Status	<input type="checkbox"/> Published <input type="checkbox"/> Accepted for Publication <input type="checkbox"/> Submitted for Publication <input checked="" type="checkbox"/> Unpublished and Unsubmitted work written in manuscript style
Publication Details	This manuscript has been written and formatted for publication in Plant Molecular Biology.

### Principal Author

Name of Principal Author (Candidate)	Daniel J. Menadue				
Contribution to the Paper	Contributed to the experimental design, grew and sampled plants, conducted the genotyping, gene expression and gene sequencing, conducted phenotyping and microscopy analysis, prepared samples for metabolomics analysis, statistically analysed and interpreted the data and wrote the manuscript.				
Overall percentage (%)	80				
Certification:	This paper reports on original research I conducted during the period of my Higher Degree by Research candidature and is not subject to any obligations or contractual agreements with a third party that would constrain its inclusion in this thesis. I am the primary author of this paper.				
Signature	<table border="1" style="width: 100%;"> <tr> <td style="width: 80%;"></td> <td style="width: 20%;">Date</td> </tr> <tr> <td></td> <td>28/5/2018</td> </tr> </table>		Date		28/5/2018
	Date				
	28/5/2018				

### Co-Author Contributions

By signing the Statement of Authorship, each author certifies that:

- i. the candidate's stated contribution to the publication is accurate (as detailed above);
- ii. permission is granted for the candidate to include the publication in the thesis; and
- iii. the sum of all co-author contributions is equal to 100% less the candidate's stated contribution.

Name of Co-Author	Rhiannon K. Schilling				
Contribution to the Paper	Contributed to the experimental design, assisted with data interpretation and contributed to revision of the manuscript.				
Signature	<table border="1" style="width: 100%;"> <tr> <td style="width: 80%;"></td> <td style="width: 20%;">Date</td> </tr> <tr> <td></td> <td>4/6/2018</td> </tr> </table>		Date		4/6/2018
	Date				
	4/6/2018				

Name of Co-Author	Darren C. Plett		
Contribution to the Paper	Contributed to the experimental design, assisted with data interpretation and contributed to revision of the manuscript.		
Signature		Date	4/6/2018

Name of Co-Author	Stuart J. Roy		
Contribution to the Paper	Conceived the research project, contributed to the experimental design, assisted with data interpretation and contributed to revision of the manuscript.		
Signature		Date	28/5/2018

## Expression of the proton-pumping pyrophosphatase gene, *AVP1*, influences metabolite concentrations in *Arabidopsis thaliana* seedlings

**Running title:** Metabolite profiling of *AVP1* over-expressing and loss-of-function *Arabidopsis*

Daniel Jamie Menadue<sup>1,2</sup>, Rhiannon Kate Schilling<sup>1,2</sup>, Darren Craig Plett<sup>1,2</sup> and Stuart John Roy<sup>1,2\*</sup>

<sup>1</sup>School of Agriculture, Food and Wine, The University of Adelaide, SA, 5005, Australia

<sup>2</sup>Australian Centre for Plant Functional Genomics, Glen Osmond, SA, 5064, Australia

\*Corresponding author: Daniel Menadue, School of Agriculture, Food and Wine, The University of Adelaide, SA 5005 Australia, daniel.menadue@adelaide.edu.au, Tel: +61 8 8313 7162, Fax: +61 8 8313 7102

**Tables:** 2

**Figures:** 6

**Word count:** 6255

**Keywords:** *35S:AVP1*, ascorbic acid, auxin, *fugu5*, H<sup>+</sup>-PPase, sucrose

## Key message

Constitutive over-expression of *AVP1* increased concentrations of multiple metabolites in transgenic *Arabidopsis* seedlings, while reduced *AVP1* expression decreased concentrations, indicating *AVP1* expression is important for regulating metabolism in *Arabidopsis* seedlings.

## Abstract

In *Arabidopsis* (*Arabidopsis thaliana*) the function of endogenous *AVP1*, a vacuolar proton-pumping pyrophosphatase ( $H^+$ -PPase), is important during heterotrophic growth, having beneficial impacts on growth under non-stressed and stressed conditions. While sucrose concentrations have been reported to be enhanced in *AVP1* over-expressing *Arabidopsis*, and reduced in *AVP1* loss-of-function (*fugu5*) mutants, alterations in the overall metabolome of these lines are yet to be compared. In this study, metabolites in 8 d-old transgenic *Arabidopsis* seedlings, constitutively over-expressing *AVP1* (*AVP1-1*, *AVP1-2*, *35S:AVP1*), as well as *AVP1* loss-of-function mutants (*fugu5-1*, *fugu5-2*, *fugu5-3*) were analysed via gas chromatography-mass spectrometry (GC-MS). The concentration of metabolites within the glycolysis, gluconeogenesis and shikimate pathways, as well as those in the tricarboxylic acid cycle and several ascorbic acid pathways, increased in *35S:AVP1* lines and decreased in *fugu5* mutants, compared to wild-type. In contrast to earlier studies, *35S:AVP1* seedlings contained less sucrose compared to wild-type, while in *fugu5* mutants, sucrose concentrations increased. In contrast to previous characterisation, the *AVP1-1* and *AVP1-2* lines were found to have extremely low levels of the *AVP1* transgene, limiting the conclusions that could be made from the analysis of these lines. These results indicate that *AVP1* is likely to regulate various  $PP_i$  dependent metabolic pathways, with multiple factors likely to influence the role of *AVP1*.

## Introduction

*AVP1* is a membrane bound protein in Arabidopsis, which regulates cytosolic pyrophosphate ( $PP_i$ ) levels (Sarafian et al 1992) and generates an electrochemical potential difference for protons ( $H^+$ ) across the tonoplast (Rea and Sanders 1987). Transgenic plants expressing *AVP1* have numerous phenotypes, which have implicated *AVP1* in the regulation of several processes, including vacuolar ion sequestration (Gaxiola et al 2001), auxin transportation (Li et al 2005), gluconeogenesis (Ferjani et al 2011) and sucrose respiration (Gaxiola et al 2012), as well as the Smirnoff-Wheeler ascorbic acid pathway (Schilling 2014; Schilling et al 2017).

Evidence for the involvement of *AVP1* in regulating cytosolic  $PP_i$  concentrations was first reported in Arabidopsis mutants, in which *AVP1* function was either reduced (*fugu5-1*, *fugu5-2*) or inhibited (*fugu5-3*) (Ferjani et al 2007; Ferjani et al 2011). On basal Murashige and Skoog (MS) media lacking vitamins and sugars (Murashige and Skoog 1962), heterotrophic growth was significantly reduced in *fugu5* mutants compared to wild-type (Ferjani et al 2011). On basal MS media, 8 d-old *fugu5-1* mutants had a 60 % reduction in cotyledon cell number compared to wild-type, while the mutant leaf cells were 1.4-fold larger than wild-type (Ferjani et al 2011). Tissue analysis revealed 3 d-old *fugu5-3* seedlings had 2.5-fold higher  $PP_i$  and 50 % less sucrose in the leaf than wild-type seedlings, while the vacuolar pH in cells from 10 d-old seedlings was 0.25 pH units higher than wild-type (Ferjani et al 2011). Addition of glucose, sucrose, or a combination of both to the growth medium restored seedling growth to the *fugu5* mutants, similar to that of wild-type (Ferjani et al 2011). With high levels of cytosolic  $PP_i$  known to inhibit gluconeogenesis (Stitt 1989), it was hypothesised that reduced heterotrophic growth in the *fugu5* mutants was the result of  $PP_i$  accumulation within the cytosol, thereby inhibiting sucrose production via gluconeogenesis (Ferjani et al 2011). This hypothesis has been further supported by analysis of 3.5 d-old etiolated *fugu5-1* mutants, in which a 50 % reduction in sucrose and



1.6-fold increase in  $PP_i$  concentration was reported (Segami et al 2018). However, despite evidence in *fugu5* mutants, it remains unclear whether this hypothesis is responsible for the improved growth observed in transgenic plants over-expressing *AVP1*.

In addition to regulating gluconeogenesis, a role for *AVP1* in sucrose respiration and phloem loading has also been proposed (Gaxiola et al 2012; Pizzio et al 2017). While initially considered to localise exclusively to the vacuole membrane, several  $H^+$ -PPase proteins, including *AVP1*, have also been shown to localise to the plasma membrane of sieve element-companion cells in *Ricinus communis* (Langhans et al 2001), *Arabidopsis* (Paez-Valencia et al 2011) and rice (Regmi et al 2016). In transgenic *Arabidopsis*, constitutive and phloem-cell specific expression of *AVP1* enhanced plant biomass, sucrose concentration and source to sink transportation of sucrose (Khadilkar et al 2016; Pizzio et al 2015). As such, it has been hypothesised that *AVP1* may function as a  $PP_i$  synthase when localised to the plasma membrane of sieve-element companion cells (Gaxiola et al 2012; Pizzio et al 2017). Through functioning as a  $PP_i$  synthase, it is proposed that *AVP1* enhances ATP production via sucrose respiration by increasing cytosol  $PP_i$  concentrations. This increase in ATP production is proposed to enhance activity of plasma membrane  $H^+$ -ATPase and Suc/ $H^+$  transporters, resulting in enhanced sucrose phloem loading (Gaxiola et al 2012). However, limited metabolomics analysis has been conducted to investigate this hypothesis.

In transgenic barley (cv. Golden Promise) constitutively expressing *AVP1*, the concentration of several metabolites within the Smirnoff-Wheeler ascorbic acid synthesis pathway were found to be significantly different to wild-type (Schilling 2014), suggesting another potential role for *AVP1* in plant metabolism. Within the 1<sup>st</sup> leaf of 11 d-old transgenic barley seedlings, galactose was 60-80 % lower, ascorbic acid was 1.9- to 3.8-fold higher, and dehydroascorbic acid was

15.0- to 13.1-fold higher compared to wild-type under non-stressed conditions (Schilling 2014; Schilling et al 2014). Reduced PP<sub>i</sub> activity has also been shown to reduce galactose and increase ascorbic acid and dehydroascorbic acid concentrations in tomato fruit (Osorio et al 2013), and increase ascorbic acid in potato tubers (Farré et al 2006). In addition, the growth of transgenic barley expressing *AVP1* was improved in saline and nutrient limited conditions compared to wild-type (Schilling, 2014), conditions under which ascorbic acid has also been shown to enhance plant growth (Hemavathi et al 2010; Lisko et al 2013; Ramírez et al 2013).

Ascorbic acid (vitamin C) is also known to be involved in cell division (Conklin 2001) and cell expansion (Conklin 2001; Horemans et al 1994), which were inhibited in *fugu5* mutants (Ferjani et al 2011), influence flowering time (Barth et al 2006; Gallie 2013) and fruit ripening (Osorio et al 2013), and aids in the detoxification of reactive oxygen species (Foyer et al 1995). To produce ascorbic acid via the Smirnoff-Wheeler pathway, D-mannose-1 phosphate is converted to GDP-D-mannose, producing cytosolic PP<sub>i</sub> as a by-product (Wheeler et al 1998). Therefore, the improved growth of the transgenic barley, under both stressed and non-stressed conditions, was proposed to be the result of enhanced cytosolic PP<sub>i</sub> hydrolysis by *AVP1*, leading to increased production of ascorbic acid via the Smirnoff-Wheeler pathway, or a reduced metabolic demand for ascorbic acid and dehydroascorbic acid as a result of being larger and healthier than the wild-type (Schilling 2014). This hypothesis, however, is yet to be investigated in other transgenic plants constitutively expressing *AVP1*.

Despite being implicated in various metabolic processes, the direct impact of *AVP1* function on the *Arabidopsis* metabolome has not been sufficiently assessed, with only several studies having conducted metabolomics analysis of *AVP1* over-expressing *Arabidopsis* (Gonzalez et al 2010; Khadilkar et al 2016) and *AVP1* loss-of-function *Arabidopsis* (Ferjani et al 2011; Segami

et al 2018). In the leaf of 10 d-old *AVP1-1* seedlings, concentrations of glucose, tryptophan and fructose 6-phosphate were 1.7-fold, 1.5-fold and 1.3-fold higher than wild-type, respectively (Gonzalez et al 2010). In addition, starch concentration in *AVP1-1* was unaltered compared to wild-type, while the concentration of ascorbic acid varied significantly between the two sampling times (Gonzalez et al 2010). At end of day, ascorbic acid concentration within the leaf of *AVP1-1* over-expressing *Arabidopsis* seedlings was 1.3-fold higher than wild-type, while concentrations were 120 % lower at midday (Gonzalez et al 2010). In 22 d-old *35S:AVP1* transgenic *Arabidopsis*, the concentration of glucose was 1.4-fold higher in the leaf than wild-type, but remained unaltered in the root (Khadilkar et al 2016). In addition, concentrations of malate, fumarate and glucose 6-phosphate were unaltered in both shoot and root, starch concentration was 25 % lower than wild-type, and ascorbic acid was not measured (Khadilkar et al 2016). Limited metabolomics analysis has also been conducted on *AVP1* loss-of-function mutants, with sucrose reported to be reduced up to 50 % in 3 d-old *fugu5-1* (Segami et al 2018) and *fugu5-3* (Ferjani et al 2011) mutants compared to wild-type, and a 10 % reduction in glucose and a 5 % increase in starch also reported in *fugu5-1* seedlings compared to wild-type (Segami et al 2018).

Due to the lack of comprehensive metabolomics data, the impact of *AVP1* activity on the metabolome of *Arabidopsis* remains unclear. The aim of this research was to investigate the impact of *AVP1* expression on the metabolome of *Arabidopsis* seedlings through quantifying differences in metabolite concentrations between wild-type (*Col-0*), *AVP1* over-expressing (*AVP1-1*, *AVP1-2* and *35S:AVP1*) and *AVP1* loss-of-function mutant (*fugu5-1*, *fugu5-2* and *fugu5-3*) *Arabidopsis* lines.

## Materials and Methods

### Plant material and growth conditions

The Arabidopsis lines used in this study included *Col-0* wild-type (WT), three independent transgenic lines constitutively over-expressing *AVP1* (*AVP1-1*, *AVP1-2* and *35S:AVP1*) (Gaxiola et al 2001; Pizzio et al 2015) and the mutant *fugu5-1*, *fugu5-2* and *fugu5-3* lines, in which *AVP1* function was reduced (*fugu5-1*, *fugu5-2*) or inhibited (*fugu5-3*) (Ferjani et al 2011) via fast-neutron bombardment (Horiguchi et al 2006). The *AVP1-1* and *AVP1-2* lines were generated as described in Gaxiola et al (2001), while the *35S:AVP1* lines were generated as described in Pizzio et al (2015). In all over-expressing lines, expression of the *AVP1* transgene was driven by the cauliflower mosaic virus (CaMV) 35S dual enhancer promoter and were generated via *Agrobacterium*-mediated transformation (Gaxiola et al 2001; Pizzio et al 2015). All Arabidopsis lines were kindly provided by Associate Professor Roberto Gaxiola (Arizona State University, United States). To reduce any potential variation between the lines due to seed quality, all lines were grown together in a growth chamber, with seed collected from these plants used for all further experiments. Seed were sterilised with 30 % (v/v) bleach (White King, Melbourne, Australia) and 70 % (v/v) ethanol, and rinsed in sterile water. Seed were imbibed for 48 h in the dark at 4°C in 1 mL sterile water. Following imbibition, seed were pipetted onto basal MS medium without vitamins (PhytoTechnology Laboratories®, Lenexa, United States) in Petri dishes (100 × 100 × 20 mm)(SARSTEDT, Technology Park, Australia). Plates were sealed with Micropore™ tape (3M, North Ryde, Australia) and placed vertically in a growth chamber (12 h day/night length, 22°C day and 18°C night temperatures, 100 μmol m<sup>-2</sup> s<sup>-1</sup> light intensity and 60-80 % relative humidity) for 14 d. Following germination, seedlings were transplanted into individual pots (90 × 70 × 50 mm) containing 250 g of Arabidopsis soil mix (25 % (v/v) sand, 25 % (v/v) perlite, 25 % (v/v) vermiculate and 25 % (v/v) peatmoss, supplemented with 0.1 % (v/v)

iron sulphate, 0.3 % (v/v) Osmocote® Plus (Scotts, Bella Vista, Australia), 0.2 % (v/v) dolomite, 0.05 % (v/v) gypsum, 0.1 % (v/v) agricultural lime and 0.04 % (v/v) hydrated lime) and grown until maturity.

### Genotypic analysis

To confirm presence or absence of the *AVP1* transgene in the wild-type and *AVP1* over-expressing lines, as well as verify mutations within the *fugu5* lines, genomic DNA (gDNA) was extracted from leaf tissue using a modified Edwards et al (1991) protocol. In brief, DNA was lysed from cells by digesting leaf tissue in extraction buffer (100 mM Tris-HCl (pH 7.5), 50 mM EDTA (pH 8.0), 1.25 % SDS) at 65°C for 45 min. DNA was precipitated with 6 M ammonium acetate and 100 % (v/v) isopropanol. Pelleted DNA was washed with 70 % (v/v) ethanol and resuspended in R40 (40 µg/mL RNase A (Sigma-Aldrich, St. Louis, United States) in 1× TE buffer). Presence of the Arabidopsis *Actin2* gene (*AT3G18780*) and the Arabidopsis *AVP1* transgene (*AT1G15690*) were determined by PCR amplification using gene specific primers (Table 1). All reactions were performed with an initial denaturation at 94°C for 2 min, 30 cycles of 94°C for 30 s, a primer specific annealing temperature for 30 s (Table 1), extension at 68°C for 30 s, and a final extension at 68°C for 5 min. Each reaction contained 1 µl (~0.5 µg) extracted gDNA, 1× OneTaq® 2× Master Mix (20 mM Tris-HCl, 0.2 mM dNTPs, 0.025 U DNA polymerase, 1.8 mM MgCl<sub>2</sub>) (New England Biolabs, Ipswich, United States), 0.2 µM forward primer and 0.2 µM reverse primer, in a final volume of 25 µl. PCR products were visualised using a UV-transilluminator (Clinx, Shanghai, China) on 1.5 % agarose gels containing 0.005 % (v/v) SYBR® Safe DNA stain (ThermoFisher Scientific, Waltham, United States). To confirm each of the *fugu5* lines contained mutations within the *AVP1* gene as previously described (Ferjani et al 2011),

DNA regions containing the mutations were amplified via PCR using primers specific to each mutation region (Table 1), PCR products were purified using a Nucleospin® Gel and PCR clean-up kit (Macherey-Nagel, Düren, Germany) according to the manufacturer's instructions and Sanger sequencing was performed using a BigDye™ Terminator v3.1 Cycle Sequencing Kit (ThermoFisher Scientific) for DNA labelling. Samples were sequenced via capillary separation using a 3730xl DNA Analyzer (ThermoFisher Scientific) and sequence reads were aligned, translated and annotated in Geneious® 10.1.3 (Biomatters Ltd., Auckland, New Zealand).

### Gene expression analysis

RNA was extracted from pooled samples of 8 d-old Arabidopsis seedlings using a DirectZol RNA purification kit (Zymo Research, Irvine, United States) and contaminating gDNA was removed with an in-column DNase treatment (Zymo Research) according to the manufacturer's instructions. Complementary DNA (cDNA) was reverse transcribed using an AffinityScript cDNA synthesis kit (Agilent Technologies, Santa Clara, United States) according to manufacturer's instructions. Each reaction contained 1 µl RNA, standardised to 0.25 µg using a NanoDrop 1000 spectrophotometer (ThermoFisher Scientific), 10 µl 2× first strand master mix, 0.3 µg oligo(dT), 1 µl AffinityScript RT/RNase Block enzyme mixture, and sterile water to a final volume of 20 µl. Reactions were incubated at 25°C for 5 min for primer annealing, followed by 45 min at 42°C for cDNA synthesis, and terminated at 95°C for 5 min. Expression of the *AVP1* transgene was analysed via semi-quantitative reverse-transcription PCR (RT-PCR) by amplifying fragments of the *AVP1* and *AtActin2* genes, as described above. Transgene expression, relative to *AtActin2*, was determined by comparing band intensities of each sample when visualised on a 1.5 % agarose gel using GIMP 2.8.18 image manipulation software ([www.gimp.org](http://www.gimp.org)).

### Phenotyping of *Arabidopsis* seedlings

Bulked seed from the wild-type, *AVP1* mutant (*fugu5-1*, *fugu5-2*, *fugu5-3*) and *AVP1* over-expressing (*AVP1-1*, *AVP1-2*, *35S:AVP1*) *Arabidopsis* lines, sterilised and imbibed as described above, were grown on basal MS media with and without 2 % sucrose, in a growth chamber as previously described. Following 8 d growth, 6 uniform size seedlings from each line were selected for phenotypic characterisation. For each seedling, primary root length (mm) was measured before cotyledons were detached and sealed inside Petri dishes (100 × 100 × 20 mm) on basal MS media, adaxial side upwards. Cotyledons were individually imaged using a SMZ25 stereo microscope (2 × Plan Apo objective with 0.312 numerical aperture (NA), 20 mm working distance (WD) and 0.63 × magnification) fitted with a DS-Ri1 high-resolution digital camera (Nikon, Minato, Japan). First leaf length (mm), first leaf width (mm) and first leaf area (mm<sup>2</sup>) were determined using NIS-Elements Advanced Research software (Nikon).

### Metabolomics analysis of whole *Arabidopsis* seedlings

For metabolomics analysis, wild-type, *AVP1* over-expressing (*AVP1-1*, *AVP1-2* and *35S:AVP1*) and *fugu5* mutant (*fugu5-1*, *fugu5-2* and *fugu5-3*) seed were sterilised and imbibed as previously described. Following imbibition, seed from each line were pipetted onto 3 replicate Petri dishes containing basal MS media and grown as previously described. Following 8 d growth (as per Ferjani et al 2011), whole seedlings from each Petri dish were pooled into individual 2 mL centrifuge tubes and frozen in liquid nitrogen. For each *Arabidopsis* line, metabolites were extracted from the 3 replicates of pooled freeze-dried *Arabidopsis* seedlings (2.5 ± 0.1 mg) using a methanol extraction protocol (Hill and Roessner 2013). Each sample was

homogenised in 100 % (v/v) methanol and 4 % (v/v)  $^{13}\text{C}_6$ -sorbitol/ $^{15}\text{N}$ -valine (0.5 mg/mL) at -10°C using a CryoMill (Retsch, Haan, Germany). Samples were shaken at 30°C for 15 min in a ThermoMixer® (Eppendorf, Hamburg, Germany) before centrifuging at 12 000 *g* for 10 min. Supernatants were washed in Milli-Q H<sub>2</sub>O, dried to 40 µl aliquots using a rotational vacuum concentrator (at room temperature) and derivatised with 20 µl methoxyamine hydrochloride and 20 µl N, O-Bistrifluoroacetamide (BSTFA). Metabolite concentrations were quantified via gas chromatography-mass spectrometry (GC-MS) in 1 µl aliquots of each sample using an Agilent 7890 gas chromatograph coupled with an Agilent 7000 triple-quadrupole (QqQ) mass spectrometer (Agilent Technologies, Santa Clara, United States).

### Statistical analysis

Statistically significant differences were determined via two-way ANOVA (phenotypic data) and one-way ANOVA (metabolomics data), with Tukey's 95 % confidence intervals ( $P \leq 0.05$ ), in GenStat® version 15.3.

## Results

### **Arabidopsis *fugu5* mutants contain nucleotide polymorphisms within the *AVP1* gene and transgene expression level varies between *AVP1* over-expressing lines**

To confirm mutations within the *AVP1* gene sequence in *fugu5* mutant Arabidopsis lines, amplified gDNA products were sequenced. This confirmed the presence of a nucleotide substitution (G-A at position 3072) in the *fugu5-1* mutants (Fig. 1A), a substitution (G-A at position 1201) in the *fugu5-2* mutants (Fig. 1B), and a substitution (G-A at position 2442) and deletion (2444-2458) in the *fugu5-3* mutants (Fig. 1C). These results were consistent with the



findings of Ferjani et al (2011), who found these nucleotide changes resulted in reduced *AVP1* function in the *fugu5-1* and *fugu5-2* mutants, and inhibited *AVP1* function in the *fugu5-3* mutant. Genotypic analysis of the *AVP1* over-expressing (*AVP1-1*, *AVP1-2* and *35S:AVP1*) lines identified twelve *35S:AVP1* sibling lines as transgenic, however, as expression of the *AVP1* transgene could only be detected in one of these lines (Fig. A1), this single line was selected for further experimentation. While expression of the *AVP1* transgene was detected in all *AVP1-1* and *AVP1-2* sibling lines during preliminary screening, transgene expression was 82 % and 94 % lower than the *35S:AVP1* lines respectively (Fig. A2). As such, the *AVP1-1* and *AVP1-2* lines with the highest level of transgene expression were selected for further experimentation.

### **Root length, leaf width and total leaf area are reduced in *fugu5* mutants compared to *35S:AVP1* and wild-type**

Following 8 d on basal MS lacking vitamins and sugars, *fugu5* seedlings had significantly reduced leaf and root growth compared to wild-type and *35S:AVP1* seedlings (Fig. 2 and 3). On basal MS, primary root length of *fugu5* mutants showed an average reduction of 40 % and 20 % compared to wild-type and *35S:AVP1* seedlings, respectively, while primary root length was 25 % lower in *35S:AVP1* seedlings compared to wild-type (Fig. 3A). When supplied with 2 % sucrose, primary root length of *fugu5* seedlings increased by an average of 44 % compared to *fugu5* seedlings on basal MS, while primary root length increased by 50 % in *35S:AVP1* seedlings compared to basal MS (Fig. 3A). There were (as per Ferjani et al 2011) no significant differences in the primary root length of wild-type seedlings on basal MS compared to those on MS media supplemented with 2 % sucrose (Fig. 3A).

No significant differences in leaf length were observed between any of the lines on basal MS media or MS media containing sucrose (Fig. 3B). Between treatments, leaf length increased 12 % in wild-type seedlings and 20 % in *fugu5-2* and *fugu5-3* seedlings, while leaf length did not significantly differ between treatments in either *fugu5-1* or *35S:AVP1* seedlings (Fig. 3B). On basal MS, leaf width of *fugu5* mutants was approximately 20 % lower than both wild-type and *35S:AVP1* seedlings (Fig. 3C), while no difference in leaf width occurred between wild-type and *35S:AVP1* lines (Fig. 3C). When supplied with sucrose, leaf width in the *fugu5* mutants increased 25 % compared to *fugu5* mutants on basal MS, while there were no significant increases in leaf width of wild-type or *35S:AVP1* seedlings (Fig. 3C). No significant differences in leaf width were apparent between any of the lines when supplied with sucrose (Fig. 3C).

Total leaf area was 35 % lower in *fugu5-2* seedlings and 40 % lower in *fugu5-3* seedlings compared to both wild-type and *35S:AVP1* seedlings on basal MS, while no significant differences were apparent between wild-type, *fugu5-1* or *35S:AVP1* seedlings (Fig. 3D). When supplied with sucrose, total leaf area remained unaltered compared to basal MS in wild-type and *35S:AVP1* seedlings, while the leaf area of *fugu5-1*, *fugu5-2* and *fugu5-3* seedlings increased 45 %, 80 % and 83 % respectively, compared to basal MS (Fig. 3D). No significant differences in total leaf area were observed between wild-type, *fugu5* or *35S:AVP1* seedlings on MS media supplemented with sucrose (Fig. 3D).

In the low *AVP1* expressing *AVP1-1* line, primary root length was 30 % lower on basal MS and 35 % lower on MS supplied with sucrose compared to the low *AVP1* expressing *AVP1-2* line and the highly expressing *35S:AVP1* line (Fig. A3). When supplied with sucrose, primary root length increased 46 %, 50 % and 55 % in *AVP1-1*, *AVP1-2* and *35S:AVP1* seedlings, respectively, compared to basal media (Fig. A3). On basal MS, leaf length, leaf width or leaf area did not

significantly differ between any of the lines, while *AVP1-2* was the only line to show an increase in leaf length, leaf width or leaf area when supplied with sucrose, compared to basal MS (Fig. A3). When supplied with sucrose, leaf length did not significantly differ between the lines, while leaf width and length were 10 % and 20 % higher in the *AVP1-2* line respectively, compared to the *AVP1-1* line (Fig. A3). Total leaf area was also 25 % higher in the *AVP1-2* lines compared to *AVP1-1* and *35S:AVP1* seedlings when supplied with sucrose (Fig. A3). The only significant differences between the low *AVP1* expressing lines and wild-type were leaf area in the *AVP1-2* line, which was ~ 10 % higher than wild-type when supplied with sucrose, and root length in the *AVP1-1* line, which was 20 % lower than wild-type when supplied with sucrose (Figures 3 and A3). Preliminary screening of wild-type and *fugu5* mutants showed that primary root length in the *fugu5* mutants increased 3-fold when supplied with 2 % sucrose, and 2-fold when supplied with 4 % glucose, compared to basal MS (Fig. A4).

#### **Multiple metabolites are reduced in *fugu5* mutant seedlings compared to wild-type**

In 8 d-old *fugu5* seedlings, a large proportion of the metabolites analysed were reduced compared to wild-type seedlings. Compared to wild-type, *fugu5* mutants contained reduced concentrations of fructose (-36 to -63 %), trehalose (-42 to -57 %), nicotinic acid (-25 to -36 %), ribose (-29 to -30 %), xylose (-24 to -33 %), inositol (-20 to -33 %), maleate (-12 to -33 %), erythritol (-24 to -27 %), glucose (-20 to -34 %), arabinose (-13 to -27 %), citrate (-5 to -31 %), galactose (-15 to -21 %), malate (-3 to -27 %), fumarate (-5 to -31 %), isocitrate (-3 to -20 %), succinate (-5 to -17 %), fucose (-8 to -11 %), maltose (-1 to -16 %) and raffinose (-4 to -13 %) (Table 2, Fig. 4). While the majority of the metabolites analysed in the *fugu5* mutants were reduced compared to wild-type, concentrations of several metabolites increased slightly

compared to wild-type, such as 2-ketoglutaric acid (7-18 %), shikimate (5-27 %) and glucose 6-phosphate (3-17 %) (Table 2, Fig. 4). In addition, changes in several metabolites varied considerably between the *fugu5* lines relative to wild-type. While xylitol increased 71 % and 54 % in the *fugu5-1* and *fugu5-3* lines compared to wild-type, xylitol decreased 65 % in the *fugu5-2* line compared to wild-type (Fig. 4). The *fugu5-1* and *fugu5-2* mutants also contained 28 % and 42 % higher sucrose than wild-type, while the *fugu5-3* mutant contained 18 % lower sucrose than the wild-type (Fig. 4). Fructose 6-phosphate concentrations also varied relative to wild-type, with the concentration decreasing by 9 % and 16 % in the *fugu5-1* and *fugu5-3* mutants and increasing by 43 % in the *fugu5-2* mutant (Fig. 4).

#### **Multiple metabolites are increased in *35S:AVP1* seedlings compared to wild-type**

In contrast to the *fugu5* mutants, the concentration of multiple metabolites within the *35S:AVP1* over-expressing seedlings increased compared to wild-type. Compared to wild-type, *35S:AVP1* seedlings contained higher concentrations of maltose (108 %), fructose 6-phosphate (60 %), glucose 6-phosphate (40 %), inositol (51 %), fumarate (38 %), shikimate (37 %), citrate (27 %), malonate (19 %), malate (16 %), ribose (13 %), mannose (7 %), succinate (6 %) and glucose (5 %) (Table 1, Fig. 4). While the majority of metabolites increased in concentration in the *35S:AVP1* lines, the concentration of several metabolites were lower in these lines compared to wild-type, including xylitol (-92 %), fructose (-53 %), nicotinic acid (-38 %), erythritol (-15 %), sucrose (-14 %), maleate (-12 %), arabinose (-11 %) and xylose (-5 %) (Table 1, Fig. 4).

**Metabolite concentrations vary between the low *AVP1* expressing *AVP1-1*, *AVP1-2* lines and the highly expressing *35S:AVP1* line**

While the majority of metabolites increased within *35S:AVP1* seedlings compared to wild-type, metabolite concentrations in the *AVP1-1* and *AVP1-2* lines, which had only a low level of *AVP1* transgene expression (Fig. A2), were reduced (Table A1). Compared to wild-type, the *AVP1-1* and *AVP1-2* lines contained lower concentrations of xylitol (-95 and -90 %), fructose (both -85 %), glucose (-88 and -52 %), trehalose (-56 and -37 %), sucrose (-56 and -30 %), fructose 6-phosphate (-53 and -24 %), erythritol (-34 and -37 %), xylose (-42 and -29 %), shikimate (-47 and -15 %), succinate (-29 and -32 %), maltose (-38 and -23 %), inositol (-56 and -2 %), citrate (-28 and -25 %), fumarate (-29 and -23 %), malate (-5 and -41 %), mannose (-31 and -14 %), arabinose (-26 and -16 %), glucose 6-phosphate (-25 and -15 %), maleate (-5 and -24 %), raffinose (-16 and -3 %), fucose (-15 and -9 %) and galactose (-16 and -3 %) respectively (Table A1). The only metabolite concentrations to increase compared to wild-type in the *AVP1-1* and *AVP1-2* lines were malonate (24 and 50 %), 2-hydroxy glutaric acid (25 and 3 %), turanose (5 and 20 %) and 2-keoglutaric acid (20 and 1 %) (Table A1). Concentrations of some metabolites relative to wild-type differed between the two lowly expressing *AVP1* lines, with nicotinic acid 20 % lower in *AVP1-1* and 60 % higher in *AVP1-2*, and ribose 19 % lower in *AVP1-1* and 28 % higher in *AVP1-2*, compared to wild-type (Table A1). In contrast, concentrations of aconitate and isocitrate were 7 % and 19 % higher, respectively, in *AVP1-1* compared wild-type, while concentrations in *AVP1-2* were 4 % and 13 % lower, respectively (Table A1).

## Discussion

### The *AVP1* transgene is downregulated or silenced in the *AVP1-1* and *AVP1-2* over-expressing Arabidopsis lines

While the amino acid alterations and deletions in the *fugu5* mutant lines were consistent with that of previous reports (Ferjani et al 2011), the expression levels of *AVP1* within the well characterised *AVP1-1* and *AVP1-2* lines (Fig. A2) were significantly lower than previously reported (Gaxiola et al 2001; Khadilkar et al 2016; Pizzio et al 2015). In addition, expression of the *AVP1* transgene was detected in only a single *35S:AVP1* line (Fig. A1). A high level of *AVP1* transgene-silencing was previously reported in *AVP1-1* and *AVP1-2* Arabidopsis lines (Kriegel et al 2015), while a high level of *AVP1* transgene expression was detected in newly produced transgenic Arabidopsis lines (Khadilkar et al 2016). The low level of *AVP1* transgene expression in the *AVP1-1* and *AVP1-2* lines, in addition to *AVP1* transgene expression only being detected in a single *35S:AVP1* transgenic line, indicates that transgene silencing occurs at a high rate in subsequent generations of *AVP1* expressing transgenic plants. Consequently, the results of this study will predominately be discussed in relation to the *35S:AVP1* transgenic line, however, it should be noted to only one independent *35S:AVP1* line was analysed in this study. Furthermore, as many subsequent studies have characterised the *AVP1-1* and *AVP1-2* lines generated by Gaxiola et al (2001), the high occurrence of transgene silencing in these lines should be considered when interpreting results from these studies.

### Sucrose concentrations vary between *fugu5* mutants on basal MS

In general, metabolites within the *fugu5* mutants (lacking *AVP1*) were reduced compared to wild-type (Fig. 5), while in *35S:AVP1* seedlings (over-expressing *AVP1*), metabolite

concentrations increased compared to wild-type (Fig. 6). In the *fugu5* mutants, the concentration of sugars, such as glucose, galactose, maltose, fructose and trehalose, as well as metabolites within the tricarboxylic acid (TCA) cycle were reduced compared to wild-type (Fig. 5), while the majority of these metabolites increased in *35S:AVP1* seedlings (Fig. 6). However, several metabolites were exceptions to this, the most notable of which was sucrose. In the *fugu5-3* mutant, the concentration of sucrose was 18 % lower than wild-type, which supports the findings of Ferjani et al (2011), in which sucrose concentrations were 50 % that of the wild-type. However, sucrose concentrations within *fugu5-1* and *fugu5-3* mutants increased by 28 % and 42 % respectively, which conflicts with the findings of Segami et al (2018), where sucrose was reported to be 50 % lower than wild-type in the *fugu5-1* mutant. In both of these previous studies, the large reductions in sucrose within *fugu5* mutants was proposed to be evidence for the inhibition of sucrose production via gluconeogenesis (Ferjani et al 2011; Segami et al 2018). While lower concentrations of sucrose may be limiting heterotrophic growth in the *fugu5-3* mutant (Fig. 2), as reported by Ferjani et al (2011), the increased levels of sucrose in the *fugu5-1* and *fugu5-2* mutants (Fig. 4) conflict with the hypothesis of Ferjani et al (2011). When transported to sink tissues, sucrose is either metabolised, converted to hexose or stored as starch (Lemoine et al 2013). Therefore, the increased sucrose observed in the *fugu5-1* and *fugu5-2* mutants (Fig. 4) could be due to an inability to transport sucrose to sink tissues, resulting in accumulation within source tissues. To further investigate this possibility, metabolite analysis would need to be conducted on separate leaf and root tissues of the *fugu5* mutants, rather than whole plants.

### **Sucrose concentrations are reduced in *35S:AVP1* seedlings on basal MS**

In contrast to the *fugu5* mutants, a large proportion of metabolites in *35S:AVP1* seedlings increased compared to wild-type (Fig. 4). An exception to this was the concentration of sucrose, which decreased by 14 % in whole *35S:AVP1* plants compared to wild-type (Fig. 4). As only one *35S:AVP1* line was analysed in this study, however, analysis of additional lines is required to further investigate these results. The concentration of sucrose in the *AVP1-1* and *AVP1-2* lines, however, was also reduced compared to wild-type (Table A1). Previous studies have reported sucrose concentrations to be unaltered in the leaf of 28 d-old soil grown *AVP1-1* and *35S:AVP1* plants (without supplied sucrose) compared to wild-type (Khadijkar et al 2016), and 70 % higher than wild-type in 10 d-old *AVP1-1* seedlings on MS media supplemented with 1 % sucrose (Gonzalez et al 2010). These conflicting results suggest that the role of AVP1 in sucrose metabolism may be influenced by variation in growth conditions or *AVP1* expression level. The addition of sucrose to the growth media of *AVP1-1* seedlings (Gonzalez et al 2010) could have enhanced the uptake or transport of sucrose from source to sink tissues (Pizzio et al 2015), which could account for the unaltered (Khadijkar et al 2016) and reduced (Fig. 4) concentrations of sucrose on basal MS media. Differences in transgene expression level between *AVP1* over-expressing lines could also be contributing to the phenotypic variation between the lines, as could the high level of transgene silencing within the *AVP1-1* and *AVP1-2* lines. Sub-cellular and tissue localisation of AVP1 is also known vary in response to *AVP1* expression level in transgenic Arabidopsis (Segami et al 2014), variation in which may be responsible for differences in AVP1 function and, therefore, phenotypic differences between the *AVP1* over-expressing lines.



**AVP1 may regulate tryptophan and auxin biosynthesis via the shikimate pathway**

In addition to influencing sucrose production and transport, *AVP1* has also been proposed to facilitate auxin transportation (Li et al 2005), which could be contributing to the reduced growth of *fugu5* mutants, and the enhanced growth of *AVP1* over-expressing seedlings. Shikimate is an important metabolite and the precursor to aromatic amino acid biosynthesis via the shikimate pathway (Herrmann 1995). In this pathway, shikimate is metabolised to chorismate, which is utilised for the biosynthesis of several metabolites, including tryptophan. During tryptophan biosynthesis, phosphoribosyl diphosphate (PRPP) is hydrolysed, generating cytosolic PP<sub>i</sub> as a by-product (Herrmann 1995). Tryptophan generated via this pathway can subsequently be used to produce indole-3-acetic acid (IAA), the most common auxin-class plant hormone (Won et al 2011). While the initial phenotype on which the proposed role for *AVP1* in auxin transport was based (Li et al 2005) was subsequently shown to be due to a second t-DNA insertion within the mutant lines (Kriegel et al 2015), rather than the lack of *AVP1* function, enhanced auxin abundance has been reported in multiple transgenic plants constitutively expressing *AVP1* (Gonzalez et al 2010; Li et al 2010; Yang et al 2014), the reason for which is yet to be identified. The large increase in shikimate concentration in the *35S:AVP1* line compared to wild-type (Fig. 4) suggests that shikimate biosynthesis is enhanced in the transgenic lines, potentially due to enhanced activity of the shikimate pathway (Fig. 6). While the *fugu5* mutants also contained somewhat higher concentrations of shikimate compared to wild-type (Fig. 4), this could be explained by a reduction in the demand for shikimate. Accumulation of PP<sub>i</sub> within the *fugu5* mutants, due to a lack of PP<sub>i</sub> hydrolysis via *AVP1*, could inhibit PP<sub>i</sub>-dependent tryptophan production, reducing the demand for shikimate, thus increasing accumulation within the mutants (Fig. 5). Alterations in tryptophan-dependent IAA biosynthesis, as a result of altered *AVP1* expression and, therefore, cytosolic PP<sub>i</sub> regulation (Ferjani et al 2012), could account for

the enhanced growth reported in *AVP1* over-expressing transgenic Arabidopsis (Gaxiola et al 2001; Gonzalez et al 2010; Khadilkar et al 2016; Li et al 2005; Pizzio et al 2015) and the reduced growth of *fugu5* mutants (Fig. 3) (Asaoka et al 2016; Ferjani et al 2011; Kriegel et al 2015; Segami et al 2018). To further investigate this hypothesis, metabolites within the shikimate and tryptophan dependant IAA pathways should be analysed in both *AVP1* over-expressing and *fugu5* mutant lines.

### ***AVP1* may regulate multiple ascorbic acid biosynthesis pathways**

*AVP1* has also been implicated in ascorbic acid biosynthesis via the Smirnoff-Wheeler pathway, with transgenic barley expressing *AVP1* under the control of a *35S* promoter, containing 1.9- to 3.8-fold higher levels of ascorbic acid and 13.1- to 15-fold higher dehydroascorbic acid, compared to wild-type seedlings (Schilling 2014). In *35S:AVP1* Arabidopsis seedlings, concentrations of glucose, glucose 6-phosphate and fructose 6-phosphate (the initial three metabolites within the Smirnoff-Wheeler pathway) increased compared to wild-type (Figure 6). In addition, concentrations of inositol, required for ascorbic acid synthesis via the *myo*-inositol pathway (Lorence et al 2004) also increased by 51 % in *35S:AVP1* seedlings compared to wild-type, while xylitol and arabinose, precursors to the galacturonic acid ascorbic acid pathway (Agius et al 2003) decreased compared to wild-type (Fig. 6). In *fugu5* mutant seedlings, concentrations of glucose, arabinose and xylitol were reduced compared to wild-type, while glucose 6-phosphate increased slightly compared to wild-type, and the concentrations of fructose 6-phosphate and xylitol varied between the three mutant lines (Fig. 5). Although alterations in these metabolites in both *35S:AVP1* and *fugu5* seedlings suggest these pathways are responsive to changes in *AVP1* expression, it remains unclear whether the activity of these pathways is enhanced or inhibited. For instance, the increased concentrations of metabolites

within the initial stages of the Smirnoff-Wheeler and *myo*-inositol pathways in *35S:AVP1* seedlings could be due to upregulation of these pathways, resulting in increased production of these metabolites. Alternatively, higher concentrations of these metabolites could indicate reduced demand for ascorbic acid, resulting in reduced synthesis of ascorbic acid and, therefore, increased accumulation of these metabolites. Although the *fugu5* and *AVP1* over-expressing samples have been prepared for ascorbic acid and amino acid analysis, the results of these analyses have not yet been obtained. Therefore, to further elucidate the impact of *AVP1* function on these pathway, future research should investigate the activity of enzymes within these pathways, and quantify the concentration of all metabolites involved in ascorbic acid synthesis (Linster et al 2007) through a targeted metabolomics analysis (Römisch-Margl et al 2012).

### **The role of *AVP1* in plant metabolism is likely to be influenced by multiple factors**

Due to the high level of variation between replicate samples in this study, few of the alterations in metabolite concentrations were statistically significant (Table 2). With several roles proposed for *AVP1*, it is likely that these roles are influenced by expression level (Segami et al 2014) and tissue type (Gaxiola et al 2016; Segami et al 2010). Levels of expression may have differed between replicate seedlings within the pooled samples, preventing differences from being identified. Similarly, tissue differences would also not have been detected due to analysis of entire seedlings (due to the amount of tissue required for metabolic analysis), rather than separate root and shoot tissues. Sampling times are another factor that need to be considered, as metabolites within *AVP1* over-expressing transgenic *Arabidopsis* have been shown to vary throughout the day (Gonzalez et al 2010; Pizzio et al 2015), while expression of H<sup>+</sup>-PPase genes is also known to vary throughout plant development (Chapter 4). With evidence suggesting that

*AVP1* function may also be dependent on the stage of plant development, or environmental conditions (Gaxiola et al 2016; Schilling et al 2017), the results of this study are likely to be indicative of metabolite differences after 8 d of growth, and may differ between tissues and developmental stages. To further investigate the differences between the *fugu5* mutant and *35S:AVP1* over-expressing *Arabidopsis* lines, metabolites should be analysed in specific tissue types, throughout development. Furthermore, while the majority of research has focussed on characterising the role of *AVP1* in *Arabidopsis*, research should also investigate the role of H<sup>+</sup>-PPases in other species, including non-transgenic plants, as function may differ among H<sup>+</sup>-PPase orthologs and between transgenic and non-transgenic plants.

## Conclusions

In *Arabidopsis* seedlings, constitutive over-expression of *AVP1* increased the concentration of multiple metabolites within several important metabolic pathways compared to wild-type, while the concentration of various metabolites were reduced in *fugu5* mutants compared to wild-type. These results indicate that the expression of *AVP1* has an important role in regulating the metabolism of *Arabidopsis* during heterotrophic growth. While further research is required to investigate metabolite changes during different developmental stages, plant tissues and plant species, these results support the hypothesis that the expression of *AVP1* has a key role in multiple metabolic processes. Furthermore, these results suggest *AVP1* may have a role in regulating the shikimate pathway, which could influence the biosynthesis of tryptophan and indole-3-acetic acid.

## Acknowledgements

The authors wish to thank Associate Professor Roberto Gaxiola (Arizona State University) for providing the *Arabidopsis* seed used in this study, Dr Gwenda Mayo (Adelaide Microscopy) for advice regarding microscopy techniques, and Professor Ute Roessner and Dr Siria Natera (Metabolomics Australia/The University of Melbourne) for performing metabolite extraction and GC-MS analysis. This research was funded by the Grains Research and Development Corporation (UA00145), and the Grains Research and Development Corporation and International Wheat Yield Partnership (IWYP39/ACP0009). Daniel Menadue is the recipient of a GRDC Grains Industry Research Scholarship (GRS10931).

## References

- Agius F, González-Lamothe R, Caballero JL, Muñoz-Blanco J, Botella MA and Valpuesta V (2003) Engineering increased vitamin C levels in plants by overexpression of a D-galacturonic acid reductase. *Nat Biotechnol* 21:177-181
- Asaoka M, Segami S, Ferjani A and Maeshima M (2016) Contribution of PP<sub>i</sub>-hydrolyzing function of vacuolar H<sup>+</sup>-Pyrophosphatase in vegetative growth of Arabidopsis: Evidenced by expression of uncoupling mutated enzymes. *Front Plant Sci* 7:1-12
- Barth C, De Tullio M and Conklin PL (2006) The role of ascorbic acid in the control of flowering time and the onset of senescence. *J Exp Bot* 57:1657-1665
- Conklin PL (2001) Recent advances in the role and biosynthesis of ascorbic acid in plants. *Plant Cell Environ* 24:383-394
- Edwards K, Johnstone C and Thompson C (1991) A simple and rapid method for the preparation of plant genomic DNA for PCR analysis. *Nucleic Acids Res* 19:1349
- Farré EM, Tech S, Trethewey RN, Fernie AR and Willmitzer L (2006) Subcellular pyrophosphate metabolism in developing tubers of potato (*Solanum tuberosum*). *Plant Mol Biol* 62:165-179
- Ferjani A, Horiguchi G, Yano S and Tsukaya H (2007) Analysis of leaf development in *fugu* mutants of Arabidopsis reveals three compensation modes that modulate cell expansion in determinate organs. *Plant Physiol* 144:988-999
- Ferjani A, Segami S, Horiguchi G, Muto Y, Maeshima M and Tsukaya H (2011) Keep an eye on PP<sub>i</sub>: The vacuolar-type H<sup>+</sup>-pyrophosphatase regulates postgerminative development in *Arabidopsis*. *Plant Cell* 23:2895-2908
- Ferjani A, Segami S, Horiguchi G, Sakata A, Maeshima M and Tsukaya H (2012) Regulation of pyrophosphate levels by H<sup>+</sup>-PPase is central for proper resumption of early plant development. *Plant Signal Behav* 7:38-42
- Foyer CH, Souriau N, Perret S, Lelandais M, Kunert KJ, Pruvost C and Jouanin L (1995) Overexpression of glutathione reductase but not glutathione synthetase leads to increases in antioxidant capacity and resistance to photoinhibition in poplar trees. *Plant Physiol* 109:1047-1057
- Gallie DR (2013) L-ascorbic acid: A multifunctional molecule supporting plant growth and development. *Scientifica* 2013: <https://doi.org/10.1155/2013/795964>
- Gaxiola RA, Li J, Undurraga S, Dang LM, Allen GJ, Alper SL and Fink GR (2001) Drought- and salt-tolerant plants result from overexpression of the *AVP1* H<sup>+</sup>-pump. *Proc Natl Acad Sci* 98:11444-11449
- Gaxiola RA, Regmi KC, Paez-Valencia J, Pizzio GA and Zhang S (2016) Plant H<sup>+</sup>-PPases: Reversible enzymes with contrasting functions dependent on membrane environment. *Mol Plant* 9:317-319
- Gaxiola RA, Sanchez CA, Paez-Valencia J, Ayre BG and Elser JJ (2012) Genetic manipulation of a “vacuolar” H<sup>+</sup>-PPase: From salt tolerance to yield enhancement under phosphorus-deficient soils. *Plant Physiol* 159:3-11
- Gonzalez N, De Bodt S, Sulpice R, Jikumaru Y, Chae E, Dhondt S, Van Daele T, De Milde L, Weigel D, Kamiya Y, Stitt M, Beemster GTS and Inzé D (2010) Increased leaf size: Different means to an end. *Plant Physiol* 153:1261-1279
- Hemavathi, Upadhyaya C, Akula N, Young K, Chun S, Kim D and Park S (2010) Enhanced ascorbic acid accumulation in transgenic potato confers tolerance to various abiotic stresses. *Biotechnol Lett* 32:321-330

- Herrmann KM (1995) The shikimate pathway: Early steps in the biosynthesis of aromatic compounds. *The Plant Cell* 7:907-919
- Hill C and Roessner U (2013) Metabolic profiling of plants by GC–MS. In: Weckwerth W, Kahl G (eds) *The Handbook of Plant Metabolomics*, pp. 3-18. Wiley-Blackwell, Weinheim, Germany
- Horemans N, Asard H and Caubergs RJ (1994) The role of ascorbate free radical as an electron acceptor to cytochrome b-mediated trans-plasma membrane electron transport in higher plants. *Plant Physiol* 104:1455-1458
- Horiguchi G, Fujikura U, Ferjani A, Ishikawa N and Tsukaya H (2006) Large-scale histological analysis of leaf mutants using two simple leaf observation methods: identification of novel genetic pathways governing the size and shape of leaves. *Plant J* 48:638-644
- Khadilkar AS, Yadav UP, Salazar C, Shulaev V, Paez-Valencia J, Pizzio GA, Gaxiola RA and Ayre BG (2016) Constitutive and companion cell-specific overexpression of *AVP1*, encoding a proton-pumping pyrophosphatase, enhances biomass accumulation, phloem loading, and long-distance transport. *Plant Physiol* 170:401-414
- Kriegel A, Andrés Z, Medzihradszky A, Krüger F, Scholl S, Delang S, Patir-Nebioglu MG, Gute G, Yang H, Murphy AS, Peer WA, Pfeiffer A, Krebs M, Lohmann JU and Schumacher K (2015) Job sharing in the endomembrane system: Vacuolar acidification requires the combined activity of V-ATPase and V-PPase. *The Plant Cell* 27:3383-3396
- Langhans M, Ratajczak R, Lutzelschwab M, Michalke W, Wachter R, Fischer-Schliebs E and Ullrich CI (2001) Immunolocalization of plasma-membrane H<sup>+</sup>-ATPase and tonoplast-type pyrophosphatase in the plasma membrane of the sieve element-companion cell complex in the stem of *Ricinus communis* L. *Planta* 213:11-19
- Lemoine R, Camera SL, Atanassova R, Dédaldéchamp F, Allario T, Pourtau N, Bonnemain J-L, Laloi M, Coutos-Thévenot P, Maurousset L, Faucher M, Gironse C, Lemonnier P, Parrilla J and Durand M (2013) Source-to-sink transport of sugar and regulation by environmental factors. *Front Plant Sci* <https://doi.org/10.3389/fpls.2013.00272>
- Li J, Yang H, Ann Peer W, Richter G, Blakeslee J, Bandyopadhyay A, Titapiwantakun B, Undurraga S, Khodakovskaya M, Richards EL, Krizek B, Murphy AS, Gilroy S and Gaxiola R (2005) *Arabidopsis* H<sup>+</sup>-PPase AVP1 regulates auxin-mediated organ development. *Science* 310:121-125
- Li Z, Baldwin CM, Hu Q, Liu H and Luo H (2010) Heterologous expression of *Arabidopsis* H<sup>+</sup>-pyrophosphatase enhances salt tolerance in transgenic creeping bentgrass (*Agrostis stolonifera* L.). *Plant Cell Environ* 33:272-289
- Linster CL, Gomez TA, Christensen KC, Adler LN, Young BD, Brenner C and Clarke SG (2007) *Arabidopsis* VTC2 encodes a GDP-I-Galactose phosphorylase, the last unknown enzyme in the Smirnoff-Wheeler pathway to ascorbic acid in plants. *J Biol Chem* 282:18879-18885
- Lisko KA, Torres R, Harris RS, Belisle M, Vaughan MM, Jullian B, Chevone BI, Mendes P, Nessler CL and Lorence A (2013) Elevating vitamin C content via overexpression of *myo*-inositol oxygenase and L-gulonolactone oxidase in *Arabidopsis* leads to enhanced biomass and tolerance to abiotic stresses. *In Vitro Cell Dev Biol Plant* 49:643-655
- Lorence A, Chevone BI, Mendes P and Nessler CL (2004) *myo*-Inositol oxygenase offers a possible entry point into plant ascorbate biosynthesis. *Plant Physiol* 134:1200-1205
- Murashige T and Skoog F (1962) A revised medium for rapid growth and bio assays with tobacco tissue cultures. *Physiol Plant* 15:473-497

- Osorio S, Nunes-Nesi A, Stratmann M and Fernie A (2013) Pyrophosphate levels strongly influence ascorbate and starch content in tomato fruit. *Front Plant Sci* 4
- Paez-Valencia J, Patron-Soberano A, Rodriguez-Leviz A, Sanchez-Lares J, Sanchez-Gomez C, Valencia-Mayoral P, Diaz-Rosas G and Gaxiola R (2011) Plasma membrane localization of the type I H<sup>+</sup>-PPase AVP1 in sieve element–companion cell complexes from *Arabidopsis thaliana*. *Plant Sci* 181:23-30
- Pizzio GA, Hirschi KD and Gaxiola RA (2017) Conjecture regarding posttranslational modifications to the arabidopsis type I proton-pumping pyrophosphatase (AVP1). *Front Plant Sci* 8: <https://doi.org/10.3389/fpls.2017.01572>
- Pizzio GA, Paez-Valencia J, Khadilkar AS, Regmi K, Patron-Soberano A, Zhang S, Sanchez-Lares J, Furstenau T, Li J, Sanchez-Gomez C, Valencia-Mayoral P, Yadav UP, Ayre BG and Gaxiola RA (2015) *Arabidopsis* type I proton-pumping pyrophosphatase expresses strongly in phloem, where it is required for pyrophosphate metabolism and photosynthate partitioning. *Plant Physiol* 167:1541-1553
- Ramírez L, Bartoli CG and Lamattina L (2013) Glutathione and ascorbic acid protect *Arabidopsis* plants against detrimental effects of iron deficiency. *J Exp Bot* 64:3169-3178
- Rea PA and Sanders D (1987) Tonoplast energization: Two H<sup>+</sup> pumps, one membrane. *Physiol Plant* 71:131-141
- Regmi KC, Zhang S and Gaxiola RA (2016) Apoplasmic loading in the rice phloem supported by the presence of sucrose synthase and plasma membrane-localized proton pyrophosphatase. *Ann Bot* 117:257-268
- Römisch-Margl W, Prehn C, Bogumil R, Röhring C, Suhre K and Adamski J (2012) Procedure for tissue sample preparation and metabolite extraction for high-throughput targeted metabolomics. *Metabolomics* 8:133-142
- Sarafian V, Kim Y, Poole RJ and Rea PA (1992) Molecular cloning and sequence of cDNA encoding the pyrophosphate-energized vacuolar membrane proton pump of *Arabidopsis thaliana*. *Proc Natl Acad Sci* 89:1775-1779
- Schilling RK (2014) "Evaluating the abiotic stress tolerance of transgenic barley expressing an *Arabidopsis* vacuolar H<sup>+</sup>-pyrophosphatase gene (*AVP1*)". PhD Thesis, The University of Adelaide, Adelaide, Australia
- Schilling RK, Tester M, Marschner P, Plett DC and Roy SJ (2017) AVP1: One protein, many roles. *Trends Plant Sci* 22:154-162
- Segami S, Asaoka M, Kinoshita S, Fukuda M, Nakanishi Y and Maeshima M (2018) Biochemical, structural, and physiological characteristics of vacuolar H<sup>+</sup>-pyrophosphatase. *Plant Cell Physiol* <https://doi.org/10.1093/pcp/pcy054>
- Segami S, Makino S, Miyake A, Asaoka M and Maeshima M (2014) Dynamics of vacuoles and H<sup>+</sup>-pyrophosphatase visualized by monomeric green fluorescent protein in *Arabidopsis*: Artifactual bulbs and native intravacuolar spherical structures. *The Plant Cell* 26:3416-3434
- Segami S, Nakanishi Y, Sato MH and Maeshima M (2010) Quantification, organ-specific accumulation and intracellular localization of type II H<sup>+</sup>-pyrophosphatase in *Arabidopsis thaliana*. *Plant Cell Physiol* 51:1350-1360
- Stitt M (1989) Product inhibition of potato tuber pyrophosphate:fructose-6-phosphate phosphotransferase by phosphate and pyrophosphate. *Plant Physiol* 89:628-633
- Wheeler GL, Jones MA and Smirnoff N (1998) The biosynthetic pathway of vitamin C in higher plants. *Nature* 393:365-369



- Won C, Shen X, Mashiguchi K, Zheng Z, Dai X, Cheng Y, Kasahara H, Kamiya Y, Chory J and Zhao Y (2011) Conversion of tryptophan to indole-3-acetic acid by Tryptophan Aminotransferases of *Arabidopsis* and YUCCAs in *Arabidopsis*. *Proc Natl Acad Sci* 108:18518-18523
- Yang H, Zhang X, Gaxiola RA, Xu G, Peer WA and Murphy AS (2014) Over-expression of the *Arabidopsis* proton-pyrophosphatase *AVP1* enhances transplant survival, root mass, and fruit development under limiting phosphorus conditions. *J Exp Bot* 65:3045-3053

## Tables

**Table 1** Details of PCR primers and related thermocycling settings used for gene presence and expression analysis of all Arabidopsis

lines

Primer	Description	Forward primer (5'-3')	Reverse primer (5'-3')	Annealing temperature (°C)	Amplicon size (bp)
<i>AtAct2</i>	Used to amplify a product from the native <i>AtAct2</i> gene	TGAGCAAAGAAATCACAGCACT	CCTGGACCTGCCTCATCATAC	54	166
<i>AVP1</i> transgene	Used to amplify a product from the <i>AVP1</i> transgene from <i>AVP1-1</i> and <i>AVP1-2</i>	GGACAACGCCCAAGAAATACATC	AGACTGGTGATTTGGCGGACTC	53	200
<i>35S:AVP1</i> transgene	Used to amplify a product from the <i>AVP1</i> transgene from <i>35S:AVP1</i>	CACTCACGGTGGTATCCTTT	GTTTGAACGATCGGGGAAATTC	55	256
<i>fugu5-1</i>	Used to amplify the region containing the <i>fugu5-1</i> mutation	GGTGTTTCAGATCGCCATATCAG	ATGAGCTTGATGAGGATGTTTC	51	205
<i>fugu5-2</i>	Used to amplify the region containing the <i>fugu5-2</i> mutation	TATGGTCTTGGTGGGTCTTCC	TGAGCAATGGGTAGCACATGG	54	300
<i>fugu5-3</i>	Used to amplify the region containing the <i>fugu5-3</i> mutation	GGTATTGCTGAAATGGCTGG	CACCTCCACACTCTTCATTG	51	270

**Table 2** Metabolite concentrations (picomole mg<sup>-1</sup> dry weight  $\pm$  standard error of the mean) in 8 d-old pooled seedlings of wild-type (WT), *AVP1* mutant (*fugu5-1*, *fugu5-2* and *fugu5-3*) and *35S:AVP1* over-expressing Arabidopsis lines on basal MS media. Different letters indicate statistically significant differences for each metabolite (one-way ANOVA, Tukey's 95 % confidence intervals,  $P \leq 0.05$ ). Shading indicates metabolite concentrations that are higher (green shading), lower (orange shading) and unaltered (no shading) compared to wild-type, with metabolites that are significantly different to wild-type highlighted and shown in bold. Values are means of 3 replicates of pooled seedlings.

	<i>WT</i>	<i>fugu5-1</i>	<i>fugu5-2</i>	<i>fugu5-3</i>	<i>35S:AVP1</i>
2-hydroxy glutaric acid	144 $\pm$ 4 <sup>a</sup>	145 $\pm$ 4 <sup>a</sup>	145 $\pm$ 2 <sup>a</sup>	142 $\pm$ 4 <sup>a</sup>	148 $\pm$ 5 <sup>a</sup>
2-ketoglutaric acid	1,699 $\pm$ 60 <sup>a</sup>	1,957 $\pm$ 57 <sup>a</sup>	2,008 $\pm$ 110 <sup>a</sup>	1,818 $\pm$ 141 <sup>a</sup>	1,757 $\pm$ 77 <sup>a</sup>
Aconitate	198 $\pm$ 9 <sup>a</sup>	210 $\pm$ 11 <sup>a</sup>	237 $\pm$ 34 <sup>a</sup>	192 $\pm$ 12 <sup>a</sup>	203 $\pm$ 19 <sup>a</sup>
Arabinose	189 $\pm$ 7 <sup>b</sup>	165 $\pm$ 9 <sup>ab</sup>	148 $\pm$ 11 <sup>ab</sup>	<b>137 <math>\pm</math> 4<sup>a</sup></b>	170 $\pm$ 21 <sup>ab</sup>
Citrate	3,743 $\pm$ 715 <sup>a</sup>	2,789 $\pm$ 762 <sup>a</sup>	3,553 $\pm$ 1,207 <sup>a</sup>	2,567 $\pm$ 524 <sup>a</sup>	4,768 $\pm$ 993 <sup>a</sup>
Erythritol	355 $\pm$ 23 <sup>b</sup>	<b>259 <math>\pm</math> 6<sup>a</sup></b>	<b>265 <math>\pm</math> 23<sup>a</sup></b>	271 $\pm$ 5 <sup>ab</sup>	301 $\pm$ 38 <sup>ab</sup>
Fructose	158,566 $\pm$ 92,235 <sup>a</sup>	101,224 $\pm$ 7,752 <sup>a</sup>	88,561 $\pm$ 25,413 <sup>a</sup>	58,025 $\pm$ 17,214 <sup>a</sup>	74,840 $\pm$ 18,564 <sup>a</sup>
Fructose 6-phosphate	934 $\pm$ 118 <sup>a</sup>	782 $\pm$ 121 <sup>a</sup>	1,341 $\pm$ 349 <sup>a</sup>	847 $\pm$ 93 <sup>a</sup>	1,499 $\pm$ 378 <sup>a</sup>
Fucose	133 $\pm$ 9 <sup>a</sup>	122 $\pm$ 6 <sup>a</sup>	118 $\pm$ 4 <sup>a</sup>	118 $\pm$ 7 <sup>a</sup>	132 $\pm$ 10 <sup>a</sup>
Fumarate	123,330 $\pm$ 27,007 <sup>a</sup>	109,651 $\pm$ 18,178 <sup>a</sup>	129,698 $\pm$ 29,034 <sup>a</sup>	84,990 $\pm$ 19,533 <sup>a</sup>	170,001 $\pm$ 59,607 <sup>a</sup>
Galactose	193 $\pm$ 9 <sup>a</sup>	158 $\pm$ 4 <sup>a</sup>	164 $\pm$ 13 <sup>a</sup>	153 $\pm$ 9 <sup>a</sup>	186 $\pm$ 17 <sup>a</sup>
Glucose	515,782 $\pm$ 293,526 <sup>a</sup>	411,030 $\pm$ 20,461 <sup>a</sup>	447,909 $\pm$ 128,820 <sup>a</sup>	339,052 $\pm$ 75,508 <sup>a</sup>	540,616 $\pm$ 131,799 <sup>a</sup>
Glucose 6-phosphate	21,736 $\pm$ 898 <sup>a</sup>	23,747 $\pm$ 3,093 <sup>ab</sup>	25,362 $\pm$ 1,950 <sup>ab</sup>	22,404 $\pm$ 736 <sup>ab</sup>	<b>30,324 <math>\pm</math> 2,891<sup>b</sup></b>
Inositol	1,529 $\pm$ 480 <sup>ab</sup>	1,020 $\pm$ 32 <sup>a</sup>	1,221 $\pm$ 173 <sup>ab</sup>	1,164 $\pm$ 31 <sup>ab</sup>	2,314 $\pm$ 509 <sup>b</sup>
Isocitrate	175 $\pm$ 13 <sup>a</sup>	158 $\pm$ 20 <sup>a</sup>	170 $\pm$ 16 <sup>a</sup>	141 $\pm$ 9 <sup>a</sup>	174 $\pm$ 18 <sup>a</sup>
Malate	157,297 $\pm$ 24,064 <sup>a</sup>	115,145 $\pm$ 36,674 <sup>a</sup>	152,748 $\pm$ 47,155 <sup>a</sup>	119,429 $\pm$ 52,187 <sup>a</sup>	181,915 $\pm$ 52,892 <sup>a</sup>
Maleate	4,301 $\pm$ 504 <sup>a</sup>	2,867 $\pm$ 914 <sup>a</sup>	3,775 $\pm$ 214 <sup>a</sup>	2,956 $\pm$ 688 <sup>a</sup>	3,789 $\pm$ 389 <sup>a</sup>
Malonate	841 $\pm$ 151 <sup>a</sup>	817 $\pm$ 67 <sup>a</sup>	977 $\pm$ 81 <sup>a</sup>	885 $\pm$ 56 <sup>a</sup>	1,002 $\pm$ 21 <sup>a</sup>
Maltose	190 $\pm$ 28 <sup>a</sup>	159 $\pm$ 2 <sup>a</sup>	188 $\pm$ 14 <sup>a</sup>	168 $\pm$ 12 <sup>a</sup>	<b>394 <math>\pm</math> 31<sup>b</sup></b>
Mannose	193 $\pm$ 24 <sup>a</sup>	206 $\pm$ 16 <sup>a</sup>	210 $\pm$ 19 <sup>a</sup>	187 $\pm$ 9 <sup>a</sup>	207 $\pm$ 23 <sup>a</sup>
Nicotinic acid	214 $\pm$ 84 <sup>a</sup>	161 $\pm$ 16 <sup>a</sup>	138 $\pm$ 29 <sup>a</sup>	147 $\pm$ 15 <sup>a</sup>	133 $\pm$ 23 <sup>a</sup>
Raffinose	135 $\pm$ 11 <sup>a</sup>	118 $\pm$ 3 <sup>a</sup>	130 $\pm$ 11 <sup>a</sup>	119 $\pm$ 5 <sup>a</sup>	134 $\pm$ 11 <sup>a</sup>
Ribose	171 $\pm$ 14 <sup>ab</sup>	120 $\pm$ 6 <sup>a</sup>	120 $\pm$ 8 <sup>a</sup>	122 $\pm$ 6 <sup>a</sup>	193 $\pm$ 25 <sup>b</sup>
Shikimate	548 $\pm$ 65 <sup>a</sup>	575 $\pm$ 52 <sup>a</sup>	697 $\pm$ 73 <sup>a</sup>	596 $\pm$ 54 <sup>a</sup>	752 $\pm$ 121 <sup>a</sup>
Succinate	1,916 $\pm$ 323 <sup>a</sup>	1,700 $\pm$ 114 <sup>a</sup>	1,814 $\pm$ 347 <sup>a</sup>	1,582 $\pm$ 376 <sup>a</sup>	2,027 $\pm$ 342 <sup>a</sup>
Sucrose	105,548 $\pm$ 25,372 <sup>a</sup>	135,7626 $\pm$ 27,783 <sup>a</sup>	150,106 $\pm$ 40,667 <sup>a</sup>	86,226 $\pm$ 25,481 <sup>a</sup>	90,329 $\pm$ 12,342 <sup>a</sup>
Trehalose	119 $\pm$ 22 <sup>a</sup>	66 $\pm$ 7 <sup>a</sup>	69 $\pm$ 14 <sup>a</sup>	51 $\pm$ 6 <sup>a</sup>	123 $\pm$ 32 <sup>a</sup>
Turanose	154 $\pm$ 11 <sup>a</sup>	152 $\pm$ 3 <sup>a</sup>	165 $\pm$ 7 <sup>a</sup>	149 $\pm$ 3 <sup>a0.</sup>	158 $\pm$ 7 <sup>a</sup>
Xylitol	2,328 $\pm$ 827 <sup>a</sup>	3,977 $\pm$ 2,653 <sup>a</sup>	807 $\pm$ 765 <sup>a</sup>	3,585 $\pm$ 2,834 <sup>a</sup>	178 $\pm$ 53 <sup>a</sup>
Xylose	258 $\pm$ 33 <sup>a</sup>	195 $\pm$ 10 <sup>a</sup>	187 $\pm$ 19 <sup>a</sup>	173 $\pm$ 7 <sup>a</sup>	247 $\pm$ 41 <sup>a</sup>

## Figure Legends

**Fig. 1** Molecular characterisation of *AVP1* over-expressing and *fugu5* mutant Arabidopsis lines. Partial sequence alignments of three regions within the *AVP1* genomic DNA sequence showing the nucleotide substitutions (highlighted in red) and deletions (-) responsible for reduced *AVP1* activity in the (a) *fugu5-1*, (b) *fugu5-2* and (c) *fugu5-3* mutant Arabidopsis lines. (d) Semi-quantitative gene expression analysis of the *AVP1* transgene in wild-type (WT), *AVP1* mutant (*fugu5-1*, *fugu5-2* and *fugu5-3*) and *35S:AVP1* over-expressing relative to *AtActin2* (*AT3G18780*). Values are means (n=3) with error bars indicating standard error of the mean.

**Fig. 2** Growth phenotypes of Arabidopsis seedlings on basal MS media and MS + 2 % sucrose. Eight d-old wild-type (WT), *AVP1* mutant (*fugu5-1*, *fugu5-2*, *fugu5-3*) and *AVP1* over-expressing (*35S:AVP1*) Arabidopsis seedlings on (a) basal MS media and (b) MS media with 2 % sucrose (Suc), were imaged using a SMZ25 stereo microscope (2 × Plan Apo, NA 0.312, WD 20 mm, 0.63 × magnification) and NIS-Elements Advanced Research software (Nikon, Minato, Japan). Representative images are shown for each line and were selected from 6 replicate seedlings. Scale bar = 1 mm (1000 μm).

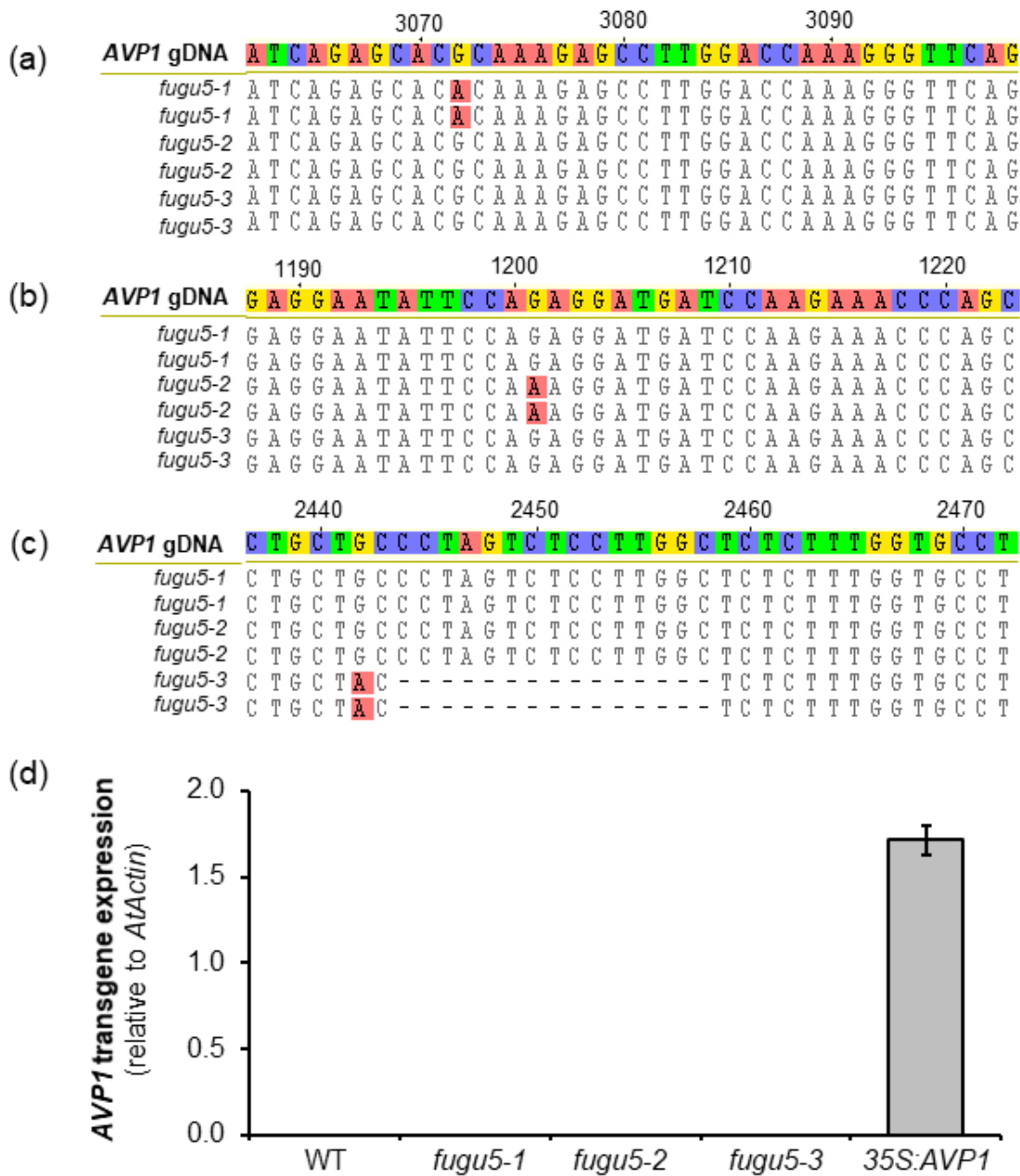
**Fig. 3** Growth parameters of wild-type (WT), *AVP1* mutant (*fugu5-1*, *fugu5-2*, *fugu5-3*) and *35S:AVP1* over-expressing seedlings on basal MS media with and without 2 % sucrose (Suc) for 8 d. (a) Primary root length (mm), (b) first leaf length (mm), (c) first leaf width (mm), and (d) first leaf total area (mm<sup>2</sup>) of 8 d-old seedlings. Different letters indicate statistically significant differences (two-way ANOVA, Tukey's 95 % confidence intervals,  $P \leq 0.05$ ), with error bars showing standard error of the mean (n=6).

**Fig. 4** Percent (%) change in metabolite concentrations relative to wild-type in 8 d-old *AVP1* mutant (*fugu5-1*, *fugu5-2*, and *fugu5-3*) and *35S:AVP1* over-expressing Arabidopsis seedlings on basal MS media without nutrients or sugars. Changes that are significantly different to wild-type (one-way ANOVA, Tukey's 95 % confidence intervals,  $P \leq 0.05$ ) are annotated (\*) and shown in bold.

**Fig. 5** Metabolite changes in 8 d-old *fugu5* mutant *Arabidopsis* seedlings relative to wild-type. Green (↑) and red (↓) arrows indicate a  $\geq 5\%$  increase and decrease, respectively, in metabolite concentrations relative to wild-type. Size of arrow indicates relative change, with larger arrows representing a larger change compared to wild-type. Differences in metabolite concentrations  $< 5\%$  are considered unaltered compared to wild-type (⊕), while (≡) indicates no data. Simplified versions of the glycolysis (blue shading), gluconeogenesis (blue shading) and shikimate (green shading) pathways are indicated, as are key metabolites within the Smirnoff-Wheeler (orange shading), *myo*-inositol (yellow shading) and galacturonic acid (purple shading) ascorbic acid pathways, and the tricarboxylic acid (TCA) cycle (blue shading). Arrows indicate the direction of each simplified pathway, with arrows indicating direct (→), indirect (↘) and reversible (↔) steps. The enzymes involved in the steps of each pathway are not shown. During gluconeogenesis,  $PP_i$  is produced as a by-product during the conversion of (1) fructose 6-phosphate to glucose 6-phosphate and (2) glucose 1-phosphate to UDP-glucose. During the Smirnoff-Wheeler ascorbic acid pathway,  $PP_i$  is produced during the conversion of (3) mannose-1-P to GDP-Mannose. In the Shikimate pathway, the conversion of (4) anthranilate to phosphoribosyl anthranilate produces  $PP_i$  through the reduction of phosphoribosyl pyrophosphate (PRPP).

**Fig. 6** Metabolite changes in 8 d-old *35S:AVP1* transgenic *Arabidopsis* seedlings relative to wild-type. Green (↑) and red (↓) arrows indicate a ≥ 5 % increase and decrease, respectively, in metabolite concentrations relative to wild-type. Size of arrow indicates relative change, with larger arrows representing a larger change compared to wild-type. Differences in metabolite concentrations < 5 % are considered unaltered compared to wild-type (⊕), while (≡) indicates no data. Simplified versions of the glycolysis (blue shading), gluconeogenesis (blue shading) and shikimate (green shading) pathways are indicated, as are key metabolites within the Smirnoff-Wheeler (orange shading), *myo*-inositol (yellow shading) and galacturonic acid (purple shading) ascorbic acid pathways, and the tricarboxylic acid (TCA) cycle (blue shading). Arrows indicate the direction of each simplified pathway, with arrows indicating direct (→), indirect (↘) and reversible (↔) steps. The enzymes involved in the steps of each pathway are not shown. During gluconeogenesis, PP<sub>i</sub> is produced as a by-product during the conversion of (1) fructose 6-phosphate to glucose 6-phosphate and (2) glucose 1-phosphate to UDP-glucose. During the Smirnoff-Wheeler ascorbic acid pathway, PP<sub>i</sub> is produced during the conversion of (3) mannose-1-P to GDP-Mannose. In the Shikimate pathway, the conversion of (4) anthranilate to phosphoribosyl anthranilate produces PP<sub>i</sub> through the reduction of phosphoribosyl pyrophosphate (PRPP).

## Figures

Fig. 1 Molecular characterisation of *AVP1* over-expressing and *fugu5* mutant Arabidopsis lines



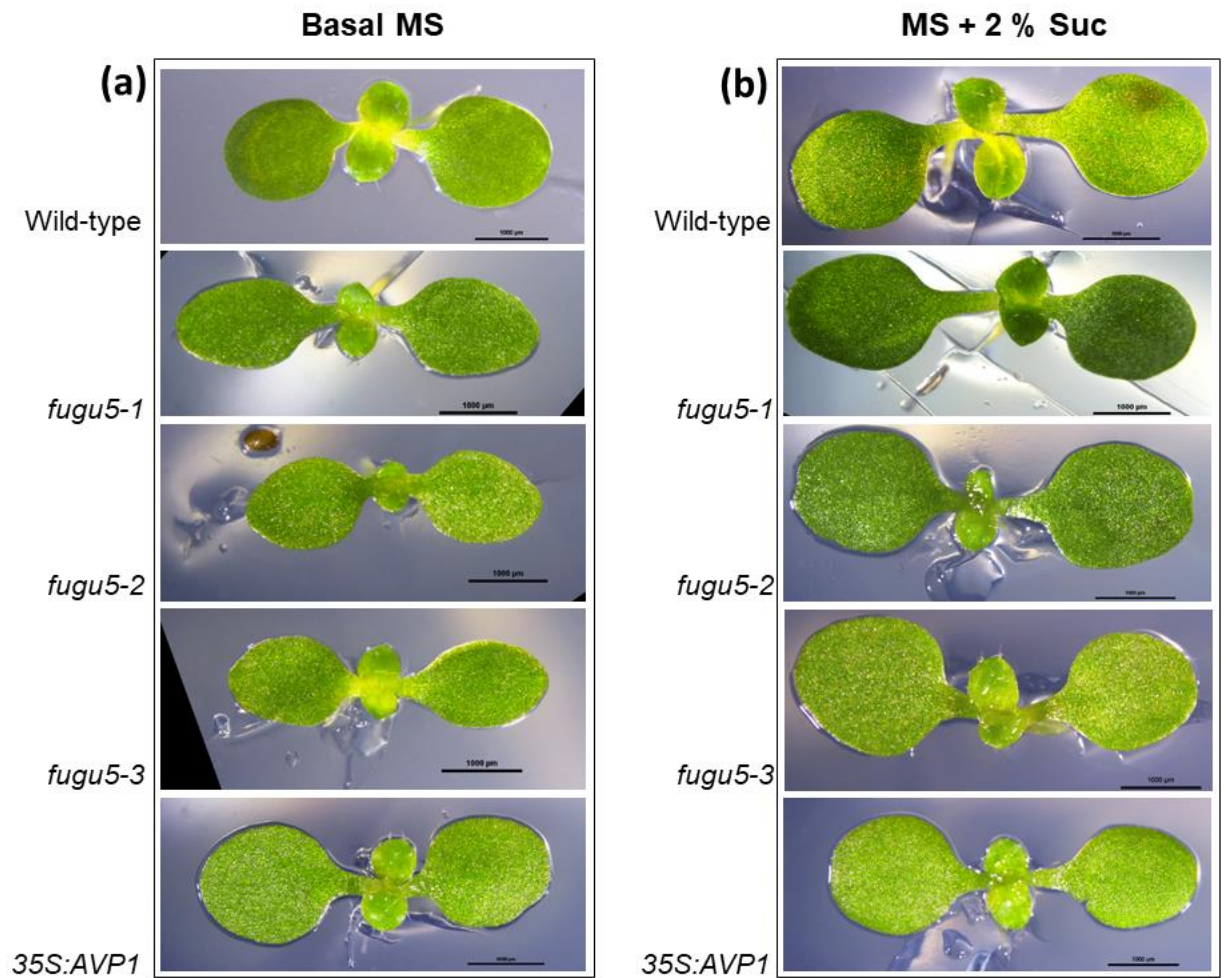


Fig. 2 Growth phenotypes of Arabidopsis seedlings on basal MS media and MS + 2 % sucrose

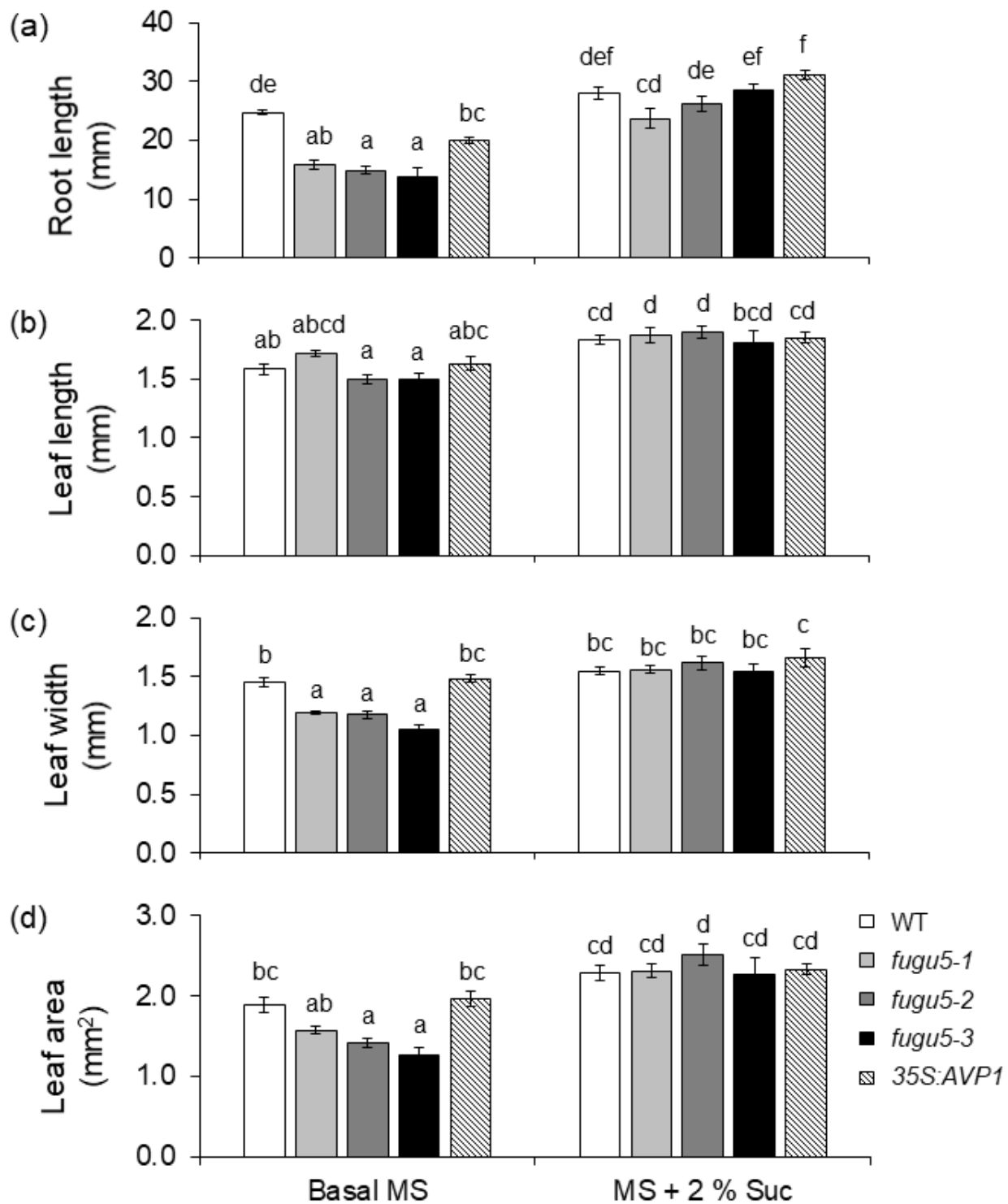
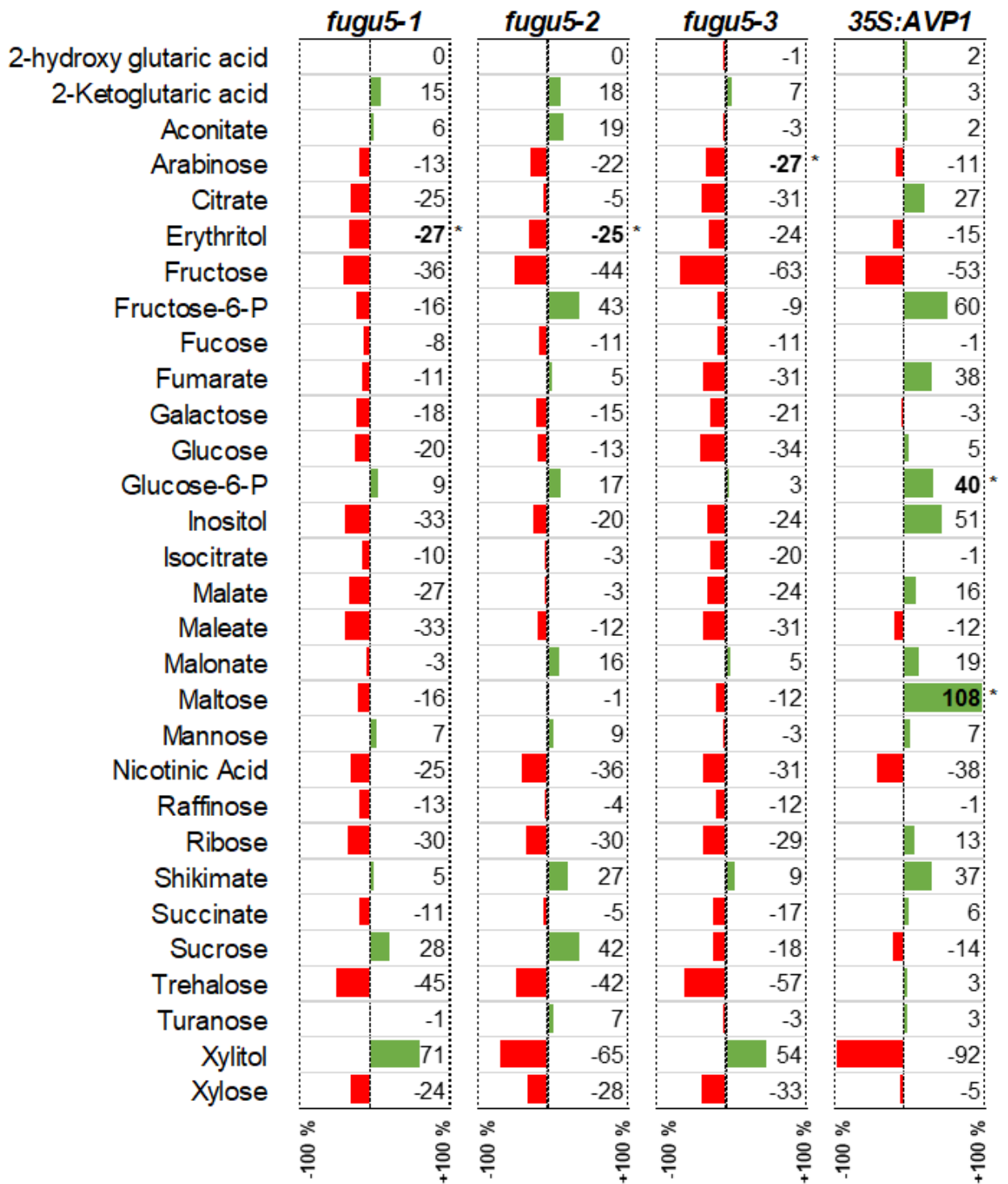


Fig. 3 Growth parameters of wild-type (WT), *AVP1* mutant (*fugu5-1*, *fugu5-2*, *fugu5-3*) and *35S:AVP1* over-expressing seedlings on basal MS media with and without 2 % sucrose (Suc) for 8 d.



**Fig. 4** Percent (%) change in metabolite concentrations relative to wild-type in 8 d-old *AVP1* mutant (*fugu5-1*, *fugu5-2*, and *fugu5-3*) and *35S:AVP1* over-expressing Arabidopsis seedlings on basal MS media without nutrients or sugars.

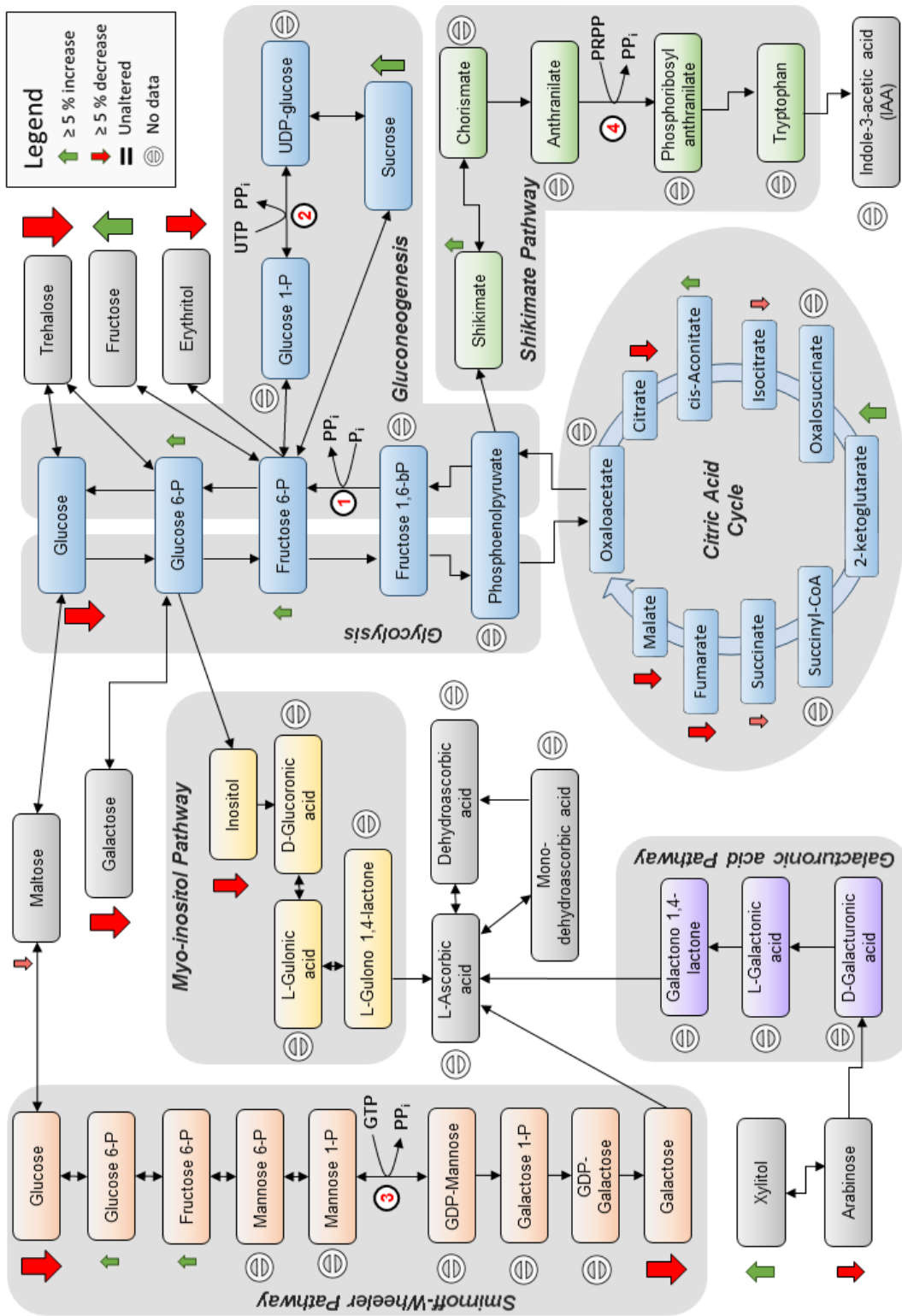


Fig. 5 Metabolite changes in 8 d-old *fugu5* mutant Arabidopsis seedlings relative to wild-type.

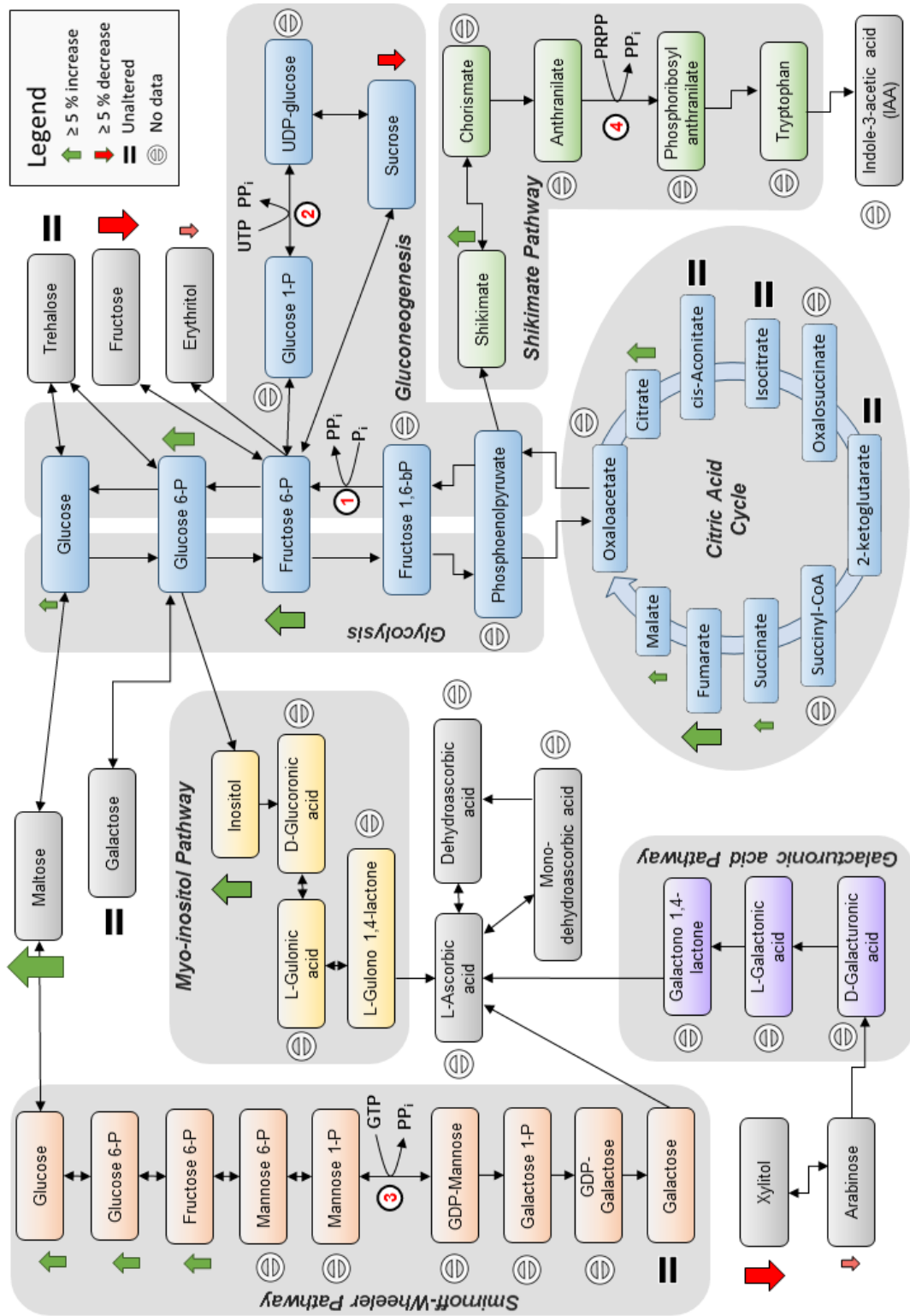
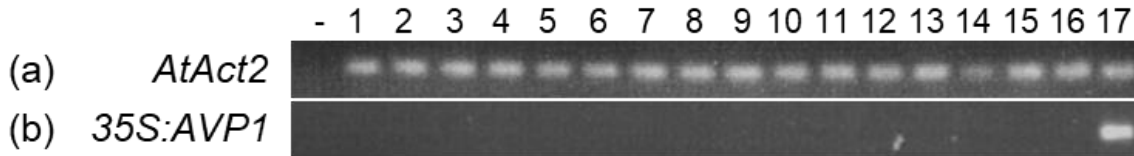


Fig. 6 Metabolite changes in 8 d-old 35S:AVP1 transgenic Arabidopsis seedlings relative to wild-type.

## Additional Data

**Table A1** Metabolite concentrations (picomole  $\text{mg}^{-1}$  dry weight  $\pm$  standard error of the mean) in 8 d-old pooled seedlings of wild-type (WT), and *AVP1-1* and *AVP1-2* transgenic Arabidopsis lines on basal MS media. Different letters indicate statistically significant differences for each metabolite (one-way ANOVA, Tukey's 95 % confidence intervals,  $P \leq 0.05$ ). Shading indicates metabolite concentrations that are higher (green shading), lower (orange shading) and unaltered (no shading) compared to wild-type, with metabolites that are significantly different to wild-type highlighted and shown in bold. Values are means of 3 replicate samples of pooled seedlings.

	<i>WT</i>	<i>AVP1-1</i>	<i>AVP1-2</i>
2-hydroxy glutaric acid	144 ± 4 <sup>a</sup>	<b>180 ± 8<sup>b</sup></b>	149 ± 14 <sup>ab</sup>
2-ketoglutaric acid	1,699 ± 60 <sup>a</sup>	2,035 ± 209 <sup>a</sup>	1,720 ± 63 <sup>a</sup>
Aconitate	198 ± 9 <sup>a</sup>	212 ± 5 <sup>a</sup>	190 ± 15 <sup>a</sup>
Arabinose	189 ± 7 <sup>b</sup>	<b>141 ± 8<sup>a</sup></b>	<b>159 ± 1<sup>a</sup></b>
Citrate	3,743 ± 715 <sup>a</sup>	2,677 ± 223 <sup>a</sup>	2,790 ± 422 <sup>a</sup>
Erythritol	355 ± 23 <sup>b</sup>	233 ± 17 <sup>a</sup>	223 ± 9 <sup>a</sup>
Fructose	158,566 ± 92,235 <sup>a</sup>	24,019 ± 8,042 <sup>a</sup>	23,441 ± 18,049 <sup>a</sup>
Fructose-6-P	934 ± 118 <sup>a</sup>	443 ± 114 <sup>a</sup>	710 ± 243 <sup>a</sup>
Fucose	133 ± 9 <sup>a</sup>	113 ± 5 <sup>a</sup>	127 ± 12 <sup>a</sup>
Fumarate	123,330 ± 27,007 <sup>a</sup>	87,778 ± 24,003 <sup>a</sup>	94,625 ± 16,385 <sup>a</sup>
Galactose	193 ± 9 <sup>a</sup>	162 ± 3 <sup>a</sup>	187 ± 23 <sup>a</sup>
Glucose	515,782 ± 293,526 <sup>a</sup>	60,282 ± 9,539 <sup>a</sup>	249,905 ± 182,685 <sup>a</sup>
Glucose-6-P	21,736 ± 898 <sup>b</sup>	<b>16,301 ± 1,109<sup>a</sup></b>	18,503 ± 1,374 <sup>ab</sup>
Inositol	1,529 ± 480 <sup>a</sup>	670 ± 88 <sup>a</sup>	1,505 ± 566 <sup>a</sup>
Isocitrate	175 ± 13 <sup>ab</sup>	<b>208 ± 16<sup>b</sup></b>	152 ± 16 <sup>a</sup>
Malate	157,297 ± 24,064 <sup>a</sup>	149,529 ± 85,033 <sup>a</sup>	92,655 ± 27,332 <sup>a</sup>
Maleate	4,301 ± 504 <sup>a</sup>	4,079 ± 927 <sup>a</sup>	3,289 ± 524 <sup>a</sup>
Malonate	841 ± 151 <sup>a</sup>	1,047 ± 23 <sup>ab</sup>	<b>1,258 ± 64<sup>b</sup></b>
Maltose	190 ± 28 <sup>a</sup>	119 ± 9 <sup>a</sup>	146 ± 24 <sup>a</sup>
Mannose	193 ± 24 <sup>a</sup>	133 ± 4 <sup>a</sup>	166 ± 27 <sup>a</sup>
Nicotinic acid	214 ± 84 <sup>a</sup>	172 ± 8 <sup>a</sup>	342 ± 99 <sup>a</sup>
Raffinose	135 ± 11 <sup>a</sup>	113 ± 1 <sup>a</sup>	131 ± 17 <sup>a</sup>
Ribose	171 ± 14 <sup>a</sup>	139 ± 6 <sup>a</sup>	220 ± 45 <sup>a</sup>
Shikimate	548 ± 65 <sup>b</sup>	<b>289 ± 34<sup>a</sup></b>	464 ± 47 <sup>ab</sup>
Succinate	1,916 ± 323 <sup>a</sup>	1,356 ± 364 <sup>a</sup>	1,294 ± 178 <sup>a</sup>
Sucrose	105,548 ± 25,372 <sup>a</sup>	46,234 ± 10,709 <sup>a</sup>	74,239 ± 14,659 <sup>a</sup>
Trehalose	119 ± 22 <sup>b</sup>	<b>52 ± 4<sup>a</sup></b>	75 ± 9 <sup>ab</sup>
Turanose	154 ± 11 <sup>a</sup>	162 ± 2 <sup>a</sup>	185 ± 16 <sup>a</sup>
Xylitol	2,328 ± 827 <sup>b</sup>	<b>113 ± 9<sup>a</sup></b>	<b>235 ± 83<sup>a</sup></b>
Xylose	258 ± 33 <sup>b</sup>	<b>150 ± 5<sup>a</sup></b>	184 ± 17 <sup>ab</sup>



**Fig. A1** Gene expression analysis of *35S:AVP1* over-expressing Arabidopsis. (a) Expression of the constitutively expressed *AtAct2* gene and (b) the *35S:AVP1* transgene in leaf tissue cDNA of 17 *35S:AVP1* sibling lines during preliminary screening. Genes were PCR amplified with gene specific primers as previously described, with water used as a negative control (-). Expression of the *AVP1* transgene was only detected within a single *35S:AVP1* line.



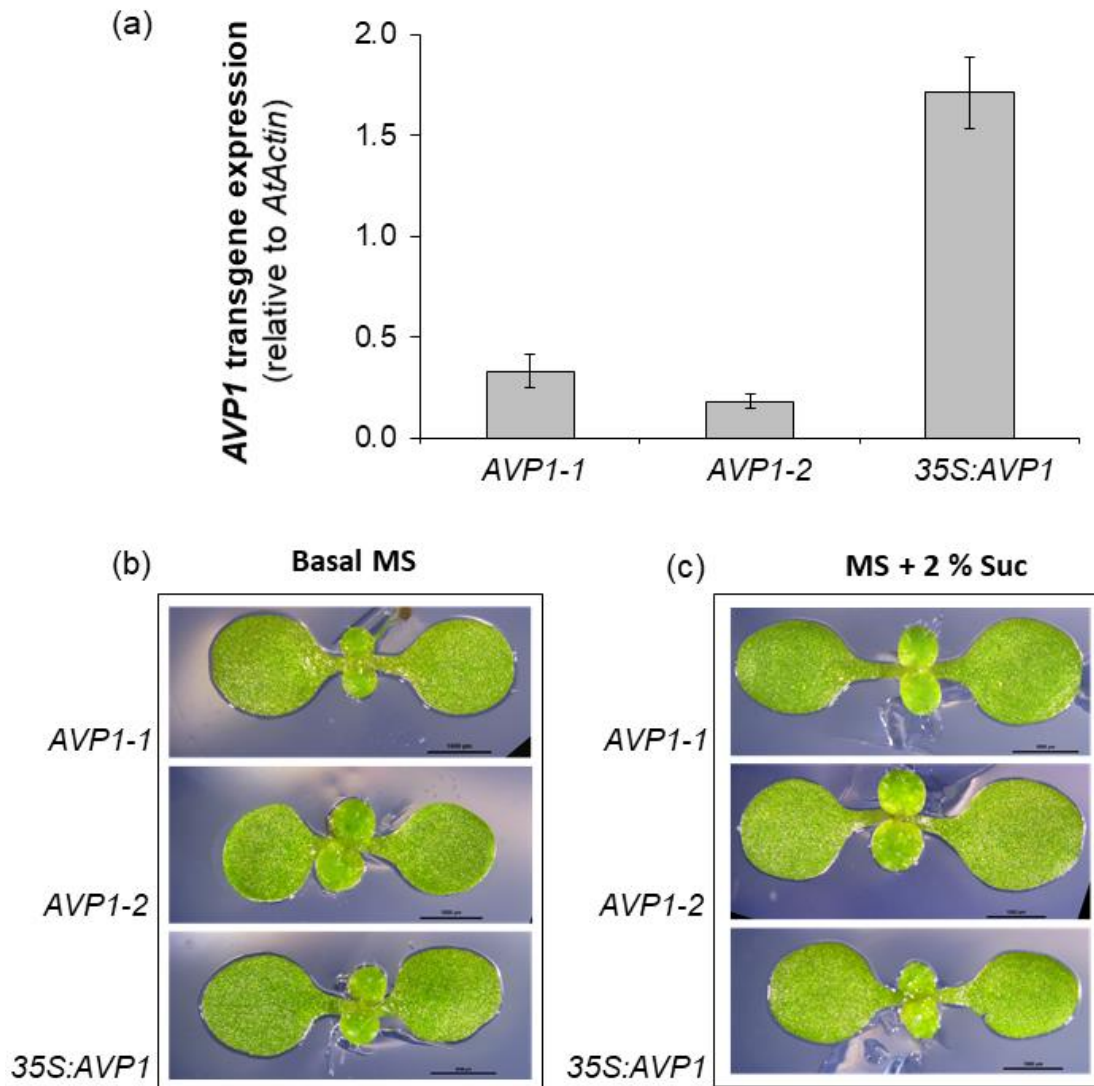


**Fig. A2** Transgene expression and growth phenotypes of *AVP1-1*, *AVP1-2* and *35S:AVP1* transgenic *Arabidopsis* seedlings. (a) Semi-quantitative gene expression analysis of the *AVP1* transgene in *AVP1-1*, *AVP1-2* and *35S:AVP1* transgenic lines relative to *AtActin2* (*AT3G18780*). Eight d-old wild-type *AVP1-1*, *AVP1-2* and *35S:AVP1* transgenic *Arabidopsis* seedlings on (b) basal MS media and (c) MS media with 2 % sucrose (Suc). Seedling cotyledons were imaged using a SMZ25 stereo microscope (2 × Plan Apo, NA 0.312, WD 20 mm, 0.63 × magnification) and NIS-Elements Advanced Research software (Nikon, Minato, Japan). Representative images are shown for each line and were selected from 6 seedlings. Scale bar = 1 mm (1000 μm).

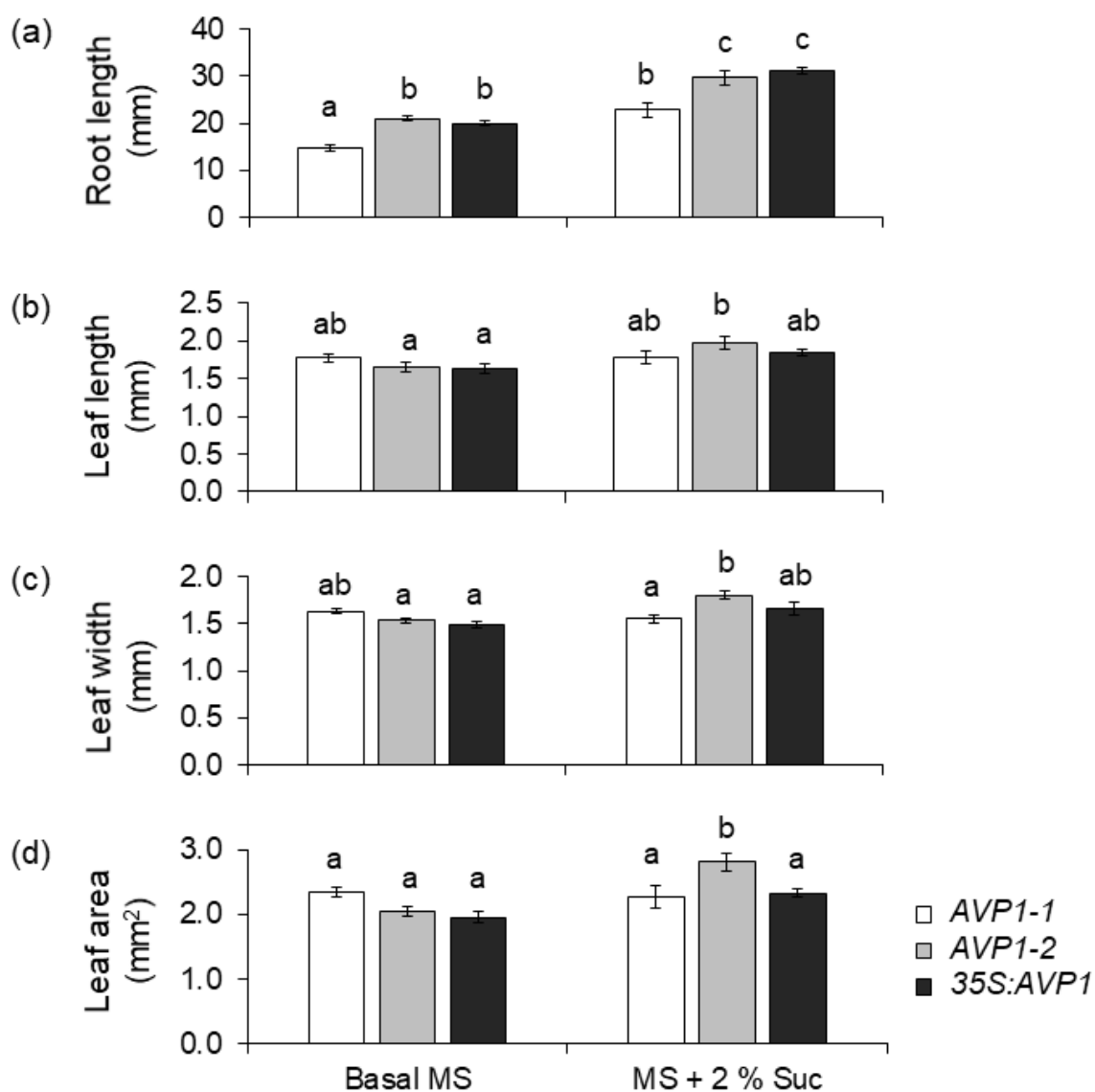


**Fig. A3** Growth parameters of 8 d-old *AVP1-1*, *AVP1-2* and *35S:AVP1* transgenic Arabidopsis on basal MS media with and MS media with 2 % sucrose (Suc). (a) Primary root length (mm), (b) first leaf length (mm), (c) first leaf width (mm), and (d) first leaf total area (mm<sup>2</sup>) of 8 d-old seedlings are displayed, with different letters indicating statistically significant differences (two-way ANOVA, Tukey's 95 % confidence intervals,  $P \leq 0.05$ ) and error bars representing standard error of the mean (n=6).

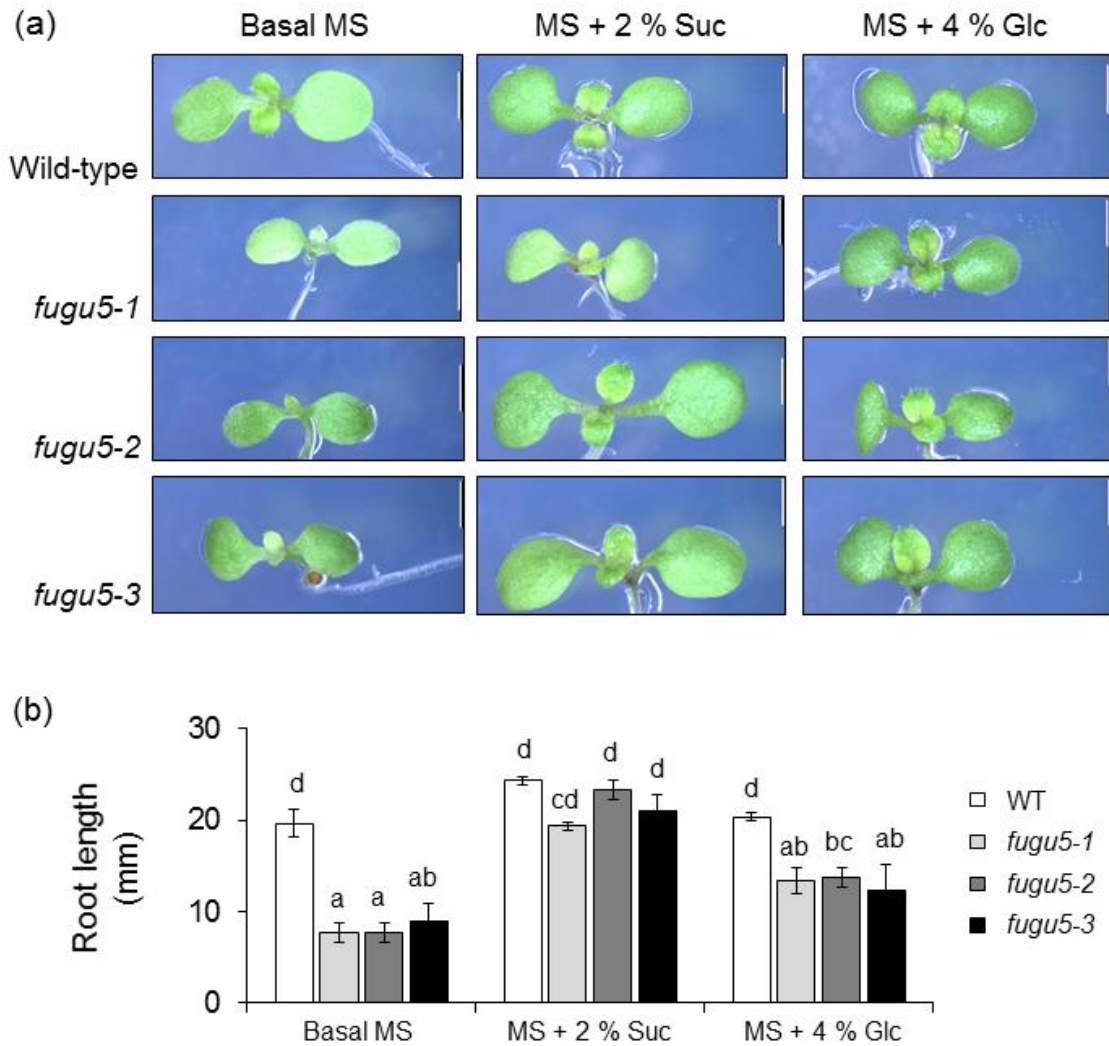


**Fig. A4** Preliminary phenotypic analysis of wild-type and *fugu5* Arabidopsis mutants. (a) Visual growth phenotype and (b) root length (mm) measurements of 8 d-old wild-type, *fugu5-1*, *fugu5-2*, *fugu5-3* mutant Arabidopsis seedlings on basal MS media, MS media with 2 % sucrose (Suc), and MS media with 4 % glucose (Glc). Seedlings were observed using a Leica MZ FLIII Fluorescence Stereomicroscope (Leica Microsystems, Wetzlar, Germany) and images were obtained and analysed using a Leica DC300F digital camera and IM50 software (Leica Microsystems). Different letters indicate statistically significant differences (two-way ANOVA, Tukey's 95 % confidence intervals,  $P \leq 0.05$ ), with error bars representing standard error of the mean ( $n=5$ ). Scale bar = 1 mm (1000  $\mu\text{m}$ ).



**Chapter 3** - Assessing the salt tolerance of *AVP1* expressing  
transgenic wheat

## Statement of Authorship

Title of Paper	Expression of the <i>Arabidopsis thaliana</i> H <sup>+</sup> -PPase gene, <i>AVP1</i> , does not improve growth or salinity tolerance in bread wheat ( <i>Triticum aestivum</i> )
Publication Status	<input type="checkbox"/> Published <input type="checkbox"/> Accepted for Publication <input type="checkbox"/> Submitted for Publication <input checked="" type="checkbox"/> Unpublished and Unsubmitted work written in manuscript style
Publication Details	Although this chapter is written and formatted as a manuscript, this work is not intended to be submitted for publication.

### Principal Author

Name of Principal Author (Candidate)	Daniel J. Menadue		
Contribution to the Paper	Contributed to the experimental design, grew and sampled plants, conducted the genotyping, gene expression analysis, ion analysis and root acidification assay, statistically analysed the data, interpreted the results, and wrote the manuscript.		
Overall percentage (%)	80		
Certification:	This paper reports on original research I conducted during the period of my Higher Degree by Research candidature and is not subject to any obligations or contractual agreements with a third party that would constrain its inclusion in this thesis. I am the primary author of this paper.		
Signature		Date	28/5/2018

### Co-Author Contributions

By signing the Statement of Authorship, each author certifies that:

- i. the candidate's stated contribution to the publication is accurate (as detailed above);
- ii. permission is granted for the candidate to include the publication in the thesis; and
- iii. the sum of all co-author contributions is equal to 100% less the candidate's stated contribution.

Name of Co-Author	Rhiannon K. Schilling		
Contribution to the Paper	Contributed to the experimental design, assisted with the rhizosphere acidification experiment and contributed to revision of the manuscript.		
Signature		Date	4/6/2018

Name of Co-Author	Darren C. Plett		
Contribution to the Paper	Contributed to the experimental design, generated the <i>ubi:AVP1</i> and <i>rab17:AVP1</i> constructs used for plant transformation and contributed to revision of the manuscript.		
Signature		Date	4/6/2018

Name of Co-Author	Stuart J. Roy		
Contribution to the Paper	Conceived the research project, contributed to the experimental design and assisted with revision of the manuscript.		
Signature		Date	28/05/2018

**Expression of the *Arabidopsis thaliana* H<sup>+</sup>-PPase gene, *AVP1*, does not improve growth or salinity tolerance in bread wheat (*Triticum aestivum*)**

**Running title:** Assessing the salt tolerance of *AVP1* expressing transgenic wheat

Daniel Jamie Menadue<sup>1,2</sup>, Rhiannon Kate Schilling<sup>1,2</sup>, Darren Craig Plett<sup>1,2</sup> and Stuart John Roy<sup>1,2\*</sup>

<sup>1</sup>School of Agriculture, Food and Wine, The University of Adelaide, Adelaide, SA, 5005, Australia

<sup>2</sup>Australian Centre for Plant Functional Genomics, Glen Osmond, SA, 5064, Australia

\*Corresponding author: Daniel Menadue, School of Agriculture, Food and Wine, The University of Adelaide, SA 5005 Australia, daniel.menadue@adelaide.edu.au, Tel: +61 8 8313 7162, Fax: +61 8 8313 7102

**Keywords:** constitutive expression, proton-pumping pyrophosphatase, *rab17*, rhizosphere acidification, stress-inducible expression, transgene promoter, *ubiquitin*

**Word count:** 5800



## Abstract

The *Arabidopsis* (*Arabidopsis thaliana*) vacuolar proton-pumping pyrophosphatase gene, *AVP1*, improves growth and abiotic stress tolerance in many plant species when constitutively expressed. However, the impact of *AVP1* expression on the growth and salt tolerance of transgenic bread wheat (*Triticum aestivum*) remains unknown. To investigate this, transgenic wheat (cv. Bob White) lines were generated with constitutive (*ubi:AVP1*) and stress inducible (*rab17:AVP1*) expression of *AVP1*. In control conditions, 6 d-old seedlings of one *ubi:AVP1* line had enhanced total biomass and greater root zone acidification compared to wild-type seedlings. In hydroponic conditions, no difference in shoot or root biomass was observed in any of the *ubi:AVP1* lines under control (0 mM NaCl) or salinity (150 mM NaCl) treatment. Under saline conditions, there were no significant differences in Na<sup>+</sup>, Cl<sup>-</sup> or K<sup>+</sup> concentrations in the 4<sup>th</sup> leaf or root of the *ubi:AVP1* transgenic lines, compared to null segregants. The *rab17:AVP1* lines also displayed no phenotypic difference to the null segregants under control or saline conditions. Based on these results, expression of *AVP1* does not appear to have a beneficial impact on the growth of Bob White transgenic wheat under salinity treatment. Further investigation is required to determine whether expression of *AVP1*, or orthologous H<sup>+</sup>-PPase genes, can be used to enhance the growth and salt tolerance of bread wheat.

## Introduction

With the global population growing exponentially, significant increases in food production are required to maintain food security. However, increasing food production is limited by abiotic stresses (Tester and Langridge, 2010), the occurrence of which are predicted to increase as a result of climate change (Hochman et al., 2017). Bread wheat is the most widely grown cereal crop in the world, with 22 M T of grain produced in Australia annually (Australian Bureau of Statistics, 2017). Approximately 69 % of Australia's wheat production zone is affected by salinity, which contributes to an estimated economic loss of \$1.5 B each year (Rengasamy, 2010). Despite commercial cultivars having the potential to produce 6 t/ha under optimal conditions, the average wheat yield in Australia has remained at 2 t/ha for the last 20 years, largely as a result of abiotic stresses, such as salinity, heat, drought and low nutrient availability (Gilliham et al., 2017; Hochman et al., 2017). To increase wheat production in Australia, wheat varieties with the ability to maintain yield under abiotic stress conditions, without sacrificing high yield under non-stress conditions, are required.

Plants have two main tolerance mechanisms that enable them to maintain growth when exposed to high levels of sodium ( $\text{Na}^+$ ) and chloride ( $\text{Cl}^-$ ); shoot ion independent tolerance (also known as osmotic tolerance), and shoot ion dependent tolerance (also known as ionic tolerance) (Roy et al., 2014). Shoot ion dependent tolerance involves ion transport processes, such as ion exclusion and ion sequestration, as well as the breakdown of reactive oxygen species and the synthesis of compatible solutes (Roy et al., 2014). In ion exclusion, transport proteins such as high-affinity potassium ( $\text{K}^+$ ) transporters (HKTs) (Byrt et al., 2014; James et al., 2011) and those within the Salt Overly Sensitive (SOS) pathway (Cuin et al., 2011; Shi et al., 2000) function within the root to reduce ions from being transported to, and accumulated within, shoot tissues. Ions that are excluded from the shoot are either sequestered into root

cell vacuoles, or transported out of the root via  $\text{Na}^+$  efflux pathways (Britto and Kronzucker, 2015; Munns and Gilliam, 2015).

Under saline conditions, ions such as  $\text{Na}^+$  and  $\text{Cl}^-$  accumulate within the cytosol, where they can disrupt cellular function and inhibit plant growth (Munns, 2002). Vacuolar ion sequestration decreases ion accumulation within the cytosol by transporting these ions into the vacuole or extra cellular space, thus reducing the toxic effects of  $\text{Na}^+$  and  $\text{Cl}^-$  within the cytosol (Munns et al., 2016; Roy et al., 2014). Ion sequestration requires an electrochemical potential difference for protons ( $\text{H}^+$ ) across the tonoplast, which is generated by vacuolar proton-pumping ATPases ( $\text{H}^+$ -ATPase, *EC 3.6.1.3*) and vacuolar proton-pumping pyrophosphatases ( $\text{H}^+$ -PPase, *EC 3.6.1.1*) (Rea and Sanders, 1987).  $\text{H}^+$ -ATPases and  $\text{H}^+$ -PPases generate this electrochemical gradient through hydrolysing cytosolic adenosine triphosphate (ATP) and inorganic pyrophosphate ( $\text{PP}_i$ ), respectively (Rea and Sanders, 1987). The energy generated by these reactions is used to transport  $\text{H}^+$  across the tonoplast (Zhen et al., 1997), which can be utilised by ion transporters, such as the cation/proton antiporter NHX, to transport ions from the cytosol into the vacuole (Gaxiola et al., 1999). As such,  $\text{H}^+$ -ATPases and  $\text{H}^+$ -PPases have an important role in promoting salt tolerance through reducing the accumulation of toxic ions within the cytosol (Gaxiola et al., 2001). However, under stress conditions, the production of ATP is reduced, thereby limiting the function of  $\text{H}^+$ -ATPases (Ashraf and Harris, 2013). Unlike  $\text{H}^+$ -ATPases,  $\text{H}^+$ -PPases utilise  $\text{PP}_i$  as an energy source, which is produced as a by-product of many cellular reactions and is not limited under stress conditions (Maeshima et al., 1996). Furthermore, while the  $\text{H}^+$ -ATPase protein consists of multiple sub-units, which are encoded by several genes (Manolson et al., 1988),  $\text{H}^+$ -PPases consist of one sub-unit and are encoded by a single gene (Sarafian et al., 1992). For these reasons,  $\text{H}^+$ -PPase genes have been favoured over  $\text{H}^+$ -ATPases as a mechanism to improve the salinity tolerance of plants.

Constitutive expression of the Arabidopsis H<sup>+</sup>-PPase gene, *AVP1*, has been demonstrated to enhance the growth of many plant species under saline conditions (Bao et al., 2009; Gao et al., 2006; Gaxiola et al., 2001; Pasapula et al., 2011; Qin et al., 2013; Schilling et al., 2014). Constitutive over-expression of *AVP1* was first shown to enhance plant biomass in Arabidopsis, when treated with 250 mM NaCl (Gaxiola et al., 2001). The enhanced growth of these lines was attributed to an increase in leaf ion sequestration, as the transgenic lines accumulated significantly higher levels of Na<sup>+</sup> and K<sup>+</sup> within the leaf, compared to wild-type (Gaxiola et al., 2001). Constitutive expression of *AVP1* has also been shown to improve the growth of tobacco (*Nicotiana tabacum*) (Gao et al., 2006) and alfalfa (*Medicago sativa*) (Bao et al., 2009) under saline conditions, with the transgenic lines accumulating significantly higher levels of Na<sup>+</sup> within the leaf compared to wild-type. In barley (*Hordeum vulgare*), constitutive expression of *AVP1* enhanced biomass under control and salinity treatment, both in the greenhouse and in the field (Schilling et al., 2014). However, in contrast to other studies, leaf Na<sup>+</sup> concentrations in salt treated *AVP1* expressing barley lines remained unaltered compared to wild-type (Schilling et al., 2014), suggesting *AVP1* may have a role in other processes related to plant growth, in addition to aiding in vacuolar ion sequestration (Schilling et al., 2017).

Despite constitutive expression of *AVP1* improving growth in several plant species, the impact of *AVP1* expression on the growth and stress tolerance of wheat is yet to be investigated. In addition, the potential of stress inducible *AVP1* expression as a strategy to improve plant growth and stress tolerance also remains unknown. When expressed under constitutive promoters, such as the maize (*Zea mays*) *ubiquitin1* and cauliflower mosaic virus (CaMV) 35S promoters, transgene expression occurs at a high level in most cell and tissue types, throughout plant development (Cornejo et al., 1993; Sunilkumar et al., 2002; Torney et al., 2004). High expression in certain plant tissues, or at specific developmental stages in which a gene is not

normally expressed, can have negative consequences, including disrupted growth (Abebe et al., 2003), suppression of endogenous genes (Thompson et al., 2000) and reduced yield (Tung et al., 2008). In contrast, when controlled by an inducible promoter, transgene expression occurs at a high level only when induced, often in response to a stress condition (Rai et al., 2009). In transgenic wheat and barley, constitutive expression of genes encoding the TaDREB2 and TaDREB3 transcription factors, while enhancing drought tolerance, resulted in reduced biomass, delayed flowering and decreased yield under control conditions compared to wild-type (Morran et al., 2011). When controlled by the drought-inducible *rab17* promoter, expression of *TaDREB2* and *TaDREB3* significantly increased plant survival and yield under drought treatment, without producing a negative phenotype under non-stress conditions (Morran et al., 2011). The maize *rab17* promoter is known to induce gene expression in response to drought stress and abscisic acid (ABA) treatment, with transcript levels of the *ZmRab17* gene shown to increase in maize leaves when exposed to salinity stress (Busk et al., 1997). Salinity stress has also been shown to induce *rab17:AVP1* expression in the root of transgenic barley (Schilling, 2014), while only a low level of expression was detected under control conditions (Morran et al., 2011; Schilling, 2014). As such, the *rab17* promoter is a good candidate for investigating the impact of inducible *AVP1* expression in response to salinity stress in wheat.

The aim of this study was to evaluate the impact of constitutive and stress inducible *AVP1* expression on the growth of transgenic bread wheat, under both control and saline conditions, and determine whether *AVP1* expression alters root or shoot ion accumulation.

## Experimental Methods

### Plant Material

The complete cDNA coding sequence (CDS) of the Arabidopsis type I H<sup>+</sup>-pyrophosphatase gene, *AVP1* (*AT1G15690*), was cloned from Arabidopsis (*Col-0*) cDNA into the *pCR8* entry vector (Invitrogen, Carlsbad, United States). The *AVP1* CDS was then transferred into the *pMDC32* destination vector (FJ172534) using Gateway<sup>TM</sup> recombination, containing either the constitutive maize *ubiquitin1* (DQ141598) promoter (*ubi:AVP1* lines) or the stress inducible *rab17* (X15994) promoter (*rab17:AVP1* lines), according to manufacturer's instructions (Invitrogen). Bread wheat callus (cv. Bob White) was transformed via biolistic transformation following the protocol of Ismagul et al. (2014). T<sub>1</sub> seed from 3 transgenic and 1 null segregant line of both *ubi:AVP1* (*ubi:AVP1-1*, *ubi:AVP1-2* and *ubi:AVP1-3*) and *rab17:AVP1* (*rab17:AVP1-1*, *rab17:AVP1-2* and *rab17:AVP1-3*) wheat were selected for further analysis based on transgene expression level, which was assessed via semi-quantitative RT-PCR as described below. For all experiments, seed were UV sterilised for 5 min and germinated in Petri dishes (100 x 100 mm) (SARSTEDT, Technology Park, Australia) on paper towel moistened with reverse osmosis (RO) water. To maintain humidity, Petri dishes were sealed inside polyethylene bags and placed in a growth chamber for 6 d (12 h day length, 22°C day and 18°C night temperatures, 800 μmol m<sup>-2</sup> s<sup>-1</sup> light intensity and 60-80 % relative humidity).

### Plant growth conditions for assessing salinity tolerance

After 6 d from germination, seedlings were transferred to a greenhouse at The Plant Accelerator<sup>®</sup> in Urrbrae, South Australia (latitude: -34.971353; longitude: 138.639933) with a 22°C day and 15°C night temperature, and 60-80 % relative humidity. Representative seedlings

from each line were placed into 18 individual PVC tubes (40 mm × 280 mm) containing polycarbonate plastic beads (Plastics Granulated Services, Adelaide, Australia), 2 cm from the surface. Tubes were placed in a supported hydroponics system (Shavrukov et al., 2012) with a nutrient solution containing 0.2 mM  $\text{NH}_4\text{NO}_3$ , 5 mM  $\text{KNO}_3$ , 2 mM  $\text{Ca}(\text{NO}_3)_2$ , 2 mM  $\text{MgSO}_4$ , 0.1 mM  $\text{KH}_2\text{PO}_4$ , 0.5 mM  $\text{Na}_2\text{Si}_3\text{O}_7$ , 50  $\mu\text{M}$   $\text{NaFe}(\text{III})\text{EDTA}$ , 5  $\mu\text{M}$   $\text{MnCl}_2$ , 10  $\mu\text{M}$   $\text{ZnSO}_4$ , 0.5  $\mu\text{M}$   $\text{CuSO}_4$ , 0.1  $\mu\text{M}$   $\text{Na}_2\text{MoO}_4$ , and rainwater up to 80 L. The pH of the solution was maintained weekly at pH 6.5-7.0 by adjusting with 3.2 % (v/v) HCl, and the growth solutions were replaced every 7 d to prevent nutrient limitation. Automatic pumps supplied the nutrient solution from a 120 L tank to the containers, which held the plants in their tubes, in a 30 min flood, 30 min drain cycle. Plants were grown under natural light for a total of 28 d between the 22<sup>nd</sup> of July and the 19<sup>th</sup> of August 2015. At 3<sup>rd</sup> leaf emergence, NaCl was added to the treatment tank in 25 mM NaCl increments, twice daily, to a final concentration of 150 mM. To maintain similar calcium ( $\text{Ca}^{2+}$ ) activity in the salt treatment tank, as in the control tank, 0.43 mM  $\text{CaCl}_2$  was added with each 25 mM NaCl application. After 21 d of salt treatment, plants were removed from the hydroponics system and 4<sup>th</sup> leaf, shoot and root fresh weights were recorded for salt treated plants, while 4<sup>th</sup> leaf and whole plant weights were recorded for control plants. To remove adhering  $\text{Na}^+$  from the roots, root tissue collected from the salt treated plants were rinsed in 10 mM  $\text{CaSO}_4$ . For transgene presence and expression analysis, the 3<sup>rd</sup> leaf and a section of root tissue were collected from each plant and frozen in liquid nitrogen. The 4<sup>th</sup> leaf of all plants, and root of the salt treated plants were collected for ion analysis and dried at 70°C for 48 h (root samples were not collect from control plants as these plants were transferred to soil to obtain  $T_2$  seed).

### Root acidification assay

To assess differences in root acidification between the transgenic and null segregant *ubi:AVP1* and *rab17:AVP1* lines, seed were selected by weight ( $43 \pm 1.0$  mg) and germinated as previously described. After 6 d, the total biomass of each seedling was recorded. A bromocresol purple ( $C_{21}H_{16}Br_2O_5S$ ) (Sigma-Aldrich, St. Louis, United States) and agarose (Bioline, London, United Kingdom) solution, adjusted to pH 6.5 with 1 M NaOH, was heated in a microwave and 75 mL was poured into individual plastic trays (170 mm  $\times$  170 mm). The solutions were allowed to cool for several minutes before placing seedlings into individual trays containing the media. Root acidification was visually assessed by monitoring colour change, from purple to yellow, within the media. Visual measurements were recorded every 60 min for a total of 4 h.

### DNA extraction and genotyping

To confirm the presence of the *AVP1* transgene, leaf genomic DNA (gDNA) was extracted according to the protocol of Edwards et al. (1991), with some modifications. In brief, cells were lysed by digesting leaf tissue in extraction buffer (100 mM Tris-HCl (pH 7.5), 50 mM EDTA (pH 8.0), 1.25 % SDS) at 65°C for 45 min. DNA was precipitated with 6 M ammonium acetate and 100 % (v/v) isopropanol. Pelleted DNA was washed with 70 % (v/v) ethanol and resuspended in R40 (40  $\mu$ g/mL RNase A (Sigma-Aldrich) in 1 $\times$  TE buffer). Presence of the *AVP1* transgene was determined via polymerase chain reaction (PCR) amplification using *AVP1* specific primers (5' TGTTTTGACCCCTAAAGTTATC 3' and 5' TGGCTCTGAACCCTTGGTC 3') with the following thermocycling conditions; 94°C for 2 min, followed by 30 cycles of 94°C for 30 s, 53°C for 30 s and 68°C for 30 s, with a final extension of 5 min at 68°C. *TaVP1*, a native wheat H<sup>+</sup>-PPase (AY296911), was used as a control gene. *TaVP1* was PCR amplified with gene specific primers



(5' GACGACGACCCTGGAAGCAAGGAA 3' and 5' ATAGAAGCAACAACAAGAGCAGCG 3') with the following thermocycling conditions; 94°C for 2 min, followed by 30 cycles of 94°C for 30 s, 57°C for 30 s and 68°C for 30 s, with a final extension of 5 min at 68°C. Each PCR contained 1 µl (0.5 - 1.0 µg) extracted gDNA, 0.625 U OneTaq® DNA polymerase (New England Biolabs, Ipswich, United States), 1× OneTaq® GC rich Buffer, 100 µM dNTP, 0.2 µM forward primer and 0.2 µM reverse primer in a final volume of 25 µl.

### **RNA purification and expression analysis**

Total RNA was extracted from leaf and root tissue using a DirectZol RNA purification kit (Zymo Research, Irvine, USA) according to the manufacturer's instructions. To prevent contamination by gDNA, an in-column DNase treatment was used following the manufacturer's instructions (Zymo Research). Complementary DNA (cDNA) was reverse transcribed using a SuperScript III reverse transcription kit (Invitrogen). Reactions containing 1 µl purified RNA, standardised to 500 ng using a NanoDrop 1000 spectrophotometer (ThermoFisher Scientific, Waltham, United States), 50 µM oligo(dT)<sub>20</sub>, 10 mM dNTP and sterile water up to 10 µl, were incubated at 65°C for 5 min. Following incubation, 10 µl cDNA Synthesis Mix (10× reverse transcription buffer, 25 mM MgCl<sub>2</sub>, 0.1 M DTT, 40 U RNaseOUT™ and 200 U SuperScript III reverse-transcriptase) was added to each reaction and incubated at 50°C for 50 min, before terminating the reaction at 85°C for 5 min. Semi-quantitative reverse-transcription PCR (RT-PCR) was used to quantify expression levels of the *AVP1* transgene. Synthesised cDNA from leaf and root RNA samples were analysed using the *AVP1* primers and thermocycling conditions described above. The wheat glyceraldehyde 3-phosphate dehydrogenase gene, *TaGAPDH* (EF592180.1), was used as a control gene for RT-PCR and was amplified using the following primers (5'

TTCAACATCATTCCAAGCAGCA 3' and 5' CGTAACCCAAAATGCCCTTG 3'). Reactions were set up as previously described, with thermocycling conditions as follows; 94°C for 2 min, followed by 30 cycles of 94°C for 30 s, 52°C for 30 s and 68°C for 30 s, with a final extension of 5 min at 68°C. *AVP1* expression, relative to *TaGAPDH*, was determined by comparing band intensities of each sample on a 1.5 % agarose gel using GIMP2.8.18 Image Manipulation Software ([www.gimp.org](http://www.gimp.org)).

### Sequencing of the *AVP1* transgene

The full-length *AVP1* transgene was PCR amplified from *ubi:AVP1* gDNA samples using primers specific to the 5' and 3' ends of the *AVP1* transgene (5' ATGGTGGCGCCTGCTTTG 3' and 5' TTAGAAGTACTTGAAAAGGATACCACC 3'). Reactions contained 1 µl (0.5 - 1.0 µg) extracted gDNA, 0.5 U Phusion® High-Fidelity DNA polymerase (New England Biolabs), 1× Phusion HF Buffer, 200 µM dNTP, 0.5 µM forward primer and 0.5 µM reverse primer, in a final volume of 25 µl. Thermocycling conditions were as follows; 98°C for 2 min, followed by 30 cycles of 98°C for 30 s, 65°C for 30 s and 72°C for 30 s, with a final extension of 10 min at 72°C. Amplified DNA was purified using a Nucleospin® Gel and PCR clean-up kit (Macherey-Nagel, Düren, Germany) according to the manufacturer's instructions. A BigDye™ Terminator v3.1 Cycle Sequencing Kit (ThermoFisher Scientific) was used for DNA labelling and samples were sequenced with four gene specific primer pairs (Supplementary Table 1) via capillary separation using a 3730xl DNA Analyzer (ThermoFisher Scientific). Sequence reads were aligned, translated and annotated in Geneious® 10.1.3 (Biomatters Ltd., Auckland, New Zealand).

### Flame photometry and chloride analysis

After drying at 70°C for 48 h, 4<sup>th</sup> leaf and root samples were weighed and digested in 10 mL of 1 % (v/v) nitric acid for 4 h in a Hotblock (Environmental Express, Mount Pleasant, USA) at 80°C. Na<sup>+</sup> and K<sup>+</sup> concentrations were analysed in the digested leaf and root solutions using a Model 420 flame photometer (Sherwood, Cambridge, UK) and Cl<sup>-</sup> concentrations were determined with a Sherwood 926 chloride analyser.

### Statistical analysis

Statistical analysis was performed in Microsoft® Office Excel 2013, with significant differences determined via one-way analysis of variance (ANOVA) and Tukey's 95 % confidence intervals.

## Results

### *AVP1* expression levels vary between *AVP1* transgenic lines

PCR amplification from gDNA samples confirmed the presence of the *AVP1* transgene in the three transgenic *ubi:AVP1* wheat lines, while the transgene was shown to be absent in the null segregant line (Figure 1a). Expression analysis via RT-PCR revealed *AVP1* expression levels varied between the three *ubi:AVP1* wheat lines (Figure 1a). Despite the *AVP1* transgene being present in gDNA of the *rab17:AVP1* transgenic lines (Supplementary Figure 1A), no expression of the transgene was detected in either leaf (Supplementary Figure 1b) or root (Supplementary Figure 1c) samples in control (data not shown) or saline conditions (Supplementary Figure 1). Sanger sequencing revealed a 90 bp deletion within the *AVP1* CDS in the *ubi:AVP1-3* line (Figure 2a). In the translated amino acid sequence, this deletion created a stop codon at position 252, five residues upstream of the PP<sub>i</sub> binding site (Figure 2b).

### **Biomass and root zone acidification is enhanced in *ubi:AVP1-1* seedlings**

In 6 d-old seedlings, the *ubi:AVP1-1* line showed a 20 % increase in total biomass, and were significantly larger than the null segregant, *ubi:AVP1-2* and *ubi:AVP1-3* lines (Figure 3a). Neither *ubi:AVP1-2* or *ubi:AVP1-3* lines had an increase in seedling biomass compared to null segregants. After 4 h, *ubi:AVP1-1* seedlings had a greater colour change in the pH-sensitive bromocresol purple media surrounding the root zone than all other lines (Figure 3b). Media surrounding the root zone of these lines changed from purple (pH 6.5) to yellow (pH 5.5-5.0). Media surrounding the roots of null segregant, *ubi:AVP1-2* and *ubi:AVP1-3* seedlings displayed minimal colour changes (Figure 3b), indicating an increase in root-zone acidification in *ubi:AVP1-1* seedlings.

### **Growth of *AVP1* transgenic wheat is not enhanced in control or saline hydroponic conditions**

After 5 weeks in control conditions, neither the *ubi:AVP1* or *rab17:AVP1* lines had an increase in total plant biomass compared to null segregants (Figure 4a, Supplementary Figure 3a). The average number of tillers in the *ubi:AVP1-1* line was slightly higher than both the null segregant and other *ubi:AVP1* transgenic lines, however, this increase was not statistically significant (Figure 4b). Similarly, after 3 weeks in saline conditions, no significant differences in total plant biomass or tiller number were observed between the *ubi:AVP1*, *rab17:AVP1* and null segregant lines (Figure 4, Supplementary Figure 3). With the addition of 150 mM NaCl, growth was significantly reduced in all lines compared to control conditions, with no lines developing more than 1 tiller after 5 weeks of growth (Figure 4b, Supplementary Figure 3b).

***AVP1* expression does not significantly enhance 4<sup>th</sup> leaf Na<sup>+</sup>, K<sup>+</sup> or Cl<sup>-</sup> accumulation**

Under saline conditions, 4<sup>th</sup> leaf Na<sup>+</sup> concentrations in all lines increased from approximately 10 µmol/g DW in 0 mM NaCl, to approximately 1000 µmol/g DW in 150 mM NaCl (Figure 5, Supplementary Figure 4). However, no significant differences in Na<sup>+</sup>, Cl<sup>-</sup> or K<sup>+</sup> concentrations within the 4<sup>th</sup> leaf or root were observed between null segregants, *ubi:AVP1* or *rab17:AVP1* lines (Figure 5, Supplementary Figure 4). Although not significant, the *ubi:AVP1-1* line displayed a slight increase in shoot Na<sup>+</sup> and Cl<sup>-</sup> concentration under salt treatment compared to the other *ubi:AVP1* lines (Figure 5b). The 4<sup>th</sup> leaf Na<sup>+</sup> concentration in the *ubi:AVP1-2* and *ubi:AVP1-3* lines were 10 % and 50 % lower under salt treatment than the null segregants, respectively. The 4<sup>th</sup> leaf Cl<sup>-</sup> concentration was also 20 % and 7 % higher in the *ubi:AVP1-2* and *ubi:AVP1-3* lines compared to null segregants (Figure 5b). In *ubi:AVP1-3*, the 4<sup>th</sup> leaf Cl<sup>-</sup> concentration was approximately 15 % lower than the null segregants, while no difference in 4<sup>th</sup> leaf K<sup>+</sup> concentration was observed in any of the *ubi:AVP1* or *rab17:AVP1* lines in saline conditions (Figure 5b, Supplementary Figure 4). No difference in root Na<sup>+</sup>, Cl<sup>-</sup> or K<sup>+</sup> concentrations were apparent in either the *ubi:AVP1* or *rab17:AVP1* lines (Figure 5c, Supplementary Figure 4c). The 4<sup>th</sup> leaf Na<sup>+</sup>/K<sup>+</sup> ratio of *ubi:AVP1-1* was 20 % higher than null segregants, 30 % higher than *ubi:AVP1-2* and 60 % higher than *ubi:AVP1-3* (Figure 5d). The Na<sup>+</sup>/K<sup>+</sup> ratio of *ubi:AVP1-2* was similar to the null segregants, while *ubi:AVP1-3* was approximately 50 % lower. No differences in the Na<sup>+</sup>/K<sup>+</sup> ratio were observed between the *rab17:AVP1* and null segregant lines (Supplementary Figure 4d).

## Discussion

### **Enhanced seedling vigour may be responsible for the increase in rhizosphere acidification by 6 d-old *ubi:AVP1-1* seedlings**

In media containing the pH indicator bromocresol purple, the line with the highest level of *AVP1* expression (*ubi:AVP1-1*) noticeably reduced the pH of the media surrounding the root zone. A reduction in pH was not apparent in the media surrounding the root zone of the other *ubi:AVP1* transgenic lines or null segregants. This increase in acidification was likely the result of the *ubi:AVP1-1* line having a larger root system and, therefore, a higher level of proton exudation than the other lines. Six d-old seedlings of the *ubi:AVP1-1* line also had a significant increase in total biomass compared to the *ubi:AVP1-2*, *ubi:AVP1-3* and null segregants lines. Increased root proton exudation is an advantageous trait that can increase nutrient availability through altering rhizosphere pH (Marschner et al., 1986). Expression of *AVP1* has previously been shown to enhance growth in conditions with low nutrient availability, which has been attributed to increased root proton exudation (Paez-Valencia et al., 2013). As the 6 d-old *ubi:AVP1* seedlings were grown on filter paper without supplied nutrients and were in the heterotrophic growth phase, during which growth is dependent on nutrient reserves within the seed (Elamrani et al., 2008), the greater level of acidification by *ubi:AVP1-1* seedlings is unlikely to have contributed to the larger biomass of this line. Previous research has shown that, when *AVP1* function in *Arabidopsis* is impaired, seedling growth is significantly reduced (Ferjani et al., 2011). This growth reduction was hypothesised to be due to an inhibition of sucrose production via gluconeogenesis, as a result of cytosolic  $PP_i$  accumulation (Ferjani et al., 2011). The improved biomass of 6 d-old *ubi:AVP1-1* seedlings, therefore, could be the result of enhanced cytosolic  $PP_i$  hydrolysis, leading to increased sucrose production and, therefore, enhanced seedling growth. Alternatively, higher *AVP1* expression within the previous ( $T_0$ ) generation may

have improved nutrient uptake and remobilisation (Paez-Valencia et al., 2013; Yang et al., 2007), photosynthate assimilation (Pizzio et al., 2015) or sugar transport (Gaxiola et al., 2012; Khadilkar et al., 2016). Increased available grain reserves within the T<sub>1</sub> seed, which were utilised during the heterotrophic growth phase, could account for the larger biomass of *ubi:AVP1-1* seedlings. In the *ubi:AVP1-3* line, a 90 bp deletion within the *AVP1* transgene was identified, which is likely to have prevented the formation of a functional AVP1 protein in this line. A lack of AVP1 function may be responsible for the lack of phenotypic difference in this line compared to the null segregants. However, the reason for the lack of enhanced biomass and root acidification in the *ubi:AVP1-2* line compared to the null segregant and *ubi:AVP1-3* lines remains unclear.

**Lack of *rab17* promoter activation is likely responsible for the absence of *AVP1* expression in *rab17:AVP1* lines**

When controlled by the *rab17* promoter, transgene expression is known to occur at a low level under control conditions (Morran et al., 2011; Schilling, 2014), and to be induced under stress conditions (Busk et al., 1997; Schilling, 2014; Vilardell et al., 1991). While the *rab17:AVP1* transgenic lines were confirmed to contain sequences specific to the *AVP1* transgene, expression of the transgene could not be detected in either leaf or root tissue sampled from control or salt treated plants. The lack of *AVP1* expression in the salt treated plants suggests that the 150 mM NaCl treatment may not have been sufficient to induce expression of the transgene. In a previous study, a 24 h NaCl treatment  $\geq$  250 mM was required to induce expression of *rab17* within the shoot of 8 d-old maize seedlings, while a 500 mM NaCl treatment was required to induce *rab17* expression within the root (Busk et al., 1997).

Therefore, it is possible that a higher level of NaCl treatment is required to induce *AVP1* expression under the *rab17* promoter. However, as bread wheat is only a moderately salt tolerant species (Munns and Tester, 2008), this would be a severe stress treatment. While the application of salt treatments are frequently applied gradually, both to prevent osmotic shock and to accurately simulate field conditions, this method may have failed to induce the *rab17* promoter, which is highly responsive to osmotic stress (Busk et al., 1997; Vilardell et al., 1991). Despite being less representative of salt stress conditions within the field, applying the salt treatment over a shorter period of time may be required to induce *AVP1* expression by the *rab17* promoter in wheat.

The lack of *AVP1* expression in the *rab17:AVP1* lines may also have been due to transgene silencing, which has been reported to occur in up to 75 % of T<sub>1</sub> Bob White wheat lines (Anand et al., 2003), or fragmentation of the *AVP1* transgene as a result of the biolistic transformation process (Chauhan and Khurana, 2017). Alternatively, expression within a specific cell type may have prevented detection of the transgene, with *rab17:AVP1* expression in barley shown to be specific to root stelar cells (Schilling, 2014). As total root RNA was extracted from a small section sampled from the base of the root system, the sampling method may have prevented detection of *AVP1* expression in these samples. Specificity of *AVP1* within the root could provide an explanation for the increased rhizosphere acidification observed in several of the lines in the bromocresol purple media, however, further characterisation of the *rab17:AVP1* lines is required to investigate this. Generation of transgenic wheat lines containing reporter genes, such as the  $\beta$ -glucuronidase (GUS) and green fluorescent protein (GFP) (Kavita and Burma, 2008) controlled by the *rab17* promoter, would be beneficial for investigating the effectiveness of this promoter in driving transgene expression in wheat. Such reporter lines would also aid in



determining conditions in which the *rab17* promoter is induced in wheat, which may differ to those in other plant species (Vilardell et al., 1994).

#### **AVP1 may not have a beneficial impact on salt tolerance in bread wheat**

Under 150 mM NaCl, the *ubi:AVP1* transgenic lines had no significant difference in 4<sup>th</sup> leaf ion concentration compared to null segregants. However, there was large variation in both 4<sup>th</sup> leaf Na<sup>+</sup> and Cl<sup>-</sup> concentrations between the three transgenic lines. While the *ubi:AVP1-1* line had a slight increase in 4<sup>th</sup> leaf Na<sup>+</sup> under salinity stress compared to null segregants, the *ubi:AVP1-2* line had slightly lower Na<sup>+</sup>, and a similar level of Cl<sup>-</sup> to the null segregants. The *ubi:AVP1-3* line had 50 % less Na<sup>+</sup> in the 4<sup>th</sup> leaf and 15 % lower Cl<sup>-</sup> than the null segregants. Despite these differences, growth under salt treatment was not improved in any of the transgenic lines compared to null segregants. While increased tissue ion concentrations are often cited as evidence for enhanced vacuolar ion sequestration, ion concentrations do not have to be enhanced for vacuole sequestration to be improved (Munns and Tester, 2008). The overall lack of enhanced ion accumulation in the transgenic lines under salt treatment compared to wild-type may be due to several factors, including targeting and function of the AVP1 protein, suitability of the *ubiquitin* promoter and the preference for ion exclusion in bread wheat.

Localisation of AVP1 has been investigated in *Arabidopsis* using the GFP reporter gene (Segami et al., 2014). In this study, GFP was inserted into a non-conserved region encoding a cytoplasmic loop, allowing AVP1 localisation to be visualised under control of the native *AVP1* promoter without affecting protein function. In the majority of lines analysed, the AVP1 protein localised exclusively to the tonoplast, while in lines with artificially high levels of AVP1, the protein localised to the plasma membrane (Segami et al., 2014). These results indicate that AVP1 can

be mis-targeted in *Arabidopsis* when highly expressed (Segami et al., 2014). As *AVP1* expression levels varied among the *ubi:AVP1* lines, differences in *AVP1* localisation could have contributed to the phenotypic variation between the lines. A lack of *AVP1* targeting to the tonoplast could have prevented an increase in  $\text{Na}^+$  and  $\text{Cl}^-$  accumulation in the transgenic lines compared to wild-type. The phenotypic variation may also have been influenced by the maize *ubiquitin* promoter, which was used to drive transgene expression in these lines. Despite being classified as a constitutive promoter, transgene expression controlled by the *ubiquitin* promoter has been reported to be highly variable in transgenic rice (Cornejo et al., 1993), maize (Torney et al., 2004) and wheat (Rooke et al., 2000), with activity highest in young, rapidly developing tissues and decreasing through time (Christensen et al., 1992). In wheat, transgene expression level and localisation was found to vary considerably between transgenic lines when controlled by the *ubiquitin* promoter (Rooke et al., 2000), while differences in tissue specificity have been observed among transgenic maize lines using the *ubiquitin* promoter (Torney et al., 2004). Therefore, use of the *ubiquitin* promoter to drive expression of *AVP1* may also have contributed to the phenotypic variation observed between the transgenic lines.

When accumulation of ions within plant tissues increases, plants require greater production of compatible solutes to maintain osmotic balance (Hasegawa et al., 2000; Munns, 2005). Wheat varieties with the ability to maintain osmotic balance, through increased production of compatible solutes, have been shown to maintain growth under saline conditions more effectively than varieties in which compatible solute levels remain unaltered (Sairam et al., 2002; Saneoka et al., 1999). An inability to maintain osmotic balance could have reduced the ability of the transgenic lines to accumulate higher levels of  $\text{Na}^+$  and  $\text{Cl}^-$  within the vacuole compared to null segregants.

Previous research has also shown that ion exclusion, rather than ion sequestration, is the primary salt tolerance mechanism in several bread wheat varieties (Husain et al., 2004). A strong ability to exclude ions from the shoot would prevent  $\text{Na}^+$  from accumulating within the cytosol of shoot tissue, thus making an enhanced ability to sequester ions into the vacuole unnecessary (Byrt et al., 2014; Horie et al., 2009). A preference for ion exclusion could explain the lack of significant increases in leaf ion accumulation in the transgenic lines under saline conditions compared to null segregants, as well as the variability between transgenic *ubi:AVP1* lines.

Despite considerable research, the role of *AVP1* in enhancing vacuole ion sequestration remains unclear. While several studies have reported constitutively expressing *AVP1* plants to have enhanced ion accumulation and growth compared to wild-type under saline conditions (Bao et al., 2009; Gaxiola et al., 2001; Kim et al., 2013), several studies have reported enhanced growth under saline conditions without alterations in leaf ion accumulation (Lv et al., 2015; Schilling et al., 2014; Yang et al., 2015). In addition, several studies in which constitutive expression of  $\text{H}^+$ -PPase genes has improved growth, compared to wild-type under saline conditions, have not reported tissue ion concentrations (Kumar et al., 2014; Pasapula et al., 2011; Qin et al., 2013; Shen et al., 2015). Although ion concentrations do not necessarily have to increase for ion sequestration within the vacuole to be enhanced (Munns and Tester, 2008), the variation in ion accumulation between these studies, as well as the improved growth observed in these lines under other abiotic stress conditions, suggests the beneficial phenotypes observed in *AVP1* expressing transgenic plants are likely due to the involvement of *AVP1* in multiple cellular processes (Gaxiola et al., 2012; Gaxiola et al., 2016; Schilling et al., 2017). As such, while growth of the *ubi:AVP1* lines was not improved under saline conditions, these lines may have a beneficial phenotype when exposed to other abiotic stress conditions.

While *Arabidopsis* contains a single H<sup>+</sup>-PPase gene, multiple H<sup>+</sup>-PPase genes have been identified in cereal species, with 3 H<sup>+</sup>-PPase genes identified in barley (Shavrukov, 2014) and 6 H<sup>+</sup>-PPases known in rice (*Oryza sativa*) (Liu et al., 2010). Differences in expression level and tissue localisation among barley and rice homologs have also been identified, with different genes within each species demonstrated to be involved in different stress responses (Fukuda et al., 2004; Liu et al., 2010; Shavrukov et al., 2013). It has been hypothesised that, in cereal species, H<sup>+</sup>-PPases have diversified and developed individual and specialised functions (Wang et al., 2009). Consequently, further research should focus on the identification and characterisation of native wheat H<sup>+</sup>-PPase genes, to help elucidate the role of H<sup>+</sup>-PPases in bread wheat. Such knowledge is crucial to identifying wheat H<sup>+</sup>-PPase genes that are beneficial for improving the growth of wheat under control and stress conditions.

## Conclusions

The lack of significant phenotypic differences between the *ubi:AVP1* wheat lines and null segregants may have been due to several factors, including the ability of bread wheat to naturally exclude ions from the shoot, or a lack of AVP1 function in the transgenic plants. Few phenotypic differences were observed in the *rab17:AVP1* lines, which was likely due to the *rab17* promoter failing to induce transgene expression, or these lines having cell-type specific and/or low levels of expression. Based on the results of this study it appears that expression of *AVP1*, under control of the maize *ubiquitin* and *rab17* promoters, does not have a beneficial impact on the growth of transgenic Bob White wheat, under control or saline conditions. To further investigate the role of H<sup>+</sup>-PPase genes in wheat, transgenic bread wheat expressing *AVP1*, or *AVP1* orthologs, using both constitutive and stress inducible promoters, need to be

characterised. In addition, greater knowledge of the native wheat H<sup>+</sup>-PPase genes, and their function in stressed and non-stress conditions, would provide useful insights as to how these genes can be further utilised to improve the growth and stress tolerance of bread wheat.

### **Acknowledgements**

The authors wish to thank the ACPFG Transformation Group for generating the transgenic wheat lines used in this study. This research was funded by the Grains Research Development Corporation (UA00145). Daniel Menadue is the recipient of a GRDC Grains Industry Research Scholarship (GRS10931).

## References

- Abebe, T., Guenzi, A.C., Martin, B. and Cushman, J.C. (2003) Tolerance of mannitol-accumulating transgenic wheat to water stress and salinity. *Plant Physiol.* **131**, 1748-1755.
- Anand, A., Trick, H.N., Gill, B.S. and Muthukrishnan, S. (2003) Stable transgene expression and random gene silencing in wheat. *Plant Biotechnol. J.* **1**, 241-251.
- Ashraf, M. and Harris, P.J.C. (2013) Photosynthesis under stressful environments: An overview. *Photosynthetica* **51**, 163-190.
- Australian Bureau of Statistics (2017) Agricultural Commodities, Australia, 2015-16.
- Bao, A.K., Wang, S.M., Wu, G.Q., Xi, J.J., Zhang, J.L. and Wang, C.M. (2009) Overexpression of the *Arabidopsis* H<sup>+</sup>-PPase enhanced resistance to salt and drought stress in transgenic alfalfa (*Medicago sativa* L.). *Plant Sci.* **176**, 232-240.
- Britto, D.T. and Kronzucker, H.J. (2015) Sodium efflux in plant roots: What do we really know? *J. Plant Physiol.* **186-187**, 1-12.
- Busk, P.K., Jensen, A.B. and Pages, M. (1997) Regulatory elements *in vivo* in the promoter of the abscisic acid responsive gene *rab17* from maize. *Plant J.* **11**, 1285-1295.
- Byrt, C.S., Xu, B., Krishnan, M., Lightfoot, D.J., Athman, A., Jacobs, A.K., Watson-Haigh, N.S., Plett, D., Munns, R., Tester, M. and Gilliam, M. (2014) The Na<sup>+</sup> transporter, TaHKT1;5-D, limits shoot Na<sup>+</sup> accumulation in bread wheat. *Plant J.* **80**, 516-526.
- Chauhan, H. and Khurana, P. (2017) Wheat genetic transformation using mature embryos as explants. In: *Wheat Biotechnology: Methods and Protocols* (Bhalla, P.L. and Singh, M.B. eds), pp. 153-167. New York, NY: Springer New York.
- Christensen, A., Sharrock, R. and Quail, P. (1992) Maize polyubiquitin genes: Structure, thermal perturbation of expression and transcript splicing, and promoter activity following transfer to protoplasts by electroporation. *Plant Mol. Biol.* **18**, 675-689.
- Cornejo, M.J., Luth, D., Blankenship, K., Anderson, O. and Blechl, A. (1993) Activity of a maize ubiquitin promoter in transgenic rice. *Plant Mol. Biol.* **23**, 567-581.
- Cuin, T.A., Bose, J., Stefano, G., Jha, D., Tester, M., Mancuso, S. and Shabala, S. (2011) Assessing the role of root plasma membrane and tonoplast Na<sup>+</sup>/H<sup>+</sup> exchangers in salinity tolerance in wheat: *in planta* quantification methods. *Plant, Cell Environ.* **34**, 947-961.
- Edwards, K., Johnstone, C. and Thompson, C. (1991) A simple and rapid method for the preparation of plant genomic DNA for PCR analysis. *Nucleic Acids Res.* **19**, 1349.
- Elamrani, A., Raymond, P. and Saglio, P. (2008) Nature and utilization of seed reserves during germination and heterotrophic growth of young sugar beet seedlings. *Seed Sci. Res.* **2**, <https://doi.org/10.1017/S0960258500001045>.
- Ferjani, A., Segami, S., Horiguchi, G., Muto, Y., Maeshima, M. and Tsukaya, H. (2011) Keep an eye on PPi: The vacuolar-type H<sup>+</sup>-pyrophosphatase regulates postgerminative development in *Arabidopsis*. *Plant Cell* **23**, 2895-2908.
- Fukuda, A., Chiba, K., Maeda, M., Nakamura, A., Maeshima, M. and Tanaka, Y. (2004) Effect of salt and osmotic stresses on the expression of genes for the vacuolar H<sup>+</sup>-pyrophosphatase, H<sup>+</sup>-ATPase subunit A, and Na<sup>+</sup>/H<sup>+</sup> antiporter from barley. *J. Exp. Bot.* **55**, 585-594.
- Gao, F., Gao, Q., Duan, X., Yue, G., Yang, A. and Zhang, J. (2006) Cloning of an H<sup>+</sup>-PPase gene from *Thellungiella halophila* and its heterologous expression to improve tobacco salt tolerance. *J. Exp. Bot.* **57**, 3259-3270.

- Gaxiola, R.A., Rao, R., Sherman, A., Grisafi, P., Alper, S.L. and Fink, G.R. (1999) The *Arabidopsis thaliana* proton transporters, AtNHX1 and AVP1, can function in cation detoxification in yeast. *Proc. Natl. Acad. Sci.* **96**, 1480-1485.
- Gaxiola, R.A., Li, J., Undurraga, S., Dang, L.M., Allen, G.J., Alper, S.L. and Fink, G.R. (2001) Drought- and salt-tolerant plants result from overexpression of the *AVP1* H<sup>+</sup>-pump. *Proc. Natl. Acad. Sci.* **98**, 11444-11449.
- Gaxiola, R.A., Sanchez, C.A., Paez-Valencia, J., Ayre, B.G. and Elser, J.J. (2012) Genetic manipulation of a “vacuolar” H<sup>+</sup>-PPase: From salt tolerance to yield enhancement under phosphorus-deficient soils. *Plant Physiol.* **159**, 3-11.
- Gaxiola, R.A., Regmi, K.C., Paez-Valencia, J., Pizzio, G.A. and Zhang, S. (2016) Plant H<sup>+</sup>-PPases: Reversible enzymes with contrasting functions dependent on membrane environment. *Mol. Plant* **9**, 317-319.
- Gilliam, M., Able, J.A. and Roy, S.J. (2017) Translating knowledge about abiotic stress tolerance to breeding programmes. *Plant J.* **90**, 898-917.
- Hasegawa, P.M., Bressan, R.A., Zhu, J.-K. and Bohnert, H.J. (2000) Plant cellular and molecular responses to high salinity. *Annu. Rev. Plant Biol.* **51**, 463-499.
- Hochman, Z., Gobbett, D.L. and Horan, H. (2017) Climate trends account for stalled wheat yields in Australia since 1990. *Glob. Chang. Biol.* **23**, 2071-2081.
- Horie, T., Hauser, F. and Schroeder, J.I. (2009) HKT transporter-mediated salinity resistance mechanisms in *Arabidopsis* and monocot crop plants. *Trends Plant Sci.* **14**, 660-668.
- Husain, S., von Caemmerer, S. and Munns, R. (2004) Control of salt transport from roots to shoots of wheat in saline soil. *Funct. Plant Biol.* **31**, 1115-1126.
- Ismagul, A., Iskakova, G., Harris, J.C. and Eliby, S. (2014) Biolistic transformation of wheat with centropheoxine as a synthetic auxin. *Methods Mol. Biol.* **1145**, 191-202.
- James, R.A., Blake, C., Byrt, C.S. and Munns, R. (2011) Major genes for Na<sup>+</sup> exclusion, *Nax1* and *Nax2* (wheat *HKT1;4* and *HKT1;5*), decrease Na<sup>+</sup> accumulation in bread wheat leaves under saline and waterlogged conditions. *J. Exp. Bot.* **62**, 2939-2947.
- Kavita, P. and Burma, P.K. (2008) A comparative analysis of green fluorescent protein and beta-glucuronidase protein-encoding genes as a reporter system for studying the temporal expression profiles of promoters. *J. Biosci.* **33**, 337-343.
- Khadilkar, A.S., Yadav, U.P., Salazar, C., Shulaev, V., Paez-Valencia, J., Pizzio, G.A., Gaxiola, R.A. and Ayre, B.G. (2016) Constitutive and companion cell-specific overexpression of *AVP1*, encoding a proton-pumping pyrophosphatase, enhances biomass accumulation, phloem loading, and long-distance transport. *Plant Physiol.* **170**, 401-414.
- Kim, Y.S., Kim, I.S., Choe, Y.H., Bae, M.J., Shin, S.Y., Park, S.K., Kang, H.G., Kim, Y.H. and Yoon, H.S. (2013) Overexpression of the *Arabidopsis* vacuolar H<sup>+</sup>-pyrophosphatase *AVP1* gene in rice plants improves grain yield under paddy field conditions. *J. Agric. Sci.* **152**, 941-953.
- Kumar, T., Uzma, Khan, M.R., Abbas, Z. and Ali, G.M. (2014) Genetic improvement of sugarcane for drought and salinity stress tolerance using *Arabidopsis* vacuolar pyrophosphatase (*AVP1*) gene. *Mol. Biotechnol.* **56**, 199-209.
- Liu, Q., Zhang, Q., Burton, R.A., Shirley, N.J. and Atwell, B.J. (2010) Expression of vacuolar H<sup>+</sup>-pyrophosphatase (*OVP3*) is under control of an anoxia-inducible promoter in rice. *Plant Mol. Biol.* **72**, 47-60.
- Lv, S., Jiang, P., Nie, L., Chen, X., Tai, F., Wang, D., Fan, P., Feng, J., Bao, H., Wang, J. and Li, Y. (2015) H<sup>+</sup>-pyrophosphatase from *Salicornia europaea* confers tolerance to

- simultaneously occurring salt stress and nitrogen deficiency in *Arabidopsis* and wheat. *Plant, Cell Environ.* **38**, 2433–2449.
- Maeshima, M., Nakanishi, Y., Matsuura-Endo, C. and Tanaka, Y. (1996) Proton pumps of the vacuolar membrane in growing plant cells. *J Plant Res* **109**, 119-125.
- Manolson, M.F., Ouellette, B.F., Filion, M. and Poole, R.J. (1988) cDNA sequence and homologies of the "57-kDa" nucleotide-binding subunit of the vacuolar ATPase from *Arabidopsis*. *J. Biol. Chem.* **263**, 17987-17994.
- Marschner, H., Römheld, V., Horst, W.J. and Martin, P. (1986) Root-induced changes in the rhizosphere: Importance for the mineral nutrition of plants. *J. Plant Nutr. Soil Sci.* **149**, 441-456.
- Morran, S., Eini, O., Pyvovarenko, T., Parent, B., Singh, R., Ismagul, A., Eliby, S., Shirley, N., Langridge, P. and Lopato, S. (2011) Improvement of stress tolerance of wheat and barley by modulation of expression of DREB/CBF factors. *Plant Biotechnol. J.* **9**, 230-249.
- Munns, R. (2002) Comparative physiology of salt and water stress. *Plant, Cell Environ.* **25**, 239-250.
- Munns, R. (2005) Genes and salt tolerance: Bringing them together. *New Phytol.* **167**, 645-663.
- Munns, R. and Tester, M. (2008) Mechanisms of salinity tolerance. *Annu. Rev. Plant Biol.* **59**, 651-681.
- Munns, R. and Gilliam, M. (2015) Salinity tolerance of crops – what is the cost? *New Phytol.* **208**, 668-673.
- Munns, R., James, R.A., Gilliam, M., Flowers, T.J. and Colmer, T.D. (2016) Tissue tolerance: an essential but elusive trait for salt-tolerant crops. *Funct. Plant Biol.* **43**, 1103-1113.
- Paez-Valencia, J., Sanchez-Lares, J., Marsh, E., Dorneles, L.T., Santos, M.P., Sanchez, D., Winter, A., Murphy, S., Cox, J., Trzaska, M., Metler, J., Kozic, A., Facanha, A.R., Schachtman, D., Sanchez, C.A. and Gaxiola, R.A. (2013) Enhanced proton translocating pyrophosphatase activity improves nitrogen use efficiency in romaine lettuce. *Plant Physiol.* **161**, 1557-1569.
- Pasapula, V., Shen, G., Kuppu, S., Paez-Valencia, J., Mendoza, M., Hou, P., Chen, J., Qiu, X., Zhu, L., Zhang, X., Auld, D., Blumwald, E., Zhang, H., Gaxiola, R. and Payton, P. (2011) Expression of an *Arabidopsis* vacuolar H<sup>+</sup>-pyrophosphatase gene (*AVP1*) in cotton improves drought- and salt tolerance and increases fibre yield in the field conditions. *Plant Biotechnol. J.* **9**, 88-99.
- Pizzio, G.A., Paez-Valencia, J., Khadilkar, A.S., Regmi, K., Patron-Soberano, A., Zhang, S., Sanchez-Lares, J., Furstenau, T., Li, J., Sanchez-Gomez, C., Valencia-Mayoral, P., Yadav, U.P., Ayre, B.G. and Gaxiola, R.A. (2015) *Arabidopsis* type I proton-pumping pyrophosphatase expresses strongly in phloem, where it is required for pyrophosphate metabolism and photosynthate partitioning. *Plant Physiol.* **167**, 1541-1553.
- Qin, H., Gu, Q., Kuppu, S., Sun, L., Zhu, X., Mishra, N., Hu, R., Shen, G., Zhang, J., Zhang, Y., Zhu, L., Zhang, X., Burow, M., Payton, P. and Zhang, H. (2013) Expression of the *Arabidopsis* vacuolar H<sup>+</sup>-pyrophosphatase gene *AVP1* in peanut to improve drought and salt tolerance. *Plant Biotechnol. Rep.* **7**, 345-355.
- Rai, M., He, C. and Wu, R. (2009) Comparative functional analysis of three abiotic stress-inducible promoters in transgenic rice. *Transgenic Res.* **18**, 787-799.
- Rea, P.A. and Sanders, D. (1987) Tonoplast energization: Two H<sup>+</sup> pumps, one membrane. *Physiol. Plant.* **71**, 131-141.
- Rengasamy, P. (2010) Soil processes affecting crop production in salt-affected soils. *Funct. Plant Biol.* **37**, 613-620.



- Rooke, L., Byrne, D. and Salgueiro, S. (2000) Marker gene expression driven by the maize *ubiquitin* promoter in transgenic wheat. *Ann. Appl. Biol.* **136**, 167-172.
- Roy, S.J., Negrão, S. and Tester, M. (2014) Salt resistant crop plants. *Curr. Opin. Biotechnol.* **26**, 115-124.
- Sairam, R.K., Rao, K.V. and Srivastava, G.C. (2002) Differential response of wheat genotypes to long term salinity stress in relation to oxidative stress, antioxidant activity and osmolyte concentration. *Plant Sci.* **163**, 1037-1046.
- Saneoka, H., Shiota, K., Kurban, H., Chaudhary, M.I., Premachandra, G.S. and Fujita, K. (1999) Effect of salinity on growth and solute accumulation in two wheat lines differing in salt tolerance. *Soil Sci. Plant Nutr.* **45**, 873-880.
- Sarafian, V., Kim, Y., Poole, R.J. and Rea, P.A. (1992) Molecular cloning and sequence of cDNA encoding the pyrophosphate-energized vacuolar membrane proton pump of *Arabidopsis thaliana*. *Proc. Natl. Acad. Sci.* **89**, 1775-1779.
- Schilling, R.K. (2014) "Evaluating the abiotic stress tolerance of transgenic barley expressing an *Arabidopsis* vacuolar H<sup>+</sup>-pyrophosphatase gene (*AVP1*)". Adelaide, Australia: The University of Adelaide.
- Schilling, R.K., Marschner, P., Shavrukov, Y., Berger, B., Tester, M., Roy, S.J. and Plett, D.C. (2014) Expression of the *Arabidopsis* vacuolar H<sup>+</sup>-pyrophosphatase gene (*AVP1*) improves the shoot biomass of transgenic barley and increases grain yield in a saline field. *Plant Biotechnol. J.* **12**, 378-386.
- Schilling, R.K., Tester, M., Marschner, P., Plett, D.C. and Roy, S.J. (2017) AVP1: One protein, many roles. *Trends Plant Sci.* **22**, 154-162.
- Segami, S., Makino, S., Miyake, A., Asaoka, M. and Maeshima, M. (2014) Dynamics of vacuoles and H<sup>+</sup>-pyrophosphatase visualized by monomeric green fluorescent protein in *Arabidopsis*: Artifactual bulbs and native intravacuolar spherical structures. *The Plant Cell* **26**, 3416-3434.
- Shavrukov, Y., Genc, Y. and Hayes, J. (2012) The use of hydroponics in abiotic stress tolerance research. In: *Hydroponics - A Standard Methodology for Plant Biological Researches* (Asao, T. ed) pp. 39-66. InTech Open Access Publisher.
- Shavrukov, Y., Bovill, J., Afzal, I., Hayes, J., Roy, S., Tester, M. and Collins, N. (2013) *HVP10* encoding V-PPase is a prime candidate for the barley *HvNax3* sodium exclusion gene: evidence from fine mapping and expression analysis. *Planta* **237**, 1111-1122.
- Shavrukov, Y. (2014) Vacuolar H<sup>+</sup>-PPase (*HVP*) genes in barley: Chromosome location, sequence and gene expression relating to Na<sup>+</sup> exclusion and salinity tolerance. In: *Barley: Physical properties, genetic factors and environmental impact on growth* (Hasunuma, K. ed). New York: Nova Science Publishers.
- Shen, G., Wei, J., Qiu, X., Hu, R., Kuppu, S., Auld, D., Blumwald, E., Gaxiola, R., Payton, P. and Zhang, H. (2015) Co-overexpression of *AVP1* and *AtNHX1* in cotton further improves drought and salt tolerance in transgenic cotton plants. *Plant Mol. Biol. Rep.* **33**, 167-177.
- Shi, H., Ishitani, M., Kim, C. and Zhu, J.-K. (2000) The *Arabidopsis thaliana* salt tolerance gene *SOS1* encodes a putative Na<sup>+</sup>/H<sup>+</sup> antiporter. *Proc. Natl. Acad. Sci.* **97**, 6896-6901.
- Sunilkumar, G., Mohr, L., Lopata-Finch, E., Emani, C. and Rathore, K.S. (2002) Developmental and tissue-specific expression of CaMV 35S promoter in cotton as revealed by GFP. *Plant Mol. Biol.* **50**, 463-479.
- Tester, M. and Langridge, P. (2010) Breeding technologies to increase crop production in a changing world. *Science* **327**, 818-822.

- Thompson, A.J., Jackson, A.C., Symonds, R.C., Mulholland, B.J., Dadswell, A.R., Blake, P.S., Burbidge, A. and Taylor, I.B. (2000) Ectopic expression of a tomato 9-*cis*-epoxycarotenoid dioxygenase gene causes over-production of abscisic acid. *Plant J.* **23**, 363-374.
- Torney, F., Partier, A., Says-Lesage, V., Nadaud, I., Barret, P. and Beckert, M. (2004) Heritable transgene expression pattern imposed onto maize ubiquitin promoter by maize *adh-1* matrix attachment regions: tissue and developmental specificity in maize transgenic plants. *Plant Cell Rep.* **22**, 931-938.
- Tung, S.A., Smeeton, R., White, C.A., Black, C.R., Taylor, I.B., Hilton, H.W. and Thompson, A.J. (2008) Over-expression of *LeNCED1* in tomato (*Solanum lycopersicum* L.) with the *rbcS3C* promoter allows recovery of lines that accumulate very high levels of abscisic acid and exhibit severe phenotypes. *Plant, Cell Environ.* **31**, 968-981.
- Vilardell, J., Mundy, J., Stilling, B., Leroux, B., Pla, M., Freyssinet, G. and Pages, M. (1991) Regulation of the maize *rab17* gene promoter in transgenic heterologous systems. *Plant Mol. Biol.* **17**, 985-993.
- Vilardell, J., Martinez-Zapater, J.M., Goday, A., Arenas, C. and Pages, M. (1994) Regulation of the *rab17* gene promoter in transgenic Arabidopsis wild-type, ABA-deficient and ABA-insensitive mutants. *Plant Mol. Biol.* **24**, 561-569.
- Wang, Y., Xu, H., Zhang, G., Zhu, H., Zhang, L., Zhang, Z., Zhang, C. and Ma, Z. (2009) Expression and responses to dehydration and salinity stresses of V-PPase gene members in wheat. *J. Genet. Genomics* **36**, 711-720.
- Yang, H., Knapp, J., Koirala, P., Rajagopal, D., Peer, W.A., Silbart, L.K., Murphy, A. and Gaxiola, R.A. (2007) Enhanced phosphorus nutrition in monocots and dicots over-expressing a phosphorus-responsive type I H<sup>+</sup>-pyrophosphatase. *Plant Biotechnol. J.* **5**, 735-745.
- Yang, Y., Tang, R.J., Li, B., Wang, H.H., Jin, Y.L., Jiang, C.M., Bao, Y., Su, H.Y., Zhao, N., Ma, X.J., Yang, L., Chen, S.L., Cheng, X.H. and Zhang, H.X. (2015) Overexpression of a *Populus trichocarpa* H<sup>+</sup>-pyrophosphatase gene *PtVP1.1* confers salt tolerance on transgenic poplar. *Tree Physiol.* **35**, 663-677.
- Zhen, R., Kim, E. and Rea, P. (1997) The molecular and biochemical basis of pyrophosphate-energized proton translocation at the vacuolar membrane. *Adv. Bot. Res.* **25**, 297-337.

## Figure legends

**Figure 1: Transgene presence and expression analysis of *ubi:AVP1* transgenic and null segregant (nulls) wheat lines.** Agarose gels showing (a) presence of the native *TaVP1* wheat gene and the *AVP1* transgene in gDNA of null segregants and transgenic wheat lines (*ubi:AVP1-1*, *ubi:AVP1-2* and *ubi:AVP1-3*), and (b) expression of *TaGAPDH* and the *AVP1* transgene in leaf cDNA samples. Water was used as a negative control for all PCR reactions (-). (c) Semi-quantitative gene expression analysis of the *AVP1* transgene, relative to *TaGAPDH* expression, in cDNA samples of null segregant and transgenic wheat lines. Values are means  $\pm$  standard error of the mean (n=3).

**Figure 2: Sequence analysis of the *AVP1* transgene in *ubi:AVP1* transgenic wheat lines.** Alignment of (a) nucleotide and (b) translated amino acid sequences of the *AVP1* transgene amplified from *ubi:AVP1* gDNA samples with the *AVP1* reference sequence (*AT1G15690*). Position of nucleotide and amino acid residues are indicated by numbers above each line, with the pyrophosphate (PP<sub>i</sub>) binding site annotated in the (b) amino acid alignment. Dashes (-) indicate missing bases in (a) the *ubi:AVP1-3* coding sequence, while in the (b) amino acid alignment asterisks (\*) indicate stop codons within the *ubi:AVP1-3* amino acid sequence, due to the deletion in the nucleotide sequence as indicated above.

**Figure 3: Phenotypic characteristics of 6 d-old *ubi:AVP1* and null segregant (nulls) wheat seedlings.** (a) Fresh weights (g FW per plant) of 6 d-old null segregant and *AVP1* transgenic wheat (*ubi:AVP1-1*, *ubi:AVP1-2* and *ubi:AVP1-3*) seedlings. Values are means  $\pm$  standard error of the mean (n=3-5). Different letters indicate values with significant differences (one-way

ANOVA,  $P \leq 0.05$ , Tukey's 95 % confidence interval). (b) Representative images of 6 d-old null segregants and *ubi:AVP1* wheat lines after 4 h in a pH sensitive bromocresol purple media. Scale bar = 3.25 cm. Inset shows pH colour scale range (5.0-7.0).

**Figure 4: Growth characteristics of *ubi:AVP1* transgenic and null segregant (nulls) wheat lines following 3 weeks in hydroponic conditions under 0 mM NaCl and 150 mM NaCl.**

(a) Fresh weight (g FW per plant) and (b) tiller number of null segregants and *AVP1* transgenic lines (*ubi:AVP1-1*, *ubi:AVP1-2* and *ubi:AVP1-3*) in 0 mM NaCl (white columns) and 150 mM NaCl (grey columns) for 3 weeks. Values are means  $\pm$  standard error of the mean (n=5-9). Different letters indicate values with significant differences (one-way ANOVA,  $P \leq 0.05$ , Tukey's 95 % confidence interval).

**Figure 5: Leaf and root  $\text{Na}^+$ ,  $\text{Cl}^-$  and  $\text{K}^+$  concentrations in *ubi:AVP1* transgenic and null segregant (nulls) wheat lines in hydroponics under 0 mM NaCl and 150 mM NaCl.** Ion ( $\text{Na}^+$ ,  $\text{Cl}^-$  and  $\text{K}^+$ ) concentrations in the 4<sup>th</sup> leaf at (a) 0 mM NaCl and (b) 150 mM NaCl, and (c) in roots at 150 mM NaCl. (d) Shoot  $\text{Na}^+/\text{K}^+$  ratios of null segregants (nulls, white columns) and *ubi:AVP1-1* (light grey columns), *ubi:AVP1-2* (dark grey columns) and *ubi:AVP1-3* (black columns) transgenic wheat lines, in 150 mM NaCl for 21 d. Values are means  $\pm$  standard error of the mean (n= 4-9). Different letters indicate significant differences between lines for each ion (one-way ANOVA,  $P \leq 0.05$ , Tukey's 95 % confidence interval).

## Figures

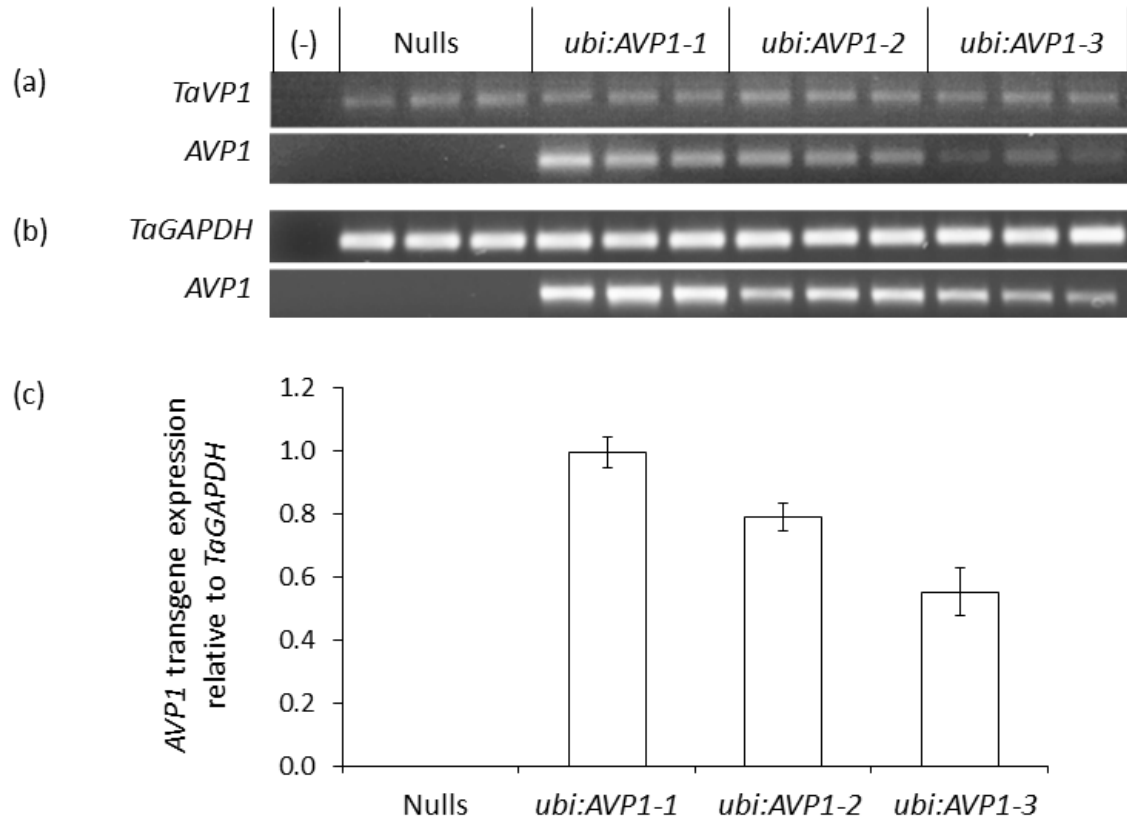


Figure 1: Transgene presence and expression analysis of *ubi:AVP1* transgenic and null segregant (nulls) wheat lines

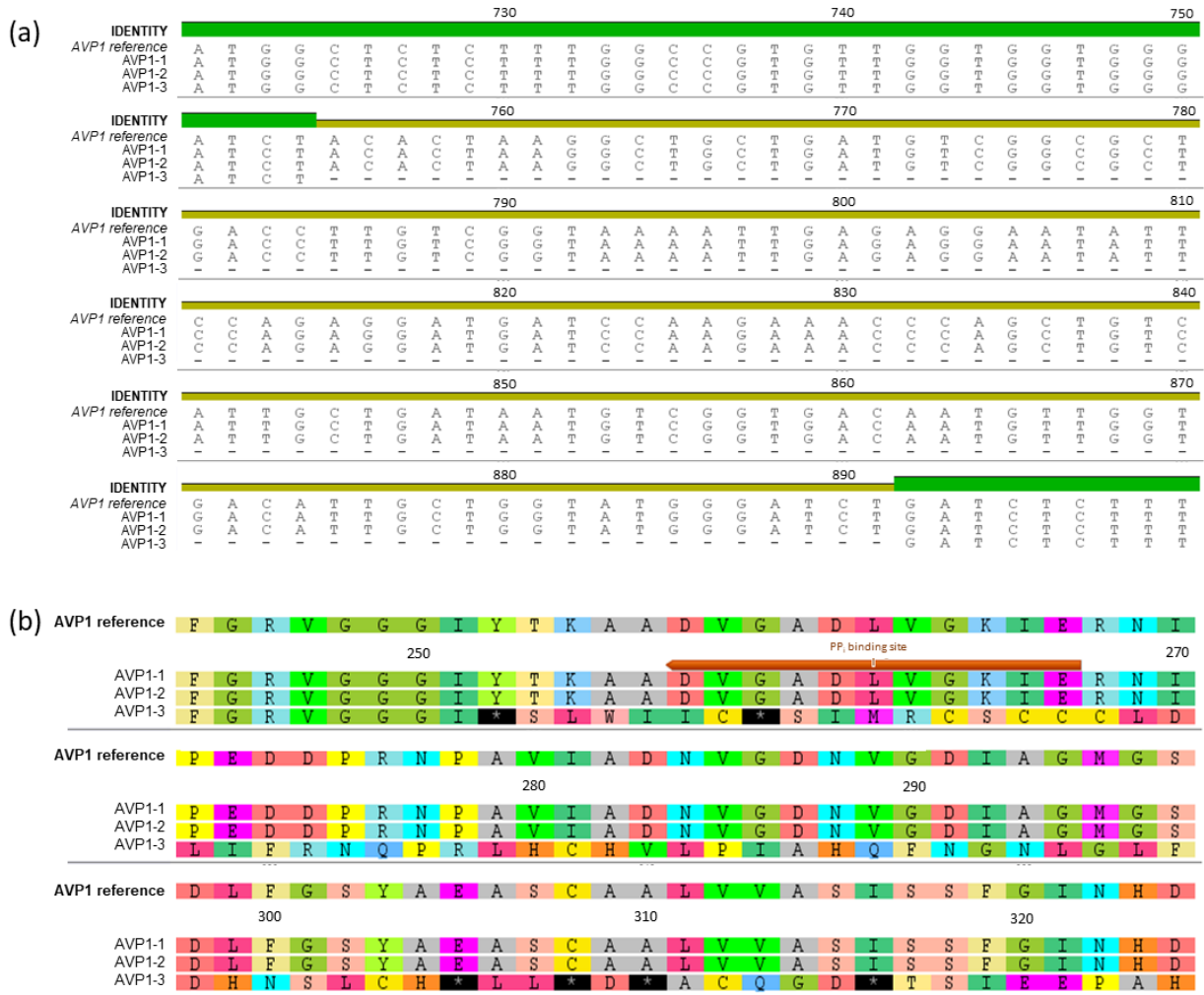


Figure 2: Sequence analysis of the *AVP1* transgene in *ubi:AVP1* transgenic wheat lines.

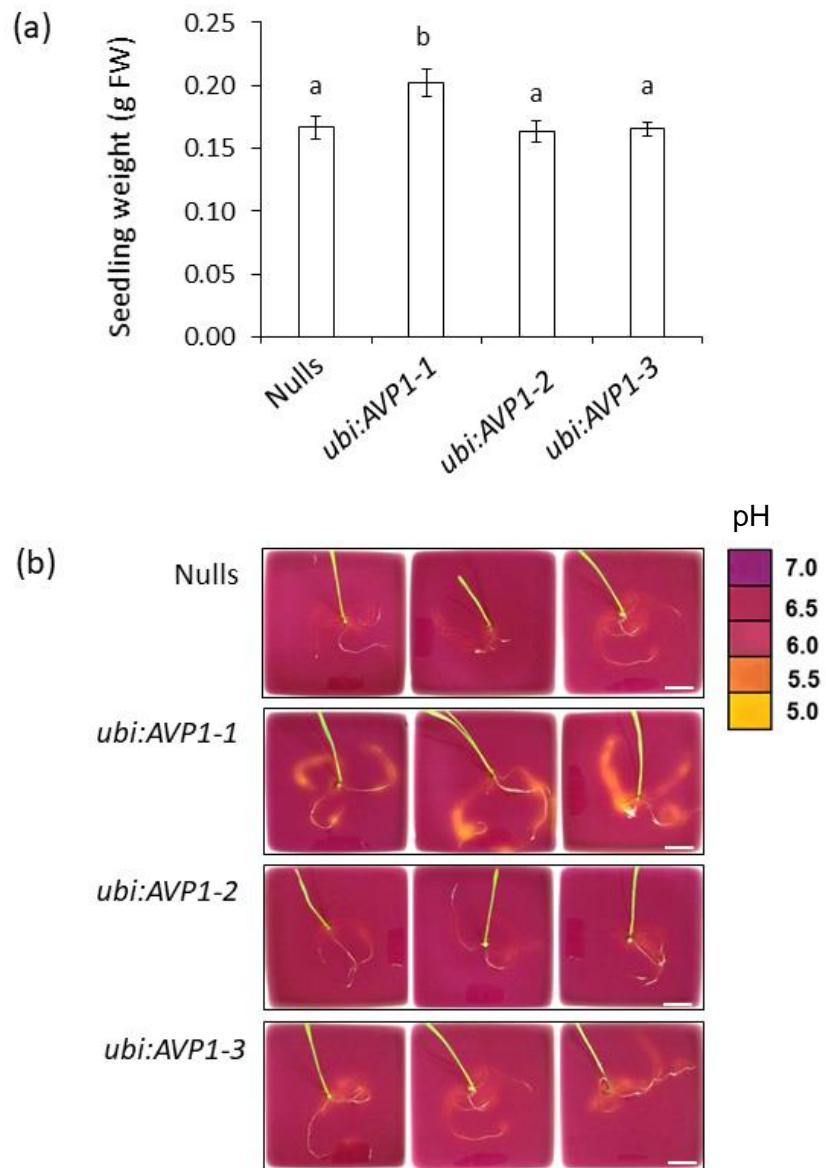


Figure 3: Phenotypic characteristics of 6 d-old *ubi:AVP1* and null segregant (nulls) wheat seedlings

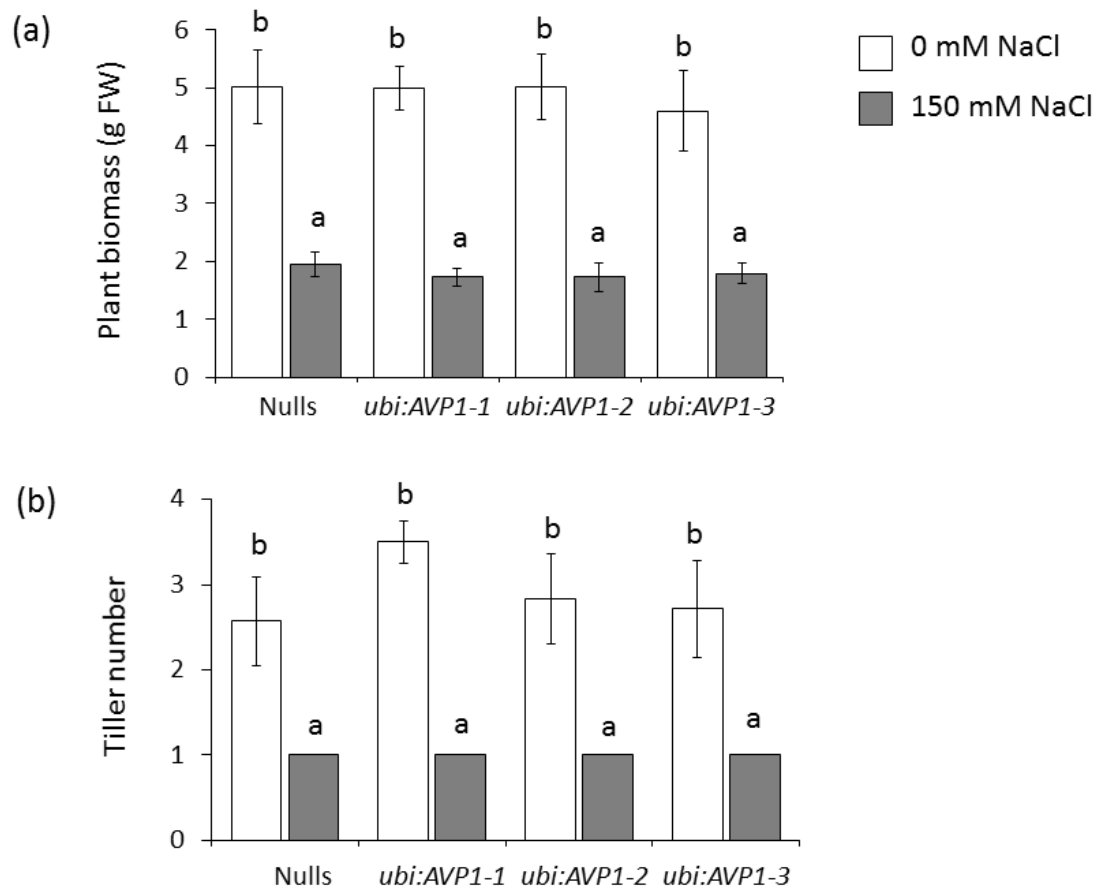


Figure 4: Growth characteristics of *ubi:AVP1* transgenic and null segregant (nulls) wheat lines following 3 weeks in hydroponic conditions under 0 mM NaCl and 150 mM NaCl.



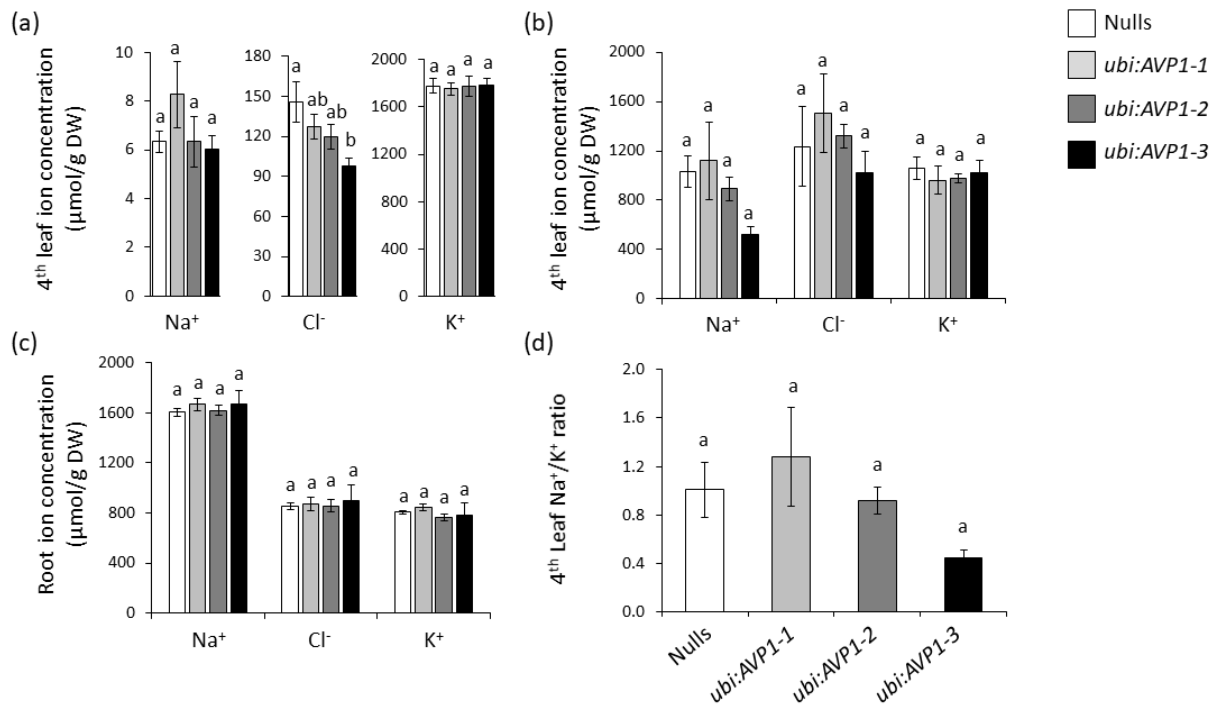


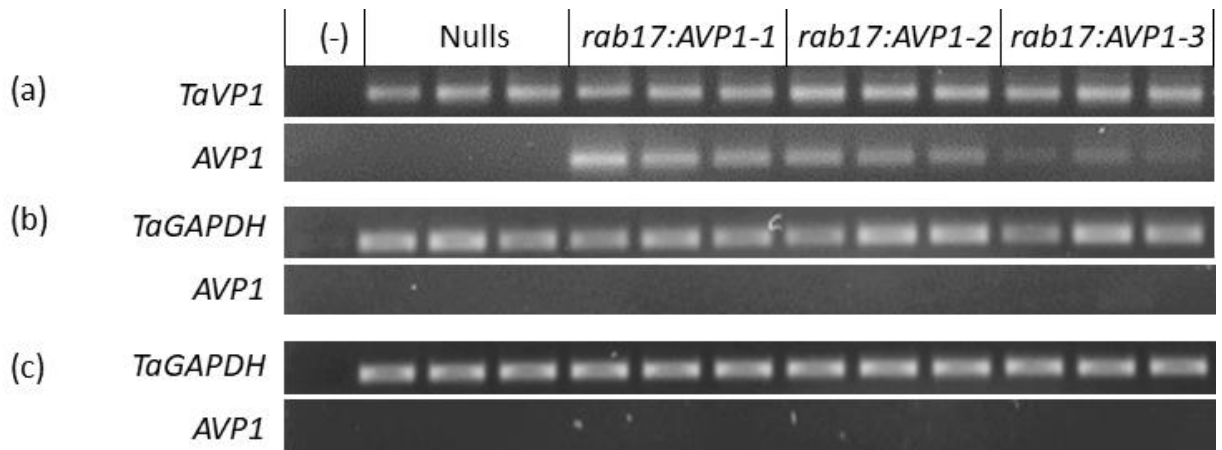
Figure 5: Leaf and root Na<sup>+</sup>, Cl<sup>-</sup> and K<sup>+</sup> concentrations in *ubi:AVP1* transgenic and null segregant (nulls) wheat lines in hydroponics under 0 mM NaCl and 150 mM NaCl.

## Supplementary Tables

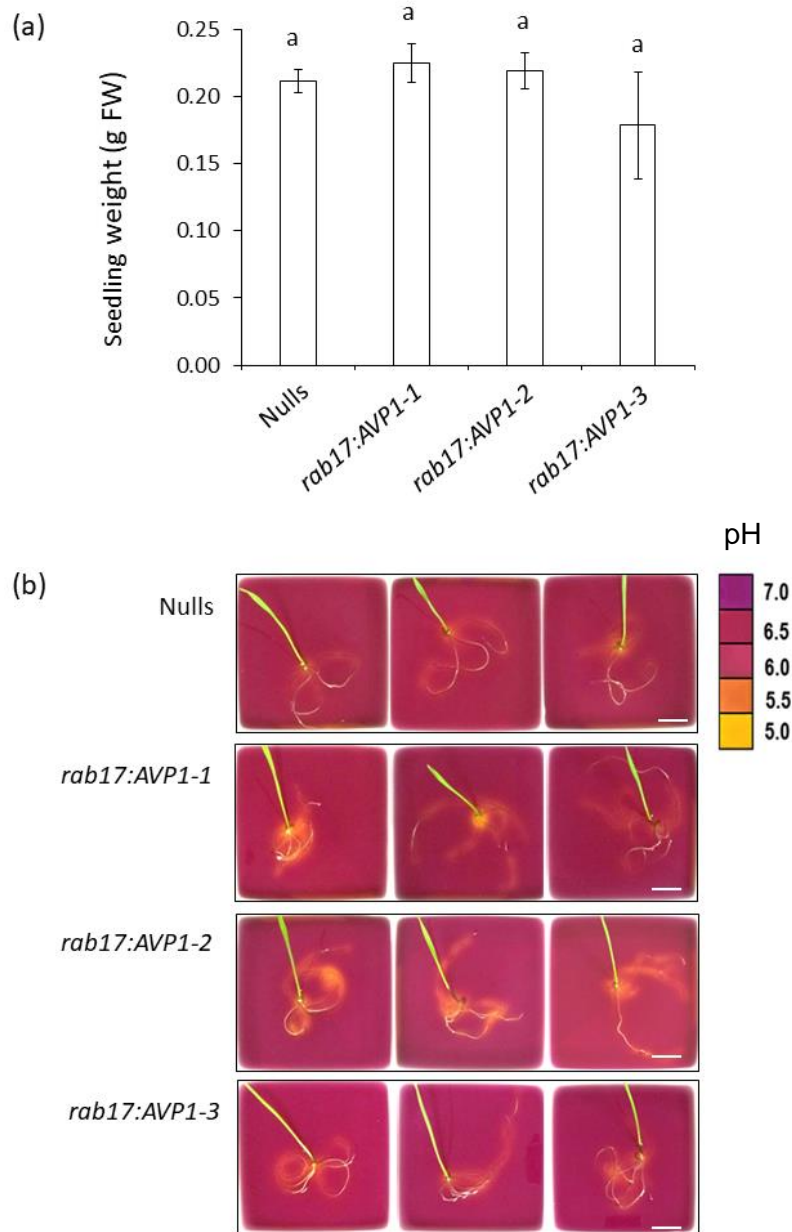
**Supplementary Table 1:** Details of primers used to amplify and sequence the *AVP1* transgene in gDNA samples of the *ubi:AVP1-1*, *ubi:AVP1-2* and *ubi:AVP1-3* transgenic wheat lines.

Primer name	Primer sequence (5'-3')	Details
AVP1cloneF	ATGGTGGCGCCTGCTTTG	Binds to 5' end of <i>AVP1</i> CDS
AVP1cloneR	TTAGAAGTACTTGAAAAGGATACCACC	Binds to 3' end of <i>AVP1</i> CDS
ZmUbiF	TTTAGCCCTGCCTTCATACG	Binds to 3' end of <i>ubiquitin</i> promoter
AVP1seq1	ATCAACCACGACTTCACTGCC	Binds 800 bp from 5' end of <i>AVP1</i> CDS
AVP1seq2	GGGACAACGCCAAGAAATAC	Binds 300 bp from 3' end of <i>AVP1</i> CDS
NOSrev	ATAATCATCGCAAGACCGGCAAC	Binds to 5' end of <i>NOS</i> terminator

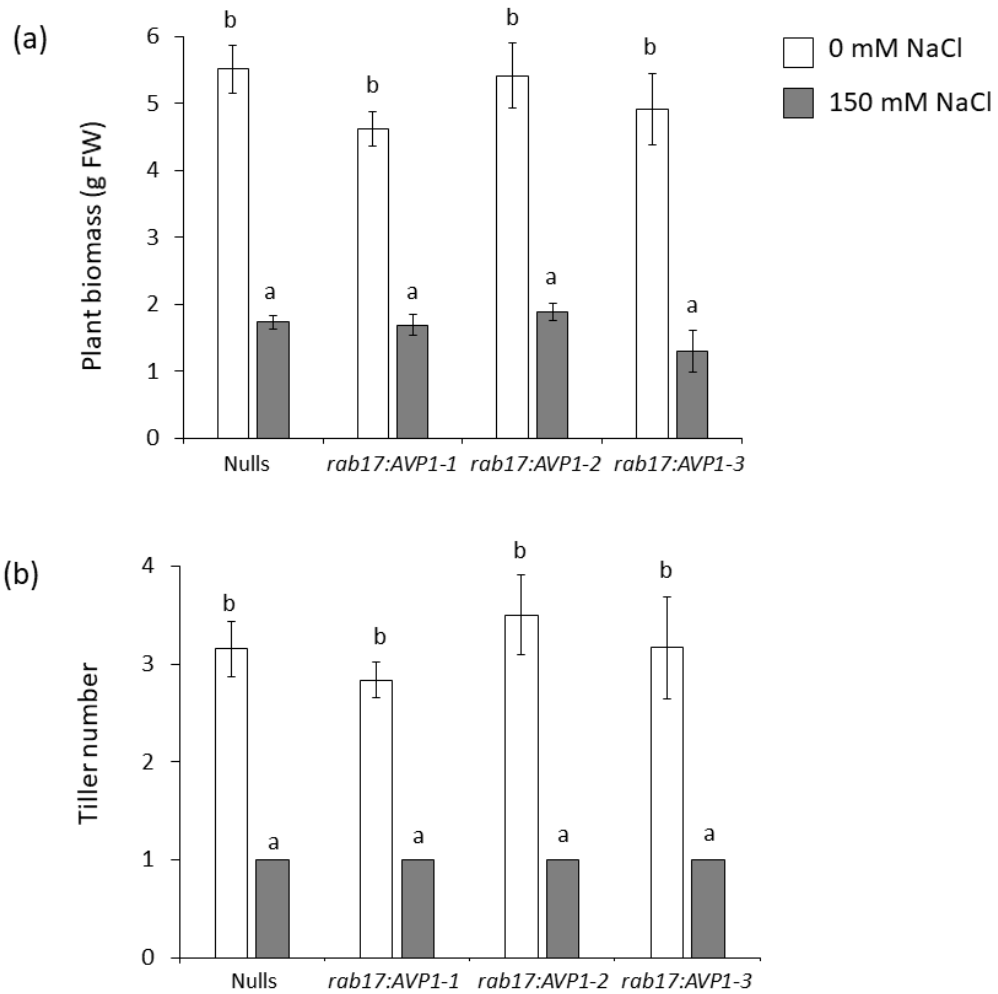
## Supplementary Figures



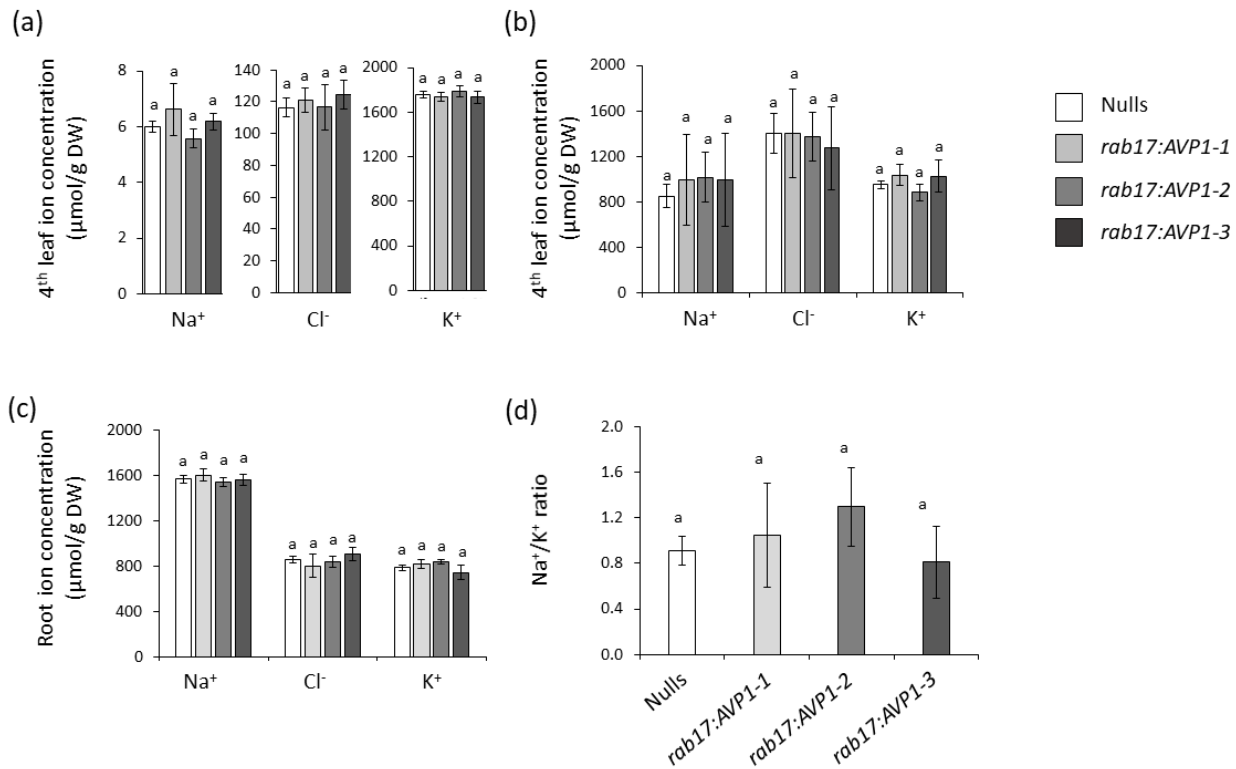
Supplementary Figure 1: Transgene presence and expression analysis of *rab17:AVP1* transgenic and null segregant (nulls) wheat lines. Agarose gels showing (a) presence of the native *TaVP1* gene and the *AVP1* transgene in gDNA of null segregants (nulls) and transgenic *rab17:AVP1* wheat lines (*rab17:AVP1-1*, *rab17:AVP1-2* and *rab17:AVP1-3*), and expression of *TaGAPDH* and absence of *AVP1* transgene expression in (b) 3<sup>rd</sup> leaf and (c) root cDNA of null segregants and transgenic *rab17:AVP1* lines in saline (150 mM NaCl) conditions. Water was used as a negative control for all PCR reactions (-).



Supplementary Figure 2: Phenotypic characteristics of 6 d-old *rab17:AVP1* and null segregant (nulls) wheat seedlings. (a) Fresh weights (g FW per plant) of 6 d-old null segregant (nulls) and *rab17:AVP1* transgenic wheat seedlings (*rab17:AVP1-1*, *rab17:AVP1-2*, *rab17:AVP1-3*). Values are means  $\pm$  standard error of the mean (n=3-5). Different letters indicate values with significant differences (one-way ANOVA,  $P \leq 0.05$ , Tukey's 95 % confidence interval). (b) Images of 6 d-old null segregants and *rab17:AVP1* transgenic wheat lines after 4 h in a pH sensitive bromocresol purple media. Scale bar = 3.25 cm. Inset shows pH colour scale range (5.0-7.0).



Supplementary Figure 3: Growth characteristics of *rab17:AVP1* transgenic and null segregant (nulls) wheat lines following 3 weeks in hydroponics under 0 mM NaCl and 150 mM NaCl. (a) Fresh weight (g FW per plant) and (b) tiller number of null segregants (nulls) and *rab17:AVP1* transgenic wheat lines (*rab17:AVP1-1*, *rab17:AVP1-2*, *rab17:AVP1-3*) in 0 mM NaCl (white columns) and 150 mM NaCl (grey columns) for 3 weeks. Values are means  $\pm$  standard error of the mean (n=5-12). Different letters indicate values with significant differences (one-way ANOVA,  $P \leq 0.05$ , Tukey's 95 % confidence interval).



Supplementary Figure 4: Leaf and root ion concentrations in *rab17:AVP1* transgenic and null segregant (nulls) wheat lines in hydroponics under 0 mM NaCl and 150 mM NaCl. Ion (Na<sup>+</sup>, Cl<sup>-</sup> and K<sup>+</sup>) concentrations in the 4<sup>th</sup> leaf of plants in (a) 0 mM NaCl and (b) 150 mM NaCl, and (c) in the root under 150 mM NaCl conditions for 21 d. (d) Shoot Na<sup>+</sup>/K<sup>+</sup> ratios of null segregants (white columns) and *rab17:AVP1-1* (light grey columns), *rab17:AVP1-2* (dark grey columns) and *rab17:AVP1-3* (black columns) transgenic wheat lines. Values are means ± standard error of the mean (n=5-12). Different letters indicate significant differences between lines for each ion analysed (one-way ANOVA,  $P < 0.05$ , Tukey's 95 % confidence interval).

**Chapter 4** - *TaVP* homeolog expression profiling in bread  
wheat

## Statement of Authorship

Title of Paper	Identification and characterisation of proton-pumping pyrophosphatase (H <sup>+</sup> -PPase) genes in bread wheat ( <i>Triticum aestivum</i> )
Publication Status	<input type="checkbox"/> Published <input type="checkbox"/> Accepted for Publication <input checked="" type="checkbox"/> Submitted for Publication <input type="checkbox"/> Unpublished and Unsubmitted work written in manuscript style
Publication Details	This manuscript has been written and formatted for publication in Plant Biotechnology.

### Principal Author

Name of Principal Author (Candidate)	Daniel J. Menadue		
Contribution to the Paper	Contributed to the experimental design, identified and confirmed the 15 <i>TaVP</i> gene sequences, designed and validated homeolog specific primers, conducted bioinformatics analysis, grew and sampled both greenhouse and field-grown plants, extracted RNA, synthesised cDNA and prepared samples for qPCR analysis, performed statistical analysis, interpreted the data and wrote the manuscript.		
Overall percentage (%)	70		
Certification:	This paper reports on original research I conducted during the period of my Higher Degree by Research candidature and is not subject to any obligations or contractual agreements with a third party that would constrain its inclusion in this thesis. I am the primary author of this paper.		
Signature		Date	28/5/2018

### Co-Author Contributions

By signing the Statement of Authorship, each author certifies that:

- i. the candidate's stated contribution to the publication is accurate (as detailed above);
- ii. permission is granted for the candidate to include the publication in the thesis; and
- iii. the sum of all co-author contributions is equal to 100% less the candidate's stated contribution.

Name of Co-Author	Matteo Riboni		
Contribution to the Paper	Performed the qRT-PCR analysis, assisted with primer validation and contributed to revision of the manuscript.		
Signature		Date	28/5/2018



Name of Co-Author	Ute Baumann		
Contribution to the Paper	Assisted with the identification of the <i>TaVP4</i> gene sequences and contributed to revision of the manuscript.		
Signature		Date	6/6/2018

Name of Co-Author	Rhiannon K. Schilling		
Contribution to the Paper	Contributed to the experimental design, field sampling, data analysis and interpretation and revision of the manuscript.		
Signature		Date	4/6/2018

Name of Co-Author	Darren C. Plett		
Contribution to the Paper	Contributed to the experimental design, generation of figures, data interpretation and revision of the manuscript.		
Signature		Date	4/6/2018

Name of Co-Author	Stuart J. Roy		
Contribution to the Paper	Conceived the research project and contributed to the experimental design, data interpretation and revision of the manuscript.		
Signature		Date	28/05/2018

## Proton-pumping pyrophosphatase (H<sup>+</sup>-PPase) homeolog expression is a dynamic trait in bread wheat (*Triticum aestivum*)

**Running title:** *TaVP* homeolog expression profiling in bread wheat

Daniel Jamie Menadue<sup>1,2</sup>, Matteo Riboni<sup>1,2#</sup>, Ute Baumann<sup>1,2</sup>, Rhiannon Kate Schilling<sup>1,2</sup>, Darren Craig Plett<sup>1,2</sup> and Stuart John Roy<sup>1,2\*</sup>

<sup>1</sup>School of Agriculture, Food and Wine, The University of Adelaide, Adelaide, SA, 5005, Australia

<sup>2</sup>Australian Centre for Plant Functional Genomics, Glen Osmond, SA, 5064, Australia

\*Corresponding author: Daniel Menadue, School of Agriculture, Food and Wine, The University of Adelaide, SA 5005 Australia, daniel.menadue@adelaide.edu.au, Tel: +61 8 8313 7162, Fax: +61 8 8313 7102

Author email addresses: daniel.menadue@adelaide.edu.au, matteo.riboni@csiro.au, ute.baumann@adelaide.edu.au, rhiannon.schilling@adelaide.edu.au, darren.plett@adelaide.edu.au, stuart.roy@adelaide.edu.au

**Keywords:** gene expression, homeolog, phylogeny, qRT-PCR, *TaVP*, time-course

**NCBI accessions:** *TaVP1-A* (MH376294), *TaVP1-B* (MH376295), *TaVP1-D* (MH376296), *TaVP2-A* (MH376297), *TaVP2-B* (MH376298), *TaVP2-D* (MH376299), *TaVP3-A* (MH376300), *TaVP3-B* (MH376301), *TaVP3-D* (MH376302), *TaVP4-A* (MH376303), *TaVP4-B* (MH376304), *TaVP4-D* (MH376305), *TaVP5-A* (MH376306), *TaVP5-B* (MH376307), *TaVP5-D* (MH376308)

**Word count:** 5025

---

# Current address: CSIRO Agriculture and Food, Glen Osmond, SA, 5064, Australia

## Summary

When constitutively expressed, proton-pumping pyrophosphatase ( $H^+$ -PPase) genes have been shown to enhance yield under non-stressed and abiotic stress conditions. However, little is known about bread wheat (*Triticum aestivum*)  $H^+$ -PPases (*TaVPs*). In this study, analysis of the 2016 IWGSC Chinese Spring NRGene wheat genome assembly identified two novel *TaVP* genes, in addition to the three known *TaVP* genes. Three homeologous sequences for each *TaVP* gene were also identified, bringing the total number of bread wheat *TaVPs* to fifteen. Gene expression levels of these *TaVP* homeologs were assessed using quantitative real-time PCR (qRT-PCR) across multiple tissue types and developmental stages, in four diverse wheat varieties. Expression levels of the *TaVP* homeologs were found to vary significantly between varieties, tissue types and plant developmental stages. During early development, Zadoks stages 10 and 13 (Z10 and Z13), expression levels of *TaVP1* and *TaVP2* homeologs were higher in shoot tissue than root tissue, with root expression increasing in later developmental stages (Z22). *TaVP2-D* was the most highly expressed homeolog at all developmental stages and was expressed in all tissue types and varieties. Expression of the *TaVP3* homeologs was restricted to developing grain (Z75), while *TaVP4* homeologs had low levels of expression at in most tissues and stages of development, and varied significantly between varieties. These findings offer a comprehensive overview of the bread wheat  $H^+$ -PPase family, and provide a basis for further research into the roles and potential uses of these genes to increase the growth, yield and stress tolerance of bread wheat.

## Introduction

Bread wheat is the most widely cultivated cereal in the world, providing 20 % of the daily calorie requirements to the global population (Shiferaw et al., 2013). With the global population predicted to reach 9.1 billion by 2050, a significant increase in wheat yield is required to maintain food security (Alexandratos and Bruinsma, 2012). Many environmental factors, however, limit our ability to achieve the yield increases required. Wheat yields are significantly limited by increasing global temperatures, rainfall variability and depletion of soil nutrients (Gilliham et al., 2017; Tester and Langridge, 2010). In order to reduce the impact of such abiotic stresses, wheat cultivars with greater nutrient uptake capacity and abiotic stress tolerance are required. Developing such cultivars can be assisted through the identification and characterisation of beneficial genes for plant development and stress tolerance (Gilliham et al., 2017).

The inorganic vacuolar proton-pumping pyrophosphatase ( $H^+$ -PPase) is a ubiquitous plant enzyme (*EC 3.6.1.1*) responsible for the breakdown of inorganic pyrophosphate ( $PP_i$ ) and the production of free energy (Baltscheffsky, 1967). A variety of roles for these enzymes have been proposed (Gaxiola et al., 2016; Schilling et al., 2017), including aiding vacuolar ion sequestration (Gaxiola et al., 1999; Gaxiola et al., 2001) and sugar transportation (Gaxiola et al., 2012; Khadilkar et al., 2016; Pizzio et al., 2015), regulating cytosolic  $PP_i$  (Ferjani et al., 2011) and assisting with nutrient uptake (Paez-Valencia et al., 2013; Yang et al., 2007; Yang et al., 2014). Numerous studies have shown that transgenic plants expressing  $H^+$ -PPases have increased biomass and yield under saline (Bao et al., 2009; Cheng et al., 2018; Gaxiola et al., 2001; Kim et al., 2013; Li et al., 2010; Pasapula et al., 2011; Qin et al., 2013; Schilling et al., 2014; Shen et al., 2015), drought (Bao et al., 2009; Gaxiola et al., 2001; Park et al., 2005; Qin et al., 2013; Shen et al., 2015), low available nitrogen (Lv et al., 2015; Paez-Valencia et al., 2013) and low available

phosphorus (Yang et al., 2007; Yang et al., 2014) conditions, as well as in non-stressed conditions (Gonzalez et al., 2010; Li et al., 2005; Pizzio et al., 2015; Schilling et al., 2014; Vercruyssen et al., 2011; Wang et al., 2014; Yang et al., 2014).

Plants have two types of H<sup>+</sup>-PPases, type I enzymes which require potassium (K<sup>+</sup>) ions for optimal function and type II enzymes, which do not require K<sup>+</sup> but are sensitive to cytosolic calcium (Ca<sup>2+</sup>) concentrations (Maeshima, 1991). Type I and type II H<sup>+</sup>-PPases also differ in protein localisation and abundance, with type I H<sup>+</sup>-PPases localised to the tonoplast and plasma membrane (Maeshima, 1991; Paez-Valencia et al., 2011), and the type II H<sup>+</sup>-PPases localised to the membrane of the Golgi apparatus (Mitsuda et al., 2001). In suspension-cultured cells extracted from *Arabidopsis* (*Arabidopsis thaliana*) seedlings from the T87 line (TAIR accession # 5529827345), protein abundance of the type II H<sup>+</sup>-PPase was found to be < 0.2 % that of the type I H<sup>+</sup>-PPase (Segami et al., 2010). As such, research involving plant H<sup>+</sup>-PPases has mainly focussed on type I H<sup>+</sup>-PPase enzymes, which have been characterised in *Arabidopsis* (Sarafian et al., 1992) and mung bean (*Vigna radiata*) (Britten et al., 1989), as well as important cereal crops including barley (*Hordeum vulgare*) (Fukuda et al., 2004; Tanaka et al., 1993), maize (*Zea mays*) (Wisniewski and Rogowsky, 2004; Yue et al., 2008), rice (*Oryza sativa*) (Choura and Rebai, 2005; Liu et al., 2010; Sakakibara et al., 1996) and wheat (Brini et al., 2005; Wang et al., 2009). To date, three H<sup>+</sup>-PPase genes, *TaVP1*, *TaVP2* and *TaVP3*, have been identified through analysis of a wheat root tissue cDNA library and the 158<sup>th</sup> GenBank expressed sequence tag (EST) database (Brini et al., 2005; Wang et al., 2009). In addition, homeologous sequences from the A, B and D genomes have also been identified for each of the three *TaVP* genes (Wang et al., 2009), however, to our knowledge these sequences remain unpublished. Based on semi-quantitative gene expression analysis of a Chinese wheat variety, Wang et al. (2009) concluded

that *TaVP1* homeologs were more highly expressed in root than shoot tissue, *TaVP2* homeologs were more highly expressed in shoot than root tissue, while expression of *TaVP3* homeologs was restricted to the developing seed. As these conclusions are based on outdated genomic information and analysis of a single wheat accession using a semi-quantifiable gene expression method, the accuracy and relevance of these findings to other wheat varieties remains unknown.

The functional role of *TaVP1* has been investigated in both *Arabidopsis* and tobacco (*Nicotiana tabacum*). Constitutive expression of *TaVP1*, improved the growth of transgenic *Arabidopsis* under salinity and drought treatments (Brini et al., 2007). Under saline conditions, the transgenic lines accumulated significantly higher levels of sodium ( $\text{Na}^+$ ) within the shoot compared to wild-type (Brini et al., 2007). In transgenic tobacco, *TaVP1* expression similarly enhanced seedling growth under salinity stress, however, ion analysis revealed that the *TaVP1* expressing lines had lower leaf  $\text{Na}^+$  than the wild-type (Gouiaa et al., 2012). As such, the native function of *TaVP1* in ion sequestration remains unclear, as does the function of other *TaVPs* in bread wheat. With several wheat genome assemblies now available (Caugant, 2016; Chapman et al., 2015; The International Wheat Genome Sequencing Consortium, 2014), there is an opportunity to further analyse the bread wheat genome for additional members of the  $\text{H}^+$ -PPase family, and to quantify expression of these genes throughout development.

## Results

### Fifteen $\text{H}^+$ -PPase homeologs are present in the bread wheat genome

Analysis of the NRGene assembly of the Chinese Spring wheat reference genome (Caugant, 2016) identified five  $\text{H}^+$ -PPase genes (Table 1). Three of these genes had previously been

identified (*TaVP1*, *TaVP2*, *TaVP3*), while two were novel genes (*TaVP4* and *TaVP5*). Homeologous sequences from the A, B and D genomes were identified for each of the five *TaVP* genes, bringing the total number of H<sup>+</sup>-PPase genes within the bread wheat genome to fifteen. Homeologous sequences of each gene shared > 98 % sequence identity. Based on NRGene scaffold information, *TaVP1* and *TaVP2* homeologs were located on the short and long arms of chromosome 7, respectively. The *TaVP1* protein sequences had 97-98 % sequence identity to the *TaVP1* consensus sequence used to query the NRGene assembly, while the *TaVP2* sequences had 84 % identity (Table 1). The *TaVP3* and *TaVP4* homeologs were located on the short and long arms of chromosome 1, respectively, and showed lower sequence identity to the *TaVP1* query sequence (72-73 %). Amino acid sequences of the *TaVP5* homeologs had the lowest sequence identity to the *TaVP1* query sequence (33 %) and were located on the long arm of chromosome 6 (Table 1).

The *TaVP2-B*, *TaVP2-D* and all *TaVP1* homeologs contained 8 exon regions, while the *TaVP2-A* homeolog contained 7 (Figure 1a). The *TaVP3* homeologs contained 5 exons, the *TaVP4* homeologs contained 4 exons, and the *TaVP5* homeologs contained 14 exons (Figure 1a). The length of the first introns in the *TaVP4* homeologs were considerably larger than the other *TaVP* sequences, which averaged 1.5 kb (Figure 1a). The first intron of *TaVP4-A* was approximately 12 kb, while the first introns of *TaVP4-B* and *TaVP4-D* were approximately 5 and 2.5 kb, respectively (Figure 1a).

Sequence alignment of *TaVP* amino acid sequences with the Arabidopsis (*AVP1-3*), barley (*HVP1*, *HVP10*, *HVP3*), maize (*ZmVPP1* and *ZmGPP*) and rice (*OVP1-6*) H<sup>+</sup>-PPases, as well as the mung bean H<sup>+</sup>-PPase (*VrVP1*) for which the protein structure has been comprehensively analysed (Protein Data Bank accession 4A01), revealed regions containing the PP<sub>i</sub> binding

domain, residues involved in proton translocation, as well as the transmembrane domains, were highly conserved among all *TaVP* homeologs (Figure 1b, Supplementary Figures 1 and 2). The only noticeable differences were among the *TaVP5* proteins, which contained several differences in amino acid sequence compared to the other *TaVP* proteins, with mutations at two of the residues required for protein translocation (R290Q and E349A) (Supplementary Figure 2). Proteins of the *TaVP5* homeologs also shared high sequence identity with the type II  $H^+$ -PPases, AVP2 (84 %), AVP3 (85 %) and ZmGPP (92 %) (Figure 1b) and formed a separate clade to the other *TaVP* homeologs, which grouped with the type I  $H^+$ -PPases (Supplementary Figure 3). Within the type I clade, the *TaVP1* proteins grouped with the HVP10, OVP2 and OVP4 sequences, the *TaVP2* proteins grouped with the HVP1, OVP1 and OVP5 proteins, the *TaVP3* proteins grouped with the OVP3 sequence, and the *TaVP4* proteins grouped with HVP3 and OVP6 (Figure 2).

Further comparison of the wheat *TaVP* homeologs revealed the *TaVP5* protein sequences were highly conserved, with only 1-2 amino acid differences between each *TaVP5* homeolog (Supplementary Figure 1). In comparison, the *TaVP1*, *TaVP2*, *TaVP3* and *TaVP4* protein sequences contained 6, 7, 8 and 11 amino acid differences amongst homeologs, respectively (Supplementary Figure 1). RNAseq data from the WheatExp database indicated *TaVP5* homeolog expression to be lower than the other *TaVPs* in the tissue types analysed (Supplementary Figure 4). ProteinPredict software also predicted the *TaVP5* proteins to localise to the membrane of the Golgi apparatus, while all other *TaVPs* were predicted to localise to the vacuole membrane (Table 1). Therefore, it is likely that the *TaVP1*, *TaVP2*, *TaVP3* and *TaVP4* homeologs are likely to encode type I  $H^+$ -PPase proteins, while the *TaVP5* homeologs encode type II  $H^+$ -PPases.



**Expression of *TaVP* homeologs varies between tissue type, developmental stage and variety in young wheat seedlings**

In young wheat seedlings at both Zadoks stage 10 and 13, expression of *TaVP* homeologs varied significantly between tissues (Figures 3-4). In all tissues at Z10, the *TaVP1* homeologs were expressed 2-fold higher than the *TaVP2* homeologs, except for *TaVP2-D*, which was the most highly expressed homeolog in the shoot of Scout (0.15 Normalised Relative Quantity (NRQ)) and Buck Atlantico (0.08 NRQ) (Figure 3). At Z10, *TaVP1*, *TaVP2* and *TaVP4* homeologs were, on average, expressed 2-fold higher in the shoot than the root, however, the overall expression level was low (0-0.14 NRQ) compared to later developmental stages (Figures 4-6). In plants with fully expanded third leaves (Z13), overall *TaVP* expression increased, with *TaVP2-D* again having the highest level of expression of all *TaVP* homeologs (Figure 4). Expression of *TaVP2-D*, however, varied significantly between varieties at Z13, with high expression in the third leaf of Scout (0.55 NRQ) and Buck Atlantico (0.22 NRQ), and low expression in Vigour18 (0.04 NRQ) and Mocho de Espiga Branca (0.01 NRQ) (Figure 4). In Vigour18 and Mocho de Espiga Branca, *TaVP1-B* was expressed 3-fold higher in the leaf and 2-fold higher in the sheath than in the root, while no significant differences in *TaVP1-B* expression between Scout and Buck Atlantico tissues were apparent (Figure 4). At both Z10 and Z13, *TaVP4-B* expression was detected only in Buck Atlantico, while expression of *TaVP4-A* was only detected in Vigour18 and Mocho de Espiga Branca (Figures 3-4).

**Expression of *TaVP* homeologs in tillering plants is dependent on variety**

In tillering plants (Z22), *TaVP* expression across all tissues increased approximately 8-fold in comparison to Z10, and 5-fold compared to Z13 (Figure 5). At the second tiller stage, *TaVP1-A* was expressed 3- to 5-fold higher in the root, and 2-fold higher in the sheath, compared to the leaf in all varieties (Figure 5). In Mocho de Espiga Branca, expression of *TaVP1-B* and *TaVP1-D* was 5-fold higher in the root than the leaf tissues, while few significant differences in *TaVP1-B* and *TaVP1-D* expression were apparent between tissue types and/or varieties (Figure 5). In tillering plants, the majority of *TaVP2* homeologs were expressed > 2-fold higher in leaf tissues than in the root. Exceptions to this were Mocho de Espiga Branca, in which there were no significant differences in *TaVP2-A* or *TaVP2-B* expression between tissues, and Vigour18, which had similar levels of *TaVP2-D* expression (0.2-0.4 NRQ) across all tissue types (Figure 5). Typically, *TaVP2-D* was the most highly expressed homeolog in all varieties, with expression in all Mocho de Espiga Branca leaf tissue significantly (3-fold) higher than all Vigour18 and Buck Atlantico tissues (Figure 5). Most varieties had low levels of *TaVP4-A* and *TaVP4-B* expression (< 0.05 NRQ) at the tillering stage, with only Buck Atlantico and Scout having significant levels of *TaVP4-B* expression (0.2-1.6 NRQ) (Figure 5).

**Expression of *TaVP3* homeologs is restricted to the developing grain**

In the developing grain of field grown plants (Z75), all *TaVP3* homeologs were expressed at a low level (< 0.2 NRQ) in all varieties, with the exception of *TaVP2-D* and *TaVP4-B* (Figure 6). Expression of *TaVP2-D* was significantly higher in Mocho de Espiga Branca (1.1 NRQ) and Scout (0.5 NRQ) than Vigour18 (0.15 NRQ), with *TaVP4-B* expression 2- to 4-fold higher in Mocho de Espiga Branca, Scout and Buck Atlantico, compared to Vigour18 (Figure 6). Minimal expression

(> 0.01 NRQ) of *TaVP2-A* and *TaVP2-B* was detected in the developing grain of all varieties, while no expression of *TaVP4-A* was detected (Figure 6). Expression of *TaVP3* homeologs were not detected in any other tissue types across the four developmental stages analysed (Supplementary Figure 5).

### ***TaVP* homeolog expression is a dynamic trait across tissue types, developmental stages and varieties**

Overall, *TaVP* homeolog expression varied greatly between tissues, developmental stages and varieties. *TaVP1-B*, *2-A* and *2-D* were consistently the most highly expressed homeologs across all tissue types and varieties (Figure 7). With the exception of the *TaVP3* homeologs, expression of which were restricted to the developing grain, expression of *TaVP* homeologs generally increased across all tissue types throughout development, increasing from an average of 0.03 NRQ at Z10, to an average of 0.28 NRQ at Z22. (Figures 4-7). The most highly expressed homeologs in the developing grain were *TaVP2-D* (0.2-1.1 NRQ) and *TaVP4-B* (0.3-1.2 NRQ), while expression of all other homeologs was comparatively low (0-0.2 NRQ) (Figures 6-7). With the exception of Vigour18 leaf tissue, in which *TaVP4-A* was expressed at a level of 0.4 NRQ (Figure 5), minimal *TaVP4-A* expression (< 0.1 NRQ) was detected across all analysed samples at Z22 (Figures 4-7). Expression of *TaVP4-B* was generally specific to Scout and Buck Atlantico, except for the grain development stage (Z75), in which *TaVP4-B* expression was detected in all four varieties (Figures 6-7).

## Discussion

In this study, two novel bread wheat H<sup>+</sup>-PPase genes, *TaVP4* and *TaVP5*, were identified, along with the three homeologous sequences of both genes from each of the three wheat sub-genomes (*TaVP4-A*, *TaVP4-B*, *TaVP4-D*, *TaVP5-A*, *TaVP5-B* and *TaVP5-D*). In addition, nucleotide and amino acid sequences were obtained for each homeolog, bringing the total number of identified bread wheat H<sup>+</sup>-PPase genes to 15. Phylogenetic analysis revealed key groupings between the wheat *TaVP* homeologs and other cereal H<sup>+</sup>-PPase proteins. In the phylogenetic tree, the *TaVP1* homeologs were most similar to the barley *HVP10* and the rice *OVP2* and *OVP4* H<sup>+</sup>-PPases. Expression of *HVP10* has been shown to be higher in root than shoot tissue (Fukuda et al., 2004; Shavrukov et al., 2013), while *OVP2* and *OVP4* are most highly expressed within the sheath and embryo, respectively (Liu et al., 2010). The *TaVP2* homeologs grouped with the barley *HVP1* and rice *OVP1* and *OVP5* proteins. Genes encoding the *HVP1* (Fukuda et al., 2004) and *OVP1* (Liu et al., 2010) proteins have been shown to be predominantly expressed within shoot tissues, while expression of the *OVP5* gene has only been detected at a low level within developing rice grain (Liu et al., 2010). The rice *OVP3* H<sup>+</sup>-PPase, expression of which is found mainly within seedling roots and embryos (Liu et al., 2010), was the most similar H<sup>+</sup>-PPase to the *TaVP3* homeologs. The *TaVP4* homeologs grouped with the barley *HVP3* protein, the expression profile of which remains unknown, and the rice *OVP6* protein, which is expressed predominantly within the leaf tissue (Liu et al., 2010). While some of the expression patterns within each group are similar across species, overall there is little correlation between phylogenetic similarities and *TaVP* expression patterns. As gene expression can also be specific to a certain cell type (Byrt et al., 2014), a more comprehensive profiling of tissue types, and within specific cell types, may be required to identify similarities in expression pattern among the *TaVP* homeologs and with other cereal H<sup>+</sup>-PPases.

With fifteen *TaVP* genes present in the wheat genome, the variation in gene expression patterns, as well as differences in protein sequences, it is likely that the *TaVP* homeologs have different roles in plant development. The *TaVP1* and *TaVP2* homeologs are the most ubiquitous wheat H<sup>+</sup>-PPase genes, and are expressed in all tissue types, varieties and developmental stages analysed. Previous research has shown that *TaVP1* plays a role in ion accumulation when constitutively expressed in *Arabidopsis* (Brini et al., 2007), however, when constitutively expressed in tobacco, ion accumulation in the transgenic lines was not enhanced under salinity stress compared to wild-type, despite showing improved growth (Gouiaa et al., 2012). As such, the function of *TaVP1* in ion accumulation remains unclear. It is also unknown whether the function of *TaVP1* when constitutively expressed in *Arabidopsis* or tobacco is indicative of the native function of this protein in wheat, or is the result of being constitutively expressed at a high level in all cells. In several plant species, H<sup>+</sup>-PPases have been shown to localise to the plasma membrane, in addition to the vacuole membrane, where they are proposed to have a role in transporting sucrose from source to sink tissues (Paez-Valencia et al., 2011; Pizzio et al., 2015; Regmi et al., 2016). The generally high expression levels of *TaVP1* and *TaVP2* across tissues during the earlier developmental stages, indicates they are likely to have important roles in plant development. These roles may include ion sequestration, source to sink transportation of sucrose or regulation of cytosolic PP<sub>i</sub> concentrations, which has been shown to have an important role in regulating heterotrophic growth (Ferjani et al., 2011; Ferjani et al., 2012).

In all analysed varieties, expression of *TaVP3* homeologs was restricted to the grain during the milk development stage (Z75), consistent with the results of Wang et al. (2009) and transcript data from the WheatEXP database (Pearce et al., 2015). In peach (*Prunus persica*), the *Vp2* H<sup>+</sup>-PPase has high expression within developing fruit, where it is hypothesised to be involved in the regulation of organic acid and sugar content (Etienne et al., 2002). H<sup>+</sup>-PPases have also

been correlated with Na<sup>+</sup> accumulation within developing apple (*Malus domestica*) fruit (Yao et al., 2011), and increased ripening and greater phosphorus content in tomato (*Solanum lycopersicum*) fruit (Yang et al., 2014). In rice, however, high expression of a H<sup>+</sup>-PPase gene has been linked to grain chalkiness, an undesirable trait resulting in reduced grain quality (Li et al., 2014). While the expression pattern of *TaVP3* homeologs suggest these genes have developed a specialised role within the grain, further research is required to determine the exact role of these homeologs in grain development.

Unlike the other *TaVP* genes, expression of *TaVP4* varied significantly between homeologs and varieties. During the early developmental stages, expression of *TaVP4-B* was lower than the other *TaVP* homeologs, with the exception of Buck Atlantico. Despite considerable efforts, suitable primers for quantifying *TaVP4-D* expression could not be developed, suggesting this homeolog either has an extremely low level of expression in the tissues and cultivars analysed, or is expressed within a specific cell type within these tissues. For example the *TaHKT1;5-D* gene, which encodes a high-affinity K<sup>+</sup> transporter, appears to have a low level of expression when analysed at a tissue level, however, this is due to expression being specific to root stelar cells (Byrt et al., 2014). Cell specific gene expression could account for the generally low levels of *TaVP4* expression detected in the tissues analysed, and would require more sophisticated techniques, such as laser-assisted microdissection (Sakai et al., 2018) or fluorescence-activated cell sorting (Coker et al., 2015), to investigate further. The significant variation in expression between the *TaVP4* homeologs may be due to several reasons, such as homeolog silencing, which can occur as a result of polyploidization (Adams et al., 2003). Homeolog expression can also be co-ordinately regulated, with expression of a particular homeolog changing in response to increased or reduced expression of another (Lloyd et al., 2017). The large differences in *TaVP4-B* expression between varieties may also be due to genetic differences. For example,

Buck Atlantico, which had higher expression in Z10 and Z13 compared to other varieties, may contain a different allele for this gene. Further investigation into the expression and allelic diversity of *TaVP4* homeologs in a wider range of wheat varieties is needed to address these questions.

To assess the relationship between *TaVP* expression and plant development, additional research is required in plants with a similar genetic background. This could be achieved through the development and characterisation of near isogenic lines (NILs), in which lines differ only in *TaVP* homeolog sequence, which would enable beneficial sequences and alleles to be identified. *TaVP* homeologs could be further investigated via techniques such as in-situ PCR (Athman et al., 2014), which would aid in identifying potential differences in cell type specificity between homeologs. As the protein localisations reported here are based on computer predictions, techniques such as immunolabelling are required to validate these predictions and further investigate potential differences in protein localisation and function between the *TaVP* homeologs (Paez-Valencia et al., 2011). Such information would be useful for determining differences in the roles of *TaVP* homeologs in plant development. Changes in *TaVP* expression in response to abiotic stresses, such as salinity, drought and low nutrient availability, would provide information regarding the potential role of these homeologs in stress tolerance. Analysis of *TaVP* homeolog promoter regions could also provide useful information for identifying wheat varieties with beneficial *TaVP* alleles. For example, the Arabidopsis *AVP1* promoter contains cis-elements involved in low-temperature response, sugar response and pollen specific expression (Pizzio et al., 2015). The rice *OVP3* promoter is known to induce gene expression under cold and oxygen stress (Liu et al), while genetic variation in the promoter region of the maize *ZmVPP1* gene is correlated with drought tolerance (Wang et al., 2016). In addition, specific amino acid residues which enhance the function of H<sup>+</sup>-PPases have been

identified, such as the E221D mutation, a gain-of-function *AVP1* allele in Arabidopsis (Zhen et al., 1997). These known promoter elements and beneficial amino acid residues provide a valuable resource for identifying beneficial *TaVP* alleles for wheat breeding.

Through analysing newly available wheat reference genomes, 6 novel *TaVP* gene sequences (*TaVP4-A*, *TaVP4-B*, *TaVP4-D*, *TaVP5-A*, *TaVP5-B* and *TaVP5-D*) were identified in this study, and full gene sequences were identified for all fifteen bread wheat *TaVP* homeologs. Analysis of the type I H<sup>+</sup>-PPase sequences revealed that *TaVP* homeolog expression is a dynamic trait, which varies between tissue types, developmental stages and wheat varieties. *TaVP3* expression was shown to be specific to the developing grain in all varieties, while *TaVP4* expression varied between varieties and was only present at detectable levels during the later developmental stages. *TaVP1-B*, *TaVP2-A* and *TaVP2-D* are the most highly expressed *TaVP* homeologs across all tissue types, developmental stages and varieties, suggesting they have an important role in bread wheat. Further characterisation is required to elucidate potential functional differences between *TaVP* homeologs and to identify beneficial *TaVP* sequences for improving the development, stress tolerance and yield of bread wheat.

## Experimental Procedures

### Identification of wheat H<sup>+</sup>-PPase homeologs

To identify homeolog specific H<sup>+</sup>-PPase sequences within the wheat genome, nucleotide coding sequences (CDS) and amino acid sequences of the previously identified *TaVP1* (AY296911.1/AAP55210.1) and *TaVP2* (EU255237.1/ABX10014.1) genes, as well as the barley *HVP3* (AK362588.1/BAJ93792.1) gene, were used to query the International Wheat Genome Sequencing Consortium (IWGSC) Chinese Spring (NRGene assembly) reference genome



(version 0.4). Sequences with > 80 % identity were considered as homologs, while those with identities > 95 % and located on the same chromosome, were considered homeologs (Wilhelm et al., 2013). Obtained putative *TaVP* homeolog CDS were aligned in Geneious® 10.1.3 (Biomatters Ltd., Auckland, New Zealand) using the MUSCLE algorithm (default parameters) and amino acid sequences were translated. The GSDS2.0 software (Hu et al., 2015) was used to determine the intron-exon structure of each homeolog, while protein sequence features such as secondary structures, proton binding sites and PP<sub>i</sub> binding sites were inferred using the known structure of the *Vigna radiata* H<sup>+</sup>-PPase (BAA23649) via ESPript3 (Robert and Gouet, 2014). Protein localisation was predicted from *TaVP* amino acid sequences using ProteinPredict (default parameters) (Yachdav et al., 2014).

#### **Sequence alignment and phylogenetic analysis of H<sup>+</sup>-PPase proteins**

Plant H<sup>+</sup>-PPase protein sequences were aligned in Jalview (Waterhouse et al., 2009) using the MUSCLE algorithm (default settings). The resulting alignment was used for molecular phylogenetic analysis in MEGA 6® (Tamura et al., 2013) and formatted with iTOL v3 (Letunic and Bork, 2016). Evolutionary history was calculated using the Maximum Likelihood methodology (Mount, 2008) and validated with 1000 bootstrap replicates.

#### **Plant growth conditions for *TaVP* expression analysis in bread wheat**

To assess *TaVP* homeolog expression through time, four wheat varieties were selected based on commonly observed phenotypes of *AVP1* over-expressing plants, such as high biomass, high yield and improved seedling vigour. Uniform size seed from Vigour18 (early seedling vigour, CSIRO), Mocho de Espiga Branca (landrace, Portugal), Scout (elite Australian cultivar,

LongReach Plant Breeding) and Buck Atlantico (high biomass cultivar, Argentina) were UV sterilised for 5 min and germinated on moist paper towel in petri dishes for 6 d in the greenhouse. Seedlings were transplanted into PVC tubes (40 mm × 280 mm) containing polycarbonate plastic beads (Plastics Granulated Services, Adelaide, Australia) and placed into a flood-drain hydroponics system (Shavrukov et al., 2012) containing 0.2 mM NH<sub>4</sub>NO<sub>3</sub>, 5.0 mM KNO<sub>3</sub>, 2.0 mM Ca(NO<sub>3</sub>)<sub>2</sub>, 2.0 mM MgSO<sub>4</sub>, 0.1 mM KH<sub>2</sub>PO<sub>4</sub>, 0.5 mM Na<sub>2</sub>Si<sub>3</sub>O<sub>7</sub>, 50 μM NaFe(III)EDTA, 5 μM MnCl<sub>2</sub>, 10 μM ZnSO<sub>4</sub>, 0.5 μM CuSO<sub>4</sub>, 0.1 μM Na<sub>2</sub>MoO<sub>4</sub> and rain water to a total of 80 L (Shavrukov et al., 2012). Plants were grown in a randomised block design in a greenhouse at The Plant Accelerator® (Urrbrae, South Australia; latitude: -34.971353, longitude: 138.639933) between the 20<sup>th</sup> of April and the 25<sup>th</sup> of May 2016. The greenhouse maintained a 22°C/15°C day/night temperature regime and 60-80 % humidity. Nutrient solutions were changed every 9 d and pH was maintained between 6.5 and 7.0 by adjusting with 3.2 % HCl. Tissues were collected from 6 replicates of each variety as follows: total shoot and total root from seedlings prior to transplantation (Z10); 3<sup>rd</sup> leaf, root and 3<sup>rd</sup> leaf sheath tissue from plants with fully expanded 3<sup>rd</sup> leaves (Z13); and 3<sup>rd</sup> leaf, root and 3<sup>rd</sup> leaf sheath tissue, as well as the first fully expanded leaf from the first and second tillers (Z22). Samples were collected once the required developmental stage was reached for each variety. For the final developmental stage (Z75), developing grain samples were collected between the 14<sup>th</sup> and 27<sup>th</sup> of October 2015 from the 2015 Australian Centre for Plant Functional Genomics (ACPGF) Wheat Diversity field trial, in which plants were grown in 5 m × 1.65 m plots, using standard agronomic practices (Tarlee, South Australia; latitude: -34.282156, longitude: 138.772988). Five samples were collected from each wheat variety grown in two replicate plots, with each sample consisting of four individual grains from the central florets. All developmental stages were assessed according to the Zadoks growth scale (Zadoks et al., 1974).

### **RNA extraction and cDNA synthesis**

RNA was extracted from tissue samples collected from greenhouse grown plants using a DirectZol RNA purification kit (Zymo Research, Irvine, United States), with contaminating DNA removed using an in-column DNase treatment (Zymo Research). Due to low RNA yield from grain samples using the DirectZol methodology, likely due to high starch content within developing wheat grains, a phenol-chloroform extraction (Chomczynski, 1993) was used to purify RNA from grain samples. Contaminating DNA was removed from the grain RNA samples using an Ambion DNA-free treatment (Invitrogen, Carlsbad, United States). RNA concentrations were standardised to 500 ng using a NanoDrop 1000 spectrophotometer (Thermo Fisher Scientific, Waltham, United States), and cDNA was synthesised using an AffinityScript cDNA synthesis kit (Agilent Technologies, Santa Clara, United States) according to the manufacturer's instructions.

### **Expression analysis of *TaVP* homeologs via quantitative real-time PCR (qRT-PCR)**

Homeolog specific primers were designed with Primer3 (version 4.0.0) (Supplementary Table 1) and the specificity of each primer pair was verified by melt curve analysis (Fletcher, 2014) and Sanger sequencing (Supplementary Figure 6). Although ten primer sets were designed to amplify the *TaVP4-D* homeolog, only one was found to be specific for the *TaVP4-D* homeolog. While this primer set successfully amplified *TaVP4-D* from gDNA and cDNA samples (pooled from various tissue types of the four wheat varieties) via standard PCR, this primer set was not suitable for qRT-PCR (Supplementary Figure 7). As such, expression data for the *TaVP4-D* homeolog was not able to be obtained. Quantitative real-time PCR was performed with KAPA SYBR® Fast qRT-PCR kit Master Mix (Kapa Biosystems, Wilmington, United States) and

amplification was monitored in real-time on a QuantStudio™ 6 Flex Real-Time PCR System (Applied Biosystems, Foster City, United States). Reference gene stability was assessed with the geNorm function of qBASE+ software using default settings (Hellemans et al., 2007). As the expression levels of the reference genes varied between the developmental stages, expression values within each growth stage were normalised relative to the two most stable reference genes. Z10 and Z13 data were normalised against *TaActin* (AY663392) and *TaGAPDH* (EU022331), Z22 data was normalised against *TaEFA2* (M90077) and *TaCyclophilin* (AY456122) and Z75 data was normalised against *TaGAPDH* and *TaEFA2*. Gene expression relative to the control genes (normalised relative quantity (NRQ)) were calculated using equations from Hellemans et al. (2007). A heat map of the expression data was generated with log transformed data using the Morpheus software created by the Broad Institute (<https://software.broadinstitute.org/morpheus/>). Gene expression data was statistically analysed in GenStat® version 15.3 (two-way ANOVA,  $P \leq 0.05$ , Tukey's 95 % confidence interval).

## Acknowledgements

The authors wish to thank Dr. Stephan Haeefele for providing field trial access, the CSIRO for providing the Vigour18 line, and GRC INRA Clermont-Ferrand for providing the Buck Atlantico (Argentina) and Mocho de Espiga Branca (Portugal) lines. This research was funded by the Grains Research and Development Corporation (UA00145), and the International Wheat Yield Partnership and Grains Research and Development Corporation (IWYP39/ACP0009). Daniel Menadue is the recipient of a Grains Research and Development Corporation Grains Industry Research Scholarship (GRS10931). The Plant Accelerator<sup>®</sup>, Australian Plant Phenomics Facility, is funded by the National Collaborative Research Infrastructure Strategy of the Commonwealth of Australia. The authors declare no conflict of interest.

## References

- Adams, K.L., Cronn, R., Percifield, R. and Wendel, J.F. (2003) Genes duplicated by polyploidy show unequal contributions to the transcriptome and organ-specific reciprocal silencing. *Proc. Natl. Acad. Sci.* **100**, 4649-4654.
- Alexandratos, N. and Bruinsma, J. (2012) World agriculture towards 2030/2050: the 2012 revision. (FAO ed). Rome.
- Athman, A., Tanz, S.K., Conn, V.M., Jordans, C., Mayo, G.M., Ng, W.W., Burton, R.A., Conn, S.J. and Gilliam, M. (2014) Protocol: a fast and simple *in situ* PCR method for localising gene expression in plant tissue. *Plant Methods* **10**, 29.
- Baltscheffsky, M. (1967) Inorganic pyrophosphate as an energy donor in photosynthetic and respiratory electron transport phosphorylation systems. *Biochem. Biophys. Res. Commun.* **28**, 270-276.
- Bao, A.K., Wang, S.M., Wu, G.Q., Xi, J.J., Zhang, J.L. and Wang, C.M. (2009) Overexpression of the *Arabidopsis* H<sup>+</sup>-PPase enhanced resistance to salt and drought stress in transgenic alfalfa (*Medicago sativa* L.). *Plant Sci.* **176**, 232-240.
- Brini, F., Gaxiola, R.A., Berkowitz, G.A. and Masmoudi, K. (2005) Cloning and characterization of a wheat vacuolar cation/proton antiporter and pyrophosphatase proton pump. *Plant Physiol. Biochem.* **43**, 347-354.
- Brini, F., Hanin, M., Mezghani, I., Berkowitz, G.A. and Masmoudi, K. (2007) Overexpression of wheat Na<sup>+</sup>/H<sup>+</sup> antiporter *TNHX1* and H<sup>+</sup>-pyrophosphatase *TVP1* improve salt- and drought-stress tolerance in *Arabidopsis thaliana* plants. *J. Exp. Bot.* **58**, 301-308.
- Britten, C.J., Turner, J.C. and Rea, P.A. (1989) Identification and purification of substrate-binding subunit of higher plant H<sup>+</sup>-translocating inorganic pyrophosphatase. *FEBS Lett.* **256**, 200-206.
- Byrt, C.S., Xu, B., Krishnan, M., Lightfoot, D.J., Athman, A., Jacobs, A.K., Watson-Haigh, N.S., Plett, D., Munns, R., Tester, M. and Gilliam, M. (2014) The Na<sup>+</sup> transporter, TaHKT1;5-D, limits shoot Na<sup>+</sup> accumulation in bread wheat. *Plant J.* **80**, 516-526.
- Caugant, I. (2016) Wheat sequencing consortium releases key resource to the scientific community. Bethesda, Maryland, USA: The International Wheat Genome Sequencing Consortium.
- Chapman, J.A., Mascher, M., Buluç, A., Barry, K., Georganas, E., Session, A., Strnadova, V., Jenkins, J., Sehgal, S., Olikier, L., Schmutz, J., Yelick, K.A., Scholz, U., Waugh, R., Poland, J.A., Muehlbauer, G.J., Stein, N. and Rokhsar, D.S. (2015) A whole-genome shotgun approach for assembling and anchoring the hexaploid bread wheat genome. *Genome Biol.* **16**, 26.
- Cheng, C., Zhang, Y., Chen, X., Song, J., Guo, Z., Li, K. and Zhang, K. (2018) Co-expression of *AtNHX1* and *TsVP* improves the salt tolerance of transgenic cotton and increases seed cotton yield in a saline field. *Mol. Breed.* **38**, 19.
- Chomczynski, P. (1993) A reagent for the single-step simultaneous isolation of RNA, DNA and proteins from cell and tissue samples. *BioTechniques* **15**, 532-534, 536-537.
- Choura, M. and Rebai, A. (2005) Identification and characterization of new members of vacuolar H<sup>+</sup>-pyrophosphatase family from *Oryza sativa* genome. *Russ. J. Plant Physiol.* **52**, 821-825.
- Coker, T., Cevik, V., Beynon, J. and Gifford, M. (2015) Spatial dissection of the *Arabidopsis thaliana* transcriptional response to downy mildew using fluorescence activated cell sorting. *Front. Plant. Sci.* **6**, 299-308

- Drozdowicz, Y.M., Kissinger, J.C. and Rea, P.A. (2000) *AVP2*, a sequence-divergent, K<sup>+</sup>-insensitive H<sup>+</sup>-translocating inorganic pyrophosphatase from *Arabidopsis*. *Plant Physiol.* **123**, 353-362.
- Etienne, C., Moing, A., Dirlwanger, E., Raymond, P., Monet, R. and Rothan, C. (2002) Isolation and characterization of six peach cDNAs encoding key proteins in organic acid metabolism and solute accumulation: involvement in regulating peach fruit acidity. *Physiol. Plant.* **114**, 259-270.
- Ferjani, A., Segami, S., Horiguchi, G., Muto, Y., Maeshima, M. and Tsukaya, H. (2011) Keep an eye on PP<sub>i</sub>: The vacuolar-type H<sup>+</sup>-pyrophosphatase regulates postgerminative development in *Arabidopsis*. *Plant Cell* **23**, 2895-2908.
- Ferjani, A., Segami, S., Horiguchi, G., Sakata, A., Maeshima, M. and Tsukaya, H. (2012) Regulation of pyrophosphate levels by H<sup>+</sup>-PPase is central for proper resumption of early plant development. *Plant Signal. Behav.* **7**, 38-42.
- Fletcher, S.J. (2014) qPCR for quantification of transgene expression and determination of transgene copy number. *Methods Mol. Biol.* **1145**, 213-237.
- Fukuda, A., Chiba, K., Maeda, M., Nakamura, A., Maeshima, M. and Tanaka, Y. (2004) Effect of salt and osmotic stresses on the expression of genes for the vacuolar H<sup>+</sup>-pyrophosphatase, H<sup>+</sup>-ATPase subunit A, and Na<sup>+</sup>/H<sup>+</sup> antiporter from barley. *J. Exp. Bot.* **55**, 585-594.
- Gaxiola, R.A., Rao, R., Sherman, A., Grisafi, P., Alper, S.L. and Fink, G.R. (1999) The *Arabidopsis thaliana* proton transporters, AtNHX1 and AVP1, can function in cation detoxification in yeast. *Proc. Natl. Acad. Sci.* **96**, 1480-1485.
- Gaxiola, R.A., Li, J., Undurraga, S., Dang, L.M., Allen, G.J., Alper, S.L. and Fink, G.R. (2001) Drought- and salt-tolerant plants result from overexpression of the *AVP1* H<sup>+</sup>-pump. *Proc. Natl. Acad. Sci.* **98**, 11444-11449.
- Gaxiola, R.A., Sanchez, C.A., Paez-Valencia, J., Ayre, B.G. and Elser, J.J. (2012) Genetic manipulation of a “vacuolar” H<sup>+</sup>-PPase: From salt tolerance to yield enhancement under phosphorus-deficient soils. *Plant Physiol.* **159**, 3-11.
- Gaxiola, Roberto A., Regmi, K., Paez-Valencia, J., Pizzio, G. and Zhang, S. (2016) Plant H<sup>+</sup>-PPases: Reversible enzymes with contrasting functions dependent on membrane environment. *Mol. Plant* **9**, 317-319.
- Gilliam, M., Able, J.A. and Roy, S.J. (2017) Translating knowledge about abiotic stress tolerance to breeding programmes. *Plant J.* **90**, 898-917.
- Gonzalez, N., De Bodt, S., Sulpice, R., Jikumaru, Y., Chae, E., Dhondt, S., Van Daele, T., De Milde, L., Weigel, D., Kamiya, Y., Stitt, M., Beemster, G.T.S. and Inzé, D. (2010) Increased leaf size: Different means to an end. *Plant Physiol.* **153**, 1261-1279.
- Gouiaa, S., Khoudi, H., Leidi, E.O., Pardo, J.M. and Masmoudi, K. (2012) Expression of wheat Na<sup>+</sup>/H<sup>+</sup> antiporter *TNHXS1* and H<sup>+</sup>- pyrophosphatase *TVP1* genes in tobacco from a bicistronic transcriptional unit improves salt tolerance. *Plant Mol. Biol.* **79**, 137-155.
- Hellemans, J., Mortier, G., De Paepe, A., Speleman, F. and Vandesompele, J. (2007) qBase relative quantification framework and software for management and automated analysis of real-time quantitative PCR data. *Genome Biol.* **8**, R19.
- Hirata, T., Nakamura, N., Omote, H., Wada, Y. and Futai, M. (2000) Regulation and reversibility of vacuolar H<sup>+</sup>-ATPase. *J. Biol. Chem.* **275**, 386-389.
- Hu, B., Jin, J., Guo, A.-Y., Zhang, H., Luo, J. and Gao, G. (2015) GSDS 2.0: an upgraded gene feature visualization server. *Bioinformatics* **31**, 1296-1297.

- Khadilkar, A.S., Yadav, U.P., Salazar, C., Shulaev, V., Paez-Valencia, J., Pizzio, G.A., Gaxiola, R.A. and Ayre, B.G. (2016) Constitutive and companion cell-specific overexpression of *AVP1*, encoding a proton-pumping pyrophosphatase, enhances biomass accumulation, phloem loading, and long-distance transport. *Plant Physiol.* **170**, 401-414.
- Kim, Y.S., Kim, I.S., Choe, Y.H., Bae, M.J., Shin, S.Y., Park, S.K., Kang, H.G., Kim, Y.H. and Yoon, H.S. (2013) Overexpression of the *Arabidopsis* vacuolar H<sup>+</sup>-pyrophosphatase *AVP1* gene in rice plants improves grain yield under paddy field conditions. *J. Agric. Sci.* **152**, 941-953.
- Letunic, I. and Bork, P. (2016) Interactive tree of life (iTOL) v3: an online tool for the display and annotation of phylogenetic and other trees. *Nucleic Acids Res.* **44**, 242-245.
- Li, J., Yang, H., Ann Peer, W., Richter, G., Blakeslee, J., Bandyopadhyay, A., Titapiwantakun, B., Undurraga, S., Khodakovskaya, M., Richards, E.L., Krizek, B., Murphy, A.S., Gilroy, S. and Gaxiola, R. (2005) *Arabidopsis* H<sup>+</sup>-PPase AVP1 regulates auxin-mediated organ development. *Science* **310**, 121-125.
- Li, Y., Fan, C., Xing, Y., Yun, P., Luo, L., Yan, B., Peng, B., Xie, W., Wang, G., Li, X., Xiao, J., Xu, C. and He, Y. (2014) *Chalk5* encodes a vacuolar H<sup>+</sup>-translocating pyrophosphatase influencing grain chalkiness in rice. *Nat. Genet.* **46**, 398.
- Li, Z., Baldwin, C.M., Hu, Q., Liu, H. and Luo, H. (2010) Heterologous expression of *Arabidopsis* H<sup>+</sup>-pyrophosphatase enhances salt tolerance in transgenic creeping bentgrass (*Agrostis stolonifera* L.). *Plant, Cell Environ.* **33**, 272-289.
- Liu, Q., Zhang, Q., Burton, R.A., Shirley, N.J. and Atwell, B.J. (2010) Expression of vacuolar H<sup>+</sup>-pyrophosphatase (*OVP3*) is under control of an anoxia-inducible promoter in rice. *Plant Mol. Biol.* **72**, 47-60.
- Lloyd, A., Blary, A., Charif, D., Charpentier, C., Tran, J., Balzergue, S., Delannoy, E., Rigaille, G. and Jenczewski, E. (2017) Homoeologous exchanges cause extensive dosage-dependent gene expression changes in an allopolyploid crop. *New Phytol.* **217**, 367-377.
- Lv, S., Jiang, P., Nie, L., Chen, X., Tai, F., Wang, D., Fan, P., Feng, J., Bao, H., Wang, J. and Li, Y. (2015) H<sup>+</sup>-pyrophosphatase from *Salicornia europaea* confers tolerance to simultaneously occurring salt stress and nitrogen deficiency in *Arabidopsis* and wheat. *Plant, Cell Environ.* **38**, 2433-2449.
- Maeshima, M. (1991) H<sup>+</sup>-translocating inorganic pyrophosphatase of plant vacuoles inhibition by Ca<sup>2+</sup>, stabilization by Mg<sup>2+</sup> and immunological comparison with other inorganic pyrophosphatases. *Eur. J. Biochem.* **196**, 11-17.
- Mitsuda, N., Enami, K., Nakata, M., Takeyasu, K. and Sato, M.H. (2001) Novel type *Arabidopsis thaliana* H<sup>+</sup>-PPase is localized to the Golgi apparatus. *FEBS Lett.* **488**, 29-33.
- Mount, D.W. (2008) The maximum likelihood approach for phylogenetic prediction. *Cold Spring Harb. Protoc.* **2008**, 34.
- Nakanishi, Y. and Maeshima, M. (1998) Molecular cloning of vacuolar H<sup>+</sup>-Pyrophosphatase and its developmental expression in growing hypocotyl of mung bean. *Plant Physiol.* **116**, 589-597.
- Paez-Valencia, J., Patron-Soberano, A., Rodriguez-Leviz, A., Sanchez-Lares, J., Sanchez-Gomez, C., Valencia-Mayoral, P., Diaz-Rosas, G. and Gaxiola, R. (2011) Plasma membrane localization of the type I H<sup>+</sup>-PPase AVP1 in sieve element-companion cell complexes from *Arabidopsis thaliana*. *Plant Sci.* **181**, 23-30.
- Paez-Valencia, J., Sanchez-Lares, J., Marsh, E., Dorneles, L.T., Santos, M.P., Sanchez, D., Winter, A., Murphy, S., Cox, J., Trzaska, M., Metler, J., Kozic, A., Facanha, A.R., Schachtman, D., Sanchez, C.A. and Gaxiola, R.A. (2013) Enhanced proton translocating pyrophosphatase



- activity improves nitrogen use efficiency in romaine lettuce. *Plant Physiol.* **161**, 1557-1569.
- Park, S., Li, J., Pittman, J.K., Berkowitz, G.A., Yang, H., Undurraga, S., Morris, J., Hirschi, K.D. and Gaxiola, R.A. (2005) Up-regulation of a H<sup>+</sup>-pyrophosphatase (*H<sup>+</sup>-PPase*) as a strategy to engineer drought-resistant crop plants. *Proc. Natl. Acad. Sci.* **102**, 18830-18835.
- Pasapula, V., Shen, G., Kuppu, S., Paez-Valencia, J., Mendoza, M., Hou, P., Chen, J., Qiu, X., Zhu, L., Zhang, X., Auld, D., Blumwald, E., Zhang, H., Gaxiola, R. and Payton, P. (2011) Expression of an *Arabidopsis* vacuolar H<sup>+</sup>-pyrophosphatase gene (*AVP1*) in cotton improves drought- and salt tolerance and increases fibre yield in the field conditions. *Plant Biotechnol. J.* **9**, 88-99.
- Pearce, S., Vazquez-Gross, H., Herin, S.Y., Hane, D., Wang, Y., Gu, Y.Q. and Dubcovsky, J. (2015) WheatExp: an RNA-seq expression database for polyploid wheat. *BMC Plant Biol.* **15**, 299.
- Pizzio, G.A., Paez-Valencia, J., Khadilkar, A.S., Regmi, K., Patron-Soberano, A., Zhang, S., Sanchez-Lares, J., Furstenau, T., Li, J., Sanchez-Gomez, C., Valencia-Mayoral, P., Yadav, U.P., Ayre, B.G. and Gaxiola, R.A. (2015) *Arabidopsis* type I proton-pumping pyrophosphatase expresses strongly in phloem, where it is required for pyrophosphate metabolism and photosynthate partitioning. *Plant Physiol.* **167**, 1541-1553.
- Qin, H., Gu, Q., Kuppu, S., Sun, L., Zhu, X., Mishra, N., Hu, R., Shen, G., Zhang, J., Zhang, Y., Zhu, L., Zhang, X., Burow, M., Payton, P. and Zhang, H. (2013) Expression of the *Arabidopsis* vacuolar H<sup>+</sup>-pyrophosphatase gene *AVP1* in peanut to improve drought and salt tolerance. *Plant Biotechnol. Rep.* **7**, 345-355.
- Regmi, K.C., Zhang, S. and Gaxiola, R.A. (2016) Apoplasmic loading in the rice phloem supported by the presence of sucrose synthase and plasma membrane-localized proton pyrophosphatase. *Ann. Bot.* **117**, 257-268.
- Robert, X. and Gouet, P. (2014) Deciphering key features in protein structures with the new ENDscript server. *Nucleic Acids Res.* **42**, 320-324.
- Sakai, K., Taconnat, L., Borrega, N., Yansouni, J., Brunaud, V., Paysant-Le Roux, C., Delannoy, E., Martin Magniette, M.-L., Lepiniec, L., Faure, J.D., Balzergue, S. and Dubreucq, B. (2018) Combining laser-assisted microdissection (LAM) and RNA-seq allows to perform a comprehensive transcriptomic analysis of epidermal cells of *Arabidopsis* embryo. *Plant Methods* **14**, 1-10.
- Sakakibara, Y., Kobayashi, H. and Kasamo, K. (1996) Isolation and characterization of cDNAs encoding vacuolar H<sup>+</sup>-pyrophosphatase isoforms from rice (*Oryza sativa* L.). *Plant Mol. Biol.* **31**, 1029-1038.
- Sarafian, V., Kim, Y., Poole, R.J. and Rea, P.A. (1992) Molecular cloning and sequence of cDNA encoding the pyrophosphate-energized vacuolar membrane proton pump of *Arabidopsis thaliana*. *Proc. Natl. Acad. Sci.* **89**, 1775-1779.
- Schilling, R.K., Marschner, P., Shavrukov, Y., Berger, B., Tester, M., Roy, S.J. and Plett, D.C. (2014) Expression of the *Arabidopsis* vacuolar H<sup>+</sup>-pyrophosphatase gene (*AVP1*) improves the shoot biomass of transgenic barley and increases grain yield in a saline field. *Plant Biotechnol. J.* **12**, 378-386.
- Schilling, R.K., Tester, M., Marschner, P., Plett, D.C. and Roy, S.J. (2017) *AVP1*: one protein, many roles. *Trends Plant Sci.* **22**, 154-162.
- Segami, S., Nakanishi, Y., Sato, M.H. and Maeshima, M. (2010) Quantification, organ-specific accumulation and intracellular localization of type II H<sup>+</sup>-pyrophosphatase in *Arabidopsis thaliana*. *Plant Cell Physiol.* **51**, 1350-1360.

- Shavrukov, Y., Genc, Y. and Hayes, J. (2012) The use of hydroponics in abiotic stress tolerance research. In: *Hydroponics - A Standard Methodology for Plant Biological Researches* (Asao, T. ed) pp. 39-66. InTech Open Access Publisher.
- Shavrukov, Y., Bovill, J., Afzal, I., Hayes, J., Roy, S., Tester, M. and Collins, N. (2013) *HVP10* encoding V-PPase is a prime candidate for the barley *HvNax3* sodium exclusion gene: evidence from fine mapping and expression analysis. *Planta* **237**, 1111-1122.
- Shen, G., Wei, J., Qiu, X., Hu, R., Kuppu, S., Auld, D., Blumwald, E., Gaxiola, R., Payton, P. and Zhang, H. (2015) Co-overexpression of *AVP1* and *AtNHX1* in cotton further improves drought and salt tolerance in transgenic cotton plants. *Plant Molecular Biology Reporter* **33**, 167-177.
- Shiferaw, B., Smale, M., Braun, H.-J., Duveiller, E., Reynolds, M. and Muricho, G. (2013) Crops that feed the world 10. Past successes and future challenges to the role played by wheat in global food security. *Food Sec.* **5**, 291-317.
- Tamura, K., Stecher, G., Peterson, D., Filipski, A. and Kumar, S. (2013) MEGA6: molecular evolutionary genetics analysis version 6.0. *Mol. Biol. Evol.* **30**, 2725-2729.
- Tanaka, Y., Chiba, K., Maeda, M. and Maeshima, M. (1993) Molecular cloning of cDNA for vacuolar membrane proton-translocating inorganic pyrophosphatase in *Hordeum vulgare*. *Biochem. Biophys. Res. Commun.* **190**, 1110-1114.
- Tester, M. and Langridge, P. (2010) Breeding technologies to increase crop production in a changing world. *Science* **327**, 818-822.
- The International Wheat Genome Sequencing Consortium (2014) A chromosome-based draft sequence of the hexaploid bread wheat *Triticum aestivum* genome. *Science* **345**.
- Vercruyssen, L., Gonzalez, N., Werner, T., Schmölling, T. and Inzé, D. (2011) Combining enhanced root and shoot growth reveals cross talk between pathways that control plant organ size in *Arabidopsis*. *Plant Physiol.* **155**, 1339-1352.
- Wang, J.W., Wang, H.Q., Xiang, W.W. and Chai, T.Y. (2014) A *Medicago truncatula* H<sup>+</sup>-pyrophosphatase gene, *MtVP1*, improves sucrose accumulation and anthocyanin biosynthesis in potato (*Solanum tuberosum* L.). *Gen. Mol. Res.* **13**, 3615-3626.
- Wang, X., Wang, H., Liu, S., Ferjani, A., Li, J., Yan, J., Yang, X. and Qin, F. (2016) Genetic variation in *ZmVPP1* contributes to drought tolerance in maize seedlings. *Nat. Genet.* **48**, 1233-1241.
- Wang, Y., Xu, H., Zhang, G., Zhu, H., Zhang, L., Zhang, Z., Zhang, C. and Ma, Z. (2009) Expression and responses to dehydration and salinity stresses of V-PPase gene members in wheat. *J. Genet. Genomics* **36**, 711-720.
- Waterhouse, A.M., Procter, J.B., Martin, D.M., Clamp, M. and Barton, G.J. (2009) Jalview version 2 - a multiple sequence alignment editor and analysis workbench. *Bioinformatics* **25**, 1189-1191.
- Wilhelm, E.P., Howells, R.M., Al-Kaff, N., Jia, J., Baker, C., Leverington-Waite, M.A., Griffiths, S., Greenland, A.J., Boulton, M.I. and Powell, W. (2013) Genetic characterization and mapping of the *Rht-1* homeologs and flanking sequences in wheat. *Theor. Appl. Genet.* **126**, 1321-1336.
- Wisniewski, J.-P. and Rogowsky, P. (2004) Vacuolar H<sup>+</sup>-translocating inorganic pyrophosphatase (*Vpp1*) marks partial aleurone cell fate in cereal endosperm development. *Plant Mol. Biol.* **56**, 325-337.
- Yachdav, G., Kloppmann, E., Kajan, L., Hecht, M., Goldberg, T., Hamp, T., Honigschmid, P., Schafferhans, A., Roos, M., Bernhofer, M., Richter, L., Ashkenazy, H., Punta, M., Schlessinger, A., Bromberg, Y., Schneider, R., Vriend, G., Sander, C., Ben-Tal, N. and Rost,

- B. (2014) PredictProtein - an open resource for online prediction of protein structural and functional features. *Nucleic Acids Res.* **42**, W337-343.
- Yang, H., Knapp, J., Koirala, P., Rajagopal, D., Peer, W.A., Silbart, L.K., Murphy, A. and Gaxiola, R.A. (2007) Enhanced phosphorus nutrition in monocots and dicots over-expressing a phosphorus-responsive type I H<sup>+</sup>-pyrophosphatase. *Plant Biotechnol. J.* **5**, 735-745.
- Yang, H., Zhang, X., Gaxiola, R.A., Xu, G., Peer, W.A. and Murphy, A.S. (2014) Over-expression of the *Arabidopsis* proton-pyrophosphatase *AVP1* enhances transplant survival, root mass, and fruit development under limiting phosphorus conditions. *J. Exp. Bot.* **65**, 3045–3053.
- Yao, YX., Dong, QL., You, CX., Zhai, H. and Hao, YJ. (2011) Expression analysis and functional characterization of apple *MdVHP1* gene reveals its involvement in Na<sup>+</sup>, malate and soluble sugar accumulation. *Plant Physiol. Biochem.* **49**, 1201-1208.
- Yue, G., Sui, Z., Gao, Q. and Zhang, J. (2008) Molecular cloning and characterization of a novel H<sup>+</sup>-translocating pyrophosphatase gene in *Zea mays*. *DNA Sequence* **19**, 79-86.
- Zadoks, J.C., Chang, T.T. and Konzak, C.F. (1974) A decimal code for the growth stages of cereals. *Weed Res.* **14**, 415-421.
- Zhen, R., Kim, E. and Rea, P. (1997) The molecular and biochemical basis of pyrophosphate-energized proton translocation at the vacuolar membrane. *Adv. Bot. Res.* **25**, 297-337.

## Tables

**Table 1: Details of the 15 *TaVP* homeologs identified in the bread wheat genome. Chromosome location, NRGene scaffold number and position, coding sequence (CDS) and protein lengths, sequence identity to the *TaVP1* consensus sequence (AAP55210.1) used to query the NRGene assembly, and predicted protein localisation and confidence level obtained with ProteinPredict are shown for each homeolog.**

Gene	Chromosome	NRGene scaffold	Scaffold position (cM)	CDS length (bp)	Protein length (amino acids)	Identity to <i>TaVP1</i> consensus (%)	Predicted protein localisation and confidence level (%)
<i>TaVP1-A</i>	7AS	Scaffold9784	58.09	2289	762	98	Vacuole membrane (99)
<i>TaVP1-B</i>	7BS	Scaffold67584	45.29	2289	762	97	Vacuole membrane (99)
<i>TaVP1-D</i>	7DS	Scaffold10918	57.69	2286	761	97	Vacuole membrane (98)
<i>TaVP2-A</i>	7AL	Scaffold2576	108.22	2328	775	84	Vacuole membrane (84)
<i>TaVP2-B</i>	7BL	Scaffold468-1	107.47	2331	776	84	Vacuole membrane (84)
<i>TaVP2-D</i>	7DL	Scaffold42320	134.96	2328	775	84	Vacuole membrane (83)
<i>TaVP3-A</i>	1AS	Scaffold44824	44.61	2298	765	72	Vacuole membrane (69)
<i>TaVP3-B</i>	1BS	Scaffold90854	44.53	2295	764	72	Vacuole membrane (69)
<i>TaVP3-D</i>	1DS	Scaffold63828	47.46	2298	765	72	Vacuole membrane (68)
<i>TaVP4-A</i>	1AL	Scaffold35254	46.68	2332	773	74	Vacuole membrane (72)
<i>TaVP4-B</i>	1BL	Scaffold153951	47.91	2328	775	73	Vacuole membrane (72)
<i>TaVP4-D</i>	1DL	Scaffold2002	52.92	2328	775	73	Vacuole membrane (72)
<i>TaVP5-A</i>	6AL	Scaffold87922	70.14	2400	799	33	Golgi apparatus membrane (81)
<i>TaVP5-B</i>	6BL	Scaffold69351	58.36	2400	799	33	Golgi apparatus membrane (81)
<i>TaVP5-D</i>	6DL	Scaffold81933-2	70.02	2400	799	33	Golgi apparatus membrane (81)

## Figure Legends

**Figure 1: Intron-exon analysis and amino acid alignment of *TaVP* homeologs.** (a) Intron-exon structures of *TaVP* wheat homeologs. Exons and introns are represented by blue and grey lines, respectively. Scale bars are indicated for both, with sequences shown in a 5' to 3' direction. (b) Amino acid sequence alignment of a highly conserved region (amino acid residues 285–355) containing a pyrophosphatase binding domain and three residues involved in proton translocation (indicated by stars). Alignment contains the *TaVP* homeologs and type I orthologs from *Vigna radiata* (VrVP1), *Arabidopsis thaliana* (AVP1), *Hordeum vulgare* (HVP1, HVP3, HVP10), *Zea mays* (ZmVPP1) and *Oryza sativa* (OVP1-6), as well as type II orthologs of *Arabidopsis thaliana* (AVP2, AVP3) and *Zea mays* (ZmGPP). Shading indicates conservation level of amino acid residues where dark blue = 100 %, light blue = 80-99 %, purple = 60-79% and no colour = < 60 %.

**Figure 2: Phylogenetic analysis of type I H<sup>+</sup>-PPases.** Unrooted phylogenetic tree of type I H<sup>+</sup>-PPase proteins from *Vigna radiata* (VrVP1), *Arabidopsis thaliana* (AVP1), *Hordeum vulgare* (HVP1, HVP10, HVP3), *Zea mays* (ZmVPP1), *Oryza sativa* (OVP1-6) and bread wheat homeologs (TaVP1-TaVP4). Phylogeny was created in MEGA6<sup>®</sup> via the Maximum-Likelihood method and formatted with iTOL. Analysis was validated with 1000 bootstrap replicates and bootstrap support for each node is indicated. Scale bar represents 0.1 amino acid substitutions per residue. Dotted lines are for labelling purposes only and are not indicative of branch length.

**Figure 3: *TaVP* expression profile at seedling stage.** Expression of *TaVP* homeologs in shoot (white columns) and roots (grey columns) of 6 d-old wheat seedlings (Z10). Expression data displayed as normalised relative quantity (NRQ) for four bread wheat varieties, Vigour18, Mocho de Espiga Branca, Scout and Buck Atlantico. Values are means of 3-5 biological replicates and 3 technical replicates. Error bars represent standard error of the mean and different letters indicate statistically significant differences (two-way ANOVA,  $P \leq 0.05$ , Tukey's 95 % confidence interval).

**Figure 4: *TaVP* expression profile at third leaf stage.** Expression of *TaVP* homeologs in 3<sup>rd</sup> leaf (white columns), 3<sup>rd</sup> leaf sheath (dotted columns) and root (grey columns) tissue of plants with fully expanded 3<sup>rd</sup> leaves (Z13). Expression data displayed as normalised relative quantity (NRQ) for four bread wheat varieties, Vigour18, Mocho de Espiga Branca, Scout and Buck Atlantico. Values are means of 3-5 biological replicates and 3 technical replicates. Error bars represent standard error of the mean and different letters indicate statistically significant differences (two-way ANOVA,  $P \leq 0.05$ , Tukey's 95 % confidence interval).

**Figure 5: *TaVP* expression profile at second tiller stage.** Expression of *TaVP* homeologs in third leaf (white columns), 3<sup>rd</sup> leaf sheath (dotted columns), first leaf of the first tiller (black columns), first leaf of the second tiller (bricked columns) and root (grey columns) tissue of tillering plants (Z22). Expression data displayed as normalised relative quantity (NRQ) for four bread wheat varieties, Vigour18, Mocho de Espiga Branca, Scout and Buck Atlantico. Values are means of 3-5 biological replicates and 3 technical replicates. Error bars represent standard error of the

mean and different letters indicate statistically significant differences (two-way ANOVA,  $P \leq 0.05$ , Tukey's 95 % confidence interval).

**Figure 6: *TaVP* expression profile at grain development stage.** Expression of *TaVP* homeologs in the developing grain of field grown plants (Z75). Expression data displayed as normalised relative quantity (NRQ) for four bread wheat varieties, Vigour18, Mocho de Espiga Branca, Scout and Buck Atlantico. Values are means of 3-5 biological replicates and 3 technical replicates. Error bars represent standard error of the mean and different letters indicate statistically significant differences (two-way ANOVA,  $P \leq 0.05$ , Tukey's 95 % confidence interval).

**Figure 7: Heat map of *TaVP* gene expression through time.** Each column represents an individual *TaVP* homeolog, with developmental stages (Z10, Z13, Z22 and Z75), varieties (Vigour18, Mocho de Espiga Branca (Mocho), Scout and Buck Atlantico) and tissue types (3<sup>rd</sup> leaf, sheath, 1<sup>st</sup> tiller leaf, 2<sup>nd</sup> tiller leaf, root and grain) displayed along the y-axis. Colours indicate *TaVP* expression levels, with white and dark blue corresponding to the lowest and highest expression levels, respectively. Grey shading indicates samples for which no qRT-PCR expression data was obtained.

Figures

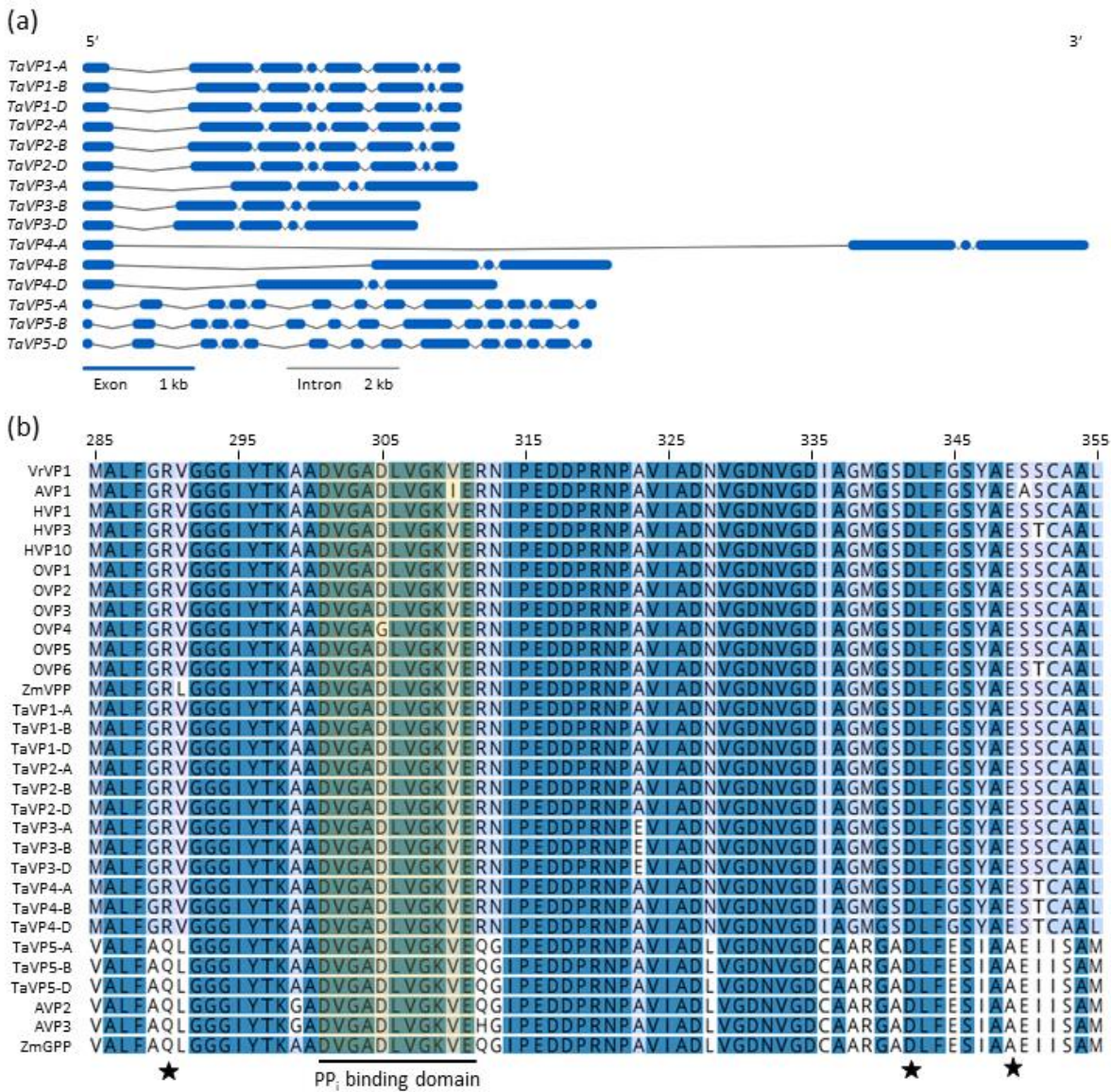


Figure 1: Intron-exon analysis and amino acid alignment of *TaVP* homeologs.



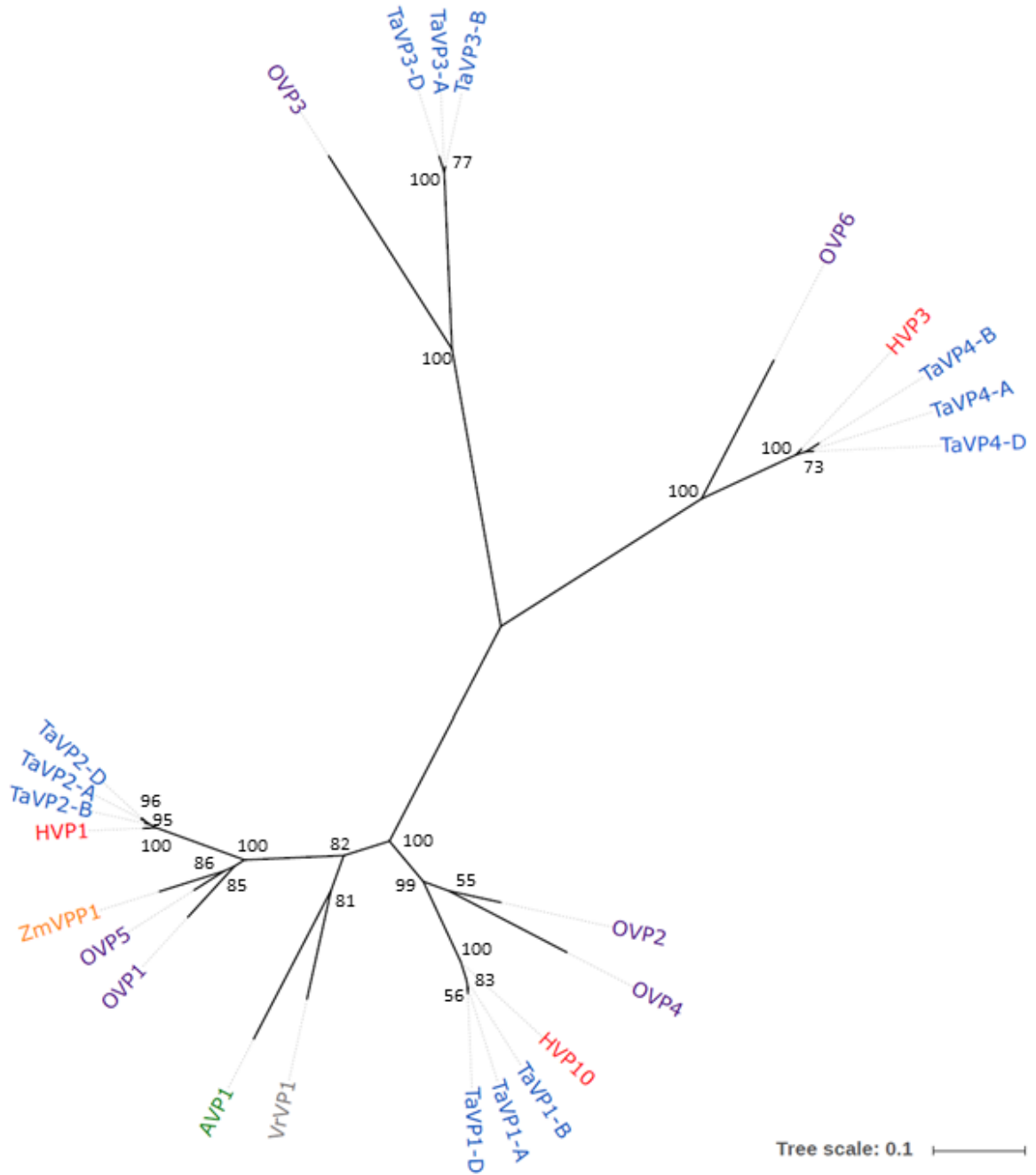


Figure 2: Phylogenetic analysis of type I H<sup>+</sup>-PPases.

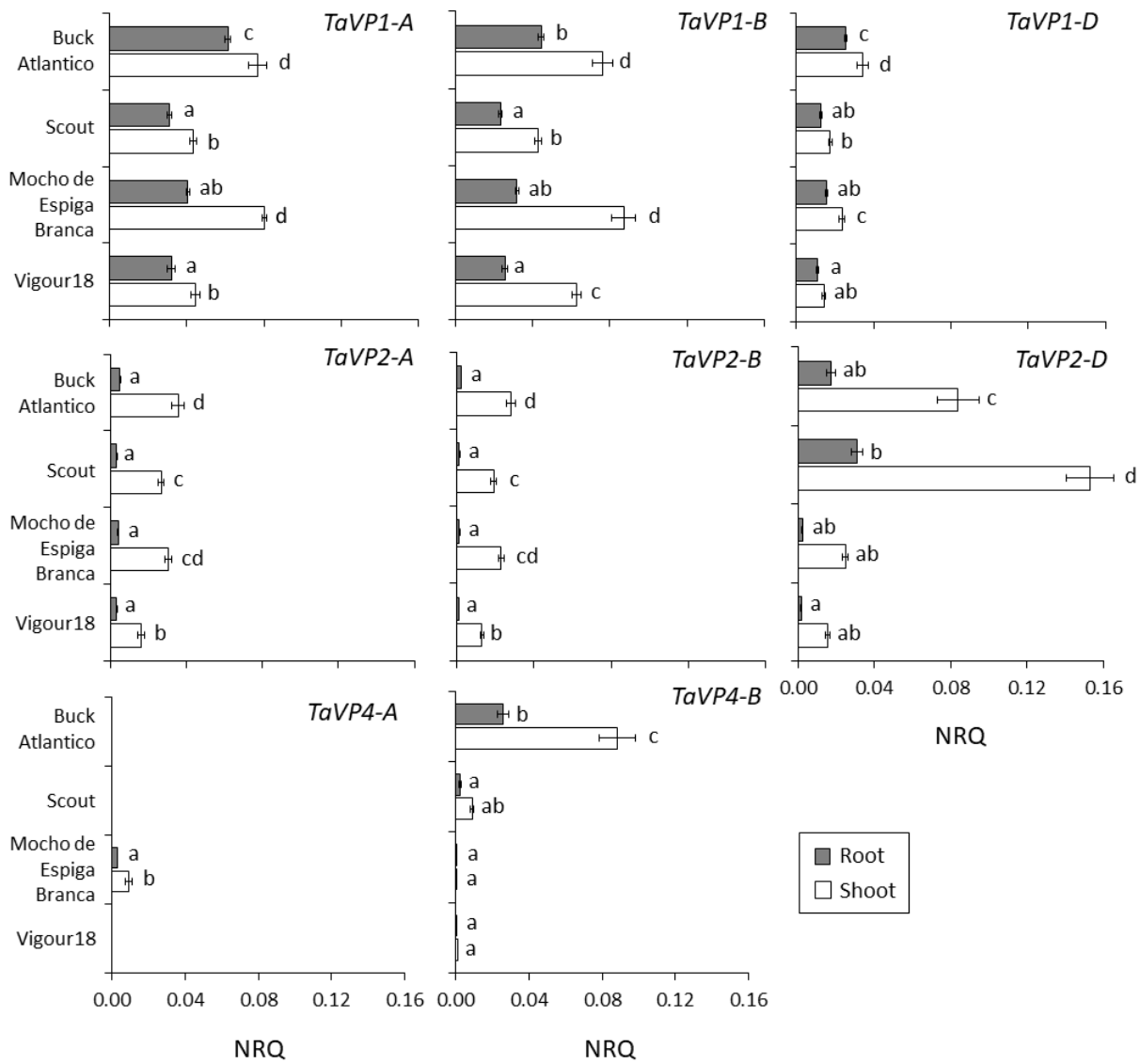


Figure 3: *TaVP* expression profile at seedling stage.

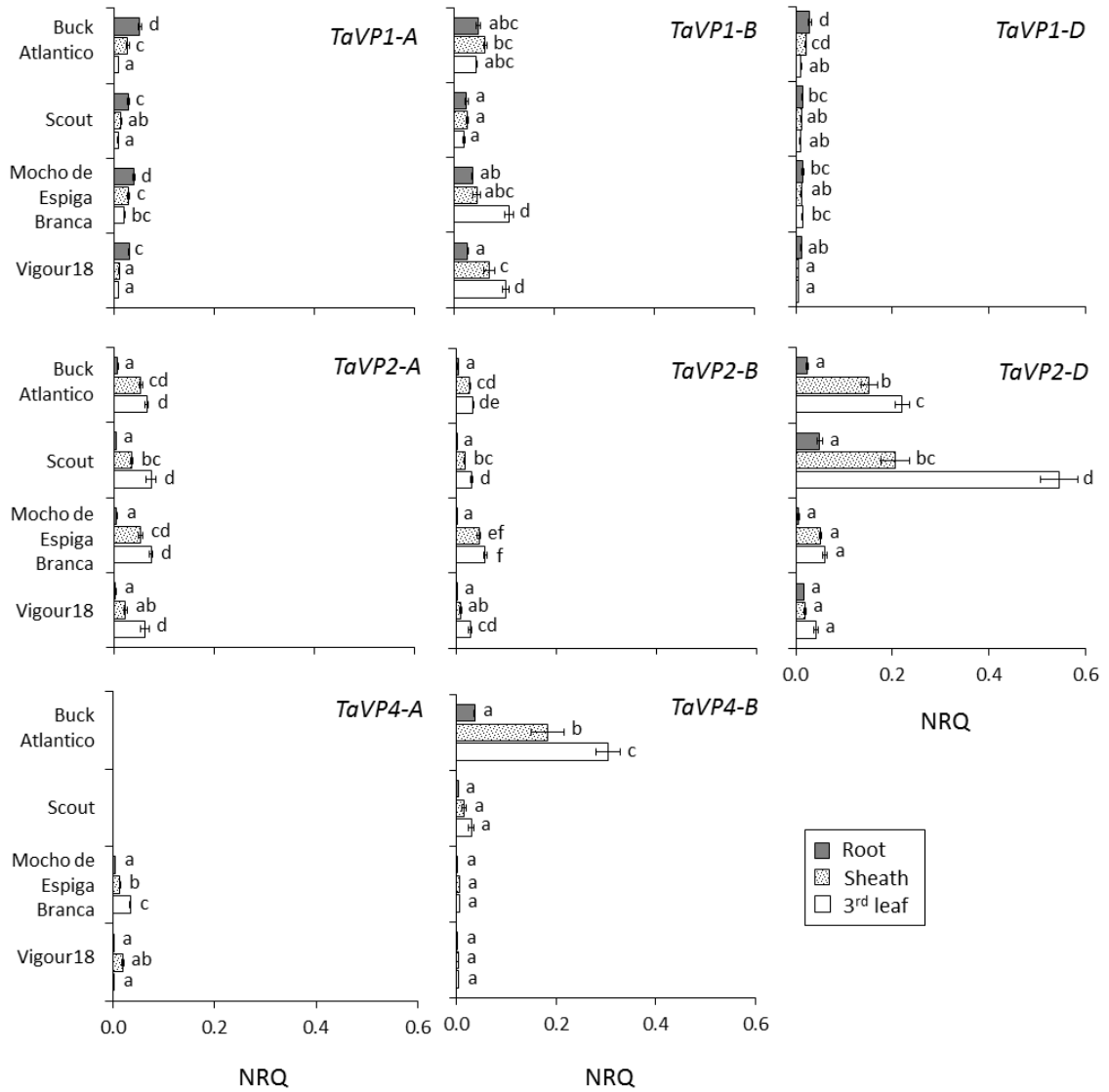


Figure 4: *TaVP* expression profile at third leaf stage.

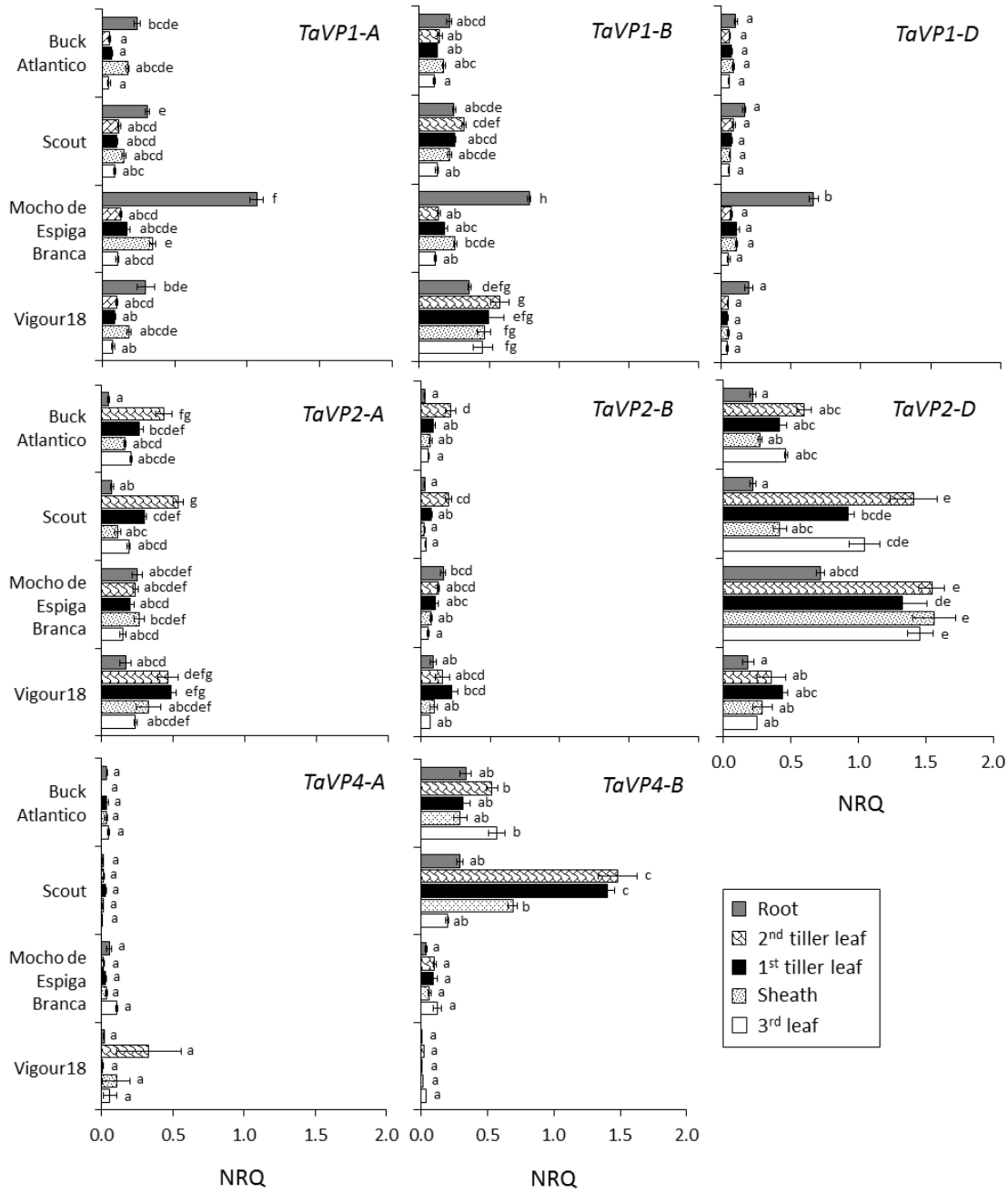


Figure 5: *TaVP* expression profile at second tiller stage.

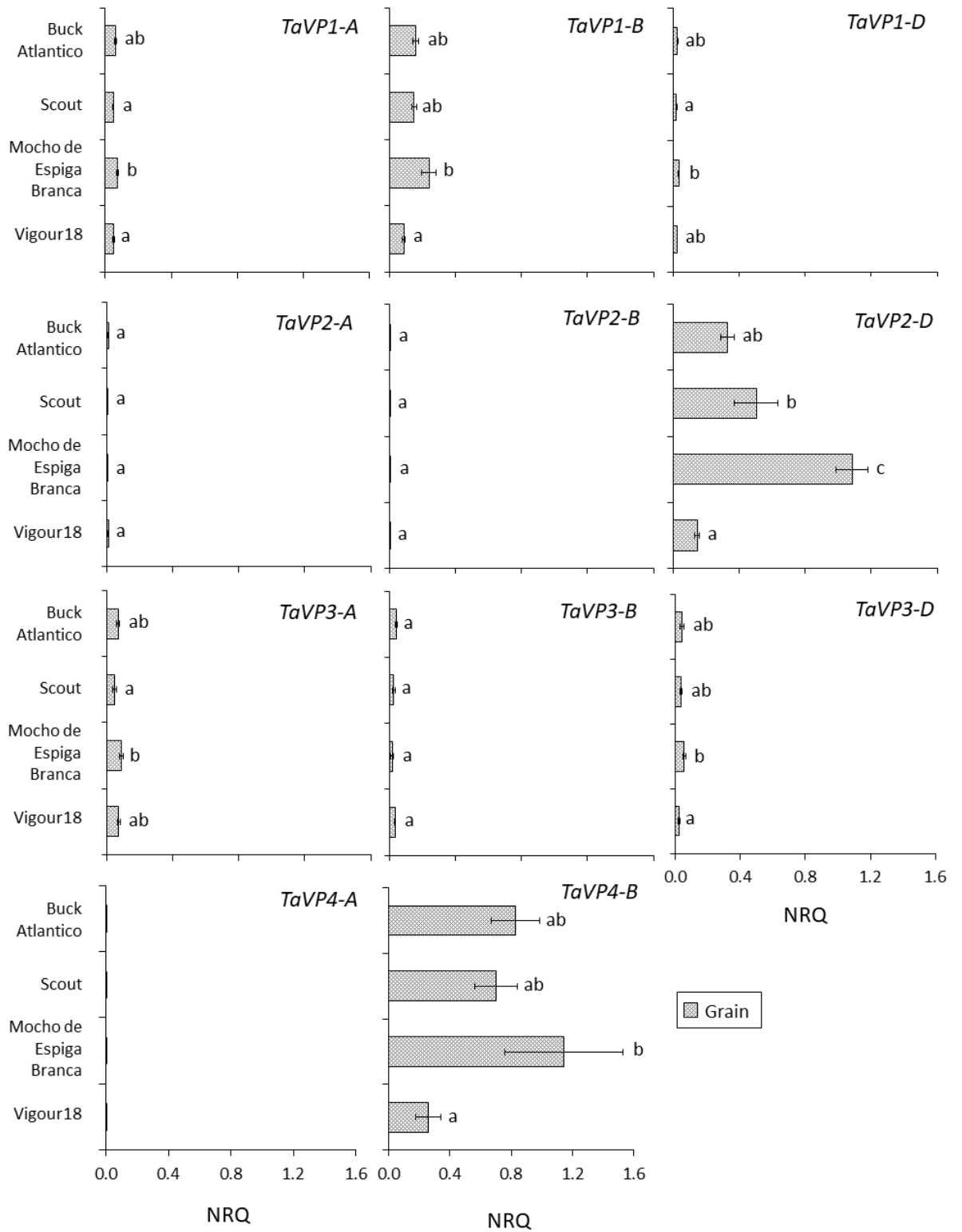


Figure 6: *TaVP* expression profile at grain development stage.

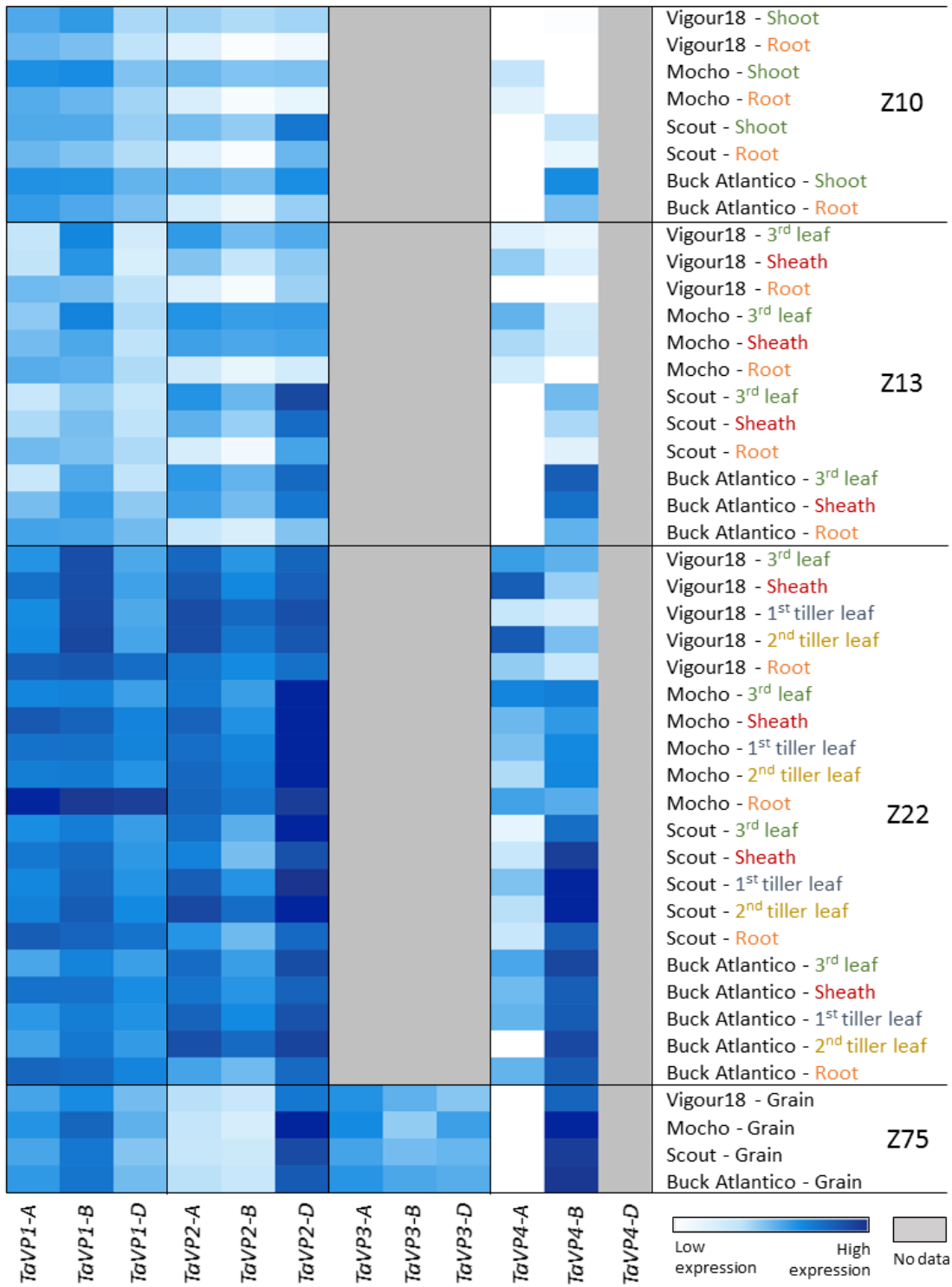


Figure 7: Heat map of *TaVP* gene expression through time.

## Supplementary Tables

Supplementary Table 1: qRT-PCR primer details.

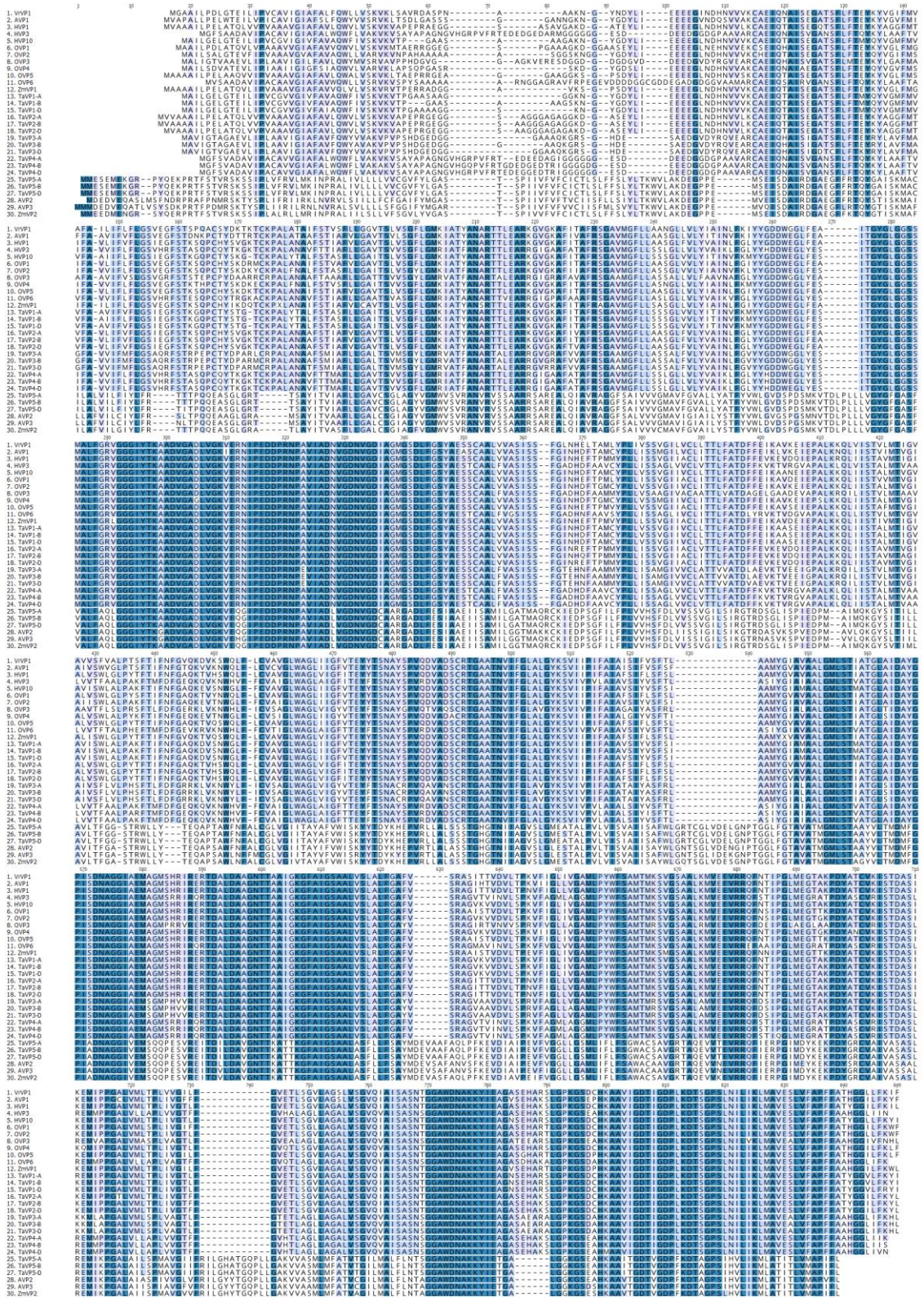
Gene	NCBI accession	Forward primer (5'-3')	Reverse primer (5'-3')	Amplicon size (bp)
<i>TaVP1-A</i>	MH376294	GAAGATGACCCCAAGGAACCCAG	CAGTCGCAAAACAGGGTGGTG	238
<i>TaVP1-B</i>	MH376295	ATAATCTTCCTCTTCCCTGGGTC	GAAAGCGGTGATGAATGCC	243
<i>TaVP1-D</i>	MH376296	GCGGCTCCAAGAACGGCTAC	GCCCTTTGTGCTGAATCCCTC	221
<i>TaVP2-A</i>	MH376297	TCGTTGCTTTCCGCTCTGG	TAAATCCACCCGCCCTACACG	193
<i>TaVP2-B</i>	MH376298	TTCATCACCGCTTTCCGCTC	TAAATCCCGCCGCCCTACACG	197
<i>TaVP2-D</i>	MH376299	GTTCAGCACCAAGAGTCAGCC	GGAGCGGAAAGCAACGGTAAAC	220
<i>TaVP3-A</i>	MH376300	TCAGCGTCCAACAGCGGGCG	GGTCCAGGCAGCAAGCCGAG	296
<i>TaVP3-B</i>	MH376301	ACGCCACGGTCCCATCAG	CGCTCCGCATCGTCATCG	291
<i>TaVP3-D</i>	MH376302	CGTCCATCTCCTCGTTCCGG	CATAGCCGATTACAAGACCTGC	332
<i>TaVP4-A</i>	MH376303	CTCGTCGTGGCACATTTCTTC	GAAAGACCAGCGACTCGACGG	293
<i>TaVP4-B</i>	MH376304	CGTCGTGGCACTTTCTTC	AGACTAGGGACTCCACAGCC	240
<i>TaVP4-D</i>	MH376305	GCTGAGGGAGATGATGCCG	GAAAGACCAGCGACTCAACGG	339
<i>TaActin</i>	AY663392	GACAATGGAACCGGAATGGTC	GTGTGATGCCAGATTTTCTCCAT	236
<i>TaCyclophilin</i>	AY456122	CAAGCCGCTGCACTACAAGG	AGGGACGGTGCAGATGAA	227
<i>TaEFA2</i>	M90077	CAGATTGGCAACGGCTACG	CGGACAGCAAAAACGACCAAG	227
<i>TaGAPDH</i>	EU022331	TTCAACATCATTTCCAAGCAGCA	CGTAACCCAAAATGCCCTTG	220

**Supplementary Table 2: Details of H<sup>+</sup>-PPase sequences used in phylogenetic analysis.** For each gene the species name, gene name, NCBI accession/locus ID (if available), enzyme type and journal reference are provided.

Species	Gene	NCBI accession/Locus ID	Type	Reference
<i>Arabidopsis thaliana</i>	<i>AVP1</i>	BAA32210/AT1G15690	I	Sarafian et al. (1992)
<i>Arabidopsis thaliana</i>	<i>AVP2</i>	AAF31163.1/AT1G78920	II	Drozdowicz et al. (2000)
<i>Arabidopsis thaliana</i>	<i>AVP3</i>	AAG09080.1	II	Hirata et al. (2000)
<i>Hordeum vulgare</i>	<i>HVP1</i>	BAB18681.1	I	Fukuda et al. (2004)
<i>Hordeum vulgare</i>	<i>HVP10</i>	BAA02717.2	I	Tanaka et al. (1993)
<i>Hordeum vulgare</i>	<i>HVP3</i>	BAJ93792.1	I	Wang et al. (2009)
<i>Oryza sativa</i>	<i>OVP1</i>	BAA08232.1/LOC_Os06g43660	I	Sakakibara et al. (1996)
<i>Oryza sativa</i>	<i>OVP2</i>	BAA31524.1/LOC_Os06g08080	I	Sakakibara et al. (1996)
<i>Oryza sativa</i>	<i>OVP3</i>	BAD02276.1/LOC_Os05g06480	I	Choura and Rebai (2005)
<i>Oryza sativa</i>	<i>OVP4</i>	CAF18416.1/LOC_Os02g55890	I	Choura and Rebai (2005)
<i>Oryza sativa</i>	<i>OVP5</i>	BAD02277.1/LOC_Os02g09150	I	Choura and Rebai (2005)
<i>Oryza sativa</i>	<i>OVP6</i>	AAQ19328.1/LOC_Os01g23580	I	Liu et al. (2010)
<i>Triticum aestivum</i>	<i>TaVP1-A</i>	MH376294	I	Current study
<i>Triticum aestivum</i>	<i>TaVP1-B</i>	MH376295	I	Current study
<i>Triticum aestivum</i>	<i>TaVP1-D</i>	MH376296	I	Current study
<i>Triticum aestivum</i>	<i>TaVP2-A</i>	MH376297	I	Current study
<i>Triticum aestivum</i>	<i>TaVP2-B</i>	MH376298	I	Current study
<i>Triticum aestivum</i>	<i>TaVP2-D</i>	MH376299	I	Current study
<i>Triticum aestivum</i>	<i>TaVP3-A</i>	MH376300	I	Current study
<i>Triticum aestivum</i>	<i>TaVP3-B</i>	MH376301	I	Current study
<i>Triticum aestivum</i>	<i>TaVP3-D</i>	MH376302	I	Current study
<i>Triticum aestivum</i>	<i>TaVP4-A</i>	MH376303	I	Current study
<i>Triticum aestivum</i>	<i>TaVP4-B</i>	MH376304	I	Current study
<i>Triticum aestivum</i>	<i>TaVP4-D</i>	MH376305	I	Current study
<i>Triticum aestivum</i>	<i>TaVP5-A</i>	MH376306	II	Current study
<i>Triticum aestivum</i>	<i>TaVP5-B</i>	MH376307	II	Current study
<i>Triticum aestivum</i>	<i>TaVP5-D</i>	MH376308	II	Current study
<i>Vigna radiata</i>	<i>VrVP2</i>	BAA23649	I	Nakanishi & Maeshima (1998)
<i>Zea mays</i>	<i>ZmVPP1</i>	CAG29369.1	I	Wisniewski & Rogowsky (2004)
<i>Zea mays</i>	<i>ZmGPP</i>	ABK51382.1	II	Yue et al. (2008)

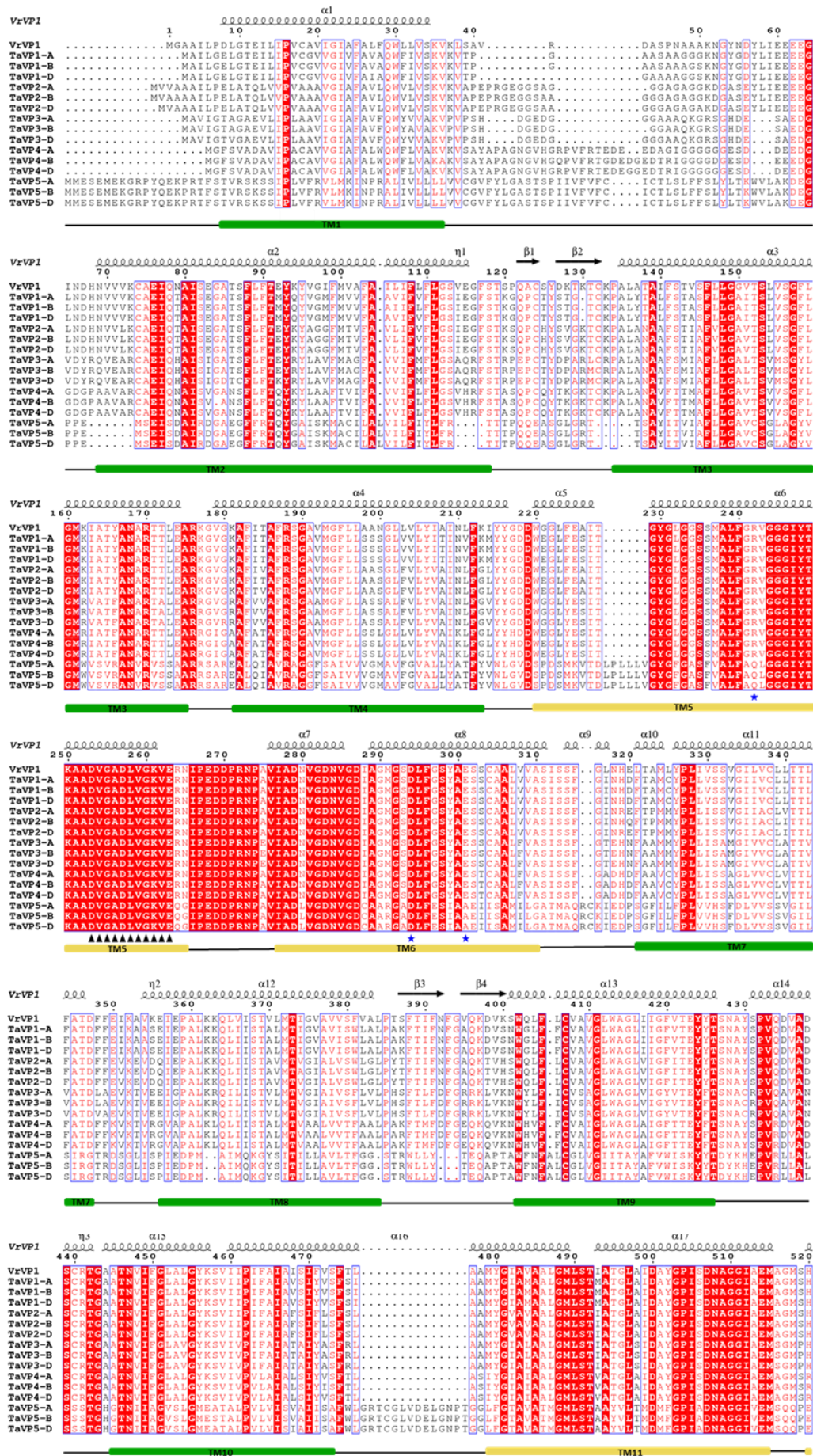


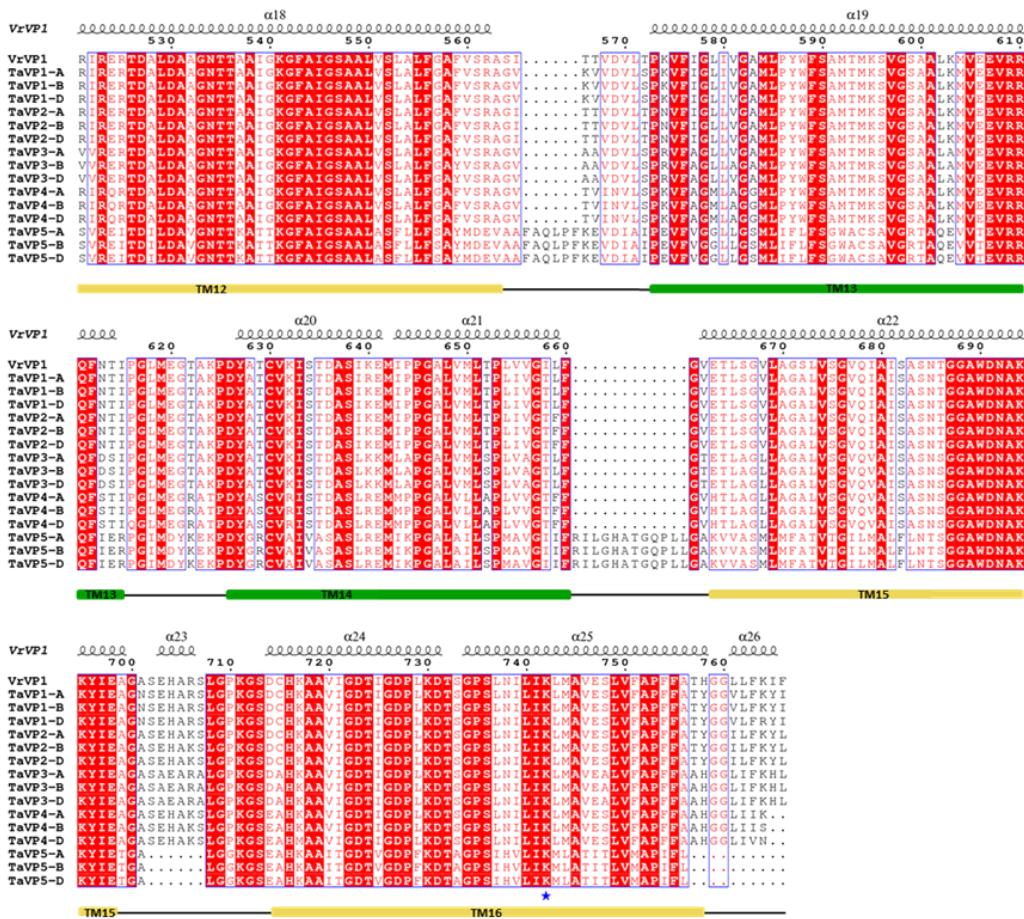
# Supplementary Figures



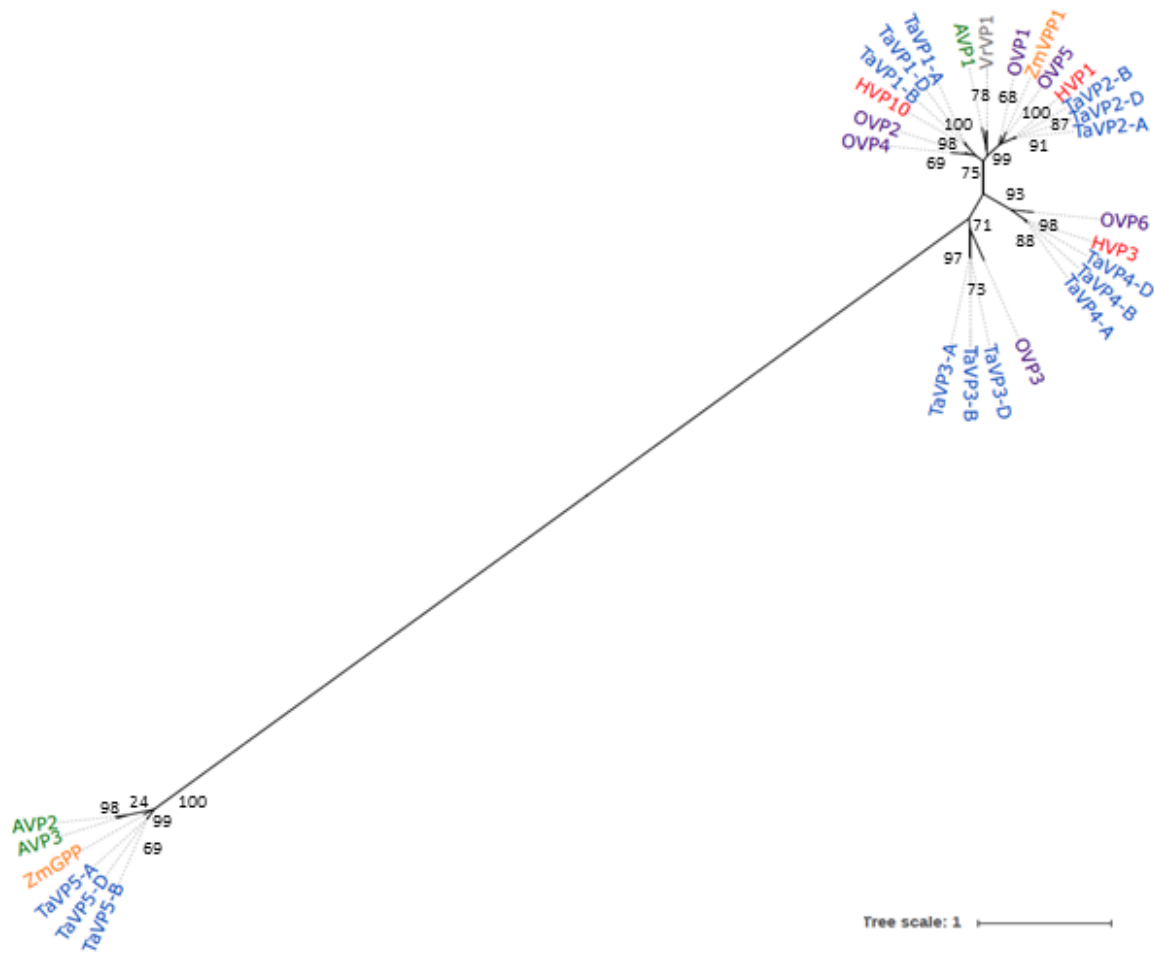
**Supplementary Figure 1: Complete type I and II H<sup>+</sup>-PPase amino acid alignment.** *TaVP* homeolog sequences aligned with type I orthologs from *Vigna radiata* (VrVP1), *Arabidopsis thaliana* (AVP1), *Hordeum vulgare* (HVP1, HVP3, HVP10), *Zea mays* (ZmVPP1 (labelled as ZmVP1)) and *Oryza sativa* (OVP1-6), as well as type II orthologs of *Arabidopsis thaliana* (AVP2, AVP3) and *Zea mays* (ZmGPP (labelled as ZmVP2)). Shading indicates conservation level of amino acid residues where dark blue = 100 %, light blue = 80-99 %, purple = 60-79% and no colour = < 60 %.

Chapter 4 – *TaVP* homeolog expression profiling in bread wheat

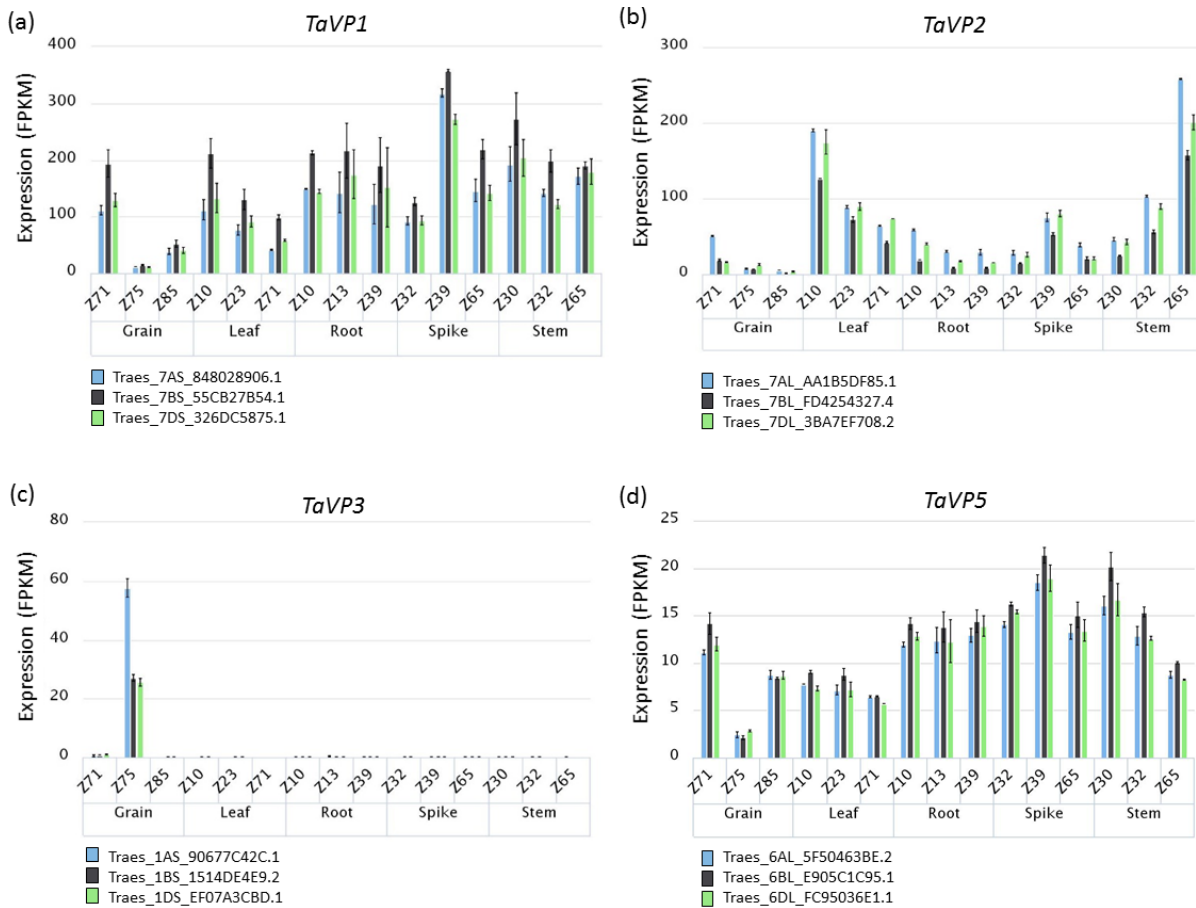




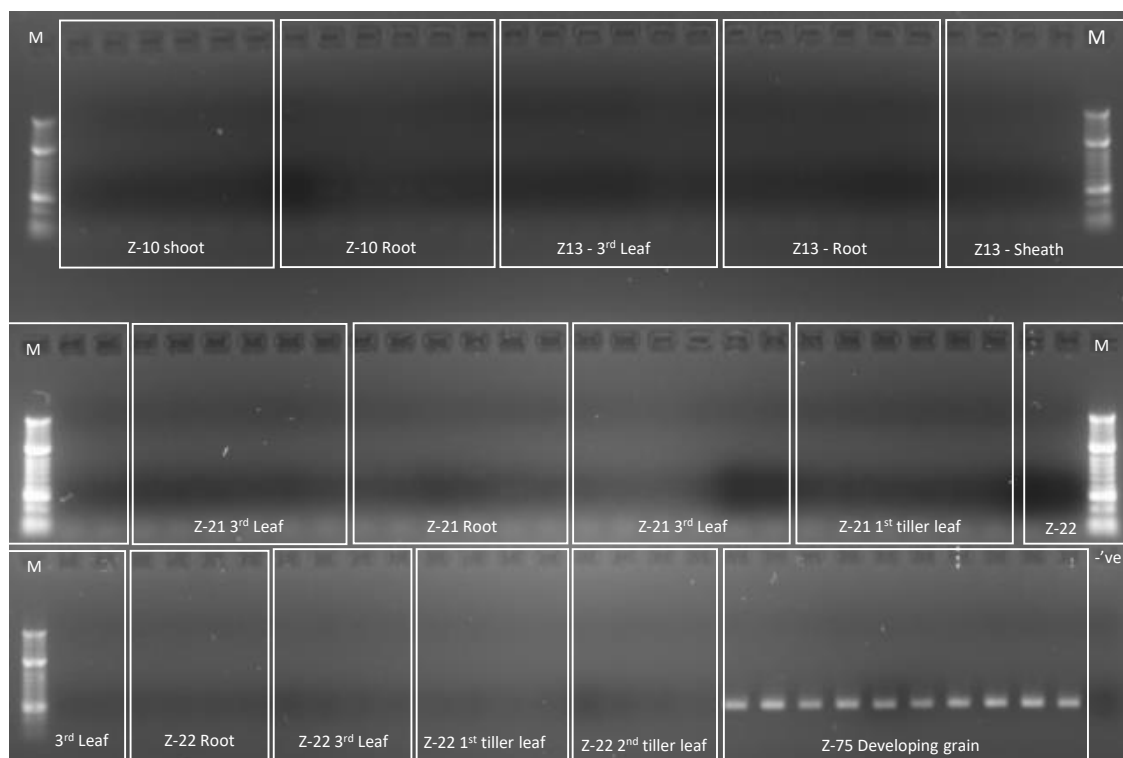
Supplementary Figure 2: Alignment of 15 identified TaVP homeologs with *Vigna radiata* H<sup>+</sup>-PPase (VrVP1) protein sequence. Red shading indicates 100 % amino acid conservation. Secondary structure elements are annotated above alignment and are based on the VrVP1 protein structure (Protein Data Bank accession 4A01). Alpha helices and beta pleated sheets are labelled with 'α' and 'β' respectively. Residues within the VrVP1 sequence known to be involved in proton translocation (stars) and pyrophosphate binding (triangles) are indicated below, as are inner (yellow) and outer (green) transmembrane domains. Alignment was created in Jalview (Waterhouse et al., 2009) using the MUSCLE algorithm (default parameters) and ESPrnt3.0 (Robert and Gouet, 2014) was used for annotation and visualisation of protein features.



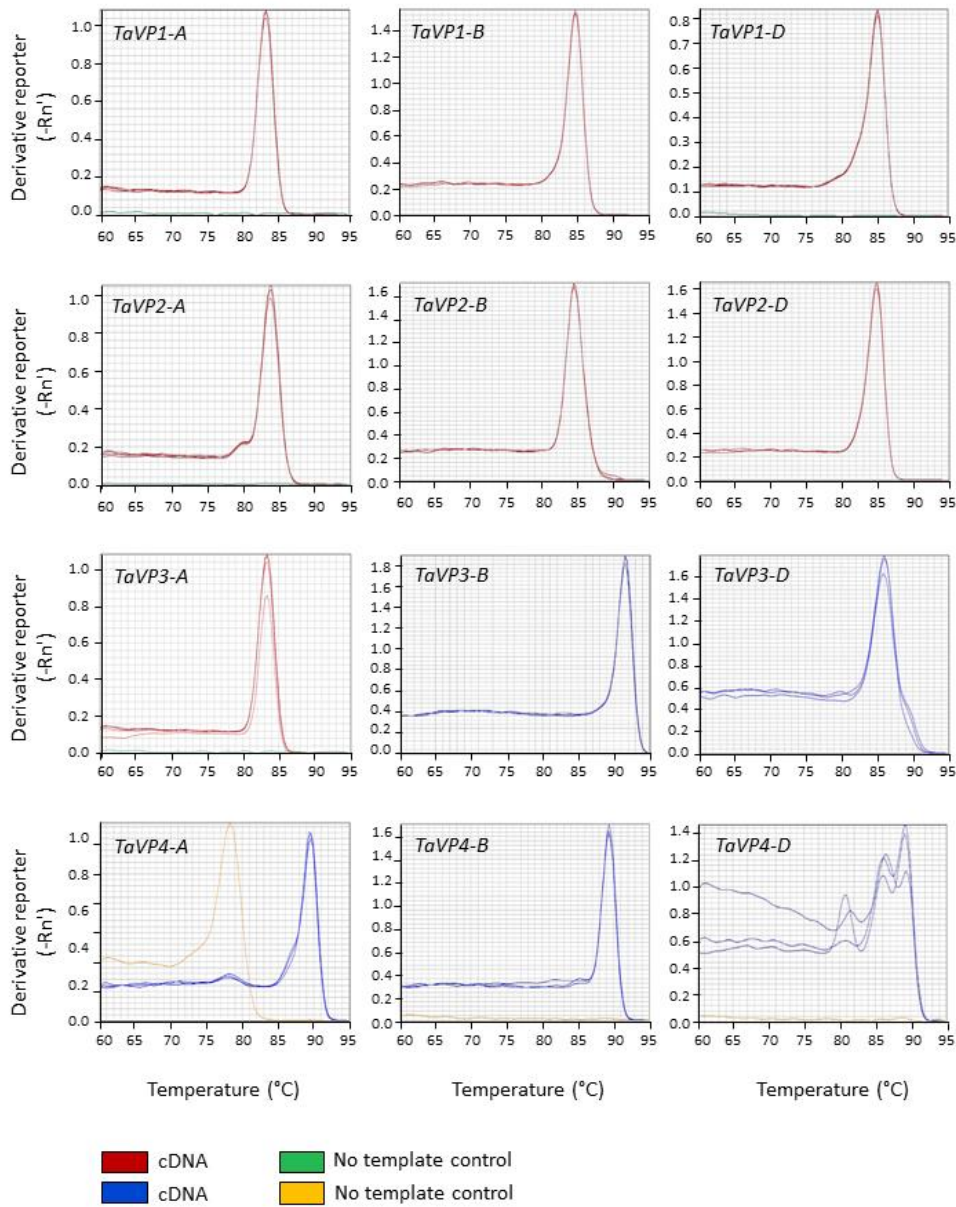
**Supplementary Figure 3: Phylogenetic analysis of type I and type II H<sup>+</sup>-PPases.** Unrooted phylogenetic tree of type I and II H<sup>+</sup>-PPase proteins from *Vigna radiata* (VrVP1), *Arabidopsis thaliana* (AVP1, AVP2, AVP3), *Hordeum vulgare* (HVP1, HVP10, HVP3), *Zea mays* (ZmVPP1, ZmGPP), *Oryza sativa* (OVP1-6) and bread wheat homeologs (TaVP1-TaVP5). Phylogeny was created in MEGA6<sup>®</sup> via the Maximum-Likelihood method and formatted with iTOL. Analysis was validated with 1000 bootstrap replicates and bootstrap support for each node is indicated. Scale bar represents 1.0 amino acid substitutions. Dotted lines are for labelling purposes only and are not included in branch lengths.



**Supplementary Figure 4: RNAseq expression data of IWGSCv2 scaffolds.** (a) *TaVP1* (Traes\_7AS\_848028906.1, Traes\_7BS\_55CB27B54.1, Traes\_7DS\_326DC5875.1), (b) *TaVP2* (Traes\_7AL\_AA1B5DF85.1, Traes\_7BL\_FD4254327.4, Traes\_7DL\_3BA7EF708.2), (c) *TaVP3* (Traes\_1AS\_90677C42C.1, Traes\_1BS\_1514DE4E9.2, Traes\_1DS\_EF07A3CBD.1), and (d) *TaVP5* (Traes\_6AL\_5F50463BE.2, Traes\_6BL\_E905C1C95.1, Traes\_6DL\_FC95036E1.1) genes from the A- (blue columns), B- (black columns) and D-genomes (green columns) in grain, leaf, root, spike and stem tissues under control conditions. Data was obtained from the WheatExp database (Pearce et al., 2015) and is displayed as FPKM (Fragments Per Kilobase of transcript per Million mapped reads). Values are means  $\pm$  standard deviation. As *TaVP4* homeologs are missing from IWGSCv2 assembly, no RNAseq data was available in the WheatExp database.

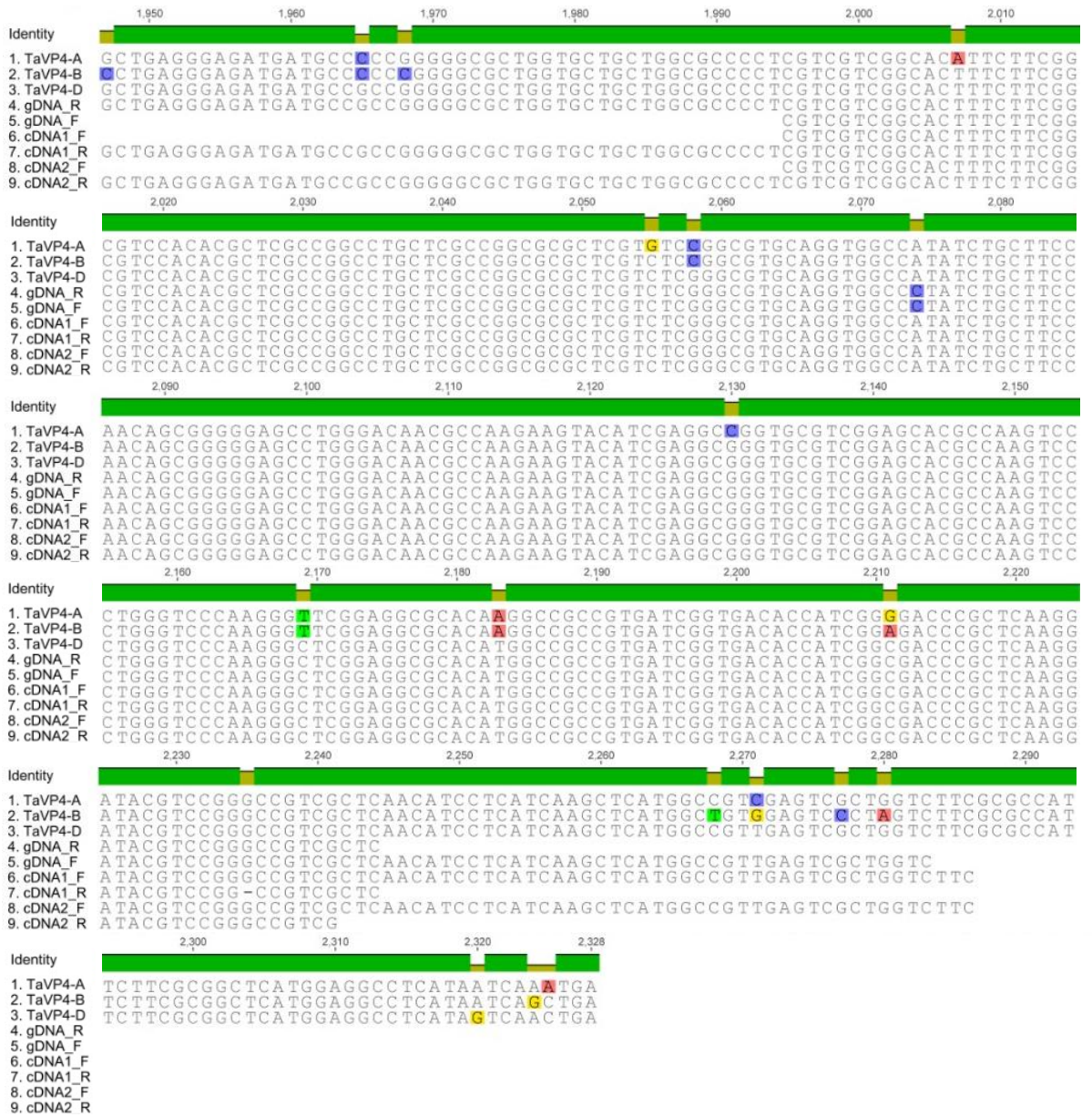


**Supplementary Figure 5: Expression of *TaVP3-A* in Vigour18 cDNA samples.** PCR amplification of *TaVP3-A* was performed with homeolog specific primers (Supplementary Table 1) and OneTaq® polymerase (New England Biosciences, Ipswich, United States) for 30 cycles (annealing temperature 59°C). Tissues analysed include: shoot and root at Z10; 3<sup>rd</sup> leaf, root and sheath at Z13; 3<sup>rd</sup> leaf, root, sheath and 1<sup>st</sup> leaf of the first tiller at Z21; 3<sup>rd</sup> leaf, root, sheath, 1<sup>st</sup> leaf of the first tiller and 1<sup>st</sup> leaf of the second tiller at Z22; developing grain at Z75. M = 100 bp marker (bright bands are 300 and 1000 bp). Final lane contains water as a negative control (-'ve). Figure is representative of all *TaVP3* homeologs in Vigour18, as well as the other analysed varieties.



**Supplementary Figure 6: Melt curve analysis of *TaVP* homeolog specific primers.** Graphs depicting melt curve analysis of amplified products from cDNA (red/blue lines) and no template control (green/yellow) via qRT-PCR (as previously described). Temperature gradient (60°C–95°C) is indicated along the x-axis, while the y-axis represents fluorescence from DNA products. Graphs indicate all primers, except *TaVP4-D*, produce a single product. Peak in *TaVP4-A* no template control shows primer dimer formation.





**Supplementary Figure 7: Sequencing of *TaVP4-D* PCR product amplified from *Gladius* genomic DNA (gDNA) and pooled cDNA.** PCR amplification was performed with *TaVP4-D* specific forward (F) and reverse (R) primers (Supplementary Table 1) and OneTaq<sup>®</sup> polymerase (New England Biosciences, Ipswich, United States) for 40 cycles (annealing temperature 67°C). Products were gel purified with a NucleoSpin Gel and PCR Clean-up kit (Macherey-Nagel, Germany) according to the manufacturer's instructions and sequenced via Sanger Sequencing. Sequencing reads were mapped to an alignment of the three *TaVP4* homeolog (*TaVP4-A*, *TaVP4-B* and *TaVP4-D*) CDS in Geneious<sup>®</sup> 10.1.3 (Biomatters Ltd., Auckland, New Zealand). Coloured nucleotides indicate differences among the aligned sequences, the identity of which is indicated above each position (green represents 100 % sequence identity and yellow represents < 100 %). The figure shows all *TaVP4-D* sequences are specific to the *TaVP4-D* homeolog in gDNA and cDNA.

## Additional Information

### Functional characterisation of *TaVP* proteins in a salt sensitive yeast strain

To investigate functional differences between bread wheat (*Triticum aestivum*) proton-pumping pyrophosphatase ( $H^+$ -PPase) proteins, complete coding sequences (CDS) for each B genome *TaVP* gene (*TaVP1-B*, *TaVP2-B*, *TaVP3-B* and *TaVP4-B*), as well as the *Arabidopsis thaliana* *AVP1* gene (*AT1G15690*), were cloned into the *pYESDEST52* yeast expression vector, 3' of the yeast (*Saccharomyces cerevisiae*) galactose inducible *GAL1* promoter (Invitrogen, Carlsbad, United States). Complete *pYESDEST52* expression vectors were transformed via lithium-acetate (Li/Ac) transformation (Gietz and Schiestl, 2007) into the B31 (*ena1Δ::HIS3::ena4Δnha1Δ::LEU2*) mutant yeast strain (Banuelos et al., 1998). Due to the absence of the plasma membrane  $Na^+$  efflux proteins, ENA1-4 (*YDR040C*) and NHA1 (*YLR138W*), B31 yeast is unable to efflux sodium ( $Na^+$ ) from the cell, resulting in reduced growth under saline conditions (Banuelos et al., 1998). Salt sensitive mutant yeast strains, such as B31, have previously been used to demonstrate the ability of  $H^+$ -PPases to prevent cytosolic  $Na^+$  accumulation and, consequently, restore yeast growth under saline conditions (Brini et al., 2005; Gao et al., 2006; Gaxiola et al., 1999).

To evaluate the role of *TaVP* proteins in salinity tolerance, transformed B31 yeast strains were phenotyped on solid media containing 0 mM, 50 mM and 100 mM NaCl. After 2 d initial growth in liquid Standard Defined (SD) media (without uracil), starting cultures were standardised to an  $OD_{600}$  of 0.6 using a spectrophotometer (UV-160A, Shimadzu, Japan) and 10  $\mu$ l serial dilutions (1 $\times$ , 10 $\times$ , 100 $\times$ , 1000 $\times$ , and 10000 $\times$ ) were plated onto SD agar media. SD media contained either 2 % glucose to inhibit transgene expression, or 2 % galactose to induce transgene expression. Three technical replicates of each B31 strain were plated on each NaCl

treatment and photographed under white light using a UV-transilluminator (Clinx, Shanghai, China) after 2 d, 3 d and 4 d incubation at 30°C.

After 2 d growth, no phenotypic differences between the B31 empty vector control and *TaVP/AVP1* expressing B31 yeast colonies were observed on 0 mM, 50 mM or 100 mM NaCl media. However, colonies of each strain showed faster growth on glucose media, compared to galactose media, regardless of NaCl treatment (Figure A1).

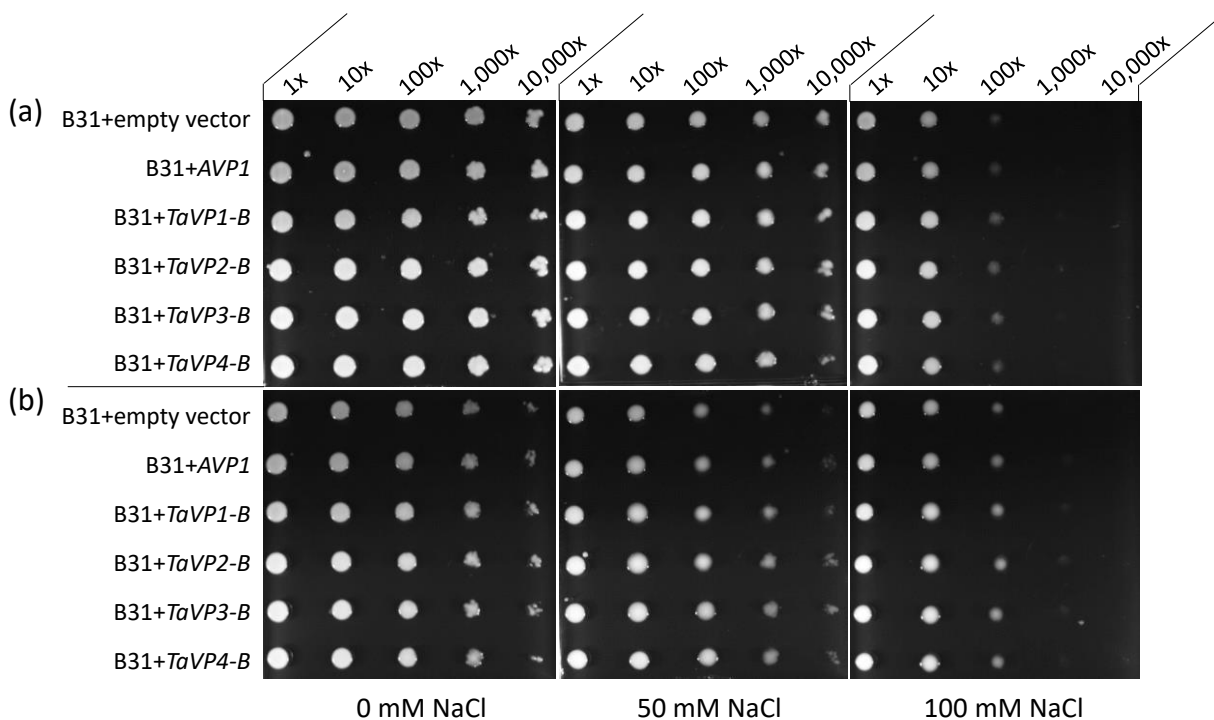


**Figure A1: Growth phenotypes of B31 yeast strains after 2 d growth with 0 mM, 50 mM and 100 mM NaCl.** Representative images of B31 yeast expressing the pYES-DEST52 empty vector, *AVP1*, *TaVP1-B*, *TaVP2-B*, *TaVP3-B* and *TaVP4-B* coding sequences grown on (a) SD + 2 % glucose and (b) SD + 2 % galactose media containing 0 mM, 50 mM and 100 mM NaCl at 30°C for 2 d. 10  $\mu$ l serial dilutions (1x, 10x, 100x, 1000x, and 10000x) of each starting culture, standardised to an  $OD_{600}$  of 0.6.

After 3 d (Figure A2) and 4 d (Figure A3) growth, colonies of all *TaVP* and *AVP1* expressing B31 yeast strains, showed enhanced growth compared to the empty vector control on media containing 100 mM NaCl. Similar growth phenotypes were observed on both glucose and galactose media, with the *AVP1* and *TaVP2-B* expressing B31 yeast strains showing the largest growth increase compared to the empty vector control (Figures A2-A3). After 3 and 4 d incubation, all transformed B31 strains showed enhanced growth on 100 mM NaCl media when supplied with galactose, compared to those supplied glucose as the primary carbon source (Figures A2-A3).

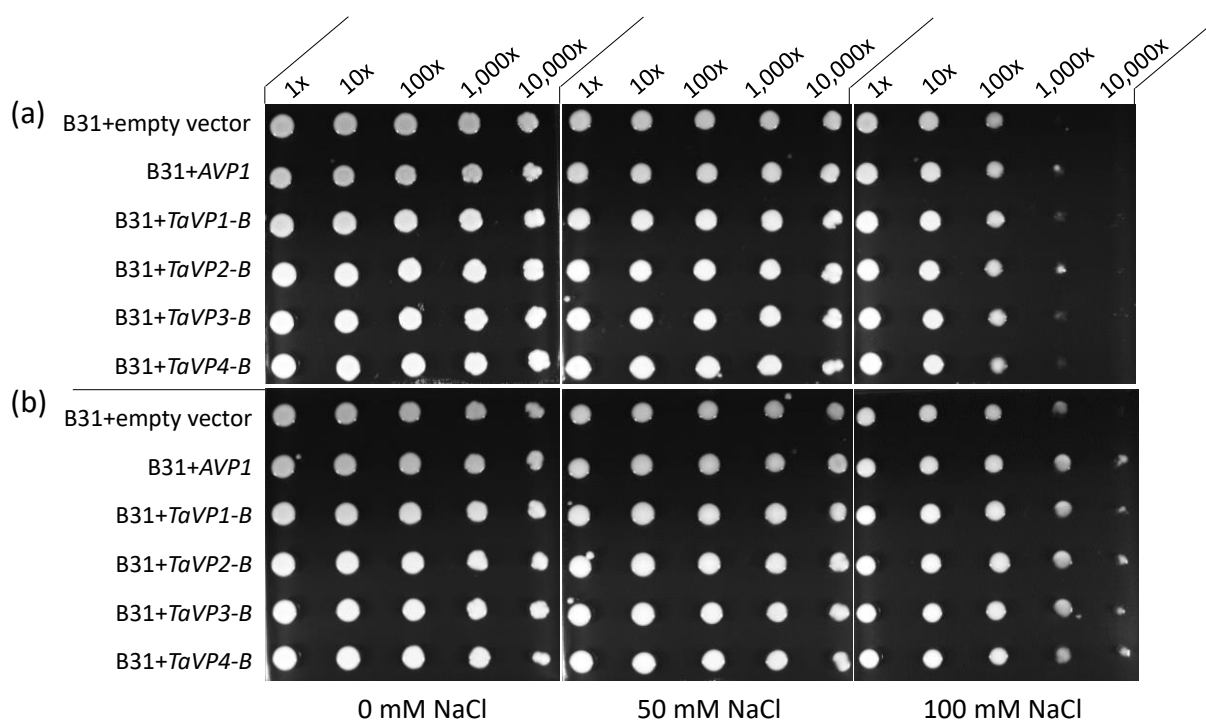


**Figure A2: Growth phenotypes of B31 yeast strains after 3 d growth with 0 mM, 50 mM and 100 mM NaCl.** Representative images of B31 yeast expressing the pYES-DEST52 empty vector, *AVP1*, *TaVP1-B*, *TaVP2-B*, *TaVP3-B* and *TaVP4-B* coding sequences grown on (a) SD + 2 % glucose and (b) SD + 2 % galactose media containing 0 mM, 50 mM and 100 mM NaCl at 30°C for 3 d. 10  $\mu$ l serial dilutions (1x, 10x, 100x, 1000x, and 10000x) of each starting culture, standardised to an  $OD_{600}$  of 0.6.

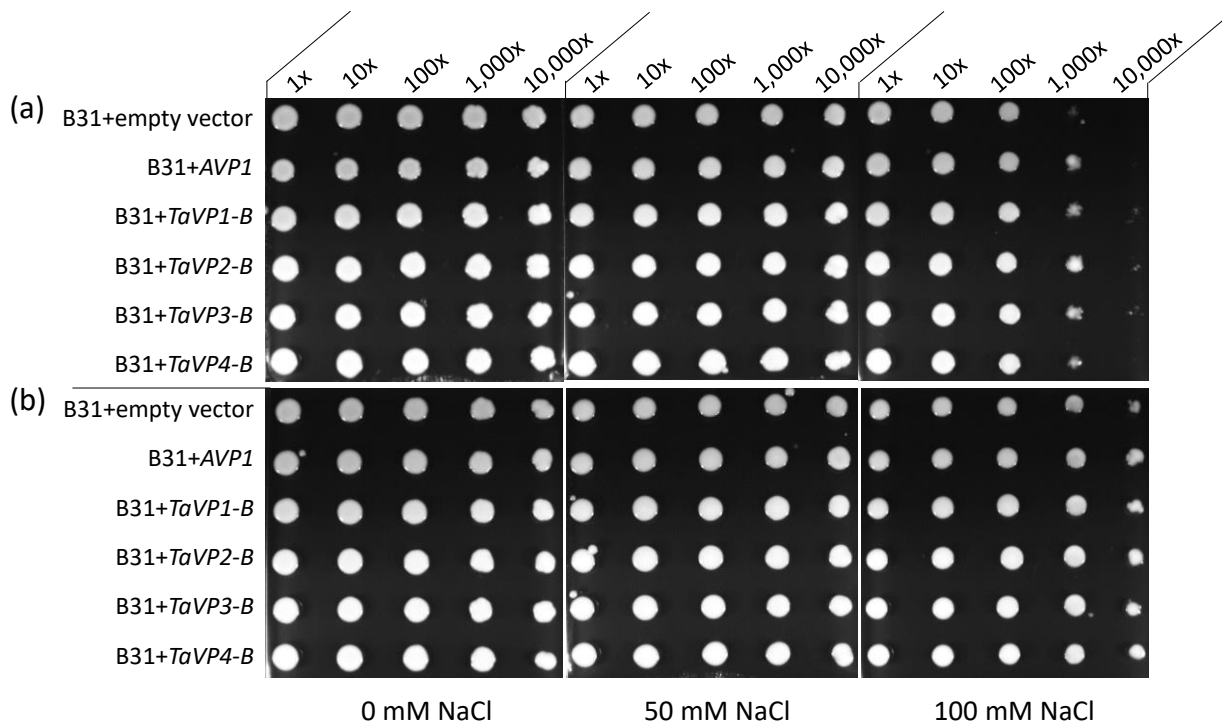


**Figure A3: Growth phenotypes of B31 yeast strains after 4 d growth with 0 mM, 50 mM and 100 mM NaCl.** Representative images of B31 yeast expressing the pYES-DEST52 empty vector, *AVP1*, *TaVP1-B*, *TaVP2-B*, *TaVP3-B* and *TaVP4-B* coding sequences grown on (a) SD + 2 % glucose and (b) SD + 2 % galactose media containing 0 mM, 50 mM and 100 mM NaCl at 30°C for 4 d. 10  $\mu$ l serial dilutions (1x, 10x, 100x, 1000x, and 10000x) of each starting culture, standardised to an  $OD_{600}$  of 0.6.

Based on these results, limited conclusions can be made regarding the role of *TaVP* proteins in the salt tolerance of yeast. The enhanced growth of the *TaVP* and *AVP1* expressing B31 yeast strains on 100 mM NaCl galactose media suggest the *TaVP* genes may be beneficial for enhancing the salt tolerance of B31 yeast. However, as the growth of these strains was also greater than the B31 empty vector on glucose media, on which transgene expression should not have been induced, the significance of these results remain unclear. As transgene

expression was not assessed in the transformed B31 yeast strains, it remains unknown whether the *TaVP* and *AVP1* transgenes were expressed in these strains on galactose media and inhibited on glucose media. As differences in transgene expression could have influenced the experimental results, future research should address this by purifying RNA from the B31 yeast strains (Rivas et al., 2001) and assessing *TaVP* and *AVP1* transgene expression via reverse-transcription polymerase chain reaction (RT-PCR) analysis, grown in the presence of both glucose and galactose.

The growth improvement observed in these lines could also be due to technical inaccuracies, such as variation in initial OD<sub>600</sub> values prior to dilution, or as a result of pipetting inconsistencies. The slower growth rate of all B31 yeast on galactose media, compared to glucose media, may have been influenced by the concentration of galactose or rate of uptake from the media. While previous research has shown 2 % galactose to be sufficient for inducing *GAL1* transgene expression (West et al., 1984), a higher concentration may be required for inducing expression in the transformed B31 strains. Alternatively, galactose is known to have a slower rate of uptake than glucose in yeast cells (Ostergaard et al., 2000), which could account for the slower growth rate of the B31 yeast on galactose media, compared to glucose media.

Yeast growth rates have also been shown to vary under salt treatment depending on the primary carbon source (Pastor et al., 2009). When treated with 100 mM NaCl, yeast growth rates were reduced to a greater extent in the presence of glucose, as opposed to galactose and glycerol. Mitochondrial metabolism, which is enhanced in the presence of galactose and inhibited in the presence of glucose, was hypothesised to influence yeast growth rates under salinity treatment (Pastor et al., 2009). Growth of the *TaVP* and *AVP1* yeast strains, as well as the empty vector control, may have been greater in the presence of 100 mM NaCl when

supplied with galactose due to enhanced mitochondrial metabolism compared to glucose media treated with 100 mM NaCl. However, further experimentation is required to investigate this possibility.

While preliminary data suggested that salted concentrations above 100 mM NaCl were detrimental to the growth of both transformed and empty-vector B31 yeast strains (data not shown), the treatment levels used in this study were considerably lower than that of other studies. In similar experiments, untransformed yeast lacking ENA1 function were able to maintain growth up to concentrations 250 mM NaCl, while transformed yeast strains expressing *AVP1* (Gaxiola et al., 1999), *TVP1* (Brini et al., 2005) and *TsVP* (Gao et al., 2006) were able to maintain growth up to concentrations of 750 mM NaCl. The higher salt sensitivity of B31 yeast, compared to *ena1* mutant yeast, may be due to the lack of both ENA1-4 and NHA1 function. Inhibition of both Na<sup>+</sup> efflux proteins could have increased the rate of Na<sup>+</sup> accumulation within the cell, and thus reduced growth at a faster rate than the *ena1* mutants, which retain some ability to efflux Na<sup>+</sup> from the cell (Gaxiola et al., 1999). An increase in salt sensitivity may have prevented significant phenotypic differences being identified between the lines *TaVP* and *AVP1* expressing B31 yeast and the empty vector control.

While expression of the *TaVP1-B*, *TaVP2-B*, *TaVP3-B* and *TaVP4-B* genes have the potential to improve yeast growth under salt treatment, further experimentation is required to clarify these results and further investigate factors that may have influenced the results of this study.



## References

- Banuelos, M.A., Sychrova, H., Bleykasten-Grosshans, C., Souciet, J.L. and Potier, S. (1998) The NHA1 antiporter of *Saccharomyces cerevisiae* mediates sodium and potassium efflux. *Microbiology* **144**, 2749-2758.
- Brini, F., Gaxiola, R.A., Berkowitz, G.A. and Masmoudi, K. (2005) Cloning and characterization of a wheat vacuolar cation/proton antiporter and pyrophosphatase proton pump. *Plant Physiol. Biochem.* **43**, 347-354.
- Gao, F., Gao, Q., Duan, X., Yue, G., Yang, A. and Zhang, J. (2006) Cloning of an H<sup>+</sup>-PPase gene from *Thellungiella halophila* and its heterologous expression to improve tobacco salt tolerance. *J. Exp. Bot.* **57**, 3259-3270.
- Gaxiola, R.A., Rao, R., Sherman, A., Grisafi, P., Alper, S.L. and Fink, G.R. (1999) The *Arabidopsis thaliana* proton transporters, AtNHX1 and AVP1, can function in cation detoxification in yeast. *Proc. Natl. Acad. Sci.* **96**, 1480-1485.
- Gietz, R.D. and Schiestl, R.H. (2007) High-efficiency yeast transformation using the LiAc/SS carrier DNA/PEG method. *Nat. Protoc.* **2**, 31-34.
- Ostergaard, S., Roca, C., Rønnow, B., Nielsen, J. and Olsson, L. (2000) Physiological studies in aerobic batch cultivations of *Saccharomyces cerevisiae* strains harboring the *MEL1* gene. *Biotechnol. Bioeng.* **68**, 252-259.
- Pastor, M.M., Proft, M. and Pascual-Ahuir, A. (2009) Mitochondrial function is an inducible determinant of osmotic stress adaptation in yeast. *J. Biol. Chem.* **284**, 30307-30317.
- Rivas, R., Vizcaíno, N., Buey, R.M., Mateos, P.F., Martínez-Molina, E. and Velázquez, E. (2001) An effective, rapid and simple method for total RNA extraction from bacteria and yeast. *J. Microbiol. Methods* **47**, 59-63.
- West, R.W., Yocum, R.R. and Ptashne, M. (1984) *Saccharomyces cerevisiae* GAL1-GAL10 divergent promoter region: Location and function of the upstream activating sequence UASG. *Mol. Cell. Biol.* **4**, 2467-2478.




**Chapter 5** - Phenotypic characterisation of *TaVP* over-  
expressing bread wheat

## Statement of Authorship

Title of Paper	Constitutive over-expression of <i>TaVP1-B</i> and <i>TaVP2-B</i> reduces time to flowering and increases Na <sup>+</sup> accumulation in wheat ( <i>Triticum aestivum</i> )
Publication Status	<input type="checkbox"/> Published <input type="checkbox"/> Accepted for Publication <input type="checkbox"/> Submitted for Publication <input checked="" type="checkbox"/> Unpublished and Unsubmitted work written in manuscript style
Publication Details	This manuscript has been written and formatted for publication in the Journal of Experimental Botany

### Principal Author

Name of Principal Author (Candidate)	Daniel J. Menadue		
Contribution to the Paper	Contributed to the experimental design, cloned the <i>TaVP</i> genes and generated the constructs used for plant transformation, grew, genotyped and phenotyped the T <sub>0</sub> , T <sub>1</sub> and T <sub>2</sub> plants, conducted plant and soil analysis for the preliminary experimental work, performed gene expression and ion analysis, recorded growth stages and daily water usage, performed statistical analysis, interpreted the data and wrote the manuscript.		
Overall percentage (%)	70		
Certification:	This paper reports on original research I conducted during the period of my Higher Degree by Research candidature and is not subject to any obligations or contractual agreements with a third party that would constrain its inclusion in this thesis. I am the primary author of this paper.		
Signature		Date	28/5/2018

### Co-Author Contributions

By signing the Statement of Authorship, each author certifies that:

- i. the candidate's stated contribution to the publication is accurate (as detailed above);
- ii. permission is granted for the candidate to include the publication in the thesis; and
- iii. the sum of all co-author contributions is equal to 100% less the candidate's stated contribution.

Name of Co-Author	Chris Brien		
Contribution to the Paper	Generated the design for the high-throughput phenotyping experiment, supervised analysis of the phenotyping data and contributed the manuscript.		
Signature		Date	5/6/2018

Name of Co-Author	Nathaniel Jewell		
Contribution to the Paper	Performed statistical analysis of the high-throughput phenotyping data.		
Signature		Date	5/6/18

Name of Co-Author	Rhiannon K. Schilling		
Contribution to the Paper	Contributed to the experimental design, assisted with method development, statistical analysis and data interpretation and contributed to revision of the manuscript.		
Signature		Date	4/6/2018

Name of Co-Author	Bettina Berger		
Contribution to the Paper	Contributed to the experimental design and supervised the high-throughput phenotyping experiment.		
Signature		Date	5/6/2018

Name of Co-Author	Darren C. Plett		
Contribution to the Paper	Contributed to the experimental design, data interpretation and revision of the manuscript.		
Signature		Date	4/6/2018

Name of Co-Author	Stuart J. Roy		
Contribution to the Paper	Conceived the research project and contributed to the experimental design, data interpretation and revision of the manuscript.		
Signature		Date	28/05/2018

## Constitutive over-expression of *TaVP1-B* and *TaVP2-B* reduces time to flowering and increases Na<sup>+</sup> accumulation in wheat (*Triticum aestivum*)

**Running title:** Phenotypic characterisation of *TaVP* over-expressing transgenic wheat

Daniel Jamie Menadue<sup>1,2</sup>, Rhiannon Kate Schilling<sup>1,2</sup>, Chris Brien<sup>1,3</sup>, Nathaniel Jewell<sup>1,3</sup>, Darren Craig Plett<sup>1,2</sup>, Bettina Berger<sup>1,3</sup> and Stuart John Roy<sup>1,2\*</sup>

<sup>1</sup>School of Agriculture, Food and Wine, The University of Adelaide, Adelaide, SA, 5005, Australia

<sup>2</sup>Australian Centre for Plant Functional Genomics, Glen Osmond, SA, 5064, Australia

<sup>3</sup>The Plant Accelerator, Australian Plant Phenomics Facility, University of Adelaide, PMB1, Glen Osmond, SA 5064, Australia.

\*Corresponding author: Daniel Menadue, School of Agriculture, Food and Wine, The University of Adelaide, SA 5005 Australia, daniel.menadue@adelaide.edu.au, Tel: +61 8 8313 7162, Fax: +61 8 8313 7102

Author email addresses:

daniel.menadue@adelaide.edu.au, rhiannon.schilling@adelaide.edu.au,

chris.brien@adelaide.edu.au, nathaniel.jewell@adelaide.edu.au,

darren.plett@adelaide.edu.au, bettina.berger@adelaide.edu.au, stuart.roy@adelaide.edu.au

**Tables:** 1

**Figures:** 6

**Supplementary Figures:** 4

**Word count:** 6367

## Highlight

When constitutively over-expressed in bread wheat, the vacuolar proton-pumping pyrophosphatase genes, *TaVP1-B* and *TaVP2-B*, increase leaf sodium accumulation, reduce biomass accumulation and trigger early flowering under control and saline conditions.

## Abstract

When constitutively expressed, vacuolar proton-pumping pyrophosphatase (H<sup>+</sup>-PPase) genes have a beneficial impact on plant growth, under both stressed and non-stressed conditions. Previously, twelve genes encoding type I H<sup>+</sup>-PPase (TaVP) proteins were identified in bread wheat, however, the functional role of these proteins remains unknown. In this work, constitutive over-expression of the *TaVP1-B* and *TaVP2-B* genes in bread wheat reduced time to flowering by approximately 5 d, under both control and saline conditions, compared to wild-type and null segregants. Under salt treatment (150 mM NaCl), accumulation of Na<sup>+</sup> and Cl<sup>-</sup> in the 4<sup>th</sup> leaf of transgenic wheat lines increased compared to wild-type and null segregants, although this did not alter salt tolerance. Furthermore, under control conditions (0 mM NaCl), plant biomass at maturity was reduced in several of the transgenic lines, compared to wild-type. These results indicate constitutive over-expression of *TaVP1-B* and *TaVP2-B* enhances wheat development by promoting early flowering, thus reducing the vegetative growth phase.

**Keywords:** flowering, growth rate, high-throughput phenotyping, H<sup>+</sup>-PPase, salt tolerance

**Abbreviations:** DAP (days after planting), H<sup>+</sup>-PPase (vacuolar proton-pumping pyrophosphatase), LSD (least significant difference), OEX (over-expressing), OST (osmotic stress tolerance), PSA (projected shoot area), RGR (relative growth rate)

## Introduction

Bread wheat (*Triticum aestivum*) is the most widely cultivated cereal crop in the world (Alexandratos and Bruinsma, 2012), with an average of 22 MT of wheat produced in Australia each year (Australian Bureau of Statistics, 2017). Abiotic stress conditions, such as soil salinity, drought and low nutrient availability, significantly constrain wheat production across Australia (Gilliham et al., 2017). Soil salinity is particularly problematic as it affects 69 % of the Australian wheat, costing Australian farmers approximately \$1.3 B per annum (Rengasamy, 2010). One approach to overcome the constraints of soil salinity on wheat yields is using genetic modification to enhance the salt tolerance of wheat varieties (Gilliham et al., 2017; Tester and Langridge, 2010). Numerous genes have been identified that have the potential to enhance plant growth and reduce yield losses in saline conditions (Roy et al., 2014). One such gene is the vacuolar proton-pumping pyrophosphatase ( $H^+$ -PPase), which has been used to improve the growth and stress tolerance of many plant species through genetic modification (Gaxiola et al., 2011; Gaxiola et al., 2016a; Gaxiola et al., 2016b; Schilling et al., 2017).

Constitutive expression of  $H^+$ -PPase genes, in particular the Arabidopsis (*Arabidopsis thaliana*) *AVP1* gene, significantly enhanced the growth of transgenic Arabidopsis (Gaxiola et al., 2001), alfalfa (*Medicago sativa*) (Bao et al., 2009), creeping bentgrass (*Agrostis stolonifera*) (Li et al., 2010) and rice (*Oryza sativa*) (Kim et al., 2013; Zhao et al., 2006) in saline conditions. In these studies, the ability of the transgenic plants to maintain growth when exposed to salt stress was attributed to enhanced ion sequestration within the vacuole. Compared to wild-type, *AVP1* over-expressing Arabidopsis contained 20-40 % higher leaf sodium ( $Na^+$ ) and 26-39 % higher leaf potassium ( $K^+$ ) concentrations than the wild-type when exposed to 150 mM NaCl (Gaxiola



et al., 2001). While other studies have also shown constitutive expression of *AVP1* to be beneficial for enhancing growth under saline conditions, this has not always been correlated with increased leaf ion accumulation. Constitutive expression of the Arabidopsis *AVP1* gene (Schilling et al., 2014), and the barley *HVP10* gene (Bovill, unpublished) in barley (*Hordeum vulgare*), as well constitutive expression of the *Salicornia europaea* *SeVP1* and *SeVP2* genes in Arabidopsis (Lv et al., 2015), enhanced growth under saline conditions relative to wild-type, without increasing leaf  $\text{Na}^+$  concentrations. In addition, poplar (*Populus trichocarpa*) constitutively over-expressing the *PtVP1.1* gene, showed improved growth under saline conditions, while leaf  $\text{Na}^+$  concentrations were 20 % lower than wild-type (Yang et al., 2015). While it is clear that constitutive expression of  $\text{H}^+$ -PPase genes improves plant growth under saline conditions, uncertainty remains regarding the role of  $\text{H}^+$ -PPase genes in facilitating vacuolar ion sequestration. Furthermore, the impact of  $\text{H}^+$ -PPase expression on shoot ion-independent tolerance is yet to be investigated.

In addition to improving growth under saline conditions, constitutive expression of  $\text{H}^+$ -PPase genes has also been found to enhance growth under water limitation (Gaxiola et al., 2001; Li et al., 2008; Park et al., 2005; Qin et al., 2013) and low nutrient supply (Lv et al., 2015; Paez-Valencia et al., 2013; Pei et al., 2012; Yang et al., 2007; Yang et al., 2014). The ability of transgenic  $\text{H}^+$ -PPase expressing plants to maintain growth under such conditions has been attributed to several mechanisms, including an improved ability to maintain water content (Gaxiola et al., 2001; Park et al., 2005) and stomatal conductance (Qin et al., 2013), enhanced ion retention (Gaxiola et al., 2001), improved root biomass (Park et al., 2005), increased carbohydrate content (Li et al., 2008; Lv et al., 2009) and enhanced nutrient uptake and

remobilisation (Paez-Valencia et al., 2013; Yang et al., 2007; Yang et al., 2014). Furthermore, several H<sup>+</sup>-PPase expressing lines have displayed enhanced growth compared to wild-type in the absence of stress conditions (Bao et al., 2014; Fan et al., 2017; Gonzalez et al., 2010; Li et al., 2005; Li et al., 2010; Lv et al., 2009; Paez-Valencia et al., 2013; Schilling et al., 2014; Vercruyssen et al., 2011; Wu et al., 2015).

As a result of the many and varied phenotypes of constitutively expressing H<sup>+</sup>-PPase plants, many mechanisms have been proposed regarding the role of H<sup>+</sup>-PPases, including enhancing vacuolar ion sequestration (Gaxiola et al., 2001), facilitating auxin transport (Li et al., 2005), regulating cytosolic pyrophosphate (PP<sub>i</sub>) levels (Ferjani et al., 2011), enhancing the synthesis and source-sink transportation of sucrose (Gaxiola et al., 2012) and promoting ascorbic acid synthesis (Schilling, 2014). Thus, it remains unclear whether the phenotypes of H<sup>+</sup>-PPase expressing transgenic plants are the result of a common function, or are specific to the particular plant species, H<sup>+</sup>-PPase gene, growth stage or experimental conditions. In addition, is it yet to be established whether the function of H<sup>+</sup>-PPases, when constitutively expressed, is representative of native H<sup>+</sup>-PPase function. It is also possible that H<sup>+</sup>-PPases have multiple functions and, therefore, could be involved in promoting seedling vigour during the seedling stage, transportation of nutrients and carbohydrates during the vegetative stage, and ion sequestration when exposed to saline conditions (Schilling et al., 2017). To further investigate this, a comprehensive analysis of H<sup>+</sup>-PPase transgenic plants through time, and under stressed and non-stressed conditions, would provide insight into the function of H<sup>+</sup>-PPases when constitutively expressed.

Despite being investigated in a wide range of plant species, including several cereal crops, little research has addressed the ability of H<sup>+</sup>-PPase genes to improve growth and stress tolerance in bread wheat. While *AVP1* expressing transgenic bread wheat had few phenotypic differences to null segregants under control or saline conditions (Chapter 3), further investigation is warranted due to the promising results of transgenic barley constitutively expressing the *AVP1* and *HVP10* genes (Bovill, unpublished; Schilling et al. 2014), as well as the improved stress tolerance reported in transgenic wheat constitutively expressing the *Salicornia europaea* *SeVP1* and *SeVP2* genes (Lv et al., 2015). The identification of 12 type I *TaVP* genes in bread wheat (Chapter 4), provides an opportunity to further investigate the role of H<sup>+</sup>-PPases in regulating growth under control and saline conditions, and to identify potential functional differences between these *TaVP* proteins. The aim of this study was to generate transgenic bread wheat constitutively over-expressing *TaVP* genes and to characterise the growth of these lines under control and saline conditions, throughout development.

## Materials and methods

### Generation of *TaVP1-B* and *TaVP2-B* transgenic wheat lines

Complete coding sequences (CDS) of the *TaVP1-B* (MH376295) and *TaVP2-B* (MH376298) wheat genes (Chapter 4) were synthesised (GenScript, Piscataway, United States) following the protocol of Ma et al. (2012), and cloned into the *EcoRV* site of the *pUC57* entry vector (Y14837). Genes were digested using *PacI* and *AscI* restriction enzymes and ligated into the multiple cloning site of the *pTOOL37* transformation vector using T4 DNA ligase (ThermoFisher Scientific, Waltham, United States), according to the manufacturer's instructions. The complete transformation vectors contained either the *TaVP1-B* or *TaVP2-B* CDS 3' of the maize (*Zea*

*mays*) *ubiquitin 1* promoter (DQ141598) and 5' of a NOS terminator sequence. Each vector also contained a *kanamycin* (*kan*) resistance gene for bacterial selection and a *hygromycin* (*hyg*) resistance gene for callus selection (Fig. S1). Transformation vectors were transformed into bread wheat (cv. Fielder) callus via *Agrobacterium*-mediated transformation (Ishida et al., 2015). Regenerated seedlings were transferred to a greenhouse in Urrbrae, South Australia (latitude: -34.968086; longitude: 138.636472) and grown until maturity (~ 14 weeks) in 180 mm pots containing University of California (UC) soil mix (1:1 peat:sand) from September to December 2016. Plants were grown under natural light (23 MJ m<sup>-2</sup> average daily solar exposure) with a maximum daily temperature of 25°C, an average minimum temperature of 16°C, and 60-80 % relative humidity. Transgene presence was determined by analysing extracted genomic DNA (gDNA) via polymerase chain reaction (PCR), as detailed below, and transgene copy number analysis via qPCR (Li et al., 2004). T<sub>1</sub> seed obtained from the primary transformants were grown in a growth chamber at The Plant Accelerator® (Urrbrae, South Australia, latitude: -34.971353; longitude: 138.639933) for seed multiplication. T<sub>1</sub> seed were grown in individual pots (150 mm depth and 100 mm diameter with drainage holes) containing UC soil mix. The growth chamber maintained a 12 h day/12 h night light regime with a light intensity of 800 μmol m<sup>-2</sup> s<sup>-1</sup>, 60-80 % relative humidity, and 22°C maximum and 15°C minimum temperatures. T<sub>2</sub> seed obtained from these plants was used for further experimentation.

### **Randomised design for high-throughput phenotyping**

Growth of T<sub>2</sub> transgenic wheat lines was assessed under control (0 mM NaCl) and saline (150 mM NaCl) conditions in the south-east Smarthouse at The Plant Accelerator® (Urrbrae, South Australia, latitude: -34.971353; longitude: 138.639933) between June and July 2017. The

experiment occupied 12 Lanes (5-12) × 14 Positions (15-20) in a split-unit design (Fig. S2). Each treatment consisted of 12 replicate plants from each line, which were assigned to a specific position (cart containing a pot) on the high-throughput phenotyping platform. To randomise the layout, a main-unit design was used, where a plant under control conditions was placed in a cart adjacent to a plant from the same line under saline conditions. Together, each pair of carts formed a Main Position (Mainposn), with each of the 12 lanes containing 7 Mainposns. A 7 × 7 Latin square, combined with a 5 × 7 Youden square, was used to assign the lines to the main units. In this design 5 lines occurred twice in a column, with the remaining 2 occurring only once, such that every line occurred once in only 2 columns. The 2 salt treatments were assigned to the 2 carts within each main unit randomly (Fig. S2). The design was randomized using *dae* (Brien, 2017c), a package for the R statistical computing environment (R Development Core Team, 2017).

### **Plant growth conditions**

Plants were grown under natural light, 22°C maximum and 15°C minimum temperatures, and 60-80 % relative humidity. Uniform size seed (~46 mg) of T<sub>2</sub> wild-type (Fielder WT), transgenic (*TaVP1* OEX Line 1, *TaVP1* OEX Line 2, *TaVP2* OEX Line 1, *TaVP2* OEX Line 2) and null segregant wheat lines (*TaVP1* null line, *TaVP2* null line) were UV sterilised for 5 min, imbibed in 50 mL centrifuge tubes (Greiner Bio-One, Kremsmünster, Austria) containing 50 mL sterile water for 4 h, and germinated in the dark at 4°C for 2 d. Three seed were sown per pot (195 mm depth and 150 mm diameter with drainage holes) at a depth of 1 cm, and thinned to 1 per pot following 1<sup>st</sup> leaf emergence. Each pot contained 2.5 kg GL soil mix (50 % (v/v) UC mix (1:1 peat:sand), 35 % (v/v) coco peat, 15 % (v/v) clay loam). Thirteen days after planting (DAP), pots

were loaded into carts on the automated high-throughput phenotyping system according to the experimental layout described above (Fig. S2). To reduce water loss, blue poly-vinyl chloride evaporation mats (Clark Rubber, Bayswater, Australia) were placed on the surface of each pot. Pots were weighed and watered daily to 17 % (w/w) soil-water content with rainwater (354 mL target water weight). The Scanalyzer 3D imaging station (LemnaTec, Aachen, Germany) was used to obtain daily RGB and steady-state fluorescence images of each plant from two side orientations (0° and 90°) and above.

### **Assessing the salinity tolerance of transgenic *TaVP1* and *TaVP2* wheat lines**

At 3<sup>rd</sup> leaf emergence (19 DAP), 208 mL of either rainwater (control treatment) or 0.25 M NaCl solution (salt treatment) was applied to individual saucers under each pot. Treatments entered the soil via capillary action, increasing the soil-water content to 27 % (w/w). Plants were imaged and weighed daily for 21 d following salt application, with watering resuming for each pot once the soil-water content returned to 17 % (w/w) (approximately 13 d post treatment). The final salt treatment level in each pot was 150 mM NaCl once 17 % (w/w) soil-water content was reached (refer to Additional Material for details regarding method development). Thirty-eight DAP, 3<sup>rd</sup> leaves were collected in liquid nitrogen for genotyping and transgene expression analysis, and 4<sup>th</sup> leaves were collected for ion analysis. All plants were transferred to a greenhouse maintaining the same environmental conditions as the Smarthouse and grown to maturity. Plants were arranged according to the randomised layout used during the high-throughput phenotyping experiment, and the soil-water content was maintained at 17 % (w/w) by watering to weight every 2 d. To monitor growth rates, developmental stages were recorded weekly for each plant according to the Zadok's growth scale (Zadoks et al., 1974). Following

commencement of the booting phase, growth rates were monitored daily until completion of flowering.

### **High-throughput phenotyping data analysis**

Imaging data was prepared using the `imageData` package (Brien, 2017b) for the R statistical computing environment (R Development Core Team, 2017). Relative growth rates (RGR) were calculated from the projected shoot area (PSA) values according to the protocol of Tilbrook *et al.* (2017). Initially, `probeDF` from `imageData` was used to subjectively examine the degree of smoothing achieved for the PSA and the PSA RGR, with different settings of the smoothing parameter `df`. The value of 5 was chosen for this parameter, as it was judged to give the most satisfactory results for both traits. Four plants (3 control and 1 salt treated) were determined to be outliers and removed from further analysis. Osmotic stress tolerance (OST) for each genotype was determined by dividing the RGR of the salt treated plants by that of the control plants in the 5 d following treatment application (19-23 DAP). To produce phenotypic means, a mixed-model analysis was performed for each trait using the R packages `ASReml-R` (Butler, 2009) and `asremlPlus` (Brien, 2017a).

### **Genotyping of transgenic wheat lines**

Genomic DNA (gDNA) was extracted from 3<sup>rd</sup> leaf samples using a modified Edwards (1991) protocol. In brief, cells were lysed by digesting leaf tissue in extraction buffer (100 mM Tris-HCl (pH 7.5), 5 mM EDTA (pH 8.0), 1.25 % SDS) at 65°C for 45 min. gDNA was then precipitated with 6 M ammonium acetate and 100 % (v/v) isopropanol. Pelleted gDNA was washed with 70 % (v/v) ethanol and resuspended in R40 (40 µg/mL RNase A (Sigma-Aldrich, St. Louis, United

States) in 1× TE buffer). Presence of the *TaVP1* and *TaVP2* transgenes were determined via PCR amplification using forward primers specific to the 3' end of each transgene, and a reverse primer specific to the NOS terminator. *TaVP1* specific primers (5'-CGCCATCTCTGCTTCCAACAC-3' and 5'-ATAATCATCGCAAGACCGGCAAC-3') were used with the following thermocycling conditions; 94°C for 2 min, followed by 30 cycles of 94°C for 30 s, 57°C for 30 s and 68°C for 30 s, with a final extension of 5 min at 68°C. *TaVP2* specific primers (5'-GCATCTGAGCACGCAAAGAGC-3' and 5'-ATAATCATCGCAAGACCGGC-3') were used with the following conditions; 94°C for 2 min, followed by 30 cycles of 94°C for 30 s, 58°C for 30 s and 68°C for 30 s, with a final extension of 5 min at 68°C. The wheat glyceraldehyde 3-phosphate dehydrogenase gene, *TaGAPDH* (EF592180.1), was used as a control and amplified using the following forward and reverse primers (5'-TTCAACATCATTCCAAGCAGCA-3' and 5'-CGTAACCCAAAATGCCCTTG-3') and thermocycling conditions as follows; 94°C for 2 min, followed by 30 cycles of 94°C for 30 s, 52°C for 30 s and 68°C for 30 s, with a final extension of 5 min at 68°C. Each PCR contained 1 µg gDNA, 1× OneTaq® 2× Master Mix (20 mM Tris-HCl, 0.2 mM dNTPs, 0.025 U DNA polymerase, 1.8 mM MgCl<sub>2</sub>) (New England Biolabs, Ipswich, United States), 0.2 µM forward primer and 0.2 µM reverse primer, in a final volume of 25 µl. PCR products were visualised under a UV-transilluminator (Clinx, Shanghai, China) on 1.5 % agarose gels containing 0.005 % (v/v) SYBR® Safe DNA stain (Thermo Fisher Scientific, Waltham, United States).

### **Gene expression analysis of transgenic wheat lines**

To analyse transgene expression, total RNA was extracted from 3<sup>rd</sup> leaf samples using a DirectZol RNA purification kit (Zymo Research, Irvine, United States), according to the



manufacturer's instructions. Contaminating gDNA was removed using an in-column DNase treatment (Zymo Research). An AffinityScript cDNA synthesis kit (Agilent Technologies, Santa Clara, United States) was used to transcribe cDNA from standardised RNA samples, following the manufacturer's instructions. Each reaction contained 0.5 µg RNA standardised using a NanoDrop 1000 spectrophotometer (ThermoFisher Scientific), 10 µl 2× first strand master mix, 0.3 µg oligo(dT), 1 µl AffinityScript RT/RNase Block enzyme mixture and sterile water to a final volume of 20 µl. Reactions were incubated at 25°C for 5 min to allow primer annealing, followed by 45 min at 42°C for cDNA synthesis, and 95°C for 5 min to terminate the reaction. *TaVP1*, *TaVP2* and *TaGAPDH* cDNA fragments were amplified via RT-PCR as previously described. *TaVP1* and *TaVP2* transgene expression, relative to *TaGAPDH*, was determined by comparing band intensities of each sample when visualised on a 1.5 % agarose gel using GIMP 2.8.18 Image Manipulation Software ([www.gimp.org](http://www.gimp.org)).

#### **4<sup>th</sup> leaf sodium, potassium and chloride measurements**

After drying at 70°C for 48 h, 4<sup>th</sup> leaf samples were digested in 10 mL of 1 % (v/v) nitric acid in a Hotblock (Environmental Express, Mount Pleasant, United States) for 4 h at 80°C. Na<sup>+</sup> and K<sup>+</sup> concentrations were analysed in the digested leaf solution using a Model 420 flame photometer (Sherwood, Cambridge, United Kingdom) and chloride (Cl<sup>-</sup>) concentrations were measured using a Sherwood Chloride Analyser.

#### **Statistical analysis**

For each trait measured using the high-throughput phenotyping platform, data was spatially adjusted according the experimental design, and a Wald F-test was conducted to determine

interactions between the lines and treatments and, if the interaction was significant, for their main effects. Data obtained from ion analysis, biomass measurements and yield measurements collected by manual phenotyping were analysed in GenStat® version 15.3 (mixed model analysis, LSD,  $P \leq 0.05$ ).

## Results

### Generation of transgenic wheat lines constitutively over-expressing *TaVP* genes

Presence of the *TaGAPDH* gene was confirmed in gDNA extracted from all wild-type and T<sub>2</sub> transgenic wheat lines (Fig. 1A). Presence of the *TaVP1-B* and *TaVP2-B* transgenes were detected within gDNA samples of the appropriate transgenic lines, and were absent in both wild-type and null segregants (Fig. 1A). Expression of *TaGAPDH* was confirmed in all samples, while *TaVP1-B* and *TaVP2-B* transgene expression was detected only within cDNA samples of the transgenic lines, and not in the wild-type or null segregants (Fig. 1B). Semi-quantitative gene expression analysis showed that the *TaVP1* OEX Line 1 had a higher level of *TaVP1-B* transgene expression than the *TaVP1* OEX Line 2, while expression of the *TaVP2-B* transgene was detected at similar levels in both *TaVP2* OEX lines (Fig. 1C).

### *TaVP* OEX wheat lines flower earlier than wild-type and null segregants under control and salt treatments

Under control conditions, the *TaVP1* over-expressing lines flowered 2-8 d earlier than the wild-type and *TaVP1* null segregant plants, while the *TaVP2* over-expressing lines flowered 4-5 d earlier than the wild-type and *TaVP2* null segregants (Fig. 2A). Under 150 mM NaCl treatment, time to flowering in of wild-type and null segregant lines reduced by approximately 5 d,

compared to control conditions, while *TaVP1* and *TaVP2* over-expressing lines flowered 7 d earlier under 150 mM NaCl treatment (Fig. 2A). Salt treated *TaVP1* over-expressing lines flowered 7 d earlier than wild-type, and 5 d earlier than *TaVP1* null segregants (Fig. 2A). *TaVP2* over-expressing lines flowered 3-5 d earlier than the wild-type, and 5-7 d earlier than *TaVP2* null segregants under 150 mM NaCl (Fig. 2A). Under both control and saline conditions, the wild-type and null segregant lines were still in the booting phase when the *TaVP1* and *TaVP2* over-expressing lines commenced flowering (Fig. 2B-E).

#### **Projected shoot area does not differ significantly between *TaVP* OEX lines and wild-type lines under control or salt treatments**

Projected shoot area (PSA) for each line was calculated for each d (13-38 DAP) based on the total number of green pixels within the daily RGB images. When treated with 150 mM NaCl, the PSA of all lines was lower, and showed a greater amount of variation, compared to plants in the control treatment (Figure 3A). Throughout the experiment, *TaVP2* OEX Line 2 had the highest PSA, while *TaVP1* OEX Line 1 and *TaVP2* OEX Line 2 had the lowest PSA, in both control and salt treatments (Fig. 3). On the first day of imaging (13 DAP), the PSA of plants selected for salt treatment were significantly higher than those in the same line selected for the control treatment (Fig. 3B). Following treatment application (18 DAP), the PSA of control and salt treated plants within each line did not significantly differ (Fig. 3C), while at the final imaging point (38 DAP), the PSA of all lines under salt treatment was significantly lower than those in the control treatment (Fig. 3D). Throughout the experiment, *TaVP2* OEX Line 2 had the highest PSA under both treatments, while *TaVP1* OEX Line 1 consistently had the lowest PSA within each treatment.

### ***TaVP* OEX lines have higher RGR than wild-type and null segregants prior to salt treatment**

Throughout the experiment, the RGR of all lines gradually decreased in both control and salt treatments. The RGR of all lines decreased at a faster rate in the salt treated plants than the control plants, following application of the respective treatments (Fig. 4A). Prior to salt application (13-17 DAP), *TaVP1* OEX Line 1 and *TaVP2* OEX Line 2 had significantly higher RGR than all other lines within the control (Fig. 4B). The RGR of wild-type and *TaVP2* OEX Line 2 were significantly higher in control plants than salt treatment plants, while all other lines did not differ between treatments (Fig. 4B). In the period following treatment application (19-25 DAP), the RGR of all lines was significantly higher within the control treatment than the salt treatment, while the RGR did not differ between lines within each treatment (Fig. 4C). Under both control and salt treatment, Fielder wild-type plants had a significantly higher RGR than the *TaVP1* OEX Lines 1 and 2, *TaVP1* Null line and *TaVP2* OEX Line 1 following treatment application (Fig. 4C). The RGR in the final interval (32-38 DAP) was significantly higher in all lines under control treatment compared to those within the salt treatment (Fig. 4D). The *TaVP2* Null line had a significantly higher RGR than all other lines under control and saline conditions, while the RGR of Fielder wild-type was significantly higher than the *TaVP1* OEX Lines 1 and 2 and *TaVP2* OEX Line 1, in both treatments (Fig. 4D).

### **Cumulative water use varies between *TaVP* OEX lines in control and saline conditions**

Following treatment application at 18 DAP, cumulative water use was significantly higher in the control treatment compared to the salt treatment, with the total water use of the control plants approximately 100 mL higher than that of salt treated plants at 38 DAP (Figure 5). Throughout the experiment, *TaVP2* OEX Line 2 tended to have the highest water use under control conditions, and wild-type tended to have the highest water use under salt treatment (Fig. 5A).

The *TaVP2* OEX Line 1 tended to have the lowest water use in both control and salt treatments (Figure 5A). Prior to salt treatment, no significant differences in cumulative water use were apparent between lines or treatments (Figure 5B). Seven days following treatment application, the cumulative water use of salt treated plants was 10-30 % lower than those within the control treatment, although this difference was only statistically significant between the wild-type, *TaVP2* OEX Line 2 and *TaVP2* null lines (Figure 5C). Within the control treatment, water use of the wild-type was significantly higher than all other lines, while no significant differences were apparent between salt treated lines (Figure 5C). At the final time point (38 DAP), the cumulative water use of all lines within the salt treatment was approximately 60 % lower than those within the control treatment (Fig. 5D), however, there were no significant differences between any of the lines in either control or salt treatments (Fig. 5D).

#### ***TaVP* OEX wheat lines have increased leaf Na<sup>+</sup> and Cl<sup>-</sup> concentration under salt treatment**

Under saline conditions, 4<sup>th</sup> leaf Na<sup>+</sup> and Cl<sup>-</sup> concentrations were significantly higher in all lines compared to control conditions, while 4<sup>th</sup> leaf K<sup>+</sup> concentrations were similar between treatments (Fig. 6). Under saline conditions, 4<sup>th</sup> leaf Na<sup>+</sup> concentrations were 72 %, 92 % and 100 % higher in *TaVP1* OEX Line 1, *TaVP1* OEX Line 2 and *TaVP2* OEX Line 2 respectively, compared to wild-type, with the *TaVP2* OEX Line 2 also significantly (74 %) higher than the *TaVP2* Null line (Fig. 6A). Compared to the control treatment, 4<sup>th</sup> leaf Na<sup>+</sup> concentrations in salt treated plants increased 2.4-fold in the wild-type line, 4.2- and 4.1-fold in the *TaVP1* and *TaVP2* OEX lines, and 3.8- and 3.0-fold in the *TaVP1B* and *TaVP2B* null lines (Fig. 6A). Under salt treatment, 4<sup>th</sup> leaf Cl<sup>-</sup> concentrations were 26 % and 23 % higher than the wild type in *TaVP1* OEX Line 2 and *TaVP2* OEX Line 2, respectively (Fig. 6B). In comparison to the control treatment, the 4<sup>th</sup> leaf Cl<sup>-</sup> concentration increased 2.7-fold in the wild-type line, 3.1-fold in the *TaVP1B* OEX

lines, 2.9-fold in the *TaVP2B* OEX lines and 2.8-fold in the *TaVP1B* and *TaVP2B* null lines (Fig. 6B). In both treatments, 4<sup>th</sup> leaf K<sup>+</sup> concentration did not vary significantly between any of the transgenic, wild type or null segregant lines (Fig. 6C). Despite significant differences in both 4<sup>th</sup> leaf Na<sup>+</sup> and Cl<sup>-</sup> concentrations, no significant differences in salt tolerance (Table 2) were observed between the transgenic, wild-type or null segregant lines.

### **Grain yield and shoot biomass are reduced in *TaVP* OEX wheat lines compared to wild-type**

At maturity, all measured growth parameters were significantly different between control and salt treated plants, with the exception of water use efficiency (Table 2). The total number of tillers in all lines was reduced by approximately 50 % under salt treatment compared to control treatment, although there were no significant differences between lines within each treatment (Table 2). Under salt treatment, plant height was reduced by approximately 30 % in all lines compared to the control treatment. Under control conditions, plant height was significantly lower in the *TaVP1* OEX Line 1 (68 cm) compared to the *TaVP1* and *TaVP2* null segregant lines (74 cm) (Table 2). Under control conditions, shoot biomass was 24 % lower than wild-type in both *TaVP1* OEX Line 1 and *TaVP2* OEX Line 2, while no significant differences in shoot biomass were observed under salt treatment (Table 2). In both treatments, the only significant differences in total grain number were in *TaVP1* OEX Line 1 and *TaVP2* OEX Line 1 under control conditions, with grain number reduced by 25 % and 23 % compared to wild-type, respectively. Compared to the control treatment, total seed weight (yield) in all lines was reduced by 70 % under salt treatment (Table 2). While no differences in total seed weight were observed under salt treatment, seed weight under control conditions was 26 % lower in *TaVP1* OEX Line 1 and *TaVP2* OEX Line 1 compared to wild type (Table 2). A difference in 100 grain weight between

control and salt treatment was observed only in *TaVP1* OEX Line 1, with 100 grain weight decreasing by 21 % under salt treatment, significantly lower compared to all other lines, with the exception of *TaVP1* OEX Line 2 and *TaVP2* OEX Line 1 (Table 2). Under salt treatment, harvest index was approximately 11 % lower in the *TaVP* over-expressing lines, 6.5 % lower in the null segregant lines and 9 % lower in the wild-type compared to the control treatment, and did not significantly differ between lines within each treatment (Table 2). Despite differences in both biomass and cumulative water use throughout the experiment (Table 2, Fig. 5, Fig. S3), no statistically significant difference in water use efficiency was observed between any of the lines under control or salt treatments (Table 2).

## Discussion

### Constitutive over-expression of *TaVP* reduces time to flowering

Constitutive over-expression of *TaVP1-B* and *TaVP2-B* significantly reduced time to flowering in the transgenic lines compared to wild-type and null segregants, under both control and salt treatments. Under control and salt treatment, *TaVP1* over-expressing wheat lines, commenced flowering approximately 7 d earlier than the wild-type, while *TaVP2* over-expressing wheat lines commenced flowering 5 d earlier compared to wild-type. The initiation of flowering is a multifaceted process and involves a complex network of signalling pathways, which are influenced by a range of molecular, genetic and environmental cues (Gol et al., 2017). As such, the reduced time to flowering in the *TaVP* over-expressing wheat lines may have been due to several factors, including differences in the expression of flowering related genes, such as vernalisation (*VRN*) and photoperiod (*Ppd*) genes (Shimada et al., 2009), or alterations in hormone, sugar or nutrient concentrations within the plants (Gol et al., 2017).

The only other reported occurrence of early flowering being associated with H<sup>+</sup>-PPase expression was in transgenic *TsVP* expressing maize (Pei et al., 2012). Under low phosphorus supply, the transgenic maize lines commenced flowered 4 d earlier, and began silking 5 d earlier than wild-type, while expression of the auxin transporter genes, *PIN1* and *AUX1*, were upregulated compared to wild-type (Pei et al., 2012). While the initial phenotype implicating the *Arabidopsis* H<sup>+</sup>-PPase, AVP1, in auxin transport (Li et al., 2005) was subsequently shown to be unrelated to AVP1 function (Ferjani et al., 2011; Kriegel et al., 2015), enhanced auxin concentrations and upregulation of auxin transport genes have been reported in many H<sup>+</sup>-PPase expressing transgenic plants (Fan et al., 2017; Gonzalez et al., 2010; Li et al., 2010; Lv et al., 2015; Pei et al., 2012; Yang et al., 2014).

Increased sucrose concentrations and enhanced transport of sucrose from source to sink tissues, are also commonly reported phenotypes in constitutively expressing H<sup>+</sup>-PPase plants (Gaxiola et al., 2012; Khadilkar et al., 2016; Li et al., 2008; Pizzio et al., 2015; Wang et al., 2014; Wu et al., 2015). Enhanced concentrations and transport of sucrose have been linked to ethylene signalling and floral transition (Wang et al., 2016b). Transgenic tomato (*Solanum lycopersicum*) constitutively expressing the pear (*Pyrus bretschneideri*) sucrose transporter gene, *PbSUT2*, had significantly reduced plant biomass, plant height and time to flowering (Wang et al., 2016a), a similar phenotype to that of *TaVP1-B* and *TaVP2-B* over-expressing wheat in this study. Furthermore, *PbSUT2* expressing tomato flowered approximately 11 d earlier than wild-type, with the mature fruit of the transgenic plants containing 25-30 % more sucrose than wild-type (Wang et al., 2016a).

Regulation of the signalling pathways responsible for floral transition and development is known to be influenced by nutrient status, in particular nitrogen and phosphorus (Gol et al.,



2017). With the uptake and transport of sucrose (Li et al., 2008; Pizzio et al., 2015; Wang et al., 2014; Wu et al., 2015), auxin (Fan et al., 2017; Gonzalez et al., 2010; Li et al., 2010; Pei et al., 2012; Yang et al., 2014), nitrogen (Lv et al., 2015; Paez-Valencia et al., 2013) and phosphorus (Pei et al., 2012; Yang et al., 2007; Yang et al., 2014) commonly enhanced in H<sup>+</sup>-PPase expressing plants compared to wild-type, it is possible that one or more of these factors are responsible for the early flowering observed in the *TaVP* over-expressing wheat lines.

However, it is also possible that the early flowering phenotype observed in the *TaVP* over-expressing transgenic wheat lines is a pleiotropic effect of *TaVP* over-expression. For instance, constitutive expression of the DREB transcription factor in bread wheat reduced plant height by 15 %, reduced tiller number by 30 %, and delayed flowering time by 2-3 weeks compared to wild-type (Morran et al., 2011). In addition, with a large range of genes involved in the initiation of flowering (Shimada et al., 2009), it is also possible that insertion of the *TaVP* transgene either disrupted or altered expression of a flowering related gene. As such, it cannot be ruled out that the early flowering phenotype in these lines may be the result of factors other than *TaVP* transgene function, and further research is required to investigate this possibility.

#### **Increased leaf Na<sup>+</sup> accumulation does not alter salinity tolerance in *TaVP* transgenic wheat**

With the exception of *TaVP2-B* OEX Line 1, Na<sup>+</sup> concentrations within the 4<sup>th</sup> leaf of the *TaVP* transgenic wheat lines increased 2-fold under salt treatment, compared to wild-type. Despite accumulating significantly higher concentrations of leaf Na<sup>+</sup>, growth and salt tolerance in the transgenic lines was not altered compared to wild-type. Ion accumulation within H<sup>+</sup>-PPase expressing transgenic plants varies considerably between studies, with improved salt tolerance reported in H<sup>+</sup>-PPase expressing transgenic lines in which leaf ion concentrations are increased,

unaltered, and reduced compared to control plants (Schilling et al., 2017). In transgenic plants in which ion accumulation was enhanced, it remains unknown whether these plants have improved vacuolar ion sequestration, or if the ions are accumulating within the cytosol. With the exception of the Zhao et al. (2006) study, the cell type in which ion accumulation occurs is rarely measured. As ion sequestration within the vacuole is dependent on the action of  $\text{Na}^+/\text{H}^+$  transporters, it is possible that  $\text{Na}^+$  within the *TaVP* wheat lines accumulated within the cytosol, rather than the vacuole, which would have had a negative impact on plant growth (Carden et al., 2003; Munns and Tester, 2008). With  $\text{Na}^+$  accumulating to significantly higher levels in most of the *TaVP* transgenic wheat lines, further investigation is required to determine where this  $\text{Na}^+$  is accumulating within the leaf and how this impacts on the growth and salt tolerance of these lines. It may be that co-expression with a  $\text{Na}^+/\text{H}^+$  transporter, such as *TaNHX1* (Wang et al., 2002), is required to enhance vacuole ion sequestration and, therefore, salt tolerance in the *TaVP* transgenic wheat lines.

### **The impact of *TaVP* over-expression on the growth rate of transgenic wheat remains unclear**

Due to the variation in PSA between plants selected for control and salt treatment within each line, differences in the initial growth rate of the *TaVP* OEX lines compared to wild-type could not be assessed. It remains unclear as to whether these differences had a further impact on the experiment. While the relative growth rate of *TaVP1* OEX Line 1 seedlings were significantly higher than the other lines at the beginning of the experiment, the initial PSA of these plants was smaller than the other lines. As such, the faster initial growth rate of this line was likely due to differences in initial biomass. Seedling vigour in the *TaVP* over-expressing wheat lines was also investigated using a mini-hydroponics system to monitor seedling growth in the first 12 d

of growth (refer to Additional Material). However, no significant differences were observed between the *TaVP* transgenic lines and null segregants in regard to seedling biomass (Table A1), root length (Table A2) or leaf length (Table A3). Based on these results, it is likely that seedling growth is not enhanced in the *TaVP* transgenic wheat lines compared to wild-type or null segregants, and that the differences in biomass are likely due to the early flowering phenotype of the transgenic lines, which reduced the length of the vegetative growth phase.

### **Over-expressing *TaVP* wheat lines require characterisation in the field**

While plant growth and yield was reduced in the *TaVP* transgenic wheat lines, field characterisation is required to further investigate the performance of these lines, as growth and yield in the greenhouse is not necessarily representative of growth in the field. Early flowering can be a desirable trait for farmers, as it reduces the risk of yield losses due to drought and heat stress, which commonly occur during the reproductive phase (Zheng et al., 2012) and can reduce input costs due to the reduction of the vegetative growth phase (An-Vo et al., 2018). However, the impact of early flowering on grain yield and quality in the *TaVP* OEX wheat lines requires further investigation in the field, as reduced yield would be an unfavourable trait. Furthermore, the impact of *TaVP* over-expression on grain quality should also be assessed, as expression of a H<sup>+</sup>-PPase gene in rice has been associated with reduced grain quality (Li et al., 2014). While expression of the *TaVP* transgenes was confirmed in the transgenic lines, the impact of *TaVP* over-expression on native *TaVP* gene expression was not analysed and should be further investigated to ensure that constitutive *TaVP* expression does not reduce native *TaVP* gene expression. In addition, the possibility of the *TaVP* transgenes being downregulated via native *TaVP* regulators should also be further investigated.

## Conclusions

Constitutive over-expression of the *TaVP1-B* and *TaVP2-B* genes produced an early flowering phenotype in bread wheat under control and saline conditions. Under saline conditions, *TaVP1-B* and *TaVP2-B* transgenic wheat lines accumulated significantly higher concentrations of Na<sup>+</sup> within the 4<sup>th</sup> leaf compared to wild-type and null segregants. However, increased leaf Na<sup>+</sup> concentrations, did not alter salt tolerance in the *TaVP* over-expressing wheat lines compared to wild-type and null segregants. Furthermore, constitutive over-expression of *TaVP* did not have a beneficial impact on biomass under control or saline conditions. Further investigation is required to determine whether constitutive over-expression of *TaVP1-B* and *TaVP2-B*, or other wheat *TaVP* genes, are able to produce a beneficial phenotype in the field or under other abiotic stress conditions.

## Supplementary data

**Fig. S1:** Transformation vectors used to generate transgenic bread wheat (cv. Fielder) constitutively over-expressing the *TaVP1-B* and *TaVP2-B* genes.

**Fig. S2:** Greenhouse layout of wild-type, *TaVP* transgenic and null segregant wheat lines.

**Fig. S3:** Cumulative water use of wild-type, *TaVP* transgenic and null segregant wheat lines under control (0 mM NaCl) and saline (150 mM NaCl) conditions 13-116 DAP.

**Fig. S4:** Osmotic stress tolerance (OST) of wild-type, *TaVP* transgenic and null segregant wheat lines in the first 5 d following salt treatment.

## Acknowledgements

The authors wish to thank the University of Adelaide Wheat Transformation group for performing wheat transformations, Ms. Jodie Kretschmer, Ms. Melissa Pickering and Mr. William Heaslip for technical assistance and Ms. Lidia Mischis, Ms. Nicole Bond, Ms. Fiona Groskreutz, Ms. Chana Borjigin and Mr. Nicholas Sitlington Hansen for assistance with the high-throughput phenotyping experiment. This research was funded by the Grains Research and Development Corporation (UA00145), and the International Wheat Yield Partnership and Grains Research and Development Corporation (IWYP39/ACP0009). Daniel Menadue is the recipient of a Grains Research and Development Corporation Grains Industry Research Scholarship (GRS10931) and a Postgraduate Internship Award from the Australian Plant Phenomics Facility. The Plant Accelerator®, Australian Plant Phenomics Facility, is funded by the National Collaborative Research Infrastructure Strategy of the Commonwealth of Australia. The authors declare no conflict of interest.

## References

- Alexandratos N and Bruinsma J 2012. World agriculture towards 2030/2050: The 2012 revision. Rome, FAO.
- An-Vo D-A, Mushtaq S, Zheng B *et al.* 2018. Direct and indirect costs of frost in the Australian wheatbelt. *Ecological Economics* **150**, 122-136.
- Australian Bureau of Statistics 2017. Agricultural Commodities, Australia, 2015-16.
- Bao AK, Wang SM, Wu GQ *et al.* 2009. Overexpression of the *Arabidopsis* H<sup>+</sup>-PPase enhanced resistance to salt and drought stress in transgenic alfalfa (*Medicago sativa* L.). *Plant Science* **176**, 232-240.
- Bao AK, Wang YW, Xi JJ *et al.* 2014. Co-expression of xerophyte *Zygophyllum xanthoxylum* ZxNHX and ZxVP1-1 enhances salt and drought tolerance in transgenic *Lotus corniculatus* by increasing cations accumulation. *Functional Plant Biology* **41**, 203-214.
- Brien CJ. 2017a. asremlPlus: Augments the use of ASReml-R in fitting mixed models. The Comprehensive R Archive Network.
- Brien CJ. 2017b. imageData: aids in processing and plotting data from a Lemna-Tec Scanalyzer. The Comprehensive R Archive Network.
- Brien CJ. 2017c. dae: Functions useful in the design and ANOVA of experiments. The Comprehensive R Archive Network.
- Butler D, Cullis, BR, Gilmour, AR, and Gogel, BJ. 2009. Analysis of mixed models for S language environments: ASReml-R reference manual. Brisbane, DPI Publications.
- Carden DE, Walker DJ, Flowers TJ *et al.* 2003. Single-cell measurements of the contributions of cytosolic Na<sup>+</sup> and K<sup>+</sup> to salt tolerance. *Plant Physiology* **131**, 676-683.
- Edwards K, Johnstone C and Thompson C. 1991. A simple and rapid method for the preparation of plant genomic DNA for PCR analysis. *Nucleic Acids Research* **19**, 1349.
- Fan W, Wang H, Wu Y *et al.* 2017. H<sup>+</sup>-pyrophosphatase *IbVP1* promotes efficient iron use in sweet potato [*Ipomoea batatas* (L.) Lam.]. *Plant Biotechnology Journal* **15**, 698-712.
- Ferjani A, Segami S, Horiguchi G *et al.* 2011. Keep an eye on PPi: The vacuolar-type H<sup>+</sup>-pyrophosphatase regulates postgerminative development in *Arabidopsis*. *Plant Cell* **23**, 2895-2908.
- Gaxiola RA, Li J, Undurraga S *et al.* 2001. Drought- and salt-tolerant plants result from overexpression of the *AVP1* H<sup>+</sup>-pump. *Proceedings of the National Academy of Sciences* **98**, 11444-11449.
- Gaxiola RA, Edwards M and Elser JJ. 2011. A transgenic approach to enhance phosphorus use efficiency in crops as part of a comprehensive strategy for sustainable agriculture. *Chemosphere* **84**, 840-845.
- Gaxiola RA, Sanchez CA, Paez-Valencia J *et al.* 2012. Genetic manipulation of a “vacuolar” H<sup>+</sup>-PPase: From salt tolerance to yield enhancement under phosphorus-deficient soils. *Plant Physiology* **159**, 3-11.
- Gaxiola RA, Regmi K and Hirschi KD. 2016a. Moving on up: H<sup>+</sup>-PPase mediated crop improvement. *Trends in Biotechnology* **34**, 347-349.
- Gaxiola RA, Regmi KC, Paez-Valencia J *et al.* 2016b. Plant H<sup>+</sup>-PPases: Reversible enzymes with contrasting functions dependent on membrane environment. *Molecular Plant* **9**, 317-319.
- Gilliham M, Able JA and Roy SJ. 2017. Translating knowledge about abiotic stress tolerance to breeding programmes. *The Plant Journal* **90**, 898-917.

- Gol L, Tomé F and von Korff M.** 2017. Floral transitions in wheat and barley: Interactions between photoperiod, abiotic stresses, and nutrient status. *Journal of Experimental Botany* **68**, 1399-1410.
- Gonzalez N, De Bodt S, Sulpice R et al.** 2010. Increased leaf size: Different means to an end. *Plant Physiology* **153**, 1261-1279.
- Ishida Y, Tsunashima M, Hiei Y et al.** 2015. Wheat (*Triticum aestivum* L.) transformation using immature embryos. In *Agrobacterium Protocols: Volume 1*, 10.1007/978-1-4939-1695-5\_15 (ed. K. Wang), pp. 189-198. New York, NY: Springer New York.
- Khadilkar AS, Yadav UP, Salazar C et al.** 2016. Constitutive and companion cell-specific overexpression of *AVP1*, encoding a proton-pumping pyrophosphatase, enhances biomass accumulation, phloem loading, and long-distance transport. *Plant Physiology* **170**, 401-414.
- Kim YS, Kim IS, Choe YH et al.** 2013. Overexpression of the *Arabidopsis* vacuolar H<sup>+</sup>-pyrophosphatase *AVP1* gene in rice plants improves grain yield under paddy field conditions. *The Journal of Agricultural Science* **152**, 941-953.
- Kriegel A, Andrés Z, Medzihradzky A et al.** 2015. Job sharing in the endomembrane system: Vacuolar acidification requires the combined activity of V-ATPase and V-PPase. *The Plant Cell* **27**, 3383-3396.
- Li B, Wei A, Song C et al.** 2008. Heterologous expression of the *TsVP* gene improves the drought resistance of maize. *Plant Biotechnology Journal* **6**, 146-159.
- Li J, Yang H, Ann Peer W et al.** 2005. *Arabidopsis* H<sup>+</sup>-PPase *AVP1* regulates auxin-mediated organ development. *Science* **310**, 121-125.
- Li Y, Fan C, Xing Y et al.** 2014. *Chalk5* encodes a vacuolar H<sup>+</sup>-translocating pyrophosphatase influencing grain chalkiness in rice. *Nature Genetics* **46**, <https://doi.org/10.1038/ng.2923>.
- Li Z, Hansen JL, Liu Y et al.** 2004. Using real-time PCR to determine transgene copy number in wheat. *Plant Molecular Biology Reporter* **22**, 179-188.
- Li Z, Baldwin CM, Hu Q et al.** 2010. Heterologous expression of *Arabidopsis* H<sup>+</sup>-pyrophosphatase enhances salt tolerance in transgenic creeping bentgrass (*Agrostis stolonifera* L.). *Plant, Cell & Environment* **33**, 272-289.
- Lv S, Jiang P, Nie L et al.** 2015. H<sup>+</sup>-pyrophosphatase from *Salicornia europaea* confers tolerance to simultaneously occurring salt stress and nitrogen deficiency in *Arabidopsis* and wheat. *Plant, Cell & Environment* **38**, 2433-2449.
- Lv SL, Lian LJ, Tao PL et al.** 2009. Overexpression of *Thellungiella halophila* H<sup>+</sup>-PPase (*TsVP*) in cotton enhances drought stress resistance of plants. *Planta* **229**, 899-910.
- Ma S, Tang N and Tian J.** 2012. DNA synthesis, assembly and applications in synthetic biology. *Current Opinion in Chemical Biology* **16**, 260-267.
- Morran S, Eini O, Pyvovarenko T et al.** 2011. Improvement of stress tolerance of wheat and barley by modulation of expression of DREB/CBF factors. *Plant Biotechnology Journal* **9**, 230-249.
- Munns R and Tester M.** 2008. Mechanisms of salinity tolerance. *Annual Review of Plant Biology* **59**, 651-681.
- Paez-Valencia J, Sanchez-Lares J, Marsh E et al.** 2013. Enhanced proton translocating pyrophosphatase activity improves nitrogen use efficiency in romaine lettuce. *Plant Physiology* **161**, 1557-1569.
- Park S, Li J, Pittman JK et al.** 2005. Up-regulation of a H<sup>+</sup>-pyrophosphatase (*H<sup>+</sup>-PPase*) as a strategy to engineer drought-resistant crop plants. *Proceedings of the National Academy of Sciences* **102**, 18830-18835.

- Pei L, Wang J, Li K *et al.* 2012. Overexpression of *Thellungiella halophila* H<sup>+</sup>-pyrophosphatase gene improves low phosphate tolerance in maize. PLoS ONE 7, <https://doi.org/10.1371/journal.pone.0043501>.
- Pizzio GA, Paez-Valencia J, Khadilkar AS *et al.* 2015. *Arabidopsis* type I proton-pumping pyrophosphatase expresses strongly in phloem, where it is required for pyrophosphate metabolism and photosynthate partitioning. Plant Physiology 167, 1541-1553.
- Qin H, Gu Q, Kuppu S *et al.* 2013. Expression of the *Arabidopsis* vacuolar H<sup>+</sup>-pyrophosphatase gene *AVP1* in peanut to improve drought and salt tolerance. Plant Biotechnology Reports 7, 345-355.
- R Development Core Team. 2017. R: A language and environment for statistical computing. Vienna, Austria, R Foundation for Statistical Computing.
- Rengasamy P. 2010. Soil processes affecting crop production in salt-affected soils. Functional Plant Biology 37, 613-620.
- Roy SJ, Negrão S and Tester M. 2014. Salt resistant crop plants. Current Opinion in Biotechnology 26, 115-124.
- Schilling RK. 2014. "Evaluating the abiotic stress tolerance of transgenic barley expressing an *Arabidopsis* vacuolar H<sup>+</sup>-pyrophosphatase gene (*AVP1*)". PhD thesis. Adelaide, Australia. The University of Adelaide.
- Schilling RK, Marschner P, Shavrukov Y *et al.* 2014. Expression of the *Arabidopsis* vacuolar H<sup>+</sup>-pyrophosphatase gene (*AVP1*) improves the shoot biomass of transgenic barley and increases grain yield in a saline field. Plant Biotechnology Journal 12, 378-386.
- Schilling RK, Tester M, Marschner P *et al.* 2017. *AVP1*: One protein, many roles. Trends in Plant Science 22, 154-162.
- Shimada S, Ogawa T, Kitagawa S *et al.* 2009. A genetic network of flowering-time genes in wheat leaves, in which an *APETALA1/FRUITFULL*-like gene, *VRN1*, is upstream of *FLOWERING LOCUS T*. The Plant Journal 58, 668-681.
- Tester M and Langridge P. 2010. Breeding technologies to increase crop production in a changing world. Science 327, 818-22.
- Tilbrook J, Schilling RK, Berger B *et al.* 2017. Variation in shoot tolerance mechanisms not related to ion toxicity in barley. Functional Plant Biology 44, 1194-1206.
- Vercruyssen L, Gonzalez N, Werner T *et al.* 2011. Combining enhanced root and shoot growth reveals cross talk between pathways that control plant organ size in *Arabidopsis*. Plant Physiology 155, 1339-1352.
- Wang JW, Wang HQ, Xiang WW *et al.* 2014. A *Medicago truncatula* H<sup>+</sup>-pyrophosphatase gene, *MtVP1*, improves sucrose accumulation and anthocyanin biosynthesis in potato (*Solanum tuberosum* L.). Genetics and Molecular Research 13, 3615-26.
- Wang LF, Qi XX, Huang XS *et al.* 2016a. Overexpression of sucrose transporter gene *PbSUT2* from *Pyrus bretschneideri*, enhances sucrose content in *Solanum lycopersicum* fruit. Plant Physiology and Biochemistry 105, 150-161.
- Wang X, Wang H, Liu S *et al.* 2016b. Genetic variation in *ZmVPP1* contributes to drought tolerance in maize seedlings. Nature Genetics 48, 1233-41.
- Wang ZN, Zhang JS, Guo BH *et al.* 2002. Cloning and characterization of the Na<sup>+</sup>/H<sup>+</sup> Antiport Genes from *Triticum aestivum*. Acta Botanica Sinica 44, 1203-1208.
- Wu GQ, Feng RJ, Wang SM *et al.* 2015. Co-expression of xerophyte *Zygophyllum xanthoxylum* *ZxNHX* and *ZxVP1-1* confers enhanced salinity tolerance in chimeric sugar beet (*Beta vulgaris* L.). Frontiers in Plant Science 6, <https://doi.org/10.3389/fpls.2015.00581>.



- Yang H, Knapp J, Koirala P et al.** 2007. Enhanced phosphorus nutrition in monocots and dicots over-expressing a phosphorus-responsive type I H<sup>+</sup>-pyrophosphatase. *Plant Biotechnology Journal* **5**, 735-745.
- Yang H, Zhang X, Gaxiola RA et al.** 2014. Over-expression of the *Arabidopsis* proton-pyrophosphatase *AVP1* enhances transplant survival, root mass, and fruit development under limiting phosphorus conditions. *Journal of Experimental Botany* **65**, 3045-3053.
- Yang Y, Tang RJ, Li B et al.** 2015. Overexpression of a *Populus trichocarpa* H<sup>+</sup>-pyrophosphatase gene *PtVP1.1* confers salt tolerance on transgenic poplar. *Tree Physiology* **35**, 663-77.
- Zadoks JC, Chang TT and Konzak CF.** 1974. A decimal code for the growth stages of cereals. *Weed Research* **14**, 415-421.
- Zhao FY, Zhang XJ, Li PH et al.** 2006. Co-expression of the *Suaeda salsa* *SsNHX1* and *Arabidopsis* *AVP1* confer greater salt tolerance to transgenic rice than the single *SsNHX1*. *Molecular Breeding* **17**, 341-353.
- Zheng B, Chenu K, Fernanda Dreccer M et al.** 2012. Breeding for the future: What are the potential impacts of future frost and heat events on sowing and flowering time requirements for Australian bread wheat (*Triticum aestivum*) varieties? *Global Change Biology* **18**, 2899-2914.

## Tables

**Table 1: Phenotypic characteristics of wild-type, *TaVP* over-expressing and null segregant wheat lines at maturity.** Tiller number, plant height (cm), aboveground biomass (g DW), total grain number, yield (total seed weight (g) per plant), 100 grain weight (g), harvest index (total grain weight (g)/aboveground biomass (g DW)), plant water use (total water use (g)/aboveground biomass (g DW)) and salt tolerance (salt yield (g)/control yield (g)) of Fielder wild-type (WT), *TaVP1* OEX Lines 1 and 2, *TaVP1* Null Line, *TaVP2* OEX Lines 1 and 2 and *TaVP2* Null Line plants in control (0 mM NaCl) and saline (150 mM NaCl) conditions. Values are means ± standard error of the mean (n=9-12). Different letters indicate statistically significant differences between lines and treatments for each parameter (mixed model analysis, LSD,  $P \leq 0.05$ ).

Line	NaCl (mM)	Tiller number	Plant height (cm)	Biomass (g DW)	Total grain (number/plant)	Yield (g/plant)	100 grain weight (g)	Harvest index (yield/biomass)	Water use (total g water/g final biomass)	Salt tolerance (salt yield/control yield)
Fielder WT	0	8.3 ± 0.5 <sup>b</sup>	73 ± 1.1 <sup>bc</sup>	21 ± 0.8 <sup>c</sup>	243 ± 15 <sup>c</sup>	10.2 ± 0.5 <sup>c</sup>	4.3 ± 0.1 <sup>abc</sup>	0.48 ± 0.01 <sup>b</sup>	165 ± 2 <sup>a</sup>	0.32 ± 0.027 <sup>a</sup>
	150	4.0 ± 0.3 <sup>a</sup>	56 ± 1.1 <sup>a</sup>	7.2 ± 0.3 <sup>a</sup>	80 ± 3 <sup>a</sup>	3.2 ± 0.1 <sup>a</sup>	4.0 ± 0.1 <sup>bc</sup>	0.44 ± 0.01 <sup>a</sup>	177 ± 5 <sup>a</sup>	
<i>TaVP1</i> OEX Line 1	0	7.1 ± 0.5 <sup>b</sup>	68 ± 0.6 <sup>b</sup>	16 ± 0.8 <sup>b</sup>	183 ± 7 <sup>b</sup>	7.6 ± 0.4 <sup>b</sup>	4.3 ± 0.1 <sup>bc</sup>	0.48 ± 0.04 <sup>b</sup>	186 ± 12 <sup>a</sup>	0.29 ± 0.021 <sup>a</sup>
	150	3.4 ± 0.2 <sup>a</sup>	55 ± 1.2 <sup>a</sup>	5.4 ± 0.2 <sup>a</sup>	65 ± 4 <sup>a</sup>	2.2 ± 0.1 <sup>a</sup>	3.4 ± 0.1 <sup>a</sup>	0.41 ± 0.02 <sup>a</sup>	199 ± 5 <sup>a</sup>	
<i>TaVP1</i> OEX Line 2	0	7.6 ± 0.6 <sup>b</sup>	72 ± 1.4 <sup>bc</sup>	19 ± 1.3 <sup>bc</sup>	222 ± 12 <sup>bc</sup>	9.6 ± 0.5 <sup>bc</sup>	4.3 ± 0.1 <sup>abc</sup>	0.51 ± 0.03 <sup>b</sup>	169 ± 14 <sup>a</sup>	0.27 ± 0.028 <sup>a</sup>
	150	3.4 ± 0.2 <sup>a</sup>	52 ± 2.2 <sup>a</sup>	5.5 ± 0.5 <sup>a</sup>	67 ± 6 <sup>a</sup>	2.5 ± 0.2 <sup>a</sup>	3.7 ± 0.2 <sup>ab</sup>	0.44 ± 0.02 <sup>a</sup>	207 ± 9 <sup>a</sup>	
<i>TaVP1</i> Null Line	0	8.3 ± 0.3 <sup>b</sup>	74 ± 0.6 <sup>c</sup>	20 ± 0.7 <sup>bc</sup>	206 ± 12 <sup>bc</sup>	8.9 ± 0.5 <sup>bc</sup>	4.3 ± 0.1 <sup>c</sup>	0.45 ± 0.01 <sup>b</sup>	170 ± 3 <sup>a</sup>	0.30 ± 0.020 <sup>a</sup>
	150	3.3 ± 0.3 <sup>a</sup>	56 ± 1.4 <sup>a</sup>	6.5 ± 0.5 <sup>a</sup>	68 ± 5 <sup>a</sup>	2.7 ± 0.2 <sup>a</sup>	3.9 ± 0.1 <sup>bc</sup>	0.41 ± 0.02 <sup>a</sup>	186 ± 12 <sup>a</sup>	
<i>TaVP2</i> OEX Line 1	0	6.8 ± 0.7 <sup>b</sup>	71 ± 0.7 <sup>bc</sup>	16 ± 1.4 <sup>b</sup>	187 ± 11 <sup>b</sup>	7.6 ± 0.6 <sup>b</sup>	4.5 ± 0.1 <sup>c</sup>	0.47 ± 0.02 <sup>b</sup>	189 ± 19 <sup>a</sup>	0.31 ± 0.022 <sup>a</sup>
	150	3.1 ± 0.3 <sup>a</sup>	55 ± 1.2 <sup>a</sup>	5.4 ± 0.5 <sup>a</sup>	61 ± 6 <sup>a</sup>	2.4 ± 0.2 <sup>a</sup>	4.1 ± 0.1 <sup>abc</sup>	0.46 ± 0.03 <sup>a</sup>	208 ± 10 <sup>a</sup>	
<i>TaVP2</i> OEX Line 2	0	7.8 ± 0.5 <sup>b</sup>	72 ± 1.1 <sup>bc</sup>	19 ± 0.7 <sup>bc</sup>	216 ± 13 <sup>bc</sup>	9.6 ± 0.5 <sup>bc</sup>	4.4 ± 0.1 <sup>c</sup>	0.50 ± 0.01 <sup>b</sup>	171 ± 12 <sup>a</sup>	0.32 ± 0.023 <sup>a</sup>
	150	3.3 ± 0.3 <sup>a</sup>	54 ± 0.7 <sup>a</sup>	6.5 ± 0.3 <sup>a</sup>	70 ± 4 <sup>a</sup>	3.0 ± 0.1 <sup>a</sup>	4.1 ± 0.1 <sup>bc</sup>	0.44 ± 0.01 <sup>a</sup>	186 ± 11 <sup>a</sup>	
<i>TaVP2</i> Null Line	0	8.1 ± 0.5 <sup>b</sup>	74 ± 1.0 <sup>c</sup>	20 ± 1.0 <sup>bc</sup>	220 ± 13 <sup>bc</sup>	9.6 ± 0.6 <sup>bc</sup>	4.3 ± 0.1 <sup>bc</sup>	0.48 ± 0.01 <sup>b</sup>	172 ± 2 <sup>a</sup>	0.32 ± 0.019 <sup>a</sup>
	150	3.3 ± 0.3 <sup>a</sup>	58 ± 0.9 <sup>a</sup>	6.6 ± 0.4 <sup>a</sup>	73 ± 3 <sup>a</sup>	2.9 ± 0.1 <sup>a</sup>	4.1 ± 0.1 <sup>bc</sup>	0.46 ± 0.01 <sup>a</sup>	185 ± 7 <sup>a</sup>	

## Figure legends

### **Fig. 1: Molecular characterisation of wild-type, *TaVP* transgenic and null segregant wheat lines.**

(A) PCR amplification of *TaGAPDH*, *TaVP1* and *TaVP2* gene fragments in gDNA samples and (B) expression of these genes in cDNA samples of Fielder wild-type, *TaVP* over-expressing (*TaVP1* OEX line 1, *TaVP1* OEX line 2, *TaVP2* OEX line 1, *TaVP2* OEX line 2) and null segregant (*TaVP1* null line, *TaVP2* null line) wheat lines. Water (-) was used as a negative control. (C) Semi-quantitative expression analysis of the *TaVP1* and *TaVP2* transgenes in cDNA samples of wild-type and transgenic lines. Transgene expression is relative to that of the constitutively expressed *TaGAPDH* gene. Error bars represent standard error of the mean of 3 biological replicates.

### **Fig. 2: Days to flowering and visual phenotype of wild-type, *TaVP* transgenic and null segregant wheat lines.**

(A) Average number of days until the initiation of flowering (Z60) of wild-type (Fielder WT), *TaVP1* OEX Lines 1 and 2, *TaVP1* Null Line, *TaVP2* OEX Lines 1 and 2 and *TaVP2* Null Line plants in control (0 mM NaCl) and saline (150 mM NaCl) conditions. Values are means (n=9-12) with error bars representing standard error of the mean. Different letters indicate statistically significant differences (mixed model analysis, LSD,  $P \leq 0.05$ ). Images of wild-type with *TaVP1* transgenic (B,D) and *TaVP2* transgenic (C,E) plants under 0 mM NaCl (B-C) and 150 mM NaCl (D-E) treatments. Images of control plants were taken 63 DAP and those of salt treated plants were taken 57 DAP. Each image contains a single representative plant from each line. Scale = 10 cm.

**Fig 3: Smoothed projected shoot area of wild-type, *TaVP* transgenic and null segregant wheat lines 13, 19 and 38 DAP.** Smoothed projected shoot area (sPSA) of wild-type (Fielder WT) and *TaVP* transgenic wheat lines under control (0 mM NaCl) and salt (150 mM NaCl) treatment. sPSA values (A) throughout the entire high-throughput phenotyping experiment (13-38 DAP), (B) from the first day of imaging (13 DAP), (C) the day following control and salt treatment application (19 DAP), and (D) the final day of imaging (38 DAP). Dotted grey lines indicate the time intervals selected for analysis (13-17, 19-25, 25-32 and 32-38 DAP) and dotted red lines indicate day of treatment application (18 DAP). Values are the adjusted mean kilo-pixels (kpixels) of each line within each treatment (n=9-12). Different letters indicate statistically significant differences (mixed model analysis, Wald's F test, LSD,  $P \leq 0.05$ ) and error bars indicate population variance ( $0.5 \times \text{LSD}$ ).

**Fig. 4: Relative growth rates of wild-type, *TaVP* transgenic and null segregant wheat lines 13-17, 19-25 and 32-38 DAP.** Relative growth rates (RGR) of wild-type (Fielder WT) and *TaVP* transgenic wheat lines under control (0 mM NaCl) and salt (150 mM NaCl) treatment. RGR were calculated by comparing sPSA from each day to that of the day before. RGR (A) across the entire high-throughput phenotyping experiment (13-38 DAP), (B) prior to treatment application (13-17 DAP), (C) following treatment application (19-25 DAP), and (D) during the final week of imaging (32-38 DAP). Dotted grey lines indicate the time intervals selected for analysis (13-17, 19-25, 25-32 and 32-38 DAP) and dotted red lines indicate day of treatment application (18 DAP). Values are the adjusted mean kilo-pixels (kpixels) of each line within each treatment (n=9-12), relative to the previous day. Different letters indicate statistically significant differences (mixed

model analysis, Wald's F test, LSD,  $P \leq 0.05$ ) and error bars indicate population variance ( $0.5 \times$  LSD).

**Fig. 5: Cumulative water use of wild-type, *TaVP* transgenic and null segregant wheat lines 17, 25 and 38 DAP.** Cumulative water use (g) of wild-type (Fielder WT) and *TaVP* transgenic wheat lines under control (0 mM NaCl) and salt (150 mM NaCl) treatment. Cumulative water use (A) throughout entire high-throughput phenotyping experiment (13-38 DAP), (B) prior to treatment application (17 DAP), (C) 7 d after application of control and salt treatments (25 DAP) and (D) on the final day of imaging (38 DAP) are shown. Dotted grey lines indicate the time intervals selected for analysis (13-17, 19-25, 25-32 and 32-38 DAP) and dotted red lines indicate day of treatment application (18 DAP). Values are means of each line within each treatment (n=9-12), with different letters indicating statistically significant differences (mixed model analysis, LSD,  $P \leq 0.05$ ). Error bars represent standard error of the mean.

**Fig. 6:  $\text{Na}^+$ ,  $\text{Cl}^-$  and  $\text{K}^+$  concentrations of wild-type, *TaVP* transgenic and null segregant wheat lines in 4<sup>th</sup> leaf samples collected at 38 DAP.** (A)  $\text{Na}^+$ , (B)  $\text{Cl}^-$  and (C)  $\text{K}^+$  concentrations ( $\mu\text{mole per g DW}$ ) in 4<sup>th</sup> leaf samples collected from wild-type (Fielder WT) and *TaVP* transgenic wheat lines (*TaVP1* OEX Line 1, *TaVP1* OEX Line 2, *TaVP1* null segregant line, *TaVP2* OEX Line 1, *TaVP2* OEX Line 2, *TaVP2* null segregant line) after 20 d growth in control (0 mM NaCl) or saline conditions (150 mM NaCl). Values are means (n=9-12) and error bars indicate standard error of the mean. Different letters indicate statistically significant differences (mixed model analysis, LSD,  $P \leq 0.05$ ).

Figures

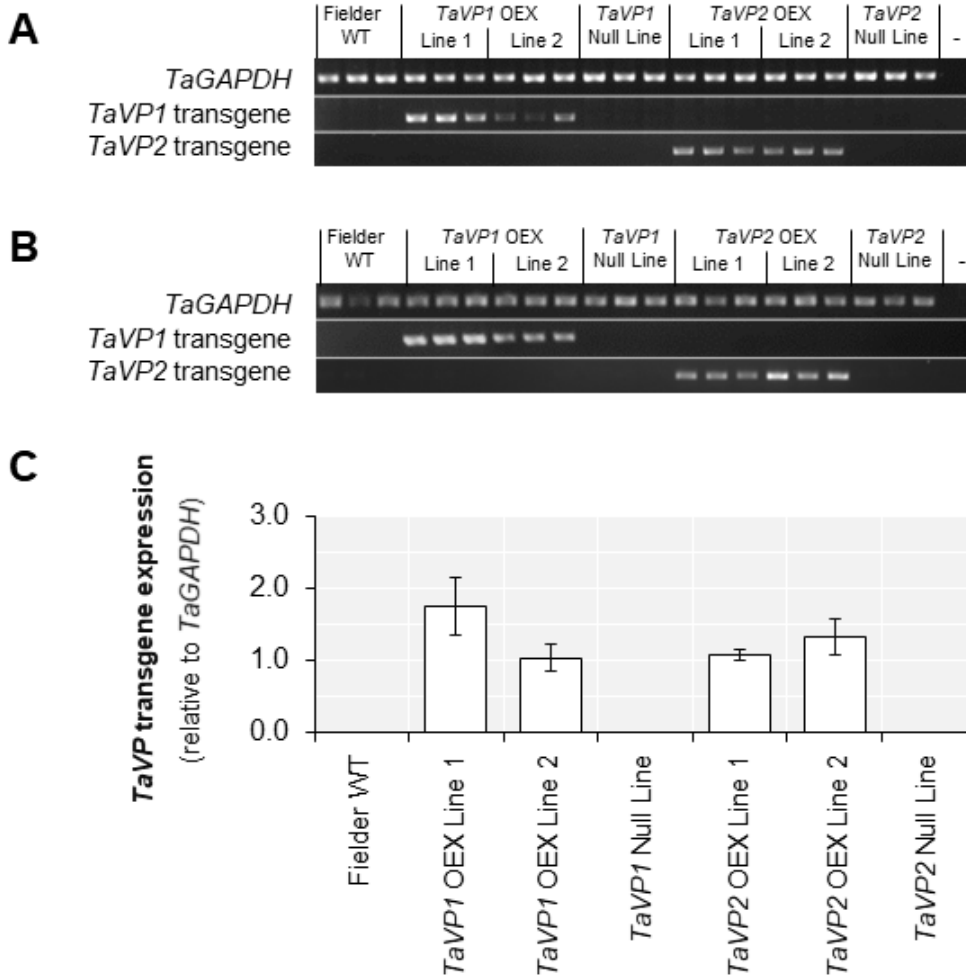


Fig. 1: Molecular characterisation of wild-type, *TaVP* transgenic and null segregant wheat lines.

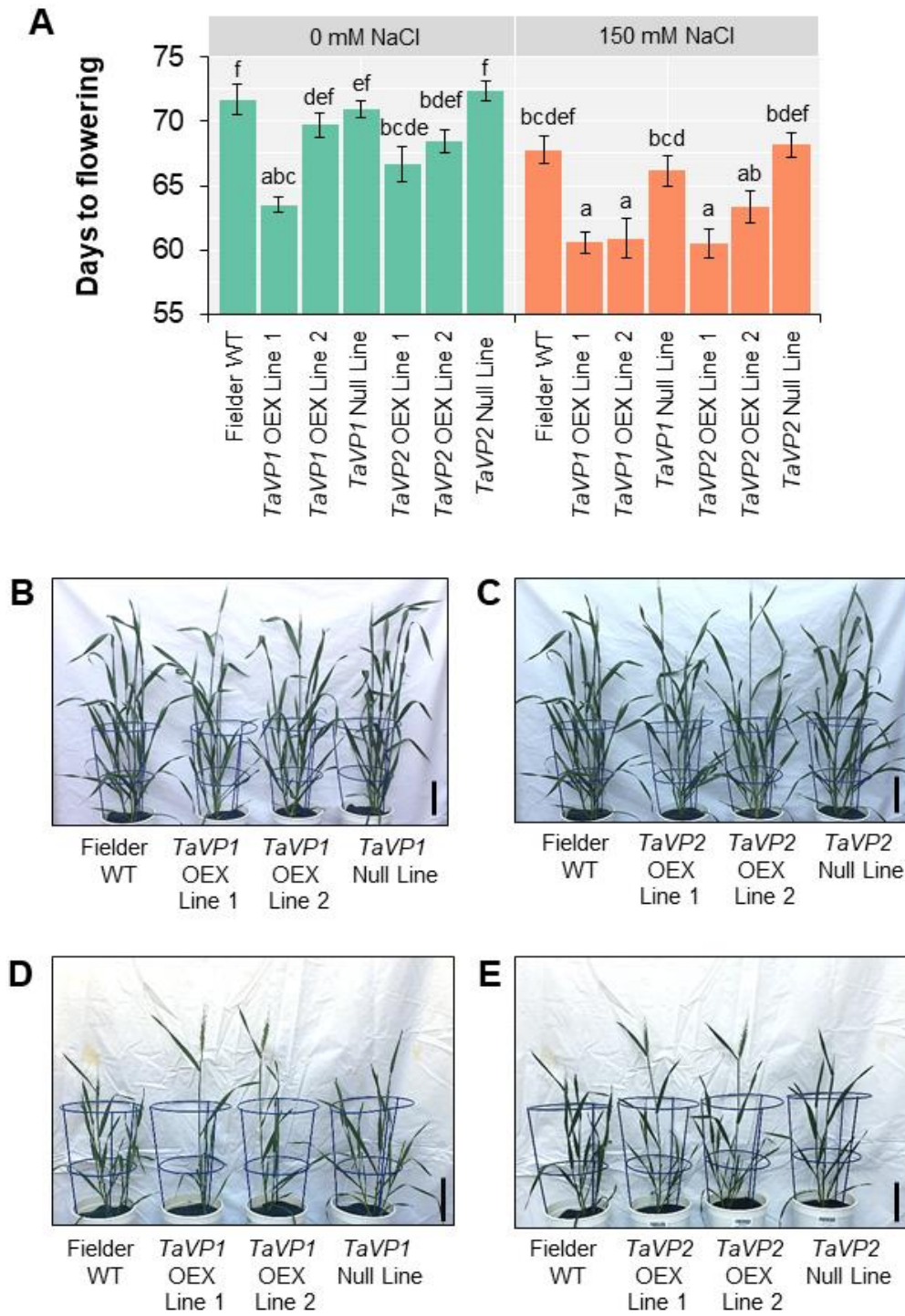


Fig. 2: Days to flowering and visual phenotype of wild-type, *TaVP* transgenic and null segregant wheat lines.

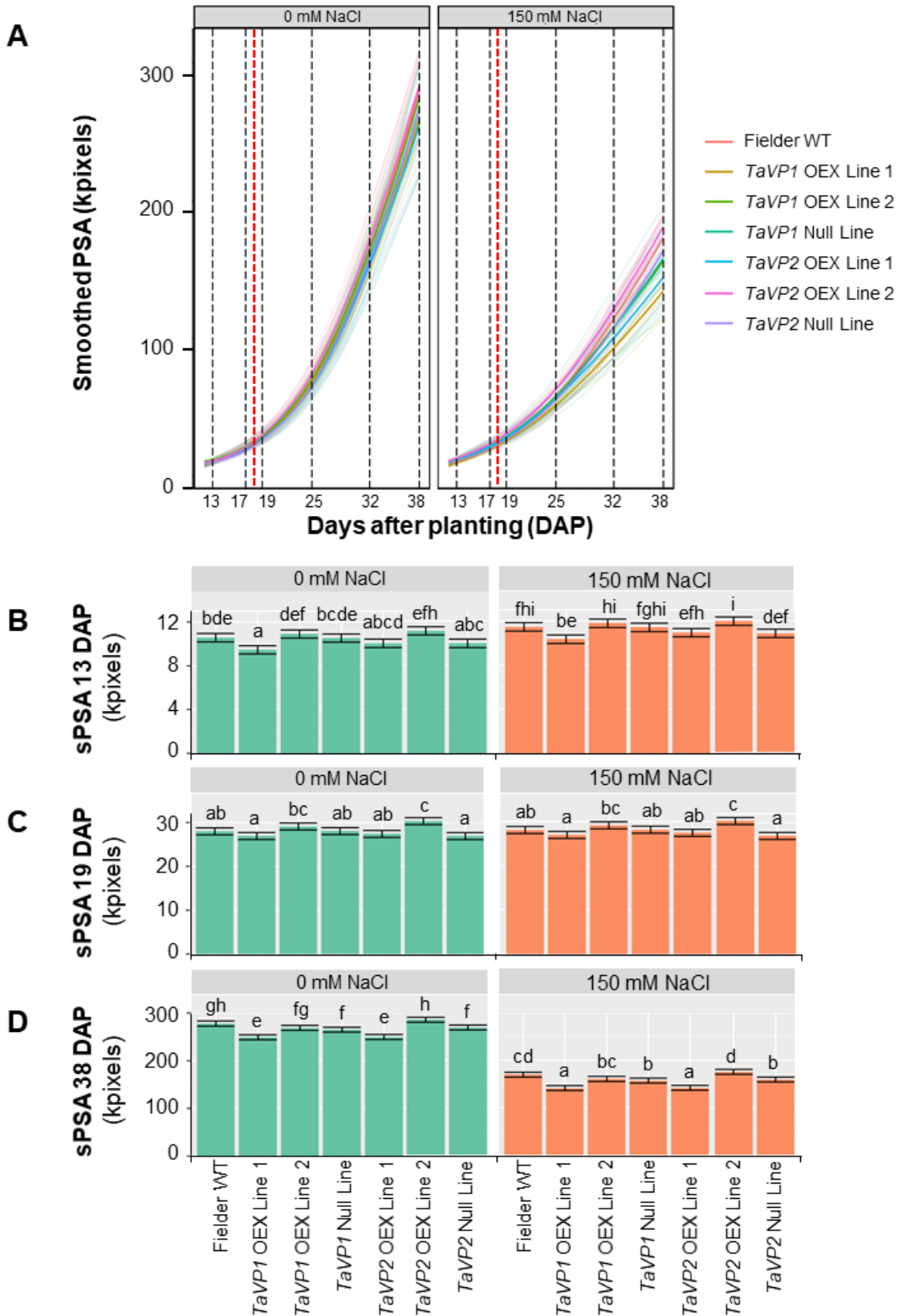


Fig 3: Smoothed projected shoot area of wild-type, *TaVP* transgenic and null segregant wheat lines 13, 19 and 38 DAP.



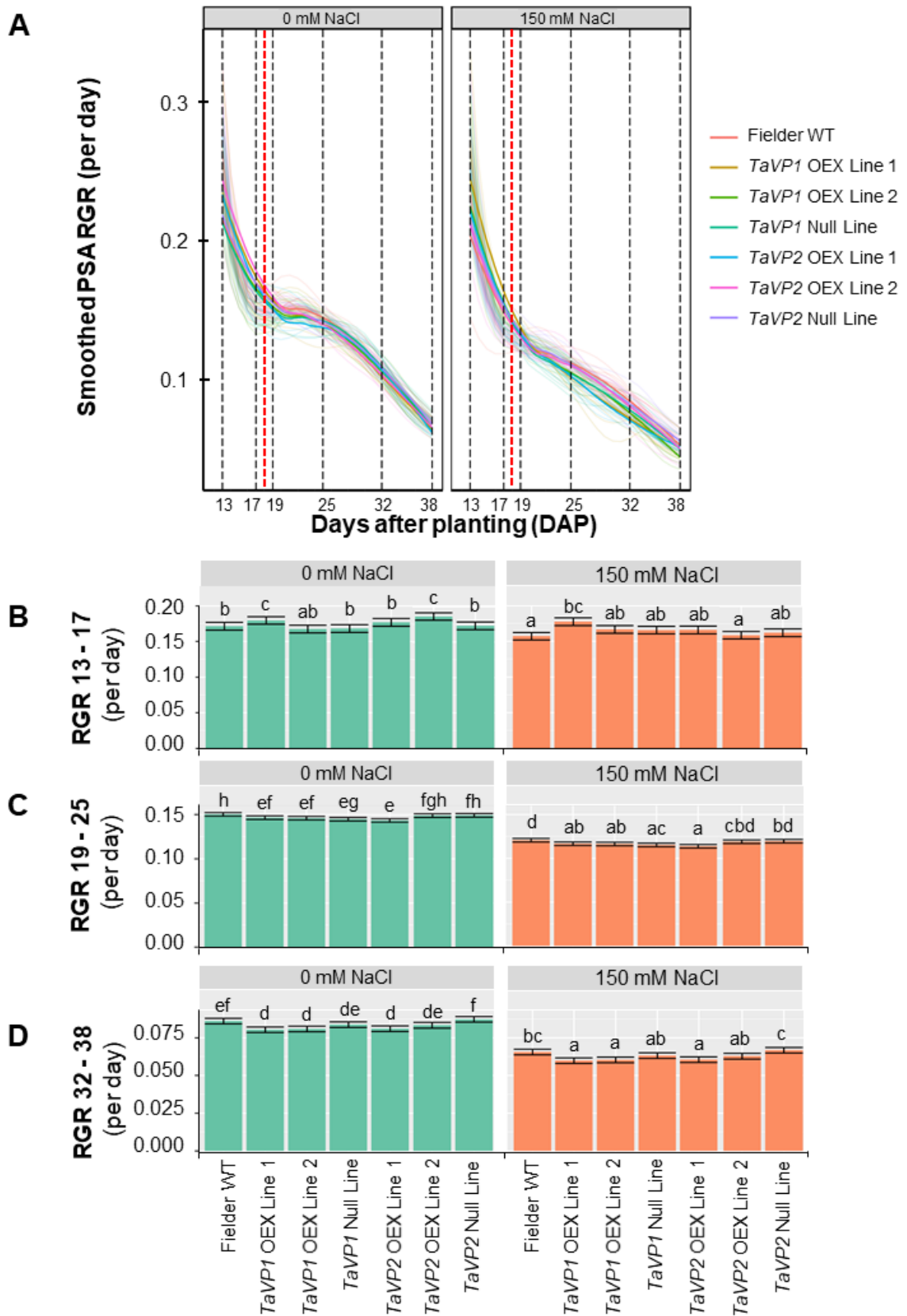


Fig. 4: Relative growth rates of wild-type, *TaVP* transgenic and null segregant wheat lines 13-17, 19-25 and 32-38 DAP.

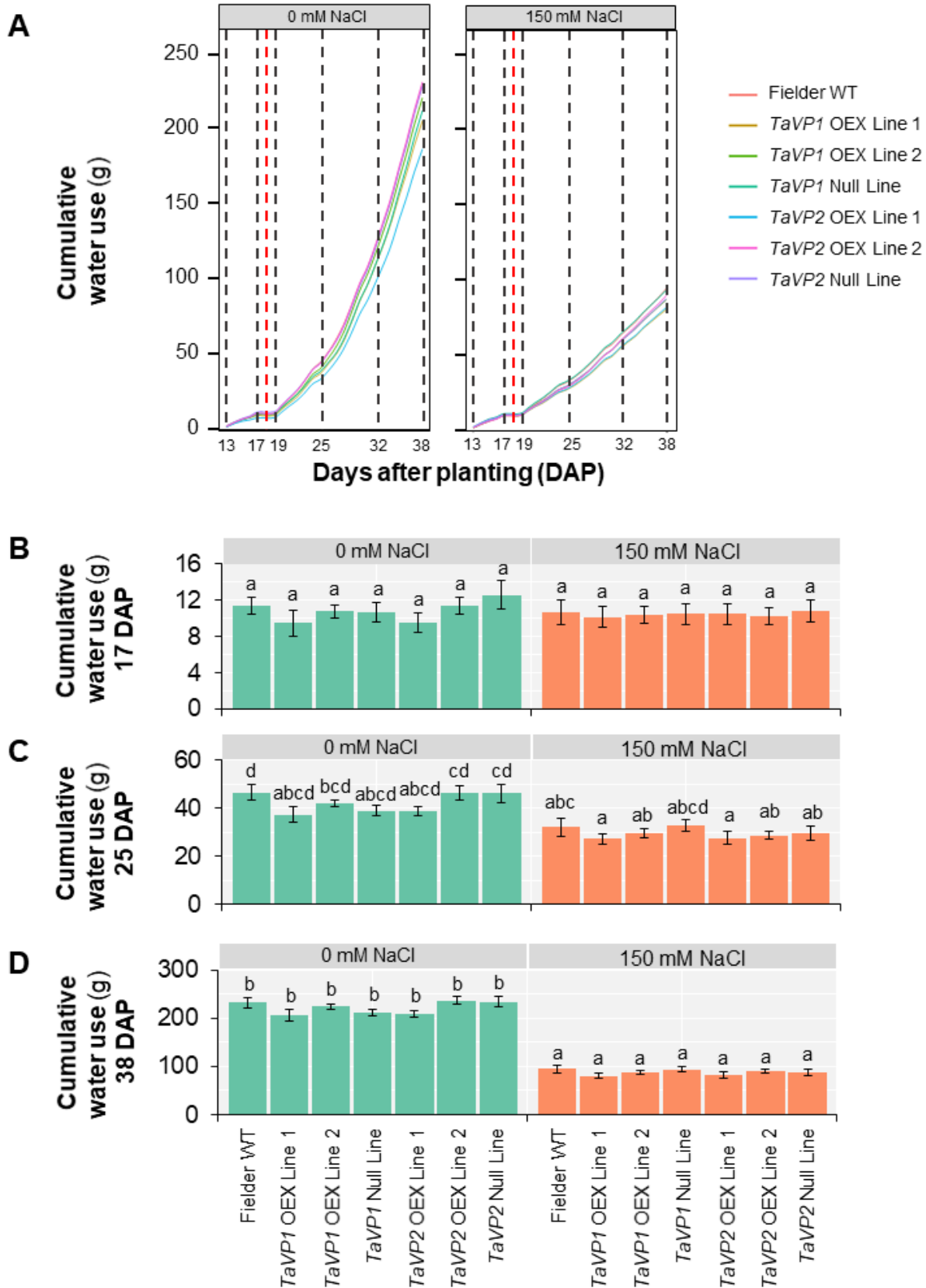


Fig. 5: Cumulative water use of wild-type, *TaVP* transgenic and null segregant wheat lines 17, 25 and 38 DAP.

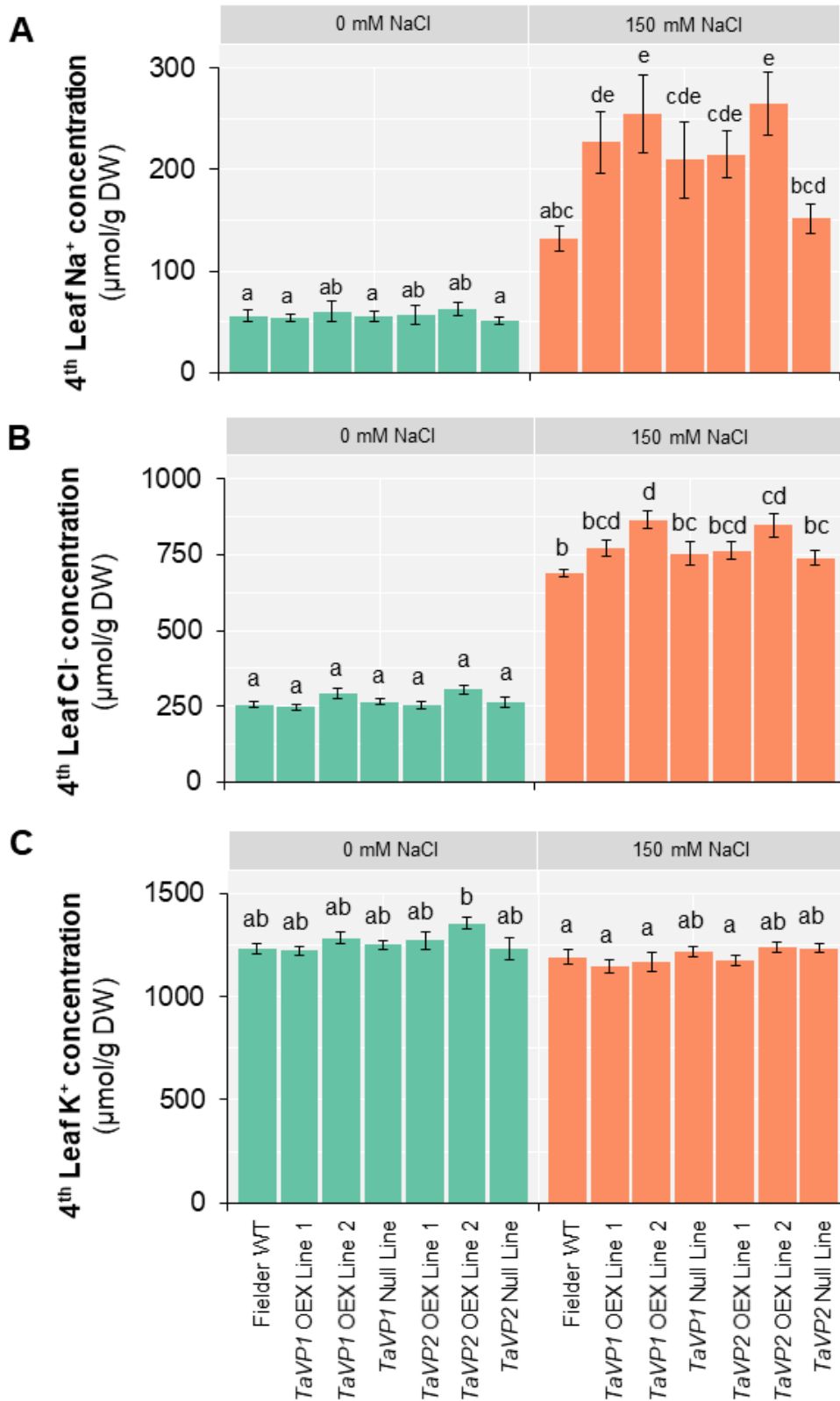
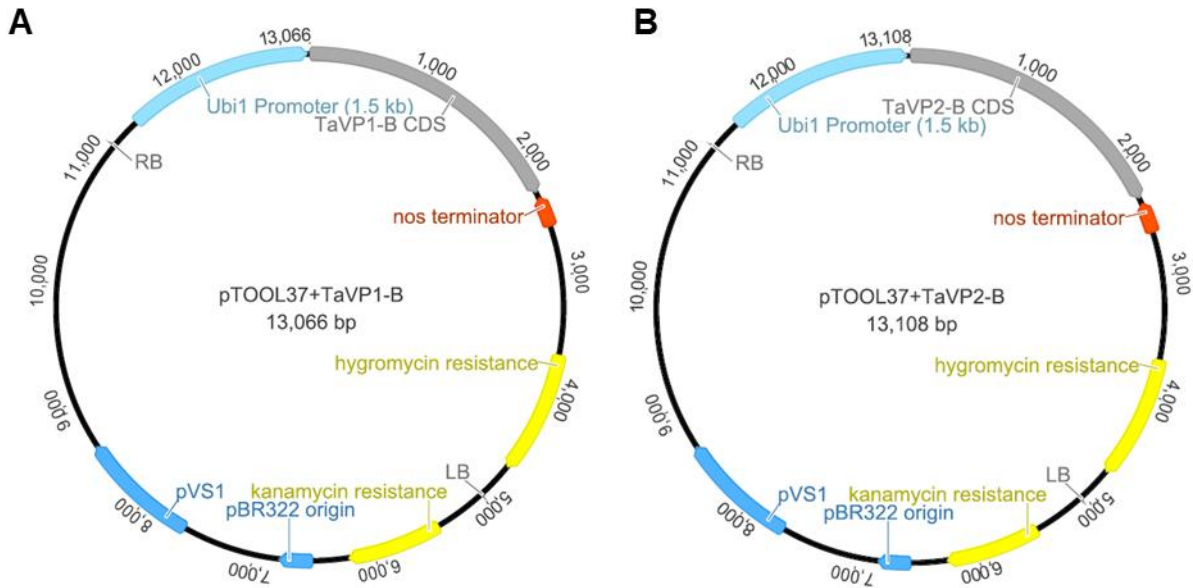
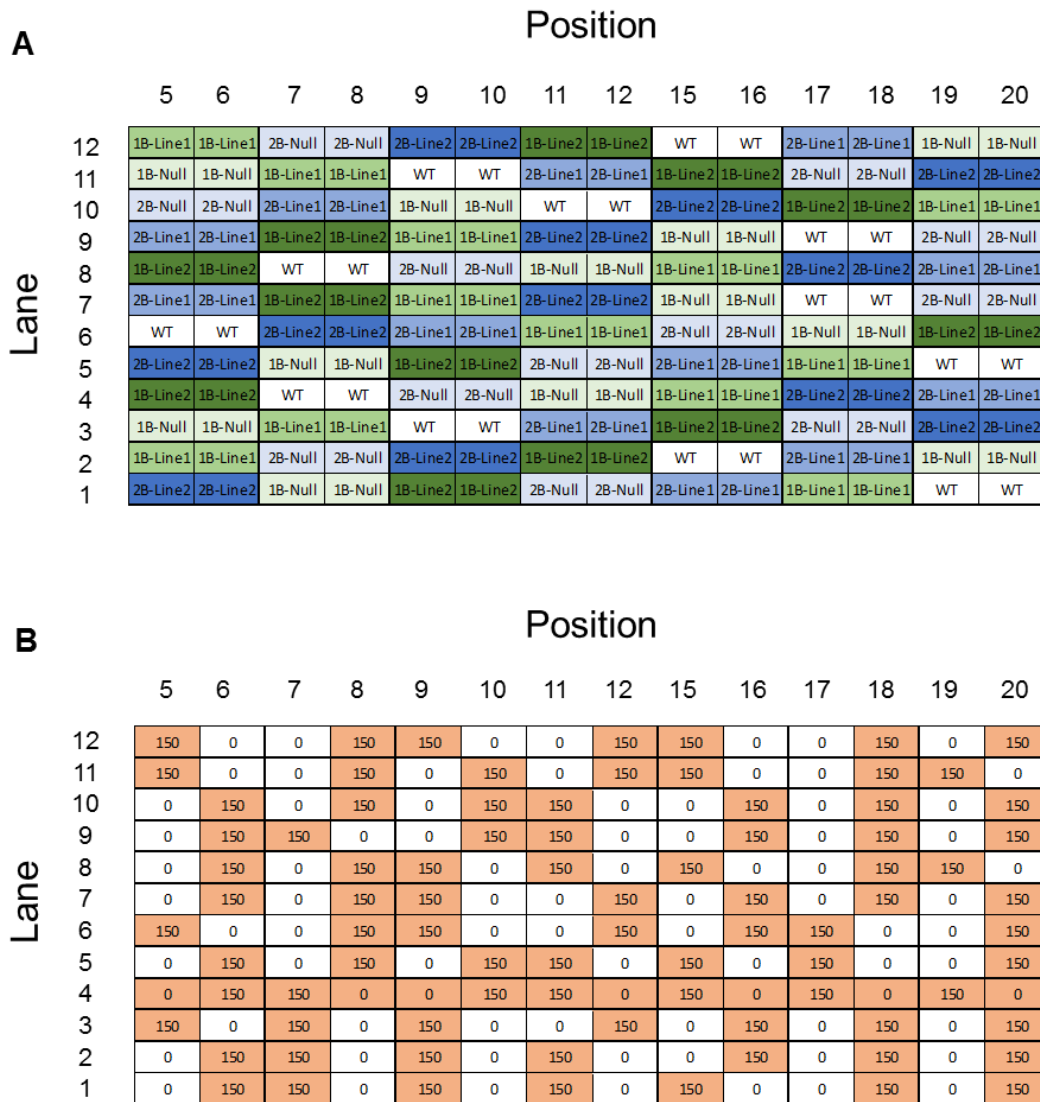


Fig. 6:  $\text{Na}^+$ ,  $\text{Cl}^-$  and  $\text{K}^+$  concentrations of wild-type, *TaVP* transgenic and null segregant wheat lines in 4<sup>th</sup> leaf samples collected at 38 DAP.

## Supplementary Figures



**Fig. S1:** Transformation vectors used to generate transgenic bread wheat (cv. Fielder) constitutively over-expressing the *TaVP1-B* and *TaVP2-B* genes. Constructed *pTOOL37* vectors containing complete (A) *TaVP1-B* and (B) *TaVP2-B* gene sequences flanked by the maize *Ubiquitin1* (DQ141598) promoter sequence and a NOS terminator sequence. Vectors also contain a *kanamycin* resistance gene for bacterial selection, a *hygromycin* resistance gene for wheat callus selection, left border (LB) and right border (RB) vector sequences, and the pBR322 and pVS1 origin of replication sequences. Vector backbones are shown in black, while exterior numbers indicate nucleotide positions within each vector sequence. Complete *TaVP1-B* (13,066 bp) and *TaVP2-B* (13,108 bp) *pTOOL37* vectors were used for *Agrobacterium*-mediated transformation of bread wheat (cv. Fielder) callus.



**Fig. S2:** Greenhouse layout of wild-type, *TaVP* transgenic and null segregant wheat lines. Details of the (A) genotype and (B) treatment of each wild-type (WT), *TaVP1* OEX Line 1 (1B-Line 1), *TaVP1* OEX Line 2 (1B-Line 2), *TaVP1* Null Line (1B-Null), *TaVP2* OEX Line 1 (2B-Line 1), *TaVP2* OEX Line 2 (2B-Line 2) and *TaVP2* Null Line (2B-Null) plant prior to, during and following high-throughput phenotyping. Layout was maintained from sowing through to maturity, including during the high-throughput phenotyping. Control (0 mM NaCl) and salt (150 mM NaCl) treatments are indicated by '0' and '150' respectively. Lane (y-axis) and Position (x-axis) correspond to those in the Smarthouse.

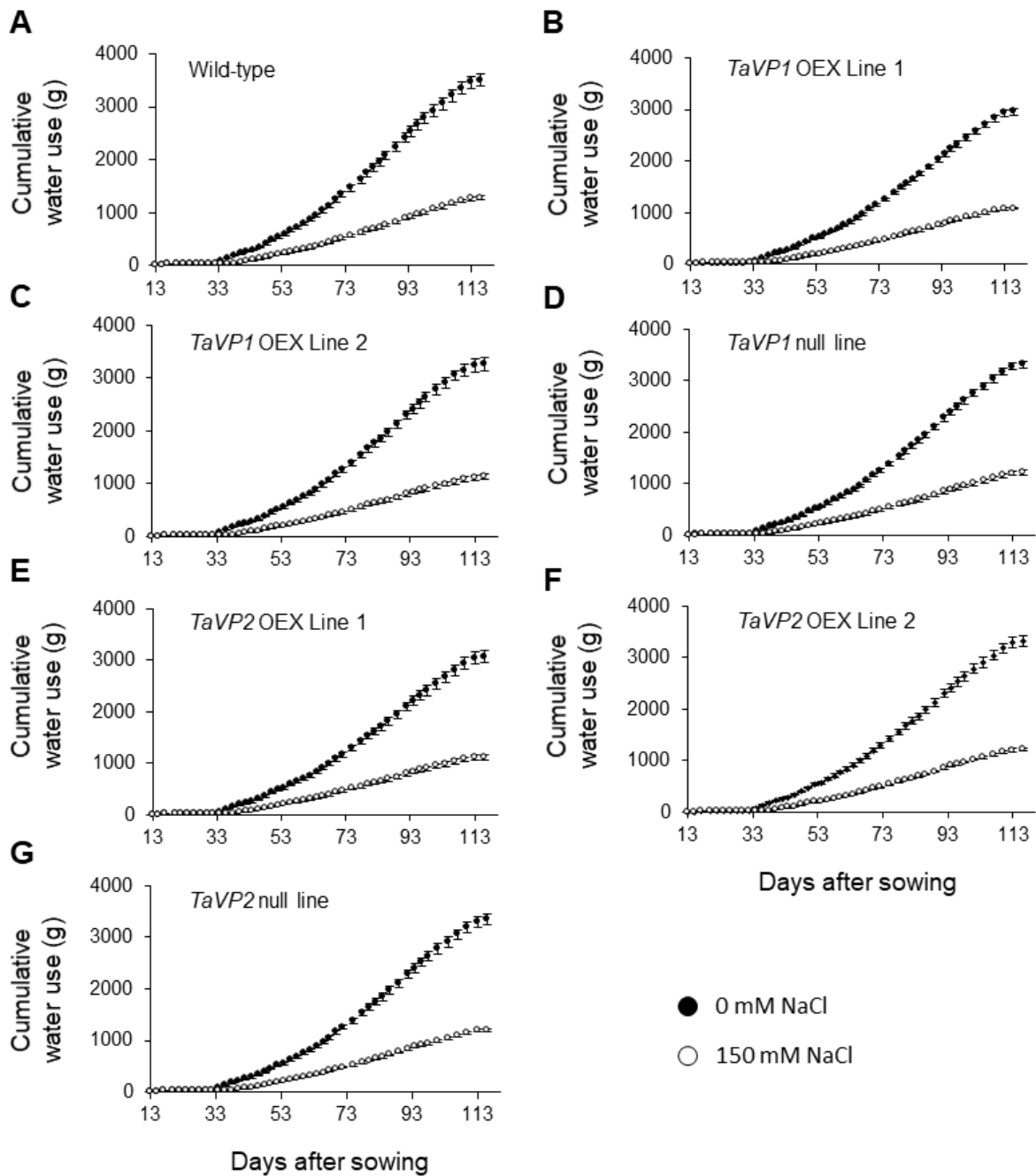


Fig. S3: Cumulative water use of wild-type, *TaVP* transgenic and null segregant wheat lines under control (0 mM NaCl) and saline (150 mM NaCl) conditions from 13-116 DAP. Total amount of water (g) used by T<sub>2</sub> (A) Fielder wild-type, (B) *TaVP1* OEX Line 1, (C) *TaVP1* OEX Line 2, (D) *TaVP1* null line, (E) *TaVP2* OEX Line 1, (F) *TaVP2* OEX Line 2 and (G) *TaVP2* null line plants in control (closed circles) and 150 mM NaCl salt treatment (open circles) until maturity (116 DAP). Values are means (n=9-12), with error bars indicating standard error of the mean.

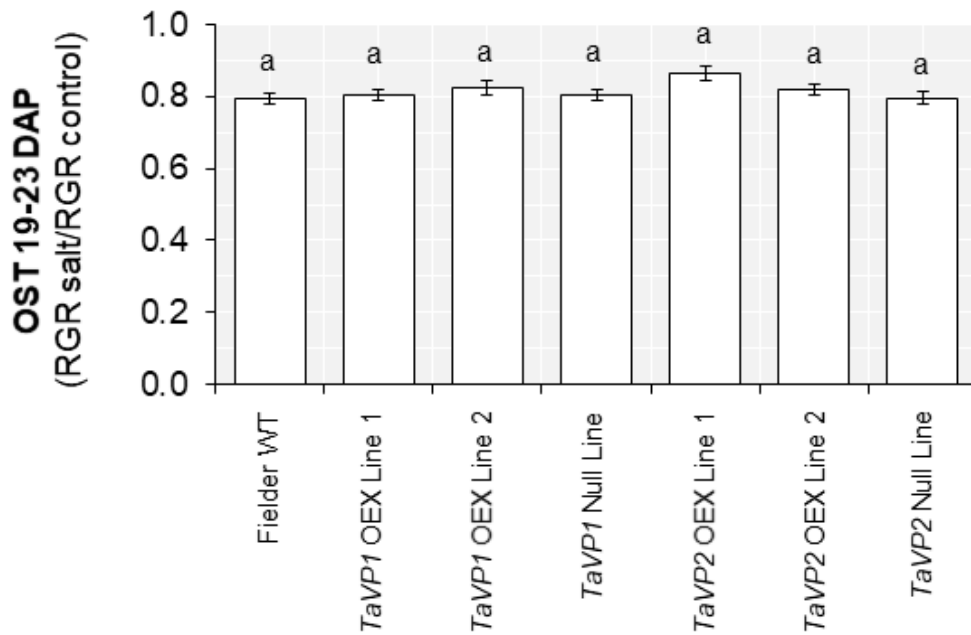


Fig. S4: Osmotic stress tolerance (OST) of wild-type, *TaVP* transgenic and null segregant wheat lines in the first 5 d following salt treatment. OST values for wild-type (Fielder WT), *TaVP1* OEX lines, *TaVP2* OEX lines and *TaVP1* and *TaVP2* Null lines were calculated by dividing the relative growth rate (RGR) of the salt treated plants by that of the control plants, in the first 5 d following salt application (19-23 DAP). Values are means (n=9-12), with different letters representing statistically significant differences (mixed model analysis, Wald's F test, LSD,  $P \leq 0.05$ ) and error bars indicating population variance ( $0.5 \times \text{LSD}$ ).

## Additional Information

### Determining an appropriate salt stress protocol for characterising Fielder wheat

A suitable treatment level for assessing salt tolerance in the transgenic *TaVP* Fielder lines was unable to be determined from the literature, as the few studies investigating the salt tolerance of Fielder wheat report conflicting results. As a wide range of methodologies have been used to assess salinity tolerance, the most suitable treatment method for this experiment was also unknown. Therefore, to establish the salt tolerance of wild-type Fielder and determine the most suitable methodology, an experiment was conducted using two common methods.

In the first method, based on Tilbrook et al. (2017), wild-type Fielder plants were grown until 3<sup>rd</sup> leaf emergence in pots with drainage holes (195 mm depth and 150 mm diameter) containing 2.7 kg GL mix (50 % (v/v) University of California (UC) mix (1:1 peat:sand), 35 % (v/v) coco peat, 15 % (v/v) clay loam) with 17 % soil water content. Various salt treatments (0 mM, 100 mM, 150 mM and 200 mM NaCl) were applied to the saucer of each pot, which entered the soil via capillary action, increasing the soil water content to 27 %. In the second method, salt solutions (0 mM, 100 mM, 150 mM and 200 mM NaCl) were mixed into the bottom 2/3 of GL soil in each pot (195 mm depth and 150 mm diameter without drainage holes) prior to sowing. Soil water content was maintained at 17 % by watering daily throughout the experiment. After 30 (Method 1) and 38 d (Method 2) plants were destructively harvested and both plant (4<sup>th</sup> leaf and root) and soil samples were analysed.

In both methodologies, cumulative water use declined with increasing NaCl levels (Fig. A1), however, only in Method 1 did shoot and root biomass decrease under salt treatment (Fig. A2). No increase in 4<sup>th</sup> leaf Na<sup>+</sup> or K<sup>+</sup> were apparent in either method, although 4<sup>th</sup> leaf Cl<sup>-</sup> increased to a higher level in Method 1 compared to Method 2 (Fig. A3). In the root tissue, Na<sup>+</sup> and Cl<sup>-</sup>



concentrations increased in all salt treatments in both methods, with Na<sup>+</sup> levels increasing to a higher level in Method 1, and Cl<sup>-</sup> levels increasing to a higher level in Method 2. (Fig. A4). Root K<sup>+</sup> concentration remained unchanged in both Method 1 and 2 in all salt treatments. In Method 1, soil electrical conductivity (EC<sub>1:5</sub>) increased from approximately 1000 μS cm<sup>-1</sup> in the control treatment to approximately 2000 μS/cm, while soil Na<sup>+</sup> concentrations increased from approximately 10 μmol/g to approximately 30 μmol/g (Fig. A5). The largest increases in EC<sub>1:5</sub> and Na<sup>+</sup> concentration occurred in soil treated with 150 mM and 200 mM NaCl treatments. In all soil layers, Cl<sup>-</sup> concentration increased with increasing levels of NaCl treatment, while K<sup>+</sup> concentrations remained constant between all treatments (Fig. A5). In Method 2, soil EC<sub>1:5</sub> increased similarly to that of Method 1 between control and salt treated pots, while Na<sup>+</sup> and Cl<sup>-</sup> concentrations increased from approximately 10 μmol/g under control treatment to 40 and 50 μmol/g respectively under NaCl treatment (Fig. A6). In each treatment, the bottom layer contained the highest EC<sub>1:5</sub>, Na<sup>+</sup> and Cl<sup>-</sup> levels, while few differences were apparent in the top soil layer. K<sup>+</sup> concentrations remained unchanged in all soil layers regardless of treatment level (Fig. A6).

In Method 1, the lack of increase in the 4<sup>th</sup> leaf Na<sup>+</sup> concentration of salt treated plants suggests Fielder has a high capacity to exclude Na<sup>+</sup> ions from the leaf, suggesting the reduction in shoot biomass may be due increased 4<sup>th</sup> leaf Cl<sup>-</sup> concentration, or an inability to maintain osmotic balance. After 30 d no phenotypic differences were observed between control and salt treated plants in Method 2, and so the treatment was extended for an addition 8 d. During harvest it was observed that the root systems in the salt treatment pots were contained within the top 1/3 soil layer and did not penetrate the saline layer of soil, explaining the lack of phenotype in plants in this method. Therefore, Method 1 and a treatment level of 150 mM NaCl was selected for characterising the salinity tolerance of the transgenic *TaVP* expressing Fielder wheat lines.

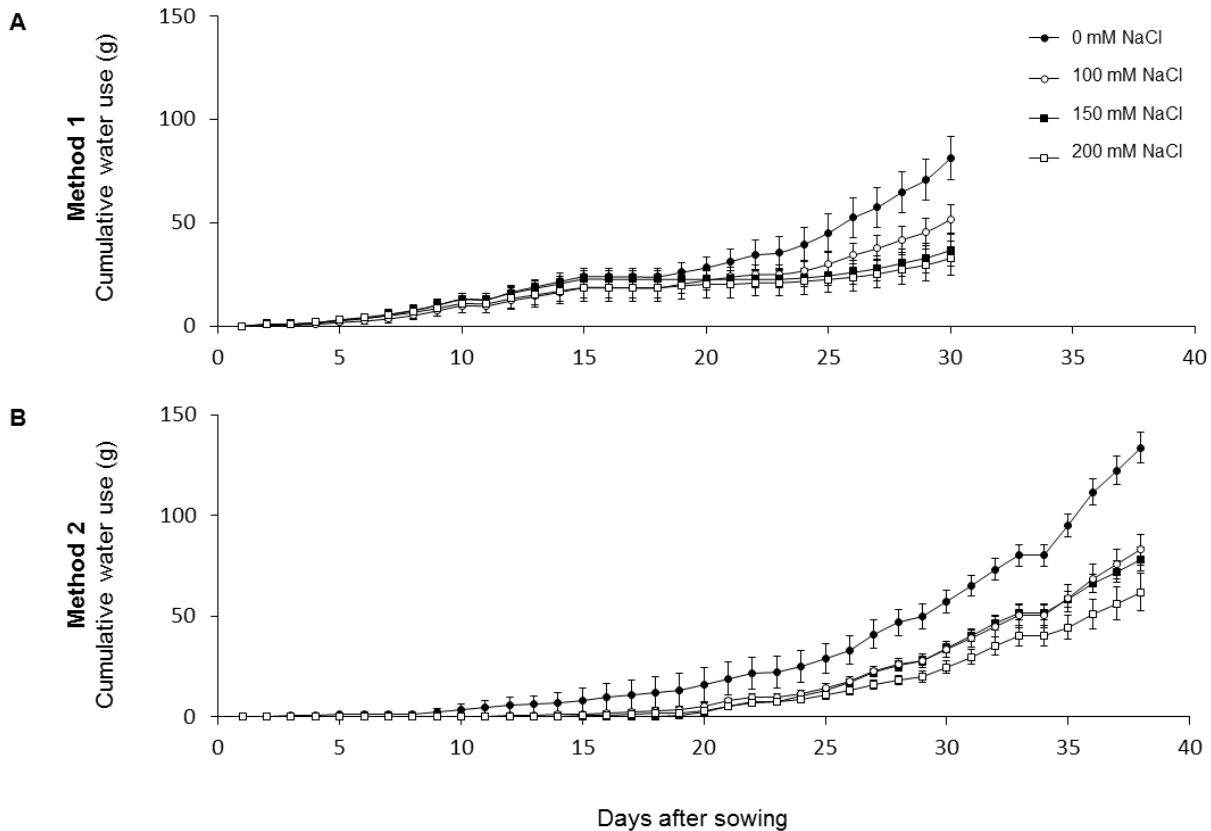


**Fig. A1: Cumulative water use of wild-type Fielder plants under various salt treatment levels in two methodologies.** Daily water use was determined by subtracting the amount of water lost from control pots (without plants) from treatment pots, which were watered daily to maintain 17 % soil water content. Graphs show cumulative water use (g) of plants treated with 0 mM (closed circles), 100 mM (open circles), 150 mM (closed squares) and 200 mM NaCl (open squares) in (A) Method 1 (salt solution applied to pot saucer at 3<sup>rd</sup> leaf emergence) 0-30 DAS, and (B) Method 2 (salt solution mixed into soil prior to sowing) 0-38 DAS. Error bars represent standard error of the mean of 5 biological replicates.

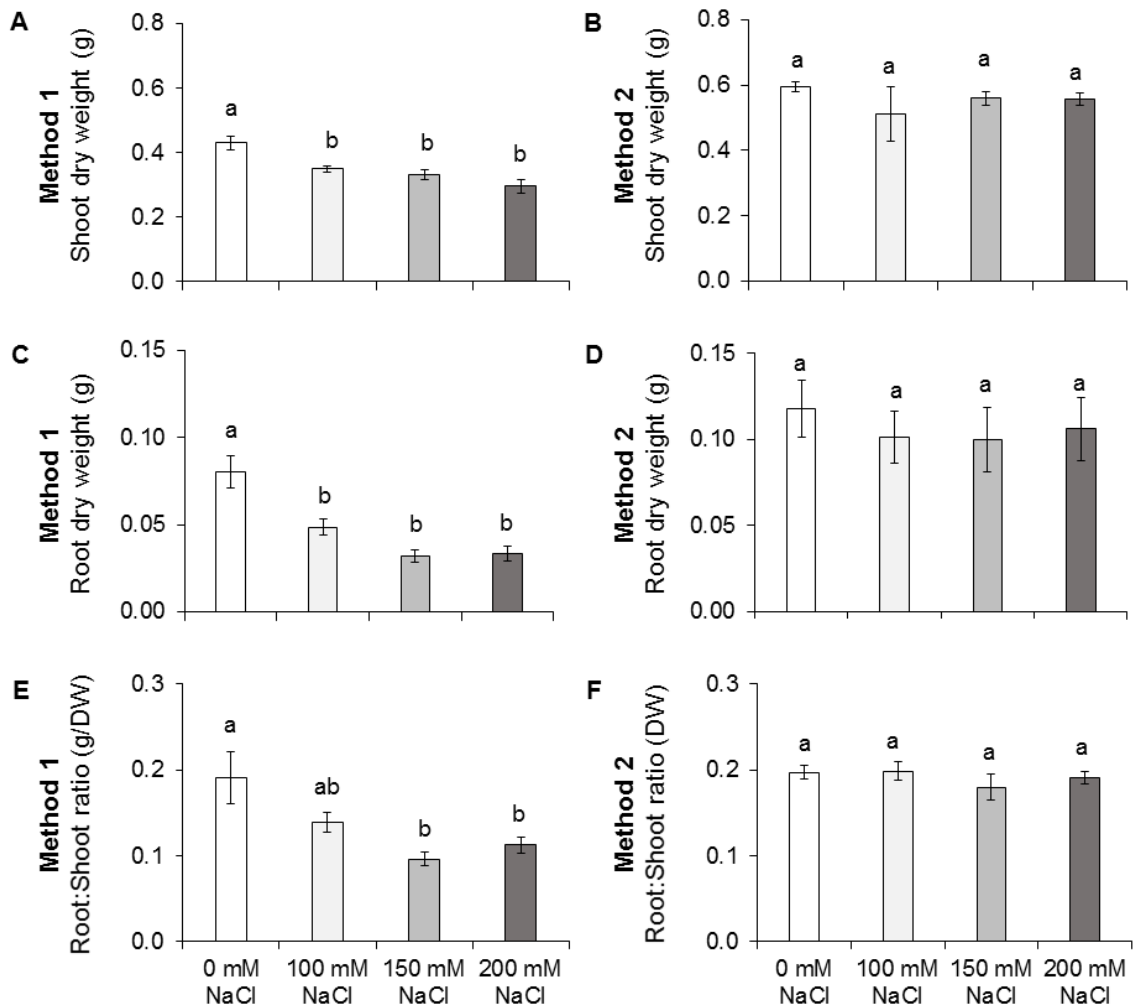


**Fig. A2: Biomass measurements of wild-type Fielder plants after 30 d and 38 d growth in two salt treatment methodologies.** (A-B) Shoot and (C-D) root dry weights (grams) and (E-F) root:shoot ratio of plants treated with 0 mM (white), 100 mM (light grey), 150 mM (dark grey) and 200 mM NaCl (black) in the two salt treatment methodologies. In Method 1 (A, C, E) the salt solution was applied to pot saucer at 3<sup>rd</sup> leaf emergence and in Method 2 (B, D, F) the salt solution was mixed into the soil prior to sowing. Different letters indicate statistically significant differences (one-way ANOVA, Tukey's 95 % confidence interval,  $P \leq 0.05$ ). Error bars represent standard error of the mean of 5 biological replicates.

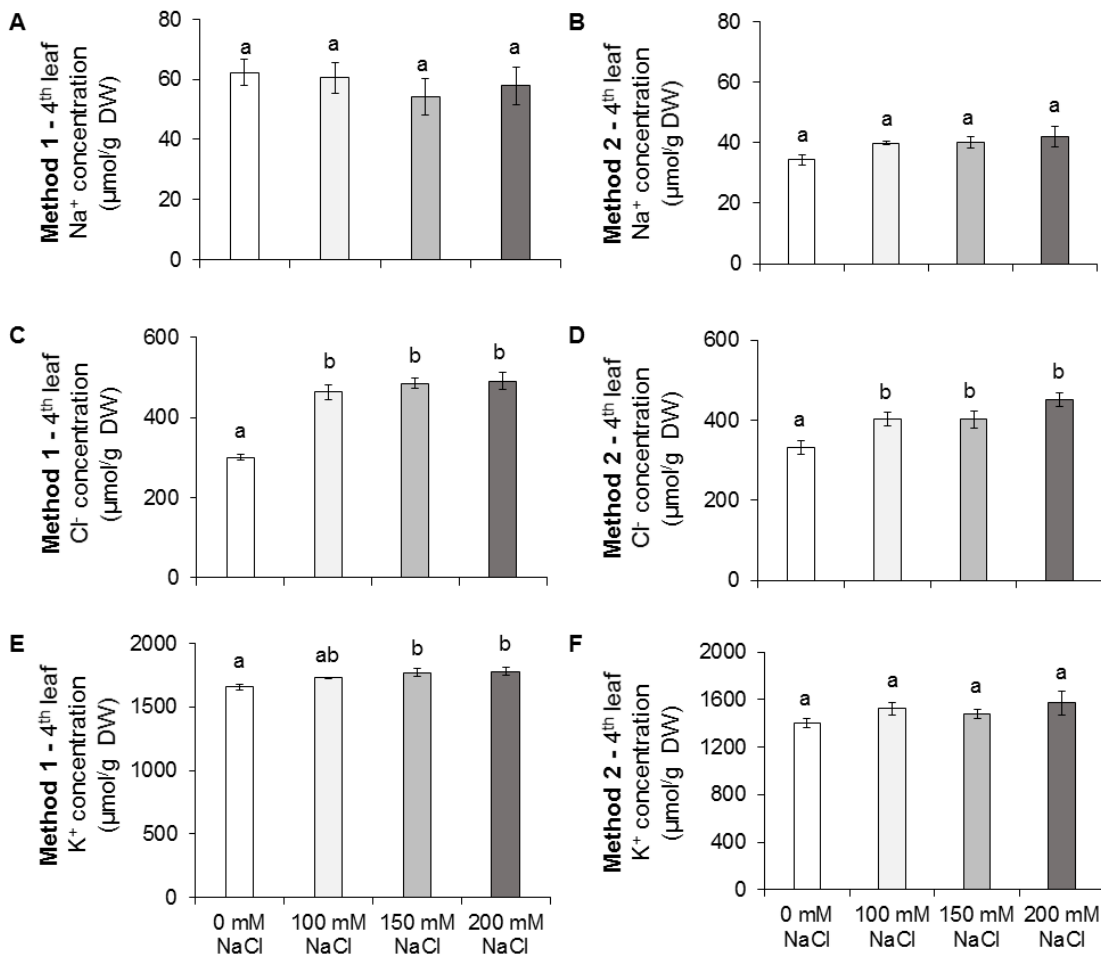


**Fig. A3: 4<sup>th</sup> leaf Na<sup>+</sup>, Cl<sup>-</sup> and K<sup>+</sup> concentration of wild-type Fielder plants under various NaCl conditions.** Fourth leaf (A-B) Na<sup>+</sup>, (C-D) Cl<sup>-</sup> and (E-F) K<sup>+</sup> concentration of plants treated with 0 mM (white), 100 mM (light grey), 150 mM (dark grey) and 200 mM NaCl (black) in the two salt treatment methodologies. In Method 1 (A, C, E) the salt solution was applied to pot saucer at 3<sup>rd</sup> leaf emergence and in Method 2 (B, D, F) the salt solution was mixed into the soil prior to sowing. A flame photometer (Sherwood, Cambridge, United Kingdom) was used to measure Na<sup>+</sup> and K<sup>+</sup> concentrations and a chloride analyser (Sherwood) was used to measure Cl<sup>-</sup> concentration in 4<sup>th</sup> leaf samples digested in 1% (v/v) nitric acid. Different letters indicate statistically significant differences (one-way ANOVA, Tukey's 95% confidence interval,  $P \leq 0.05$ ). Error bars represent standard error of the mean of 5 biological replicates.

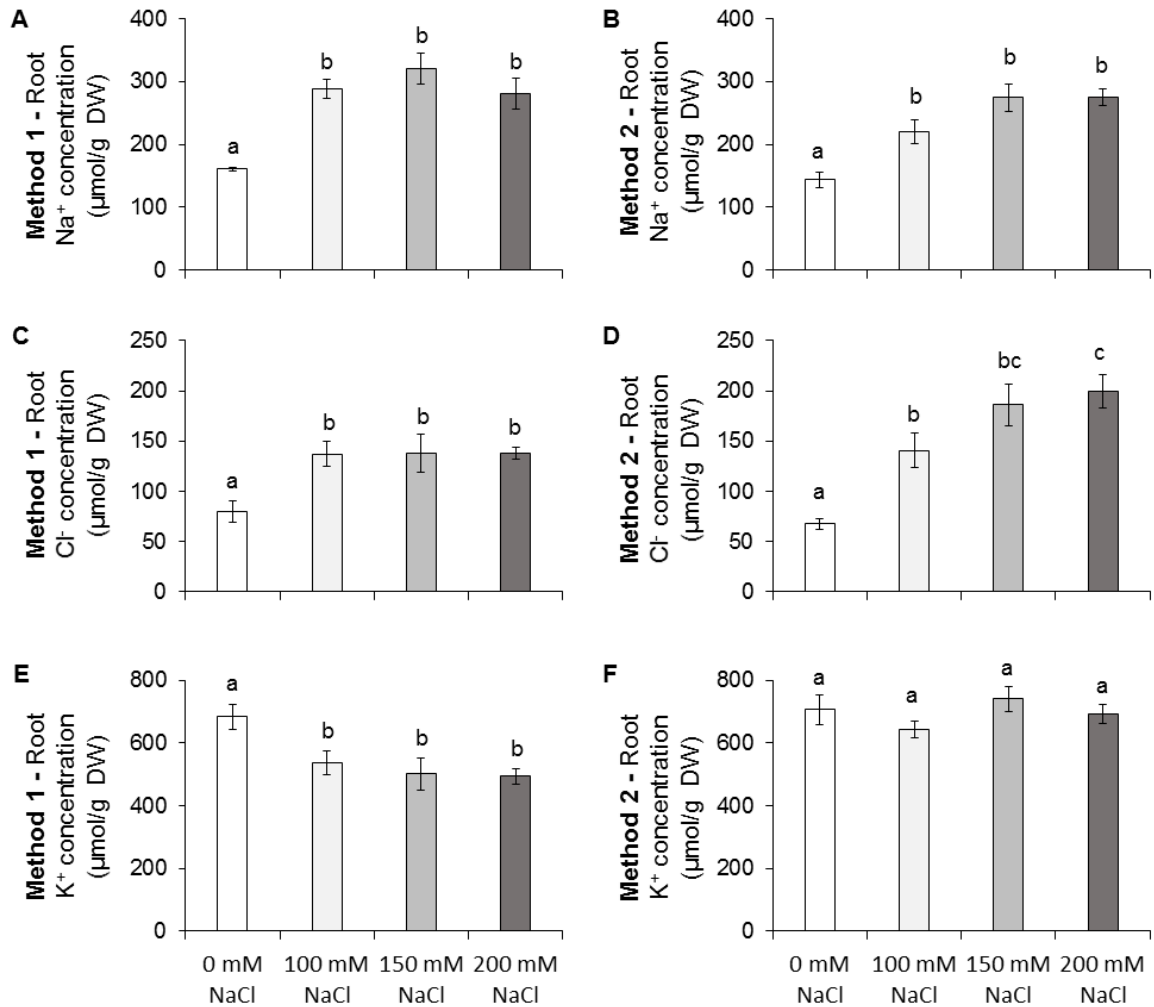


**Fig. A4:** Root Na<sup>+</sup>, Cl<sup>-</sup> and K<sup>+</sup> concentration of wild-type Fielder plants under various NaCl conditions. Root (A-B) Na<sup>+</sup>, (C-D) Cl<sup>-</sup> and (E-F) K<sup>+</sup> concentration of plants treated with 0 mM (white), 100 mM (light grey), 150 mM (dark grey) and 200 mM NaCl (black) in two salt treatment methodologies. In Method 1 (A, C, E) the salt solution was applied to pot saucer at 3<sup>rd</sup> leaf emergence and in Method 2 (B, D, F) the salt solution was mixed into the soil prior to sowing. A flame photometer (Sherwood, Cambridge,, United Kingdom) was used to measure Na<sup>+</sup> and K<sup>+</sup> concentrations and a chloride analyser (Sherwood) was used to measure Cl<sup>-</sup> concentration in 4<sup>th</sup> leaf samples digested in 1 % (v/v) nitric acid. Different letters indicate statistically significant differences (one-way ANOVA, Tukey's 95 % confidence interval,  $P \leq 0.05$ ). Error bars represent standard error of the mean of 5 biological replicates.

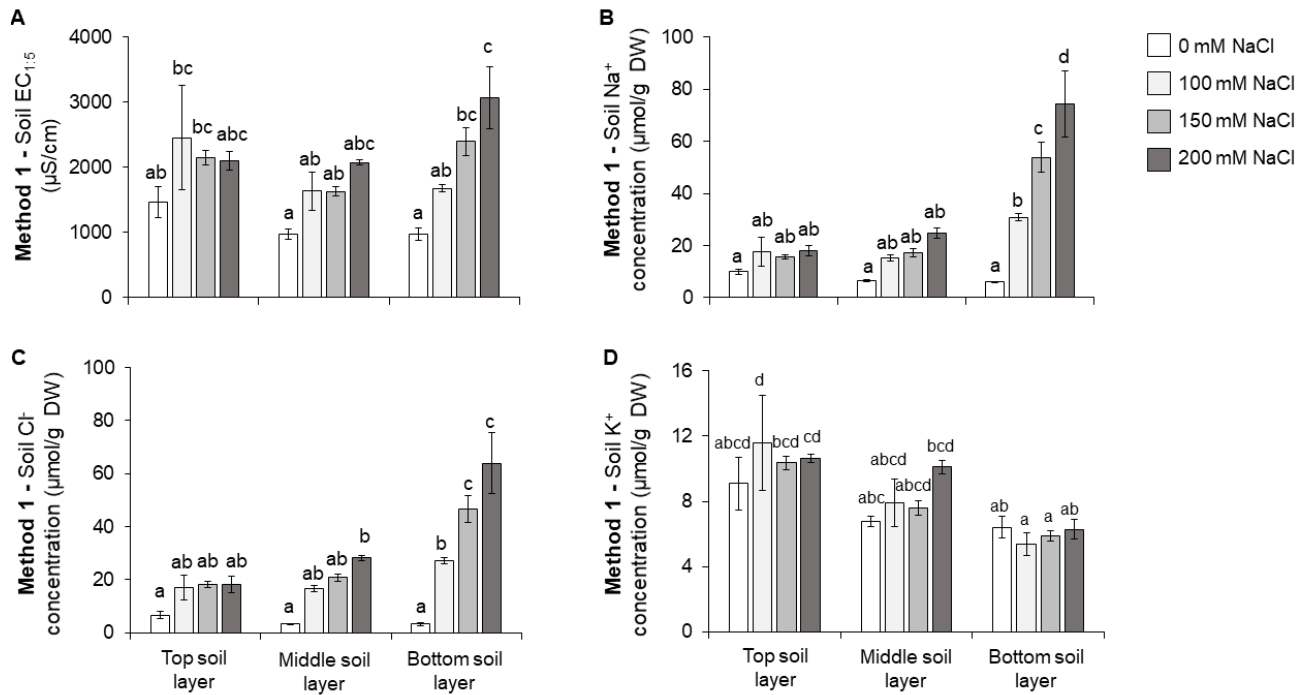


**Fig. A5: Analysis of soil in treatment Method 1.** (A) Electrical conductivity ( $\text{EC}_{1.5}$ ), (B)  $\text{Na}^+$ , (C)  $\text{Cl}^-$  and (D)  $\text{K}^+$  concentrations were measured in soil:water extracts of oven dried (72 h at  $60^\circ\text{C}$ ) soil samples from top, middle and bottom pot layers of 0 mM (white), 100 mM (light grey), 150 mM (dark grey) and 200 mM (black) NaCl treatments in Method 1 (in which the salt solution was applied to the pot saucer at 3<sup>rd</sup> leaf emergence).  $\text{EC}_{1.5}$  ( $\mu\text{S/cm}$ ) was measured with an EC meter (Thermo-Scientific, Waltham, United States) in 5 g dried soil samples mixed with 25 mL reverse osmosis (RO) water. A flame photometer (Sherwood, Cambridge, United Kingdom) was used to measure  $\text{Na}^+$  and  $\text{K}^+$  concentrations, while a chloride analyser (Sherwood) was used to measure  $\text{Cl}^-$  concentrations. Different letters indicate statistically significant differences (two-way ANOVA, Tukey's 95 % confidence interval,  $P \leq 0.05$ ). Error bars represent standard error of the mean of 5 biological and 3 technical replicates.

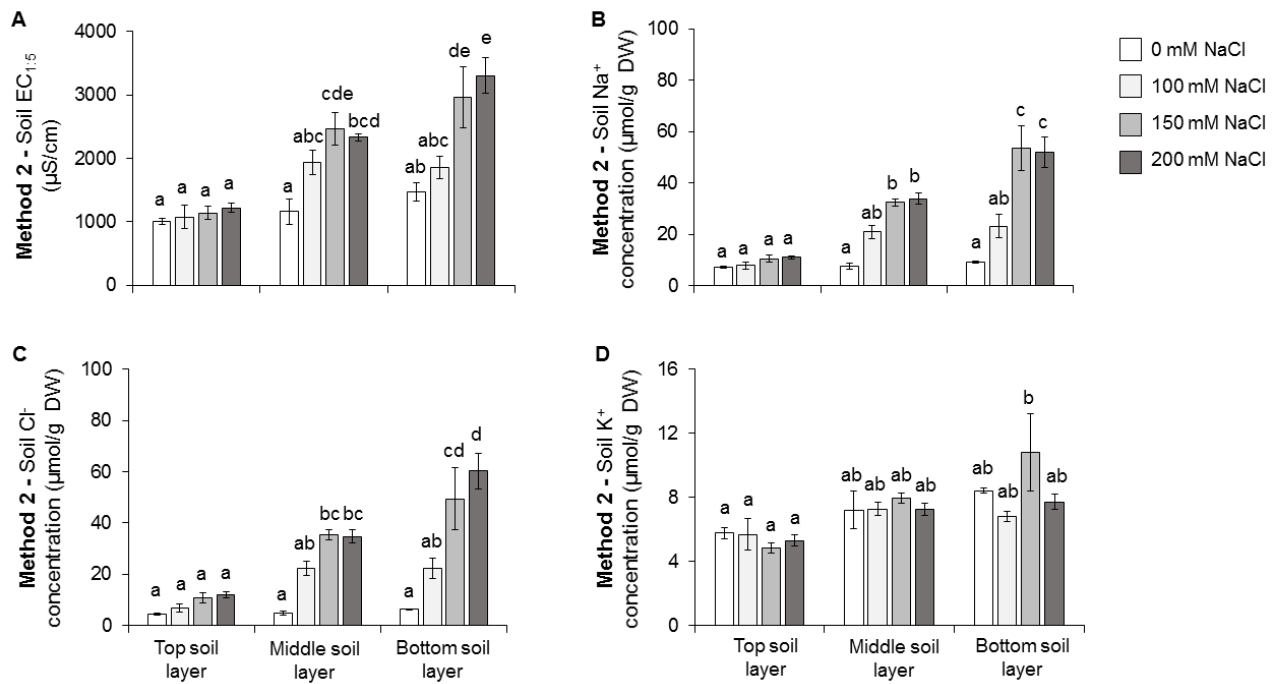


**Fig. A6: Analysis of soil in treatment Method 2.** (A) Electrical conductivity ( $\text{EC}_{1:5}$ ), (B)  $\text{Na}^+$ , (C)  $\text{Cl}^-$  and (D)  $\text{K}^+$  concentrations were measured in soil:water extracts of dried soil samples (72 h at  $60^\circ\text{C}$ ) from the top, middle and bottom pot layers 0 mM (white), 100 mM (light grey), 150 mM (dark grey) and 200 mM (black) NaCl treatments in Method 2 (in which the salt solution was mixed into the soil prior to sowing).  $\text{EC}_{1:5}$  ( $\mu\text{S/cm}$ ) was measured with an EC meter (Thermo-Scientific, Waltham, United States) in 5 g dried soil samples mixed with 25 mL reverse osmosis (RO) water. A flame photometer (Sherwood, Cambridge, United Kingdom) was used to measure  $\text{Na}^+$  and  $\text{K}^+$  concentration, while a chloride analyser (Sherwood) was used to measure  $\text{Cl}^-$  concentration. Different letters indicate statistically significant differences (two-way ANOVA, Tukey's 95 % confidence interval,  $P \leq 0.05$ ). Error bars represent standard error of the mean of 5 biological and 3 technical replicates.

### Assessing seedling vigour in *TaVP* over-expressing transgenic wheat

To investigate seedling vigour in the *TaVP* OEX wheat lines, a mini-hydroponics system (8 L) was created in which seedling growth could be measured non-destructively for 10 d (Fig. A7). The system consisted of a plastic container (40 cm length, 27 cm width, 20 cm depth) covered with black adhesive to prevent light entering the growth tank. Holes within the lid (14 mm diameter) allowed rolled paper towels to be easily placed into and removed from the tank. Twelve replicate seed (52.5 mg  $\pm$  0.5) of T<sub>1</sub> *TaVP* OEX wheat lines (Fielder wild-type, *TaVP1* OEX line 1, *TaVP1* OEX line 2, *TaVP1* null segregant line, *TaVP2* OEX line 1, *TaVP2* OEX line 2, *TaVP2* null segregant line) were UV sterilised for 5 min and placed onto individual sheets (22 cm in length and folded in half lengthways) of Scott® paper towel (Kimberly-Clark, Milsons Point, Australia), and moistened in nutrient solution. Seed were placed 1 cm from the top of the paper towel, crease side down, with the embryo oriented downwards. Paper towels were rolled and placed into the hydroponics system containing 0.2 mM NH<sub>4</sub>NO<sub>3</sub>, 5 mM KNO<sub>3</sub>, 2 mM Ca(NO<sub>3</sub>)<sub>2</sub>, 2 mM MgSO<sub>4</sub>, 0.1 mM KH<sub>2</sub>PO<sub>4</sub>, 0.5 mM Na<sub>2</sub>Si<sub>3</sub>O<sub>7</sub>, 50  $\mu$ M NaFe(III)EDTA, 5  $\mu$ M MnCl<sub>2</sub>, 10  $\mu$ M ZnSO<sub>4</sub>, 0.5  $\mu$ M CuSO<sub>4</sub>, 0.1  $\mu$ M Na<sub>2</sub>MoO<sub>4</sub> and reverse osmosis (RO) water up to 8 L. The solution was maintained at pH 6.5 by adjusting with 3.2 % (v/v) HCl and nutrient solutions were replaced after 5 d. Nutrients were supplied to the seedlings via capillary force action, with paper rolls held in place by open ended 10 mL tubes (Sarstedt Australia, Technology Park, Australia). Oxygen was continuously supplied to the solution via two stone aerators attached to an Aqua One® 2500 Precision Air-pump (Kong's Australia, Ingleburn, Australia). Seedlings were arranged in a randomised block design and grown in a growth chamber in Urrbrae, South Australia (latitude: -34.968086; longitude: 138.636472) for 10 d (12 h day/night length, 22°C day and 18°C night temperature, a light intensity of 800  $\mu$ mol m<sup>-2</sup> s<sup>-1</sup> and 60-80 % relative humidity). Seedling biomass (mg FW), shoot height (cm) and total root length (cm) were measured daily,



with seedlings destructively harvested after 10 d. Data was analysed via one-way ANOVA ( $P \leq 0.05$ ) and Tukey's 95 % confidence intervals (GenStat® version 15.3). Genotyping and expression analysis were conducted as previously described.

At each time point, the total weight of wild-type seedling was greater than that of the *TaVP* OEX transgenic seedlings, between which there were few significant differences (Table A1). The total root length was consistently higher in wild-type seedlings than the *TaVP* OEX seedlings across the 10 d, with no significant differences between the transgenic and null segregant lines (Table A2). The only significant differences in total leaf length were at Days 4 and 8, where leaf length of the *TaVP2* OEX Line 1 seedlings were 34 % and 17 % higher than the average length of the other three transgenic lines (Table A3). *TaVP2* OEX Line 1 leaves, however, were not significantly different to wild-type seedlings.

The lack of significant differences in seedling biomass, leaf length and root length between the wild-type/null segregant lines and the *TaVP* OEX lines suggests that constitutive over-expression of *TaVP1-B* and *TaVP2-B* does not improve seedling vigour. The lack of significant differences, however, may have been influenced by several factors, such as the experimental methods used and the large variation among replicate seedlings of each line. On day 8 of the experiment, an outbreak of fungus in the hydroponics systems resulted in the loss of many replicate seedlings, which likely contributed to the large variation observed within each line. To prevent the development of fungus within the system, paper rolls may need sterilisation prior to use and the exterior light barrier of the tank should be improved to ensure light does not penetrate into the tank. The total amount of solution within the tank should also be further optimised to prevent the paper rolls from becoming too moist, which may have promoted the growth of fungus within the tank and paper rolls.

**Table A1: Initial seed weight and daily total biomass measurements (mg FW  $\pm$  SEM) of wild-type, T<sub>1</sub> *TaVP* transgenic and null segregant wheat seedlings.** Seedlings were grown in a paper roll hydroponics system and destructively harvested after 10 d. Values are means ( $\pm$  standard error of the mean (SEM), n=5-11), with different letters indicating statistically significant differences based on one-way ANOVA and Tukey's 95 % confidence intervals,  $P \leq 0.05$  (GenStat® version 15.3). - indicates no recorded measurements.

Line	Initial seed weight (mg $\pm$ SEM)	Total seedling weight (mg $\pm$ SEM)									
		Day 1	Day 2	Day 3	Day 4	Day 5	Day 6	Day 7	Day 8	Day 9	Day 10
Wild-type	53 $\pm$ 0.3 <sup>a</sup>	-	89 $\pm$ 3 <sup>a</sup>	112 $\pm$ 5 <sup>b</sup>	155 $\pm$ 7 <sup>bd</sup>	205 $\pm$ 9 <sup>b</sup>	261 $\pm$ 10 <sup>bd</sup>	316 $\pm$ 11 <sup>b</sup>	352 $\pm$ 11 <sup>b</sup>	387 $\pm$ 9 <sup>bd</sup>	411 $\pm$ 7 <sup>bd</sup>
<i>TaVP1</i> OEX Line 1	53 $\pm$ 0.3 <sup>a</sup>	-	86 $\pm$ 2 <sup>a</sup>	104 $\pm$ 4 <sup>ab</sup>	137 $\pm$ 7 <sup>abccd</sup>	177 $\pm$ 8 <sup>ab</sup>	223 $\pm$ 10 <sup>abc</sup>	269 $\pm$ 11 <sup>a</sup>	302 $\pm$ 10 <sup>a</sup>	340 $\pm$ 11 <sup>abc</sup>	366 $\pm$ 11 <sup>abc</sup>
<i>TaVP1</i> OEX Line 2	53 $\pm$ 0.8 <sup>a</sup>	-	84 $\pm$ 4 <sup>a</sup>	100 $\pm$ 6 <sup>ab</sup>	128 $\pm$ 9 <sup>abc</sup>	169 $\pm$ 9 <sup>a</sup>	221 $\pm$ 10 <sup>ab</sup>	273 $\pm$ 10 <sup>a</sup>	316 $\pm$ 10 <sup>ab</sup>	357 $\pm$ 12 <sup>abccd</sup>	389 $\pm$ 16 <sup>abccd</sup>
<i>TaVP1</i> null line	53 $\pm$ 0.5 <sup>a</sup>	-	82 $\pm$ 2 <sup>a</sup>	97 $\pm$ 4 <sup>ab</sup>	126 $\pm$ 6 <sup>ab</sup>	166 $\pm$ 9 <sup>a</sup>	214 $\pm$ 11 <sup>a</sup>	258 $\pm$ 10 <sup>a</sup>	299 $\pm$ 11 <sup>a</sup>	342 $\pm$ 12 <sup>ab</sup>	371 $\pm$ 13 <sup>ab</sup>
<i>TaVP2</i> OEX Line 1	53 $\pm$ 0.3 <sup>a</sup>	-	88 $\pm$ 2 <sup>a</sup>	107 $\pm$ 3 <sup>ab</sup>	143 $\pm$ 6 <sup>abccd</sup>	185 $\pm$ 7 <sup>ab</sup>	236 $\pm$ 9 <sup>abccd</sup>	289 $\pm$ 12 <sup>ab</sup>	324 $\pm$ 10 <sup>ab</sup>	365 $\pm$ 11 <sup>abccd</sup>	399 $\pm$ 12 <sup>abccd</sup>
<i>TaVP2</i> OEX Line 2	52 $\pm$ 0.4 <sup>a</sup>	-	79 $\pm$ 2 <sup>a</sup>	91 $\pm$ 4 <sup>a</sup>	117 $\pm$ 8 <sup>a</sup>	154 $\pm$ 10 <sup>a</sup>	198 $\pm$ 11 <sup>a</sup>	244 $\pm$ 12 <sup>a</sup>	289 $\pm$ 10 <sup>a</sup>	332 $\pm$ 11 <sup>a</sup>	371 $\pm$ 10 <sup>abccd</sup>
<i>TaVP2</i> null line	53 $\pm$ 0.3 <sup>a</sup>	-	85 $\pm$ 2 <sup>a</sup>	101 $\pm$ 3 <sup>ab</sup>	134 $\pm$ 5 <sup>abccd</sup>	174 $\pm$ 7 <sup>ab</sup>	219 $\pm$ 10 <sup>a</sup>	264 $\pm$ 13 <sup>a</sup>	298 $\pm$ 15 <sup>a</sup>	331 $\pm$ 17 <sup>a</sup>	357 $\pm$ 17 <sup>a</sup>

**Table A2: Daily total root length measurements (cm ± SEM) of wild-type, T<sub>1</sub> *TaVP* transgenic and null segregant wheat seedlings. Seedlings**

were grown in a paper roll hydroponics system and destructively harvested after 10 d. Values are means (± standard error of the mean (SEM), n=5-11) with different letters indicating statistically significant differences based on one-way ANOVA and Tukey's 95 % confidence intervals,  $P \leq 0.05$  (GenStat® version 15.3). - indicates no recorded measurements.

Line	Total root length (cm ± SEM)									
	Day 1	Day 2	Day 3	Day 4	Day 5	Day 6	Day 7	Day 8	Day 9	Day 10
Wild-type	-	1.9 ± 0.5 <sup>a</sup>	7.6 ± 1.0 <sup>a</sup>	17.3 ± 1.4 <sup>b</sup>	29.5 ± 2.1 <sup>b</sup>	41.3 ± 2.0 <sup>b</sup>	50.6 ± 2.6 <sup>ac</sup>	57.5 ± 2.6 <sup>b</sup>	58.7 ± 2.3 <sup>a</sup>	60.8 ± 3.1 <sup>a</sup>
<i>TaVP1</i> OEX Line 1	-	1.6 ± 0.4 <sup>a</sup>	6.5 ± 0.9 <sup>a</sup>	14.5 ± 1.5 <sup>ab</sup>	24.4 ± 2.1 <sup>ab</sup>	35.7 ± 2.4 <sup>ab</sup>	43.7 ± 2.5 <sup>abc</sup>	50.1 ± 2.5 <sup>ab</sup>	53.6 ± 2.2 <sup>a</sup>	53.9 ± 1.5 <sup>a</sup>
<i>TaVP1</i> OEX Line 2	-	0.9 ± 0.5 <sup>a</sup>	4.8 ± 1.0 <sup>a</sup>	11.7 ± 1.9 <sup>ab</sup>	22.0 ± 2.4 <sup>ab</sup>	33.1 ± 3.0 <sup>ab</sup>	44.0 ± 2.5 <sup>abc</sup>	51.9 ± 2.1 <sup>ab</sup>	56.5 ± 3.4 <sup>a</sup>	55.5 ± 2.2 <sup>a</sup>
<i>TaVP1</i> null line	-	0.9 ± 0.3 <sup>a</sup>	4.7 ± 0.9 <sup>a</sup>	11.2 ± 1.2 <sup>ab</sup>	21.2 ± 2.1 <sup>ab</sup>	30.9 ± 2.5 <sup>ab</sup>	38.5 ± 3.0 <sup>a</sup>	44.0 ± 3.8 <sup>a</sup>	48.2 ± 4.3 <sup>a</sup>	49.3 ± 3.9 <sup>a</sup>
<i>TaVP2</i> OEX Line 1	-	1.7 ± 0.3 <sup>a</sup>	7.2 ± 0.8 <sup>a</sup>	14.3 ± 1.1 <sup>ab</sup>	23.9 ± 1.6 <sup>ab</sup>	35.3 ± 2.0 <sup>ab</sup>	41.9 ± 2.1 <sup>abc</sup>	46.3 ± 1.9 <sup>a</sup>	48.6 ± 2.0 <sup>a</sup>	51.4 ± 1.3 <sup>a</sup>
<i>TaVP2</i> OEX Line 2	-	0.9 ± 0.4 <sup>a</sup>	4.1 ± 1.1 <sup>a</sup>	10.6 ± 1.8 <sup>a</sup>	19.2 ± 2.6 <sup>a</sup>	29.9 ± 2.6 <sup>a</sup>	38.7 ± 2.4 <sup>ab</sup>	46.0 ± 1.6 <sup>a</sup>	50.9 ± 1.8 <sup>a</sup>	52.2 ± 1.7 <sup>a</sup>
<i>TaVP2</i> null line	-	1.5 ± 0.4 <sup>a</sup>	5.3 ± 1.0 <sup>a</sup>	12.4 ± 1.7 <sup>ab</sup>	23.0 ± 2.4 <sup>ab</sup>	31.7 ± 2.8 <sup>ab</sup>	41.8 ± 3.7 <sup>abc</sup>	47.9 ± 2.8 <sup>ab</sup>	50.4 ± 3.2 <sup>a</sup>	51.1 ± 2.8 <sup>a</sup>

**Table A3: Daily shoot biomass measurements (cm ± SEM) of wild-type, T<sub>1</sub> *TaVP* transgenic and null segregant wheat seedlings.** Seedlings

were grown in a paper roll hydroponics system and destructively harvested after 10 d. Values are means (± standard error of the mean (SEM), n=5-11) with different letters indicating statistically significant differences based on one-way ANOVA and Tukey's 95% confidence intervals,  $P \leq 0.05$  (GenStat® version 15.3). - indicates no recorded measurements.

Line	Total leaf length (cm ± SEM)									
	Day 1	Day 2	Day 3	Day 4	Day 5	Day 6	Day 7	Day 8	Day 9	Day 10
Wild-type	-	0.2 ± 0.06 <sup>a</sup>	0.9 ± 0.2 <sup>a</sup>	2.4 ± 0.2 <sup>ab</sup>	4.8 ± 0.4 <sup>a</sup>	7.7 ± 0.4 <sup>a</sup>	10.0 ± 0.3 <sup>a</sup>	16.0 ± 0.6 <sup>ab</sup>	18.9 ± 0.6 <sup>a</sup>	21.7 ± 0.5 <sup>a</sup>
<i>TaVP1</i> OEX Line 1	-	0.2 ± 0.04 <sup>a</sup>	0.8 ± 0.1 <sup>a</sup>	2.1 ± 0.3 <sup>ab</sup>	4.4 ± 0.4 <sup>a</sup>	7.1 ± 0.5 <sup>a</sup>	9.6 ± 0.6 <sup>a</sup>	15.5 ± 0.8 <sup>ab</sup>	18.5 ± 0.9 <sup>a</sup>	21.4 ± 1.0 <sup>a</sup>
<i>TaVP1</i> OEX Line 2	-	0.2 ± 0.08 <sup>a</sup>	0.6 ± 0.2 <sup>a</sup>	1.6 ± 0.2 <sup>a</sup>	3.7 ± 0.4 <sup>a</sup>	6.7 ± 0.4 <sup>a</sup>	9.1 ± 0.5 <sup>a</sup>	14.7 ± 0.7 <sup>ab</sup>	18.7 ± 0.3 <sup>a</sup>	21.5 ± 0.4 <sup>a</sup>
<i>TaVP1</i> null line	-	0.1 ± 0.04 <sup>a</sup>	0.6 ± 0.1 <sup>a</sup>	1.7 ± 0.3 <sup>ab</sup>	3.9 ± 0.6 <sup>a</sup>	6.9 ± 0.6 <sup>a</sup>	9.6 ± 0.6 <sup>a</sup>	15.1 ± 0.9 <sup>ab</sup>	18.2 ± 0.9 <sup>a</sup>	21.1 ± 0.9 <sup>a</sup>
<i>TaVP2</i> OEX Line 1	-	0.3 ± 0.05 <sup>a</sup>	1.1 ± 0.2 <sup>a</sup>	2.8 ± 0.2 <sup>b</sup>	5.3 ± 0.4 <sup>a</sup>	8.3 ± 0.4 <sup>a</sup>	11.0 ± 0.5 <sup>a</sup>	17.1 ± 0.8 <sup>b</sup>	20.4 ± 0.8 <sup>a</sup>	24.4 ± 1.3 <sup>a</sup>
<i>TaVP2</i> OEX Line 2	-	0.1 ± 0.05 <sup>a</sup>	0.5 ± 0.1 <sup>a</sup>	1.8 ± 0.3 <sup>ab</sup>	3.8 ± 0.5 <sup>a</sup>	6.6 ± 0.6 <sup>a</sup>	9.3 ± 0.6 <sup>a</sup>	13.4 ± 1.2 <sup>a</sup>	17.3 ± 0.9 <sup>a</sup>	20.3 ± 0.9 <sup>a</sup>
<i>TaVP2</i> null line	-	0.3 ± 0.05 <sup>a</sup>	0.9 ± 0.1 <sup>a</sup>	2.5 ± 0.3 <sup>ab</sup>	4.9 ± 0.5 <sup>a</sup>	7.8 ± 0.6 <sup>a</sup>	10.3 ± 0.7 <sup>a</sup>	15.9 ± 1.0 <sup>ab</sup>	18.8 ± 1.2 <sup>a</sup>	21.8 ± 1.2 <sup>a</sup>

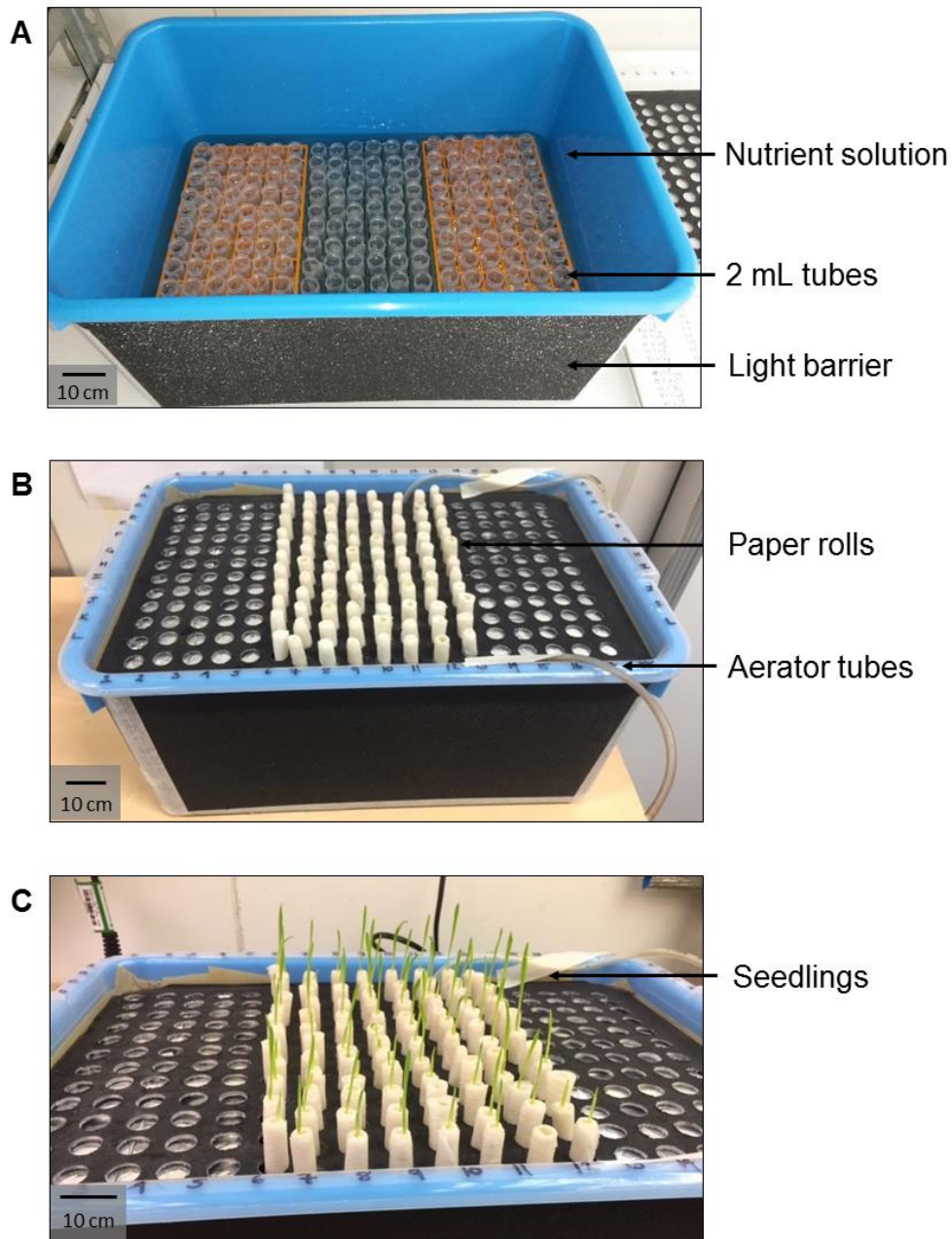


Fig. A7: Overview of the hydroponics system used to assess seedling vigour of T<sub>1</sub> *TaVP* over-expressing wheat lines. (A) Interior and (B) exterior components of the hydroponics tank, and (C) the functioning system containing (Fielder wild-type, *TaVP1* OEX Line 1, *TaVP1* OEX Line 2, *TaVP1* null segregant line, *TaVP2* OEX Line 1, *TaVP2* OEX Line 2, *TaVP2* null segregant line) wheat seedlings, supported in moist paper towel rolls. Scale bar = 10 cm.



## Chapter 6 - General discussion

## General discussion

### Review of research aims

With genetically-modified (GM) crops restricted or highly regulated in most countries (Hindmarsh and Du Plessis, 2008; Potrykus, 2013), identifying and characterising genes, which are beneficial for improving plant growth and stress tolerance, will aid in the development of high yielding and stress tolerant non-GM bread wheat (*Triticum aestivum*) cultivars (Gilliham et al., 2017). Despite considerable evidence that constitutive expression of vacuolar proton-pumping pyrophosphatase (H<sup>+</sup>-PPase) genes improves growth and abiotic stress tolerance in many transgenic plants (Gaxiola et al., 2012; Gaxiola et al., 2016a; Schilling et al., 2017), little research has investigated these genes in bread wheat, or assessed the potential of using H<sup>+</sup>-PPase genes to improve the growth and stress tolerance of bread wheat.

The specific aims of this PhD research were:

1. To investigate the role of AVP1 in plant metabolism using *Arabidopsis thaliana* as a model plant species (**Chapter 2**)
2. To evaluate the impact of constitutive and stress-inducible expression of AVP1 on the growth and salinity tolerance of transgenic bread wheat (**Chapter 3**)
3. To utilise new genomic resources to identify and profile the expression of all bread wheat H<sup>+</sup>-PPase (*TaVP*) genes (**Chapter 4**)
4. To assess the role of wheat H<sup>+</sup>-PPases (TaVPs) through generating and phenotyping constitutively over-expressing *TaVP* wheat lines (**Chapter 5**)



## Summary of research findings

Metabolomics analysis of 8 d-old *Arabidopsis thaliana* (*Arabidopsis*) plants revealed transgenic seedlings over-expressing *AVP1* (*35S:AVP1*), the *Arabidopsis* H<sup>+</sup>-PPase gene, had higher concentrations of multiple metabolites compared to wild-type, while in *AVP1* loss-of-function mutants (*fugu5*, *fugu5-2* and *fugu5-3*), the concentration of multiple metabolites were reduced compared to wild-type (Chapter 2, Table 2). In *35S:AVP1* seedlings, concentrations of several metabolites within the gluconeogenesis, shikimate and Smirnoff-Wheeler pathways were higher than wild-type and *fugu5* mutant seedlings (Chapter 2, Table 2). In contrast to previous findings, sucrose concentrations were reduced in *AVP1* over-expressing *Arabidopsis* compared to wild-type, while sucrose concentrations increased in the *fugu5* mutant seedlings (Chapter 2, Figure 4). Increased levels of shikimate in *35S:AVP1* *Arabidopsis* plants, suggests this pathway may be upregulated compared to wild-type. The shikimate pathway is responsible for producing several metabolites, including tryptophan, which is required for indole-3-acetic acid biosynthesis. These results suggest that *AVP1* may have a role in regulating auxin biosynthesis via the shikimate pathway in *35S:AVP1* over-expressing *Arabidopsis* (Chapter 2, Figure 6).

To investigate the potential of H<sup>+</sup>-PPase genes to improve the growth and salt tolerance of bread wheat, *AVP1* was expressed in transgenic bread wheat (cv. Bob White) using the constitutive maize *ubiquitin1* promoter, and the stress-inducible maize *rab17* promoter. In hydroponics, neither constitutive nor stress-inducible expression of *AVP1* improved growth or salt tolerance of the transgenic wheat lines (Chapter 3, Figures 4 and S3), while seedling biomass and rhizosphere acidification were enhanced compared to wild-type in one constitutively expressing *AVP1* wheat line (Chapter 3, Figure 3). The lack of improved growth in the transgenic *AVP1* lines, compared to when this gene is expressed in other plant species,

may have been due to the type of promoters used to express the *AVP1* transgene, differences in the function of AVP1 in wheat compared to other plant species, and/or the natural ability of wheat to exclude sodium ( $\text{Na}^+$ ) ions under saline conditions.

*In silico* analysis of the draft bread wheat genome identified 6 novel  $\text{H}^+$ -PPase (*TaVP*) genes (Chapter 4, Table 1), bringing the total number of bread wheat  $\text{H}^+$ -PPases to 15. Expression analysis revealed significant variation in expression levels between wheat varieties, tissue types and developmental stages under non-stressed conditions (Chapter 4, Figure 7). While the *TaVP1* and *TaVP2* homeologs were expressed in all wheat varieties and tissues analysed, expression of the *TaVP3* homeologs was restricted to the developing grain, while *TaVP4* homeolog expression showed both developmental stage and variety specificity (Chapter 4, Figure 7). Diversity in *TaVP* expression profiles suggests these homeologs may have specialised roles in bread wheat, depending on the specific tissues and growth stages in which they are expressed.

To further investigate the role of TaVPs in bread wheat, transgenic wheat lines (cv. Fielder) constitutively over-expressing *TaVP1-B* and *TaVP2-B* were developed and characterised under saline and non-saline conditions (Chapter 5, Figure 2). Constitutive expression of these *TaVP* genes triggered early flowering under both control and saline conditions, significantly reduced biomass accumulation compared to wild-type and null segregants, and increased leaf  $\text{Na}^+$  concentrations under saline conditions (Chapter 5, Table 2). The phenotypes observed in the *TaVP1-B* and *TaVP2-B* transgenic wheat lines are proposed to be due to alterations in metabolites in response to enhanced TaVP function, resulting in changes to the pathways which regulate flowering time.

Taken together, the results of this research provide evidence that phenotypes of H<sup>+</sup>-PPase over-expressing and knock-out plants are highly variable, and are likely to be influenced by multiple factors. Metabolomics analysis suggests that AVP1 activity is likely to regulate a wide range of cellular and metabolic processes, while the large variation in *TaVP* expression between tissue types, developmental stages and wheat varieties suggests that expression level, as well as tissue and cellular localisation, are likely to influence the function of these proteins throughout development.

## Implications for future research

### Elucidating the role of AVP1

Despite significant research, the precise role of AVP1 under both stressed and non-stressed conditions remains unclear. While individual studies have focussed on investigating the various proposed functions of AVP1 individually, it is likely that AVP1 is involved in many of these roles, depending on tissue and cellular localisation, growth stage, and the presence or absence of abiotic stress conditions (Schilling et al., 2017). Under saline conditions, AVP1 is expected to be involved in vacuolar ion sequestration, however, this is likely to be dependent on cell and tissue type, as well as plant species. With conflicting results reported in regard to ion accumulation in *AVP1* over-expressing transgenic plants (Chapter 1, Table 1), cell-specific ion measurements are needed to compare differences in cytosolic and vacuolar ion concentrations (Kotula et al., 2015).

While AVP1 is likely to have a significant role in the regulation of cytosolic pyrophosphate (PP<sub>i</sub>) concentrations, a comprehensive understanding of the contribution of this function to PP<sub>i</sub> dependent pathways is required. It has been proposed that AVP1 is important for regulating

sucrose production via gluconeogenesis during the heterotrophic growth phase, a process influenced by cytosolic PP<sub>i</sub> concentrations (Ferjani et al., 2011). In addition, the regulation of PP<sub>i</sub> by AVP1 has also been suggested to influence the biosynthesis of ascorbic acid via the Smirnoff-Wheeler pathway (Schilling, 2014). With numerous other metabolic and cellular pathways dependent upon cytosolic PP<sub>i</sub> concentrations, including the biosynthesis of cellulose, starch, cytokinin and gibberellin (Heinonen, 2001), as well as indole-3-acetic acid (auxin) (Won et al., 2011) and numerous vitamins (Gerdes et al., 2012), AVP1 has the potential to influence many additional pathways. The contribution of AVP1 to PP<sub>i</sub> regulation may also be of greater importance in specific tissues and at certain developmental stages. To further investigate the role of AVP1 in regulating PP<sub>i</sub> dependent pathways, a comprehensive and quantitative metabolomics analysis, coupled with cell-specific PP<sub>i</sub> measurements, are required across various cell and tissue types, as well as developmental stages. Furthermore, analysis should also investigate AVP1 function in non-transgenic plants, as constitutive expression of *AVP1* is likely to impact upon protein localisation and, therefore, the function of AVP1 (Gaxiola et al., 2016b; Segami et al., 2014).

AVP1 has also been proposed to function in sucrose phloem loading through enhancing the activity of H<sup>+</sup>-ATPase proteins at the plasma membrane, by increasing adenosine triphosphate (ATP) supply via sucrose respiration (Gaxiola et al., 2012). However, this function requires AVP1 to function in PP<sub>i</sub> hydrolysis when localised to the tonoplast, and PP<sub>i</sub> synthesis when localised to the plasma membrane. While photoassimilate transport has been demonstrated to be enhanced in *AVP1* over-expressing *Arabidopsis* (Pizzio et al., 2015), and amino acids with the potential to regulate AVP1 function identified via *in silico* analysis (Pizzio et al., 2017), the ability of AVP1 to function in PP<sub>i</sub> synthesis is yet to be demonstrated, either *in-vitro* or *in-planta*. While this role could be investigated *in-vitro* through measuring the incorporation of <sup>32</sup>P into

PP<sub>i</sub> synthesised within tonoplast enriched vesicles (Rocha Facanha and de Meis, 1998), techniques would need to be developed to assess this function *in-planta*. It is also possible that when constitutively expressed, increased AVP1 abundance results in greater availability of ATP, which could be utilised to enhance H<sup>+</sup>-ATPase-dependent sucrose transport (Gaxiola et al., 2012). Consequently, *in planta* evidence is required to establish whether AVP1 has the ability to function as a PP<sub>i</sub> synthase at the plasma membrane, while the contribution of AVP1 to cellular energy balance should also be investigated, as coordinated regulation of H<sup>+</sup>-PPases and H<sup>+</sup>-ATPases (Fuglsang et al., 2011) could be an important factor contributing to the phenotypes of *AVP1* over-expressing plants.

To gain a comprehensive understanding of the function of AVP1, a systems biology approach (Sheth and Thaker, 2014) would enable the role of AVP1 to be assessed in multiple plant tissues throughout development. With evidence suggesting that the function of AVP1 is likely to be different to that of cereal H<sup>+</sup>-PPases (Shavrukov, 2014; Wang et al., 2009), understanding the function and regulation of TaVP proteins in bread wheat should also be investigated, as such knowledge would contribute to genetic marker development and the breeding of high yielding, stress tolerant bread wheat cultivars.

### **Characterisation of *TaVP* gene expression patterns and stress response**

Variation in the expression of H<sup>+</sup>-PPase genes has been reported in several cereal species, both in response to stress conditions, as well as between tissue types. In rice, expression of the *OVP1* gene has been associated with cold tolerance (Zhang et al., 2011), expression of *OVP3* has been implicated in tolerance to anoxic conditions (Liu et al., 2010), while *OVP4*, *OVP5* and *OVP6* expression is upregulated under salt stress (Plett et al., 2010). Of the three identified barley H<sup>+</sup>-

PPase genes (*HVP1*, *HVP10* and *HVP3*), expression of *HVP10* (Tanaka et al., 1993) and *HVP1* (Fukuda et al., 2004) are both upregulated under salt and drought stress (Fukuda et al., 2004; Fukuda and Tanaka, 2006). Expression of *HVP10* under saline conditions, however, has been shown to vary through time, as well as between barley accessions and tissue types (Shavrukov et al., 2013). In root tissue of CPI-71284 and Barque-73 barley seedlings, *HVP10* expression peaked 3 d after the initial salt treatment and then rapidly declined, while in shoot tissue, *HVP10* expression was upregulated only in CP1-71284, with expression peaking at 10 % of the level reported in the root tissue (Shavrukov et al., 2013). In control conditions, expression of *HVP10* was found to be higher in the root compared to the shoot, while *HVP1* expression was higher in the shoot (Fukuda et al., 2004). Based on the large number of H<sup>+</sup>-PPase sequences identified in the wheat genome (Chapter 4), variation in *TaVP* expression patterns (Chapter 4), and variation in the stress responses of other cereal H<sup>+</sup>-PPases, it is likely that wheat *TaVP* genes have varied and possibly unique roles in regulating growth and stress response. For instance, the large differences in *TaVP4* homeolog expression between the 4 wheat varieties (Chapter 4, Figure 7), suggests these homeologs have a more significant role in the commercial varieties Scout and Buck Atlantico, which may contribute to a specific trait that was selected for during breeding. There is also the potential for the role of TaVPs to be co-ordinately regulated, with the expression of multiple *TaVP* genes within specific cell or tissue types contributing to a specific function. To further investigate such variation, *TaVP* gene expression needs to be characterised under a variety of stress conditions to identify under what conditions expression of each *TaVP* homeolog is upregulated. Techniques such as quantitative real-time polymerase chain reaction (qRT-PCT) and *in-situ* PCR (Athman et al., 2014) should be used to analyse the response of *TaVP* gene expression to stress conditions, across various tissue types and varieties through time. This knowledge would aid in identifying *TaVP* homeologs that are responsive to

certain stress conditions, and assist with identifying the function of these proteins. Ultimately this knowledge could be used for improving the stress tolerance of current bread wheat cultivars through selective breeding (Kumar et al., 2010) or gene-editing (Zhang et al., 2016).

### **Investigating tissue and cellular localisation of TaVPs**

In addition to identifying variation in gene expression among *TaVP* homeologs, investigating differences in tissue and cellular localisation of TaVP proteins should also be investigated, as localisation is likely to influence the function of these proteins. Determining the significance of these homeologs being specifically expressed in the developing grain (Chapter 4, Figure 7), would assist with determining the function of the TaVP3 proteins. For instance, the TaVP proteins may be responsible for regulating PP<sub>i</sub> dependent pathways such as the synthesis of sucrose (Heinonen, 2001), ascorbic acid (Smirnoff, 2000) and auxin (Won et al., 2011). These proteins may also be important for regulating the loading of carbohydrates, ions and/or nutrients into the grain during maturation, which could be beneficial for grain yield and nutrition (Ferjani et al., 2014; Li et al., 2014; Meyer et al., 2012). Furthermore, as expression of the rice H<sup>+</sup>-PPase gene, *OVP3*, has been associated with reduced grain quality (Li et al., 2014), understanding the impact of H<sup>+</sup>-PPases in grain development will be essential for determining how *TaVP* genes can be utilised to improve the yield of bread wheat. Tissue and cellular localisation of TaVP proteins could be investigated using immunolocalisation techniques (Langhans et al., 2001). However, as immunolocalisation of H<sup>+</sup>-PPase proteins use antibodies specific to a region conserved among all H<sup>+</sup>-PPase proteins (Gaxiola et al., 2001; Langhans et al., 2001; Paez-Valencia et al., 2011; Regmi et al., 2016), TaVP homeolog specific antibodies would need to be developed.

## Identifying amino acid residues that influence TaVP function

In addition to a comprehensive understanding of the variation in expression and localisation of *TaVP1*, *TaVP2*, *TaVP3* and *TaVP4* homeologs, factors that influence TaVP protein function should also be investigated. Mutation studies in *Arabidopsis* have identified several amino acid residues that are responsible for regulating both the activity and function of AVP1 (Pizzio et al., 2017; Zhen et al., 1997). When glutamic acid residues at positions 119, 229, 573, 667 and 751 in the AVP1 protein are substituted with either a glutamine or asparagine residue, the rate of PP<sub>i</sub> hydrolysis and proton (H<sup>+</sup>) translocation can be reduced up to 75 % (Zhen et al., 1997). Mutations within the AVP1 protein at positions 305 and 504, reduce the rate of PP<sub>i</sub> hydrolysis by 90 % and completely inhibit H<sup>+</sup> translocation (Zhen et al., 1997). Alternatively, the substitution of glutamic acid with aspartic acid at positions 229 and 427 within the AVP1 protein, increases the rate of PP<sub>i</sub> hydrolysis by 45 % and 6 % respectively, while H<sup>+</sup> translocation is increased 70 % and 35 %, respectively (Zhen et al., 1997).

*In silico* analysis has also identified a residue (K768) in the AVP1 protein with the potential to regulate H<sup>+</sup> flux directionality, thus potentially altering the function of AVP1 (Pizzio et al., 2017). To further investigate this hypothesis, techniques such as second-harmonic generation (SHG) microscopy (Moree et al., 2015), or fluorescence resonance energy transfer (FRET) microscopy (Fu et al., 2015), could be used to monitor conformational changes in H<sup>+</sup>-PPase proteins. Nano-mechanical sensors have also been developed which allow conformational changes within proteins to be monitored in real-time (Alonso-Sarduy et al., 2014). Cell-type specific PP<sub>i</sub> measurements coupled with H<sup>+</sup> flux measurements, using techniques such as whole-cell patch clamping (Babich et al., 2018), could be used to further investigate the function of H<sup>+</sup>-PPase proteins. Identifying amino acids within TaVP proteins that have the ability to enhance protein function, would aid in developing wheat varieties with enhanced TaVP function, either through



identifying wheat varieties that possess beneficial alleles and using selective breeding to transfer these alleles to elite wheat cultivars (Kumar et al., 2010), or by utilising gene editing techniques such as CRISPR/Cas9 (Zhang et al., 2016) to enhance the function of TaVPs within current elite wheat cultivars.

## **Other relevant areas for future research**

### **Characterisation of *TaVP* promoter sequences**

In *Arabidopsis*, expression of *AVP1* is known to be regulated by several *cis*-elements, within the *AVP1* promoter region (Mitsuda et al., 2001). These elements, located 1.7 kb 5' of the *AVP1* start codon are known to alter gene expression in response to auxin, sugar, and low-temperatures (Mitsuda et al., 2001). Deletion mutants containing various lengths of the *AVP1* promoter, fused to the GUS reporter gene, also identified two *cis*-elements 277 and 262 5' of the *AVP1* start codon, which are responsible for pollen specific expression (Mitsuda et al., 2001). Six DNA-binding One Zinc Finger 2 (DOF2) binding sites have also been identified in a region 244 bp 5' of the *AVP1* start codon (Pizzio et al., 2015). DOF transcription factors are known to both activate and inhibit the function of proteins involved in metabolism, seed development and tissue differentiation during hypocotyl elongation, pollen development, and flowering (Noguero et al., 2013). DOF proteins have also been shown to promote protein activity sieve-element companion cells (Noguero et al., 2013), which could be important elements for regulating the activity and/or localisation of *AVP1*.

H<sup>+</sup>-PPase promoter sequences are also important for regulating gene expression and protein activity in response to stress conditions. In maize, a 366-bp insertion was identified in the

promoter of the drought tolerant (CIMBL55) maize genotype, which contained 3 MYB *cis*-elements (Wang et al., 2016). MYB transcription factors have been associated with abiotic stress tolerance in many other plant species, including maize (Chen et al., 2017) and bread wheat (Bi et al., 2016). When expression of *ZmVPP1* was compared between the drought tolerant (CIMBL55) and drought sensitive (Shen5003) maize genotypes, expression of *ZmVPP1* was 2-fold higher in the tolerant genotype under drought stress (Wang et al., 2016).

With twelve type I *TaVP* homeologs now identified in bread wheat (Chapter 4), identifying regions within *TaVP* promoter sequences that are responsible for regulating gene expression and stress response, would assist with identifying beneficial *TaVP* genes for selective breeding or gene editing. Regulatory regions with *TaVP* promoters could be identified using bioinformatics tools, such as PlantPAN (Chow et al., 2016), PlantCARE (Lescot et al., 2002) and others (Solovyev et al., 2010). In addition, fusion of the  $\beta$ -glucuronidase (GUS) gene, green fluorescent protein (GFP), or luciferase (LUC) (Ruijter et al., 2003) reporter gene would be useful for identifying *TaVP* promoters that are responsive to specific stress conditions, or induce expression within specific cell or tissue types.

### **Understanding post-transcriptional regulation of TaVPs**

Currently, little is known about the regulation of H<sup>+</sup>-PPases at the post-transcriptional and post-translational level, which are likely to have an important impact on H<sup>+</sup>-PPase function. Alternative splicing is a post-transcriptional process through which multiple transcripts, and therefore proteins, are produced from a single gene (Laloum et al., 2018). The frequency of alternative splicing events has also been shown to increase under abiotic stress conditions, thus contributing to increased proteome diversity (Laloum et al., 2018). Through genomic screening,

an alternative isoform of the Arabidopsis *AVP1* gene (*AT1G15690.2*) has been identified, with sequencing data suggesting this isoform is the product of alternative splicing and contains a 550 bp deletion (Fuglsang et al., 2011). However, little is known about differences in the functionality of this isoform compared to the well characterised *AVP1* gene (*AT1G15690.1*).

Alternative splicing is known to be differentially regulated in response to developmental stages and abiotic stress conditions, and has been shown to vary significantly in frequency between wild and domesticated sorghum (*Sorghum bicolor*) varieties (Ranwez et al., 2017). Analysis of 10 wild sorghum varieties showed a greater proportion of soluble pyrophosphatase isoforms compared to the domesticated varieties, due to an increased rate of alternative splicing events, and was suggested to be a useful resource for improving the genetic and phenotypic diversity of domesticated sorghum (Ranwez et al., 2017). Transcriptomic analysis of a moss species, *Physcomitrella patens*, identified two H<sup>+</sup>-PPase isoforms, which showed differential alternative splicing between the juvenile and mature growth stages (Fesenko et al., 2017). Furthermore, alternative splicing occurred within the 5' UTR, with H<sup>+</sup>-PPase isoforms containing longer 5' UTRs associated with reduced levels of gene expression (Fesenko et al., 2017). In bread wheat, alternative splicing is known to be differentially regulated by drought and heat stress, with splicing events also differing between homeologs (Liu et al., 2018). Therefore, identification of beneficial and deleterious H<sup>+</sup>-PPase isoforms, under both stressed and non-stressed conditions, could be a useful resource for optimising *TaVP* expression and function in wheat. Such information could be obtained by comparing expression differences in various bread wheat varieties under stressed and non-stressed conditions, using techniques such as RNA sequencing (RNA-Seq) (Trapnell et al., 2010) and isoform sequencing (Iso-Seq)(Wang et al., 2018).

## Understanding post-translational regulation of TaVPs

In Arabidopsis, phosphorylation status is also known to influence AVP1 activity, with the 14-3-3 regulatory proteins having the ability to bind to the phosphorylated AVP1 protein (Hsu et al., 2018). Binding of these regulatory proteins enhances the efficiency of PP<sub>i</sub> hydrolysis and H<sup>+</sup> translocation by AVP1, and have been proposed to enhance substrate binding and prevent enzyme inhibition under stress conditions (Hsu et al., 2018). Binding sites for 14-3-3 regulatory proteins have also been identified in maize (Sun et al., 2016) and Arabidopsis (Pizzio et al., 2017) H<sup>+</sup>-PPases, as well as in H<sup>+</sup>-ATPases (Fuglsang et al., 2011), where they are responsible for regulating protein function and membrane targeting (Coblitz et al., 2005). Consequently, identifying 14-3-3 binding sites and characterising the role of these proteins in regulating TaVP function and protein targeting should be further investigated.

Ubiquitination and SUMOylation are additional post-translational regulators that influence protein function, protein stability and protein-protein interactions. Ubiquitination involves the binding of ubiquitin to lysine residues within host proteins (Sadanandom et al., 2012), while SUMOylation involves the binding of small ubiquitin-like modifier (SUMO) proteins, a process that is known to be highly influenced by abiotic stress conditions (Yates et al., 2016). *In silico* analysis predicts the AVP1 protein to contain 5 ubiquitination and 6 SUMOylation sites, which have been proposed to have an important role in regulating AVP1 function (Pizzio et al., 2017). Further investigation into post-translational regulation of TaVP protein should be further analysed, using both *in-silico* (Audagnotto and Dal Peraro, 2017) and *in-vivo* (Albuquerque et al., 2015) techniques.

## Enhancing TaVP function in bread wheat through selective breeding and gene editing

Identifying and characterising variation in gene expression and protein localisation, as well as understanding the factors that influence and regulate TaVP protein activity, will allow beneficial *TaVP* homeologs, alleles and isoforms to be identified. For instance, *TaVP* sequences which have enhanced gene expression (such as *TaVP2-D* in Scout) and protein activity, are localised within specific tissues or cell types, or are responsive to particular stress conditions could be used to enhance wheat growth via non-GM technologies, such as selective breeding (Kumar et al., 2010) and gene editing via CRISPR/Cas9 (Zhang et al., 2016). CRISPR/Cas9 has been used to enhance the expression of *AVP1* in *Arabidopsis* through insertion of a heat-shock factor 1 (HSF) activation domain into the *AVP1* promoter sequence (Park et al., 2017). As a result, *AVP1* expression increased 2- to 5-fold under non-stressed compared to wild-type (Park et al., 2017). *Arabidopsis* lines containing this HSF domain also produced a similar phenotype to previously characterised *AVP1* over-expressing transgenic plants, with a 2-fold increase in leaf area, increased leaf number, and improved drought tolerance compared to wild-type (Park et al., 2017). Using the CRISPR/Cas9 technique to alter single nucleotides, either within the gene coding sequence or the promoter region of *TaVP* homeologs is a promising approach for enhancing TaVP function in wheat, as allele editing will not be regulated in the United States (United States Department of Agriculture, 2018), and is unlikely to be regulated in Australia (Gillespie, 2017). However, a greater understanding of TaVP function and regulation would be required before such techniques could be implemented.

## Concluding remarks

Since first being identified as having a beneficial impact on the growth and stress tolerance of *Arabidopsis* (Gaxiola et al., 2001), H<sup>+</sup>-PPase research has predominantly focused on phenotypic characterisation of transgenic plants constitutively expressing the *Arabidopsis* H<sup>+</sup>-PPase (*AVP1*) gene, as well as elucidating the functional role of *AVP1* in *Arabidopsis* (Ferjani et al., 2011; Gaxiola et al., 2012; Li et al., 2005; Pizzio et al., 2015; Pizzio et al., 2017; Schilling, 2014). With considerable research into the role of *AVP1* in *Arabidopsis*, as well as other plant species, evidence suggests that *AVP1* is likely to have numerous, non-mutually exclusive roles (Gaxiola et al., 2016a; Gaxiola et al., 2016b; Gutiérrez-Luna et al., 2018; Schilling et al., 2017; Segami et al., 2018). Furthermore, characterisation of a wide range of transgenic plants constitutively expressing H<sup>+</sup>-PPase genes has produced numerous, and often contrasting phenotypes (Chapter 1, Table 1), indicating the role of H<sup>+</sup>-PPases is likely to vary between plant species. As such, future research should be focussed towards understanding the roles of H<sup>+</sup>-PPases in specific plant species, and identifying how these genes can be utilised to improve plant growth, yield and abiotic stress tolerance.

In this research, the concentration of multiple metabolites within *35S:AVP1* over-expressing *Arabidopsis* increased compared to wild-type, while in *fugu5* mutants various metabolites were reduced compared to wild-type. These results suggest that *AVP1* is likely to influence various cellular functions and metabolic pathways, and could potentially be involved ascorbic acid production via multiple biosynthesis pathways, as well as the production of tryptophan and indole-3-acetic acid via the shikimate pathway. When constitutively expressed in transgenic bread wheat, *AVP1* did not convey a beneficial phenotype under control or saline conditions compared to other plant species expressing *AVP1*, although one transgenic line constitutively

expressing *AVP1* showed evidence of enhanced seedling growth and rhizosphere acidification. Analysis of the bread wheat genome identified 6 novel H<sup>+</sup>-PPase (*TaVP*) homeologs (*TaVP4-A*, *TaVP4-B* and *TaVP4-D* which are predicted to encode type I proteins, and *TaVP5-A*, *TaVP5-B* and *TaVP5-D* which are predicted to encode type II proteins). Gene expression analysis revealed significant differences in expression levels of all 12 type I *TaVP* genes among different tissue types, developmental stages and wheat varieties. Constitutive over-expression of *TaVP1-B* and *TaVP2-B* in bread wheat, significantly reduced biomass accumulation and time to flowering under both control and saline conditions, and significantly enhanced leaf Na<sup>+</sup> accumulation compared to wild-type under salt stress. The reduced biomass observed in the *TaVP* over-expressing lines contradicts the phenotype of most H<sup>+</sup>-PPase expressing transgenic plants, the majority which have enhanced biomass compared to wild-type. In addition, this is the first instance that constitutive expression of a H<sup>+</sup>-PPase gene has reduced time to flowering.

Overall, the results of this research highlight the likelihood that H<sup>+</sup>-PPase function is influenced by multiple factors, and that the phenotypes of H<sup>+</sup>-PPase over-expressing plants may not translate to other transgenic lines, plant species or H<sup>+</sup>-PPase genes. As such, it is proposed that future research should focus on understanding the factors that regulate native H<sup>+</sup>-PPase activity, and determine how these genes can be used to improve plant growth and stress tolerance through non-GM technologies, such as selective breeding and gene editing.

## References

- Albuquerque CP, Yeung E, Ma S *et al.* 2015. A chemical and enzymatic approach to study site-specific sumoylation. *PLoS ONE* **10**, <https://doi.org/10.1371/journal.pone.0143810>.
- Alonso-Sarduy L, De Los Rios P, Benedetti F *et al.* 2014. Real-time monitoring of protein conformational changes using a nano-mechanical sensor. *PLoS ONE* **9**, <https://doi.org/10.1371/journal.pone.0103674>.
- Athman A, Tanz SK, Conn VM *et al.* 2014. Protocol: A fast and simple *in situ* PCR method for localising gene expression in plant tissue. *Plant Methods* **10**, 1-19.
- Audagnotto M and Dal Peraro M. 2017. Protein post-translational modifications: *In silico* prediction tools and molecular modeling. *Computational and Structural Biotechnology Journal* **15**, 307-319.
- Babich V, Henry MK and Di Sole F. 2018. Application of electrophysiology measurement to study the activity of electro-neutral transporters. *Journal of Visualized Experiments*, <https://doi.org/10.3791/56630>.
- Bi H, Luang S, Li Y *et al.* 2016. Identification and characterization of wheat drought-responsive MYB transcription factors involved in the regulation of cuticle biosynthesis. *Journal of Experimental Botany* **67**, 5363-5380.
- Chen YH, Cao YY, Wang LJ *et al.* 2017. Identification of MYB transcription factor genes and their expression during abiotic stresses in maize. *Biologia Plantarum*, <https://doi.org/10.1007/s10535-017-0756-1>.
- Chow C, Zheng H, Wu N *et al.* 2016. PlantPAN 2.0: An update of plant promoter analysis navigator for reconstructing transcriptional regulatory networks in plants. *Nucleic Acids Research* **44**, <https://doi.org/10.1093/nar/gkv1035>
- Coblitz B, Shikano S, Wu M *et al.* 2005. C-terminal recognition by 14-3-3 proteins for surface expression of membrane receptors. *Journal of Biological Chemistry* **280**, 36263-36272.
- Ferjani A, Segami S, Horiguchi G *et al.* 2011. Keep an eye on PP<sub>i</sub>: The vacuolar-type H<sup>+</sup>-pyrophosphatase regulates postgerminative development in *Arabidopsis*. *Plant Cell* **23**, 2895-2908.
- Ferjani A, Segami S, Horiguchi G *et al.* 2014. Roles of the vacuolar H<sup>+</sup>-PPase in seed storage oil mobilization and plant development. *Plant Morphology* **26**, 45-51.
- Fesenko I, Khazigaleeva R, Kirov I *et al.* 2017. Alternative splicing shapes transcriptome but not proteome diversity in *Physcomitrella patens*. *Scientific Reports* **7**, <https://doi.org/10.1038/s41598-017-02970-z>.
- Fu L, Lv X, Xiong Y *et al.* 2015. Investigation of protein-protein interactions and conformational changes in hedgehog signaling pathway by FRET. *Methods in Molecular Biology* **1322**, 61-70.
- Fuglsang AT, Paez-Valencia J and Gaxiola RA. 2011. Plant proton pumps: Regulatory circuits involving H<sup>+</sup>-ATPase and H<sup>+</sup>-PPase. In *Transporters and Pumps in Plant Signaling*, vol. 7 (ed. M. Geisler and K. Venema), pp. 39-64. Berlin, Heidelberg: Springer
- Fukuda A, Chiba K, Maeda M *et al.* 2004. Effect of salt and osmotic stresses on the expression of genes for the vacuolar H<sup>+</sup>-pyrophosphatase, H<sup>+</sup>-ATPase subunit A, and Na<sup>+</sup>/H<sup>+</sup> antiporter from barley. *Journal of Experimental Botany* **55**, 585-594.
- Fukuda A and Tanaka Y. 2006. Effects of ABA, auxin, and gibberellin on the expression of genes for vacuolar H<sup>+</sup>-inorganic pyrophosphatase, H<sup>+</sup>-ATPase subunit A, and Na<sup>+</sup>/H<sup>+</sup> antiporter in barley. *Plant Physiology and Biochemistry* **44**, 351-358.



- Gaxiola RA, Li J, Undurraga S et al.** 2001. Drought- and salt-tolerant plants result from overexpression of the *AVP1* H<sup>+</sup>-pump. *Proceedings of the National Academy of Sciences* **98**, 11444-11449.
- Gaxiola RA, Sanchez CA, Paez-Valencia J et al.** 2012. Genetic manipulation of a “vacuolar” H<sup>+</sup>-PPase: From salt tolerance to yield enhancement under phosphorus-deficient soils. *Plant Physiology* **159**, 3-11.
- Gaxiola RA, Regmi K and Hirschi KD.** 2016a. Moving on up: H<sup>+</sup>-PPase mediated crop improvement. *Trends in Biotechnology* **34**, 347-349.
- Gaxiola RA, Regmi KC, Paez-Valencia J et al.** 2016b. Plant H<sup>+</sup>-PPases: Reversible enzymes with contrasting functions dependent on membrane environment. *Molecular Plant* **9**, 317-319.
- Gerdes S, Lerma-Ortiz C, Frelin O et al.** 2012. Plant B vitamin pathways and their compartmentation: A guide for the perplexed. *Journal of Experimental Botany* **63**, 5379-95.
- Gillespie D.** 2017. Gene Technology Amendment (2017 Measures No. 1) Regulations 2017. Canberra, Australia, Office of the Gene Technology Regulator.
- Gilliham M, Able JA and Roy SJ.** 2017. Translating knowledge about abiotic stress tolerance to breeding programmes. *The Plant Journal* **90**, 898-917.
- Gutiérrez-Luna FM, Hernández-Domínguez EE, Valencia-Turcotte LG et al.** 2018. Review: Pyrophosphate and pyrophosphatases in plants, their involvement in stress responses and their possible relationship to secondary metabolism. *Plant Science* **267**, 11-19.
- Heinonen JK.** 2001. Biological role of inorganic pyrophosphate. New York, United States of America: Springer US.
- Hindmarsh R and Du Plessis R.** 2008. GMO regulation and civic participation at the “edge of the world”: The case of Australia and New Zealand. *New Genetics and Society* **27**, 181-199.
- Hsu Y, Huang Y, Pan Y et al.** 2018. Regulation of H<sup>+</sup>-pyrophosphatase by 14-3-3 proteins from *Arabidopsis thaliana*. *The Journal of Membrane Biology*, <https://doi.org/10.1007/s00232-018-0020-4>.
- Kotula L, Clode PL, Striker GG et al.** 2015. Oxygen deficiency and salinity affect cell-specific ion concentrations in adventitious roots of barley (*Hordeum vulgare*). *New Phytologist* **208**, 1114-25.
- Kumar GR, Sakthivel K, Sundaram RM et al.** 2010. Allele mining in crops: Prospects and potentials. *Biotechnology Advances* **28**, 451-461.
- Laloum T, Martín G and Duque P.** 2018. Alternative splicing control of abiotic stress responses. *Trends in Plant Science* **23**, 140-150.
- Langhans M, Ratajczak R, Lutzelschwab M et al.** 2001. Immunolocalization of plasma-membrane H<sup>+</sup>-ATPase and tonoplast-type pyrophosphatase in the plasma membrane of the sieve element-companion cell complex in the stem of *Ricinus communis* L. *Planta* **213**, 11-19.
- Lescot M, Déhais P, Thijs G et al.** 2002. PlantCARE, a database of plant *cis*-acting regulatory elements and a portal to tools for in silico analysis of promoter sequences. *Nucleic Acids Research* **30**, 325-327.
- Li J, Yang H, Ann Peer W et al.** 2005. *Arabidopsis* H<sup>+</sup>-PPase AVP1 regulates auxin-mediated organ development. *Science* **310**, 121-125.
- Li Y, Fan C, Xing Y et al.** 2014. *Chalk5* encodes a vacuolar H<sup>+</sup>-translocating pyrophosphatase influencing grain chalkiness in rice. *Nature Genetics* **46**, <https://doi.org/10.1038/ng.2923>.
- Liu Z, Qin J, Tian X et al.** 2018. Global profiling of alternative splicing landscape responsive to drought, heat and their combination in wheat (*Triticum aestivum* L.). *Plant Biotechnology Journal* **16**, 714-726.

**Meyer K, Stecca KL, Ewell-Hicks K et al.** 2012. Oil and protein accumulation in developing seeds is influenced by the expression of a cytosolic pyrophosphatase in *Arabidopsis*. *Plant Physiology* **159**, 1221-1234.

**Mitsuda N, Takeyasu K and Sato MH.** 2001. Pollen-specific regulation of vacuolar H<sup>+</sup>-PPase expression by multiple *cis*-acting elements. *Plant Molecular Biology* **46**, 185-192.

**Moree B, Connell K, Mortensen Richard B et al.** 2015. Protein conformational changes are detected and resolved site specifically by second-harmonic generation. *Biophysical Journal* **109**, 806-815.

**Noguero M, Atif RM, Ochatt S et al.** 2013. The role of the DNA-binding One Zinc Finger (DOF) transcription factor family in plants. *Plant Science* **209**, 32-45.

**Paez-Valencia J, Patron-Soberano A, Rodriguez-Leviz A et al.** 2011. Plasma membrane localization of the type I H<sup>+</sup>-PPase AVP1 in sieve element-companion cell complexes from *Arabidopsis thaliana*. *Plant Science* **181**, 23-30.

**Park J, Dempewolf E, Zhang W et al.** 2017. RNA-guided transcriptional activation via CRISPR/dCas9 mimics overexpression phenotypes in *Arabidopsis*. *PLoS ONE* **12**, <https://doi.org/10.1371/journal.pone.0179410>.

**Pizzio GA, Paez-Valencia J, Khadilkar AS et al.** 2015. *Arabidopsis* type I proton-pumping pyrophosphatase expresses strongly in phloem, where it is required for pyrophosphate metabolism and photosynthate partitioning. *Plant Physiology* **167**, 1541-1553.

**Pizzio GA, Hirschi KD and Gaxiola RA.** 2017. Conjecture regarding posttranslational modifications to the *Arabidopsis* type I proton-pumping pyrophosphatase (AVP1). *Frontiers in Plant Science* **8**, <https://doi.org/10.3389/fpls.2017.01572>.

**Potrykus I.** 2013. Unjustified regulation prevents use of GMO technology for public good. *Trends in Biotechnology* **31**, 131-133.

**Ranwez V, Serra A, Pot D et al.** 2017. Domestication reduces alternative splicing expression variations in sorghum. *PLoS ONE* **12**, <https://doi.org/10.1371/journal.pone.0183454>.

**Regmi KC, Zhang S and Gaxiola RA.** 2016. Apoplasmic loading in the rice phloem supported by the presence of sucrose synthase and plasma membrane-localized proton pyrophosphatase. *Annals of Botany* **117**, 257-68.

**Rocha Facanha A and de Meis L.** 1998. Reversibility of H<sup>+</sup>-ATPase and H<sup>+</sup>-pyrophosphatase in tonoplast vesicles from maize coleoptiles and seeds. *Plant Physiology* **116**, 1487-95.

**Ruijter NCA, Verhees J, Leeuwen W et al.** 2003. Evaluation and comparison of the GUS, LUC and GFP reporter system for gene expression studies in plants. *Plant Biology* **5**, 103-115.

**Sadanandom A, Bailey M, Ewan R et al.** 2012. The ubiquitin-proteasome system: Central modifier of plant signalling. *New Phytologist* **196**, 13-28.

**Schilling RK.** 2014. "Evaluating the abiotic stress tolerance of transgenic barley expressing an *Arabidopsis* vacuolar H<sup>+</sup>-pyrophosphatase gene (*AVP1*)". PhD thesis. Adelaide, Australia. The University of Adelaide.

**Schilling RK, Tester M, Marschner P et al.** 2017. AVP1: One protein, many roles. *Trends in Plant Science* **22**, 154-162.

**Segami S, Makino S, Miyake A et al.** 2014. Dynamics of vacuoles and H<sup>+</sup>-pyrophosphatase visualized by monomeric green fluorescent protein in *Arabidopsis*: Artifactual bulbs and native intravacuolar spherical structures. *The Plant Cell* **26**, 3416-3434.

**Segami S, Asaoka M, Kinoshita S et al.** 2018. Biochemical, structural, and physiological characteristics of vacuolar H<sup>+</sup>-pyrophosphatase. *Plant & Cell Physiology* <https://doi.org/10.1093/pcp/pcy054>.

- Shavrukov Y, Bovill J, Afzal I et al.** 2013. *HVP10* encoding V-PPase is a prime candidate for the barley *HvNax3* sodium exclusion gene: evidence from fine mapping and expression analysis. *Planta* **237**, 1111-1122.
- Shavrukov Y.** 2014. Vacuolar H<sup>+</sup>-PPase (*HVP*) genes in barley: Chromosome location, sequence and gene expression relating to Na<sup>+</sup> exclusion and salinity tolerance. In *Barley: Physical properties, genetic factors and environmental impact on growth*, (ed. K. Hasunuma). New York: Nova Science Publishers.
- Sheth BP and Thaker VS.** 2014. Plant systems biology: Insights, advances and challenges. *Planta* **240**, 33-54.
- Smirnoff N.** 2000. Ascorbic acid: Metabolism and functions of a multi-facetted molecule. *Current Opinion in Plant Biology* **3**, 229-235.
- Solovyev VV, Shahmuradov IA and Salamov AA.** 2010. Identification of promoter regions and regulatory sites. In *Computational Biology of Transcription Factor Binding*, (ed. I. Ladunga), pp. 57-83. Totowa, New Jersey: Humana Press.
- Sun X, Qi W, Yue Y et al.** 2016. Maize *ZmVPP5* is a truncated Vacuole H<sup>+</sup>-PPase that confers hypersensitivity to salt stress. *Journal of Integrative Plant Biology* **58**, 518-528.
- Trapnell C, Williams BA, Pertea G et al.** 2010. Transcript assembly and abundance estimation from RNA-Seq reveals thousands of new transcripts and switching among isoforms. *Nature Biotechnology* **28**, 511-515.
- United States Department of Agriculture.** 2018. Secretary Perdue issues USDA statement on plant breeding innovation. Washington, D.C., United States Department of Agriculture.
- Wang M, Wang P, Liang F et al.** 2018. A global survey of alternative splicing in allopolyploid cotton: Landscape, complexity and regulation. *New Phytologist* **217**, 163-178.
- Wang X, Wang H, Liu S et al.** 2016. Genetic variation in *ZmVPP1* contributes to drought tolerance in maize seedlings. *Nature Genetics* **48**, 1233-41.
- Wang Y, Xu H, Zhang G et al.** 2009. Expression and responses to dehydration and salinity stresses of V-PPase gene members in wheat. *Journal of Genetics and Genomics* **36**, 711-720.
- Won C, Shen X, Mashiguchi K et al.** 2011. Conversion of tryptophan to indole-3-acetic acid by Tryptophan Aminotransferases of *Arabidopsis* and YUCCAs in *Arabidopsis*. *Proceedings of the National Academy of Sciences* **108**, 18518-18523.
- Yates G, Srivastava A and Sadanandom A.** 2016. SUMO proteases: Uncovering the roles of deSUMOylation in plants. *Journal of Experimental Botany* **67**, 2541-2548.
- Zhang Y, Liang Z, Zong Y et al.** 2016. Efficient and transgene-free genome editing in wheat through transient expression of CRISPR/Cas9 DNA or RNA. *Nature Communications* **7**, <https://doi.org/10.1038/ncomms12617>.
- Zhen R, Kim E and Rea P.** 1997. The molecular and biochemical basis of pyrophosphate-energized proton translocation at the vacuolar membrane. *Advances in Botanical Research* **25**, 297-337.